

Pre-treatment and utilization of recycled fine glass dust for 3D concrete printing

Mike Spek



Pre-treatment and utilization of recycled fine glass dust for 3D concrete printing

by

Mike Spek

to obtain the degree of Master of Science
at the Delft University of Technology,
to be defended publicly on Tuesday November 8, 2022 at 11:00 AM.

Student number:	4697995
Project duration:	November 20, 2021 – November 1, 2022
Thesis committee:	Dr. O. Copuroglu, TU Delft, supervisor
	Dr. Y. Chen, TU Delft
	Ir. T. Bristogianni, TU Delft
	Ir. D. Timmers, Maltha Groep BV

This thesis is confidential and cannot be made public until December 31, 2022.

An electronic version of this thesis is available at <http://repository.tudelft.nl/>.

Acknowledgments

In 2020 I started my master Structural Engineering in 2020 with the ambition to become a structural engineer, specializing in concrete structures. My interest with concrete structures has always been in 3D Concrete Printing. Therefore it was a pleasant surprise when Dr. Oguzhan Copuroglu presented me with the opportunity for a project with 3D Concrete printing. In combination with the company Maltha B.V. this project provided an exciting challenge in the relatively new field of Concrete Printing combined with the sustainability aspect of the use of recycled fine glass dust in the mortar mixtures.

First of all, I would like to thank Dr. Copuroglu for the opportunity you gave me to graduate on an innovative topic and for contacting me with Maltha. Our meetings always gave me new insights and perspectives on the research and this was something I really appreciated. Secondly I want to thank my daily supervisor Yu Chen. Without his help and expertise I could have not finished my thesis. Your help and ideas brought my research to a higher level and learned me a lot about performing a large investigation on the specific topic of mix design and 3D Concrete Printing. Thank you very much for your help and good luck in the future with your Postdoc research. Thirdly I would like to thank my other committee member Telesilla Bristogianni for the critical, but positive feedback during the final stages of my research.

For all the experiments in the lab I would like to express my gratitude to Maiko van Leeuwen and Ton Blom. Without their help, carrying out the experiments would have never been possible. I really enjoyed the times working together and the conversations were always fun! I would also like to thank John van den Berg for his help with the oven in the early stages of my research. Without his help in finding the right crucibles, this process would have taken much more time. For the SEM analysis, the help of Arjan Thijssen was much appreciated.

During the experiments and printing sessions we needed the help of many more people. This would have not been possible without the help of Hu Shi, Luiz Miranda de Lima, Yu Zhang, Hossein Rahmani and Masi Nuri. Their help was all really appreciated.

*Mike Spek
Delft, November 2022*

Abstract

Extrusion-based 3D concrete printing (3DCP) is one of the emerging techniques in the construction industry, due to the numerous benefits for the construction of concrete elements. The use of 3DCP has many benefits with the main goal to reduce concrete construction, economical and environmental impact. However most 3D printable mix designs contain a high amount of Portland cement (PC), which partially reduces the benefits of 3DCP on sustainability, like material efficient construction work and formwork-free designs. To enhance the sustainability of the concrete mixtures for 3DCP, supplementary cementitious materials (SCMs) are added to the mixture. SCMs like fly ash, granulated blast furnace slag, silica fume are used to reduce the PC content in cementitious mixtures. However some of the conventional SCMs, which are produced as industrial byproducts, have a limited supply or a high depletion rate. A continuously produced byproduct from the glass recycling industry is fine glass dust (FGD). This fine glass dust consists of very fine glass particles and is captured in filters in the recycling plant. This byproduct is difficult to recycle to glass cullet and is nowadays mainly incinerated or disposed in landfill, due to a lack of industrial purposes.

The main goal of this thesis is to find a new utilization opportunity for recycled fine glass dust as cement replacement in 3D Printed Concrete mixtures. This is beneficial for the circularity and recycling of glass, but also advantageous for the concrete industry as more sustainable mixtures could be developed for 3DCP. In order to investigate this new utilization opportunity for the recycled fine glass dust, tests on fresh-state and hardened properties were performed for cementitious mixtures where fine glass dust was used to replace Portland cement, because there could be a potential for pozzolanic reactivity.

The first part of this thesis investigated different pre-treatment methods of the fine glass dust in order to increase the reactivity when it was used as a cement replacement in cementitious mixtures. The results showed that the optimal pre-treatment for the fine glass dust was a heat-treatment at 600°C for 1 hour combined with a grinding treatment of 1 hour. The heat-treatment was efficient in removing the organic compounds from the fine glass dust and the grinding treatment was efficient in reducing the particle size of the fine glass dust.

The second part of this thesis investigated the influence of different cement replacement percentages by pre-treated fine glass dust in cementitious mixtures. Results showed that higher FGD percentages resulted in a reduction in compressive strength. However at longer curing ages (between 28 and 90 days) a small increase in strength development was observed. This could be attributed to the pozzolanic activity of the fine glass dust, which caused secondary strength development at later curing ages. It was also shown that significant amounts of secondary products were formed in the mixture with 25% FGD, which caused volume instability of the mixture. For the mixture with 10% FGD no volume instability was observed.

The third part of this thesis investigated the suitability of pre-treated fine glass dust for 3D Concrete Printing using the set-on-demand printing technique. For the mixture with 50% FGD in the cementitious mixtures it was found that a superplasticizer (SP) dosage of 0.4% was sufficient to develop a pumpable cementitious mixture. For the mixture with 20% FGD, this SP dosage was found to be 0.35%. As a combination of cementitious mixture with an accelerator slurry with 10% and 8% CaCl_2 , Mix FGD50-SP0.35-Acc10% and FGD20-SP0.35-Acc8% provided promising results in terms of fast stiffness and strength development. Due to volume instability of the FGD50 mixture, only mix FGD20-SP0.35-Acc8% was tested on printability. This mixture proved to be printable with a nozzle moving speed of 3600 mm/min and a time interval between layers of 18.8 seconds. Therefore a 20% replacement of Portland cement with fine glass dust could be used to develop a printable cementitious mixture for 3DCP.

The fourth part of this thesis discussed the applicability of the developed mixture in practice. A concrete bus shelter was used as a case study and it was shown that the mixture developed enough strength to withstand the stresses of the designed structure. The developed mixture FGD20-SP0.35-Acc8% was promising for implementation in 3DCP in terms of sustainable development of the concrete industry and as a new utilization of a byproduct from the glass recycling industry.

Contents

1	Introduction	1
1.1	General introduction	1
1.2	The problem and research relevance	2
1.3	Research objectives	3
1.4	Research questions	3
1.5	Research scope	4
1.6	Msc thesis outline	5
2	Literature Research	7
2.1	Previous research on the fine glass dust	7
2.2	Use of glass powder or glass particles in concrete	9
2.2.1	Recycled glass cullets as aggregate replacement	10
2.2.2	Waste glass powder as cement replacement	10
2.2.3	Potential for dangerous ASR when using glass particles in concrete mixtures	13
2.3	3D Concrete Printing	14
2.3.1	Differences of 3DCP with conventionally cast concrete	14
2.3.2	3D concrete printing techniques	18
2.3.3	Accelerator for set-on-demand 3D concrete printing	22
2.4	Fresh-state properties and 3DCP terminology	23
3	Raw material characterization and optimal pre-treatment for the fine glass dust	25
3.1	Research plan	25
3.1.1	Raw material characterization tests	25
3.1.2	Pre-treatment methods for the fine glass dust	26
3.1.3	Tests after pre-treatment of fine glass dust	27
3.2	Materials and Methods	27
3.2.1	Particle size distribution	27
3.2.2	Thermogravimetric analysis	29
3.2.3	Heat-treatment of the fine glass dust	30
3.2.4	Grinding treatment of the fine glass dust	33
3.2.5	BET specific area analysis	34
3.2.6	XRD analysis	36
3.2.7	Mix design	37
3.2.8	Slump and Slump flow test	38
3.2.9	Initial setting time test	40
3.2.10	Compressive strength test	41
3.3	Results	44
3.3.1	Particle size distribution	44
3.3.2	Thermogravimetric analysis	44
3.3.3	Heat-treatment of the fine glass dust	46
3.3.4	Grinding treatment of the fine glass dust	47
3.3.5	BET specific surface area	48
3.3.6	X-Ray Diffraction	49
3.3.7	Slump and Slump flow	50
3.3.8	Initial setting time	51
3.3.9	Compressive strength	52

3.4	Discussions	57
3.4.1	The effect of different pre-treatment methods for the fine glass dust on fresh properties	57
3.4.2	The effect of different pre-treatment methods for the fine glass dust on the compressive strength development	60
3.4.3	Limitations	62
4	Cement replacement percentage investigation for fine glass dust	65
4.1	Research plan	65
4.2	Material and Methods	66
4.2.1	Mix design for replacement percentage optimization	66
4.2.2	Slump and slump flow test	67
4.2.3	Compressive strength test	67
4.2.4	Pozzolanic activity test	67
4.2.5	Secondary formations test for mixtures with different FGD percentages	68
4.3	Results	69
4.3.1	Slump and slump flow	69
4.3.2	Compressive strength	70
4.3.3	Pozzolanic activity of the fine glass dust	72
4.3.4	Secondary formations of cementitious mixtures	74
4.4	Discussions	77
4.4.1	Effect of different fine glass dust replacement percentages on the compressive strength development	77
4.4.2	Pozzolanic activity of the pre-treated fine glass dust	78
4.4.3	Effect of different fine glass dust replacement percentages on the secondary formations in the mixture	79
4.4.4	Limitations	80
5	Suitability of fine glass dust for 3D Concrete Printing	83
5.1	Research plan	83
5.1.1	Pumpable cementitious mixtures	83
5.1.2	Pumpable cementitious mixtures + accelerator slurry	84
5.2	Materials and Methods	85
5.2.1	Mix design for pumpable cementitious mixtures	85
5.2.2	Flowability test for cementitious mixtures	86
5.2.3	Compressive strength test for cementitious mixtures	87
5.2.4	Pumpability test for cementitious mixtures	87
5.2.5	Mix design for cementitious mixtures + accelerator slurry	89
5.2.6	Flowability test for cementitious mixtures + accelerator slurry	91
5.2.7	Initial setting time test for cementitious mixtures + accelerator slurry	91
5.2.8	Isothermal calorimetry test for cementitious mixtures + accelerator slurry	91
5.2.9	Compressive strength test for cementitious mixtures + accelerator slurry	93
5.2.10	Buildability test for 3D Printed Concrete	93
5.2.11	Compressive strength test on 3D Printed Concrete	96
5.3	Results	96
5.3.1	Flowability for cementitious mixtures	96
5.3.2	Compressive strength for cementitious mixtures	97
5.3.3	Pumpability for cementitious mixtures	98
5.3.4	Flowability for cementitious mixtures + accelerator slurry	99
5.3.5	Initial setting time for cementitious mixtures + accelerator slurry	100
5.3.6	Isothermal calorimetry for cementitious mixtures + accelerator slurry	101
5.3.7	Compressive strength for cementitious mixtures + accelerator slurry	101
5.3.8	Buildability for 3D Printed Concrete	103
5.3.9	Compressive strength of 3D Printed Concrete	104

5.4	Discussions	105
5.4.1	Pumpable cementitious mixtures	105
5.4.2	Pumpable cementitious mixture + accelerator slurry	108
5.4.3	3D Printed Concrete	111
5.4.4	Limitations	113
6	Applicability of the developed mixture in practice	115
6.1	Background information on concrete bus shelter	115
6.2	Design of the concrete bus shelter	117
6.3	Design verification of 3D printable mixture for concrete bus shelter	117
6.4	Suitability of developed mixture for 3D printable concrete bus shelter	121
6.5	Feasibility for the utilization of fine glass dust in 3DCP mixtures	124
7	Conclusions and recommendations	127
7.1	Conclusions	127
7.2	Recommendations for further study	130
A	SEM images for secondary formations test	131
B	Load calculation for concrete bus shelter	137

List of Figures

2.1	X-ray fluorescence of fine glass dust [48]	8
2.2	X-ray diffraction of fine glass dust [48]	8
2.3	Density of fine glass dust [48]	8
2.4	Weight loss of fine glass dust [48]	9
2.5	Effect of thermal treatment on fine glass dust [48]	9
2.6	Compressive strength for different amounts of recycled glass cullets [117]	10
2.7	Glass powder in concrete binder [15]	11
2.8	3D printed concrete layers [126]	15
2.9	3D printed concrete in practice	16
2.10	Perpendicular (I), lateral (II) and longitudinal (III) directions [125]	17
2.11	Interlayer air voids at 10 sec, 1 min and 10 min intervals [50]	18
2.12	Possible printing nozzle for 3DCP [50]	19
2.13	3D printing set-up [23]	19
2.14	3D printing set-up TUDelft [23]	20
2.15	Set-up for set-on-demand concrete printing [24]	20
2.16	Twin-pipe pumping system for 3DCP	21
2.17	Twin pump inline mixing with static mixer [114]	22
2.18	Effect of $CaCl_2$ [72]	22
3.1	Test set-up for Particle size distribution	28
3.2	Ultrasonic cleaner for preparation of PSD samples	28
3.3	Netzsch STA 499 F3 Jupiter for TGA of the fine glass dust	29
3.4	Sample carriers on the TGA apparatus	30
3.5	Carbolite HTF1700 furnace for heat-treatment of fine glass dust	31
3.6	Prepared sample for heat-treatment	31
3.7	Temperature-time program for heat-treatment of 600°C for 1 hour	32
3.8	QM-30L Ball Mill Machine for grinding treatment	33
3.9	Fine glass dust with milling balls	33
3.10	Grinding treatment sieve set-up	34
3.11	Micromeritics Gemini VII for BET analysis	35
3.12	Sample preparation for BET analysis	35
3.13	Philips PW 1830 X-ray Diffractometer	36
3.14	Preparation for XRD sample	36
3.15	Hobart N-50 mortar mixer at TUDelft	38
3.16	Set-up on compaction table for mini slump test	38
3.17	Slump test for mortar mixtures	39
3.18	Slump flow test after 25 drops of the compaction table	39
3.19	Controls Vicamatic 2 machine at TUDelft	40
3.20	Preparation of samples for the Vicat test	41
3.21	Finished Vicat test	41
3.22	Macben Servo Plus Evolution at TUDelft for compressive strength test	42
3.23	Curing procedure for mortar prisms	42
3.24	Loading jig with sample for compression test	43
3.25	Particle size distribution of cement, fine glass dust and CEN sand	45
3.26	TGA results under air	45
3.27	Comparison of mass loss at different heat-treatment temperatures and times	46
3.28	D10, D50 and D90 particle sizes of fine glass dust after different grinding treatments	48
3.29	Results XRD analysis of fine glass dust	49
3.30	XRD analysis comparison of unheated and heat-treated fine glass dust	50

3.31 Slump results for mix 1-6	51
3.32 Slump flow results for mix 1-6	52
3.33 Initial setting time results for mix 1-6	53
3.34 Compressive strength results for mix 1-6 at different curing ages	54
3.35 Compressive strength development for Mix 1, Mix 3 and Mix 5 in casting session II	55
3.36 Compressive strength development for different heat-treatment temperatures	56
4.1 Grinding the paste to a powder in isopropanol	68
4.2 Slump results for different replacement percentages of FGD	70
4.3 Slump flow results for different replacement percentages of FGD	70
4.4 Compressive strength development for different replacement percentages of FGD	71
4.5 TGA results for mix FGD-0 and mix FGD-15 after 7, 28 and 56 days of curing	73
4.6 Secondary formations test 0 days for different FGD percentages	74
4.7 Secondary formations results after 1 day for different FGD percentages	75
4.8 Secondary formation results after 7 days for different FGD percentages	76
5.1 Test set-up of the material conveying pump	88
5.2 Material conveying system	88
5.3 Pumpability test material pumping	89
5.4 TAM Air calorimeter with eight channels	92
5.5 Two material conveying pumps with separate pumping hoses	94
5.6 Helical static mixer set-up with printing nozzle (Yu Chen)	95
5.7 Flowability graph for pumpable cementitious mixtures	97
5.8 7 days compressive strength for pumpable cementitious mixtures	97
5.9 Material flow rate at different motor speeds for mix FGD50-SP0.4	99
5.10 Flowability results for cementitious mixture + accelerator slurry for different CaCl_2 dosages	100
5.11 Initial setting time results for cementitious mixture + accelerator slurry for different CaCl_2 dosages	100
5.12 Isothermal calorimetry results for mixtures FGD20 and FGD50 with different CaCl_2 dosages in accelerator slurry	102
5.13 Compressive strength results for cementitious mixture + accelerator slurry for different CaCl_2 dosages	103
5.14 Results of printing session for mix FGD20-SP0.35-Acc8%	104
5.15 Compressive strength results for the printed samples of mix FGD20-SP035-Acc8%	105
5.16 Flowability comparison for mix FGD50 and FGD20	105
5.17 Initial setting time comparison for mix FGD50 and FGD20	108
6.1 Canberra bus shelter made out of concrete	116
6.2 Canberra bus shelter with art displayed on the inside	116
6.3 Transportation of the prefabricated bus shelters [38]	117
6.4 Design drawing for the concrete bus shelters [40]	118
6.5 Diana model for the cylindrical wall of the bus shelter	119
6.6 DIANA analysis results for cylindrical wall of bus shelter	120
6.7 Force flow around a circular opening	120
6.8 Top view of printing path for cylindrical wall for on-site printing	122
6.9 Top view of printing path for cylindrical wall for precast printing	123
A.1 Overview SEM image mix FGD50 (zoom 125x)	131
A.2 Close-up SEM image 1 mix FGD50 (zoom 1000x)	132
A.3 Close-up SEM image 2 mix FGD50 (zoom 1000x)	132
A.4 Close-up SEM image 3 mix FGD50 (zoom 1000x)	133
A.5 Overview SEM image mix FGD20 (zoom 125x)	133
A.6 Close-up SEM image 1 mix FGD20 (zoom 1000x)	134
A.7 Close-up SEM image 2 mix FGD20 (zoom 1000x)	134
A.8 Close-up SEM image 3 mix FGD20 (zoom 1000x)	135
B.1 load calculation for the concrete bus shelter	137

Introduction

1.1. General introduction

Concrete is the most used building material all over the world. The reason why concrete is preferred over other building materials is because of its low cost, high fire resistance, durability and good strength. The raw materials for concrete production can be easily obtained all over the world and concrete is a flexible material before setting, which leads to freedom in shape for designers and architects [13][7]. Concrete mix consists of cementitious materials, water and sand or gravel as aggregates. Alternative additives or admixtures are added to the concrete mix to achieve specific properties or behavior of the concrete.

For the production of cement clinker (a substantial part of concrete) a lot of energy is used and large quantities of greenhouse gases are emitted into the atmosphere. This means that the large production and consumption of concrete causes a significant burden on the living environment and atmosphere. Concrete production accounts for 5-7% of the global CO₂ output [13]. There is no sign of a decrease in the demand for concrete as primary construction material, so it is necessary to improve the sustainability aspect of concrete to decrease the burden on the environment. The introduction of cement replacement by Supplementary Cementitious materials (SCMs) in the binder can reduce the high energy consumption and the environmental damage regarding high CO₂ emissions of concrete production.

Conventionally cast concrete has been facing challenges in the past few years. First of all high injury rates and several accidents have been recorded, due to dangerous formwork and reinforcement operations. Secondly high costs, dependence on labor, low efficiency and large amounts of waste are issues that are associated with cast concrete. The formwork that is used for traditionally cast concrete accounts for 30-50% of the construction time and construction costs [7] [128].

The future of the concrete construction industry can be very different due to the process of 3D concrete printing or additive manufacturing. Over the last few years, extrusion-based 3D Concrete Printing technology has accelerated in growth in the construction industry, because of its efficient method of constructing concrete elements. 3D concrete printing (3DCP) is a recently developed construction technique, which produces construction elements by using material deposition in the form of layered extrusion. The concrete is extruded from the nozzle of a concrete printer and is deposited in different layers. This printing is done according to a digitally printing route, which is designed beforehand and the printed layers are deposited without the need for any conventional formwork. This 3DCP technology has several advantages, like high architectural freedom and efficiency, but also environmental and economical benefits [85]. However due to the absence of traditional formwork, additional requirements are needed for the concrete properties for this 3DCP technology.

The 3D printing process consists of different phases and requires contradictory rheological properties of the concrete mixture. During the pumping and extruding phase the concrete mixtures should have high flowability to prevent high pumping pressures and possible damage to the printing equipment. In contrast, after extrusion of the concrete mixture from the printing head the printed layer of material should have high stability and strength in order to develop sufficient structural build-up and to withstand the loads of the filaments that will be printed on top of that layer without collapsing. After printing the filaments a very high stiffness and strength development is required to achieve stability and

withstand vertical loads.

A concrete mixture for 3D printed concrete contains a high amount of Portland cement clinker compared to cast in-situ concrete. To enhance the sustainability of the concrete mixtures, supplementary cementitious materials (SCMs) are added to the mixture. SCMs like fly ash, granulated blast furnace slag, silica fume, limestone powder or calcinated clay have cementitious properties in contact with water and therefore can be used to partially replace the high amount of Portland cement in the concrete mixture. SCMs are often byproducts from another industry or are naturally available, so implementation of SCMs in concrete can help to develop a more eco-friendly mixture and reduce the CO₂ emission of concrete production significantly [79]. The eco-friendly mixture with SCM should still possess rapid hardening with high stiffness development in order to be eligible for 3D concrete printing.

However some of the conventional SCMs have a limited supply or a high depletion rate, so this led to the investigation of other potential materials which can be utilized as cement replacement. One of these potential materials is glass powder, a byproduct or waste material of the glass recycling industry. Glass powder contains high amounts of silica and exhibits possible pozzolanic reactivity, which means it can potentially be used in the binder of concrete to partially replace Portland cement clinker.

A potential byproduct of the glass recycling industry is fine glass dust. This fine glass dust is captured in filters in the recycling plant and is nowadays mainly disposed in landfill, due to a lack of industrial purposes and limited recycling potential. The goal of the glass recycling industry and this thesis is to find a useful utilization in the construction industry for this fine glass dust. Previous research [48] has shown that fine glass dust can be used in conventionally cast in-situ concrete mixtures to replace Portland cement, but that the untreated glass dust has too low reactivity without pre-treatment measurements to effectively use in concrete.

This research aims to investigate the utilization and effect of fine glass dust in concrete mixtures for 3D printed concrete. The reason why 3D Concrete Printing is investigated in this study will be assessed in section 1.2. In the first part of the research the goal is to find the most optimal pre-treatment for the fine glass dust, so that it provides optimal results if it is used to replace Portland cement in a concrete mixture. The second part of this research focuses on the suitability and optimal mix design for using fine glass dust for 3DCP and the effect of fine glass dust replacement on the 3D printability and buildability of printed concrete mortar. In this research the impact of fine glass dust on cementitious material properties will be investigated for the fresh properties, cement hydration and hardened properties.

1.2. The problem and research relevance

The increasing demand for concrete structures worldwide induces a high amount of cement clinker that needs to be produced. This large-scale clinker production causes large energy consumption and huge quantities of CO₂ that are emitted into the atmosphere, which negatively impacts the environment. Using fine glass dust in the 3DCP mixtures would help to reduce the amount of cement consumption and therefore reduce the high CO₂ emissions for building concrete structures with 3D Concrete Printing. The total amount of fine glass powder or fine glass dust production in the glass recycling industry in Europe is around 200.000 tons every year, estimated based on the yearly production capacity of Maltha BV (D. Timmers, personal communication, August 31, 2022). This fine glass dust consists of very small glassy particles and is collected in filters in the recycling plant. Due to small particle sizes and high amounts of impurities the fine glass dust is difficult to melt and therefore almost impossible to use for the formation of recycled glass cullet. So achieving a closed-loop cycle with this material is difficult and the formation of fine glass dust as a byproduct with limited applications is one of the problems of recycling that the glass industry needs to deal with. Circularity of the glass recycling could be increased when a new utilization for this fine glass dust is found, which would otherwise be mainly disposed as landfill.

The fine glass dust production is very small compared to the yearly consumption of Portland cement for the construction industry at 250 million tons per year [108]. Next to this comes the fact that the material properties of the recycled fine glass dust fluctuate a lot, varying in mineral composition and organic content between different batches of glass in the recycling plant. For a material to be used as a new alternative SCM to replace Portland cement for cast in-situ concrete the material composition should be constant and material production should be in the same order as Portland cement production,

however for the fine glass dust this is not the case. Therefore the objective of this thesis is not to find a new alternative Supplementary Cementitious Material for Portland cement in the binder of cast in-situ concrete mixtures, but the main objective is to find a new utilization opportunity for the recycled fine glass dust in 3D Printed Concrete mixtures. The main reason for the utilization of fine glass dust for 3D printed concrete is because of the low number of regulations for 3DCP. For cast in-situ concrete there are very strict regulations for cement replacement materials. The fine glass dust has varying material compositions between batches and with the fluctuating properties of fine glass dust it would be difficult to measure up to these strict regulations for cast in-situ concrete. Therefore the utilization of fine glass dust as cement replacement in cementitious mixtures for 3DCP would be a potential solution.

Fine glass dust contains small particles with a high amount of amorphous silica, which can potentially contribute to strength development by pozzolanic activity when it is used in the binder of cementitious mixture. Therefore the use of fine glass dust as a cement replacement in 3DCP mixtures could be a promising utilization for this byproduct of the glass recycling industry, which is beneficial for the recycling of glass but also advantageous for the concrete industry. This would reduce the Portland cement consumption for cementitious mixtures, which has environmental benefits as this reduces the CO₂ that is emitted due to cement clinker production. Next to this comes the fact that the proposal of this new application would contribute to the sustainability and circularity of the glass recycling industry as utilization of recycled fine glass dust means that fewer byproducts have to be incinerated or disposed as landfill. However up until this date, investigations on the applicability of fine glass dust or waste glass powder in 3DCP mixtures are still not adequate enough. To investigate the utilization and feasibility of fine glass dust for 3DCP, the effects of cement replacement by fine glass dust on fresh properties, cement hydration and hardened properties need to be studied.

1.3. Research objectives

The main objective of this thesis is to find a new utilization opportunity for recycled fine glass dust by replacing Portland cement in the binder of cementitious mixtures for 3DCP. In order to reach the goal of this study, different research objectives are formulated.

-Investigate the effect of different pre-treatment methods for the fine glass dust (heat-treatment and grinding treatment) on the fresh state and hardened properties of mortar when fine glass dust is used to replace Portland cement in the binder.

-Investigate the effect of variable fine glass dust percentages on the fresh state and hardened properties of concrete mortar.

-Study the suitability of fine glass dust for 3D concrete printing when set-on-demand printing technique is used and propose an optimized 3D concrete printing mixture when fine glass dust is used to replace Portland cement in the binder.

1.4. Research questions

The main research question of this MSc thesis was: "What is the utilization of recycled fine glass dust as a Portland cement replacement for 3D concrete printing with set-on-demand printing technique?". In order to give a substantiated answer to this research question, the main research question was divided into the following sub-questions:

1. What is the influence of heat-treatment on the fresh state and hardened properties of fine glass dust mortar?
2. What is the influence of grinding treatment on the fresh state and hardened properties of fine glass dust mortar?
3. What is the influence of variable replacement percentages on the fresh state and hardened properties of fine glass dust mortar?
4. What is the optimal superplasticizer amount for achieving a pumpable cementitious mixtures with fine glass dust?
5. What is the optimal accelerator dosage for the accelerator slurry to achieve fast stiffness development when a cementitious mixture with fine glass dust and accelerator slurry are combined?

6. What is the impact of fine glass dust on the hydration, buildability and compressive strength development of 3D printed concrete mixture with set-on-demand printing?
7. What is the practical applicability and feasibility of a 3D printable mixture with fine glass dust?

1.5. Research scope

This research mainly investigated the optimal pre-treatment method for fine glass dust and the feasibility of using fine glass dust as a replacement for Portland cement for 3D Concrete Printing. The 3D concrete printing instrumentation with set-on-demand printing technique was not within the scope of this research. It would be very complicated and large amounts of work to include all concrete properties for the investigation of fine glass dust as Portland cement replacement for 3DCP. Therefore this research only studied some of the fresh-state properties, cement hydration properties and hardened properties related to concrete mixtures. Workability and flowability of the mixtures were evaluated, because these properties are important for 3D printable mixtures during the pumping phase, but also directly after extrusion from the printing nozzle. Initial setting time was assessed, because this property could investigate the stiffness development of the mixtures and for 3DCP fast stiffness development is important to ensure stability of the printed filaments. Hydration heat was evaluated to complement the initial setting time investigation. Hydration heat is important for 3D printable mixtures to investigate the hydration reaction rate at an early age after mixing. Buildability of the printable mixtures was studied to determine the shape stability and layer stacking ability of the printed filaments to withstand the loads from the filaments that are placed on top without collapsing. Finally compressive strength development was assessed for different curing ages, to investigate the effect of pre-treatment on the fine glass dust, to indicate the possibility of pozzolanic activity of the fine glass dust and to determine the strength development of the 3D printed samples. The concrete properties that fall within the scope of this research are summarized in Table 1.1.

A limitation for all chapters of this study was that for the mix designs of the pre-treatment investigation of the fine glass dust only mortar mixtures were investigated and no mixtures with large aggregate fractions were studied. The knowledge gained by this study could be broadened by investigating the interaction between the fine glass dust and the large aggregate particles and whether this differs from the fine aggregates in the mortar mixtures.

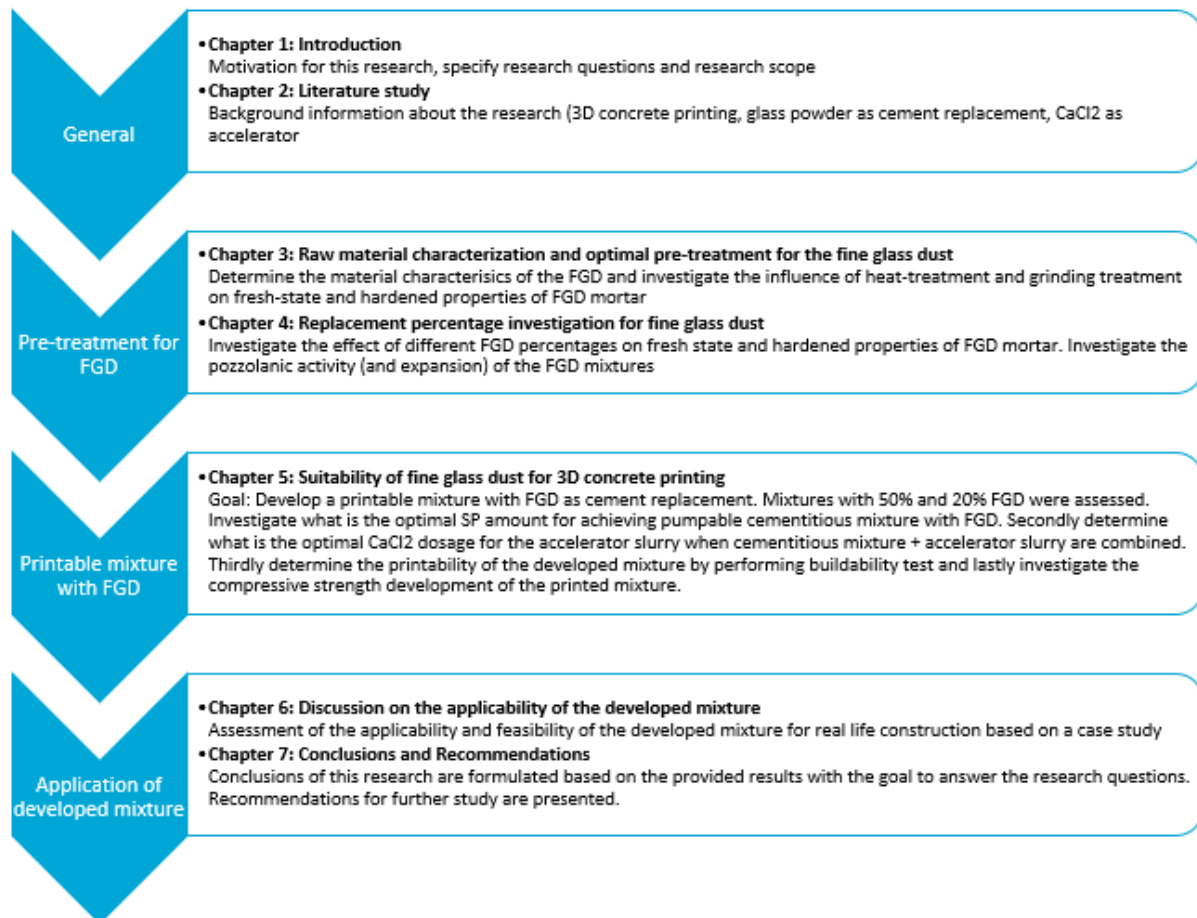
Another general limitation of the research profile was that the binder of the studied mixtures only consisted of a combination of Portland cement and fine glass dust. No other supplementary cementitious material was used to replace a part of the Portland cement to form a ternary binder. The study could be improved by investigating the interaction between the fine glass dust and other SCM's and the properties of the mortar mixtures could potentially be enhanced if a ternary binder is used, when the constituents are mixed in the optimal proportions.

Also the investigation of possible alkali-silica reaction (ASR) was not considered during this study. There was awareness for the fact that the fine glass dust consisted of silica particles that could possibly react with the alkali particles of the cement to cause unwanted expansion after hardening of the mortar mixtures. However this was not included within the scope of this research.

Fresh properties	Cement hydration	Hardened properties
Workability (Slump)	Hydration heat	Compressive strength
Flowability (Slump flow)		Pozzolanic activity
Initial setting time		
Buildability		

Table 1.1: Investigated properties that are included in this research

1.6. Msc thesis outline



2

Literature Research

This chapter aims to provide an overview of the implementation and utilization of waste glass powder in concrete mixtures and a systematic review of the available printing strategies for concrete. A high ordinary Portland cement (OPC) content is not beneficial for the sustainability of the concrete. Nowadays it becomes more important to partially replace the ordinary Portland cement in the mixture with supplementary cementitious materials (SCM). A new and challenging possibility is to try and use fine glass dust, a by-product from the glass recycling industry in the cementitious binder as a cement replacement. The fine glass dust that was used for this study was produced by Maltha Glass BV, but is produced by the entire glass recycling industry and a short overview of the previous research on the use of fine glass dust in concrete mixtures will be given in section 2.1. Furthermore, the use of waste glass powder or glass particles in conventional concrete mixtures is reviewed in section 2.2.

A potential application for using recycled fine glass dust in concrete mixtures will be 3D Concrete Printing. It will be explained what 3D concrete printing (3DCP) is and what are the different available techniques for concrete printing in section 2.3. Furthermore a review on the properties of a printable mixture will be given. For a mixture to be suitable for 3D concrete printing it is important to look at the printability and the fresh-state behavior. For set-on-demand concrete printing, a new printing technique that is recently developed, two different mixtures are mixed just before printing and this printing technique will be explained in more detail in section 2.3.2. Finally section 2.4 describes some terminology regarding 3D Concrete Printing and the fresh-state properties of concrete.

2.1. Previous research on the fine glass dust

In this section an overview is given of the previous research that was performed on the recycled fine glass dust that was used in this thesis. Fine glass dust has a relatively small particle size and a high amount of silica, so it can possibly be a good and sustainable replacement of OPC in cementitious materials. Previous studies have investigated the material composition of fine glass dust and investigated the influence of using this powder in the binder as a cement replacement. These investigations were performed for traditionally cast concrete.

SGS Intron [48] performed a study in which the materials were analyzed in terms of their mineralogical, chemical and physical characteristics and also the performance as a Portland cement replacement in concrete mixtures. Elemental compositions of the fine glass powder, cyclone powder and larger glass waste particles were determined with XRF analysis and the results can be seen in Figure 2.1.

The total weights that were determined by the XRF analysis were less than 100%, which means that there are organic materials present in the products. Organic material consists of carbon compounds that cannot be detected by XRF, because it is lighter than Fluorine. These organic materials can be seen as impurities and are not beneficial for cement replacement by the glass dust in the binder of concrete mixtures. XRD analysis was performed for the fine glass powder to determine the mineralogical composition and the results showed that the largest percentage of elements was present in amorphous phase (see Figure 2.2) [48]. The largest amount of silica-oxide was present in the glassy state.

Oxide	Glass dust	Cyclone dust	Large particles		
SiO ₂	55.90	48.10	25.80	M.-%	
CaO	10.30	9.98	8.07	M.-%	
Na ₂ O	9.46	6.34	4.46	M.-%	
Al ₂ O ₃	1.76	1.52	0.95	M.-%	
MgO	1.20	0.95	0.71	M.-%	
K ₂ O	0.67	0.66	0.59	M.-%	
Fe ₂ O ₃	1.17	0.50	0.63	M.-%	
SO ₃	0.30	0.32	0.49	M.-%	
Cl	0.35	0.30	0.67	M.-%	
P ₂ O ₅	0.16	0.16	0.69	M.-%	
TiO ₂	0.10	0.12	0.21	M.-%	
BaO	0.06	0.07	0.07	M.-%	
Cr ₂ O ₃	0.06	0.06	0.06	M.-%	
PbO	0.04	0.04	0.02	M.-%	
MnO	0.03	0.03	0.02	M.-%	
ZnO	0.06	0.03	0.03	M.-%	
SrO	0.02	0.02	0.02	M.-%	
ZrO ₂	0.02	0.02	0.02	M.-%	
CuO	0.03	0.01	0.01	M.-%	
NiO	0.00	0.00	0.01	M.-%	
As ₂ O ₃	0.00	0.00	0.02	M.-%	
Total	81.69	69.23	43.55		

Figure 2.1: X-ray fluorescence of fine glass dust [48]

Mineraal	Formula	Glass dust	Cyclone dust		
Quartz	SiO ₂	0.6	1.2	M.-%	
Calcite	CaCO ₃	0.9	1.1	M.-%	
Amorphous		98.5	97.7	M.-%	

Figure 2.2: X-ray diffraction of fine glass dust [48]

For the fine glass powder and the cyclone powder the particle density was determined and the results are shown in Figure 2.3.

Test	Glass dust	Cyclone dust	Unit
Particle density	2330	2440	kg/m ³

Figure 2.3: Density of fine glass dust [48]

Due to the fineness and the high amount of amorphous silica in the fine glass dust, it was tested if the material was suitable as a reactive filler for partial Portland cement replacement in concrete binder. K-value tests were performed by SGS INTRON in order to determine the suitability of the fine glass powder. Fine glass powder replacement of 10, 20 and 30% binder mass were investigated, but after 24 hours of curing none of the samples were ready for demoulding. Due to a lack of reactivity, the k-value tests failed for all replacement percentages [48]. Pre-treatment or material processing of the fine glass powder was needed to increase the reactivity and shorten the initial setting time of the mixtures.

Organic compounds in the fine glass powder were responsible for the retarding effect if it was used as a cement replacement. It was investigated that soluble phosphates and sugars (both known to be strong retarders for concrete) were present in small quantities in the fine glass dust to cause the retarding effect on the hydration reaction. Other found components that had a retarding effect on the hydration reaction of the glass powder were: alginic acids, fatty acids and mineral oils. Thermogravimetric analysis (TGA) was performed to determine the temperature at which the organic materials in the fine glass powder combusted. Also it can be investigated which mass fraction of organic materials combust at specific temperatures. With TGA the influence of heat-treatment on the fine glass dust could be found and the results are shown in Figure 2.4.

The fine glass powder was heat-treated by SGS INTRON at 400 and 600 °C in an oven for 24 hours [48]. After 24 hours the weight change was negligible and it was assumed that all organic materials were combusted (which combust in that temperature range). The heat-treated fine glass powder was

	Weight loss [M.-%]		Loss on Ignition [M.-%]
	50 - 400°C	400 - 780°C	
Glass dust	6.5	4.0	10.5
Cyclone dust	2.6	1.7	4.3

Figure 2.4: Weight loss of fine glass dust [48]

used for 20 and 30% mass binder replacement and the setting time was measured (see Figure 2.5).

	Replacement rate	Thermal treatment Temp (°C)	Setting time (min)		W/C (%)
			Initial	Final	
Reference	0	None	205	250	23.6
20-GD	20	None	1220	Fail	23.6
400/20-GD	20	400	270	335	24.6
400/30-GD	30	400	340	400	26.8
600/20-GD	20	600	255	285	28.0
600/30-GD	30	600	250	280	30.0

Figure 2.5: Effect of thermal treatment on fine glass dust [48]

From Figure 2.5 it can be seen that thermal treatments proved to be effective in reducing the initial setting time of the mixtures with fine glass powder. Suggestions for further research were that the fine glass powder may require a higher heat-treatment temperature (in the region of 780 °C) to remove more organic materials.

Research from University of Leuven (Belgium) [66] showed different possibilities for removing the re-tarding materials from the fine glass powder. The goal was to increase the reactivity of the fine glass powder and to decrease the initial setting time. The focus of this research was on the extraction of mineral oils and fatty acids from the fine glass powder. Supercritical CO₂ extraction was used to remove the impurities, specifically the fatty acids from the fine glass powder. Results showed a significant rise in measured compressive strength of concrete which had a replacement percentage of 15 M% treated glass powder. The compressive strength of the treated glass powder was 56-64% higher than for the untreated glass powder. Extracting the fatty acids from the glass powder with critical CO₂ extraction had a positive influence on the compressive strength of the concrete.

Utilization of fine glass dust in cementitious mixtures

The objective of this thesis was to find a practical implementation or utilization for this recycled glass dust, because a large amount of this dust is collected each year and currently this has to be disposed as landfill. The objective of this thesis is not to find a new alternative Supplementary Cementitious Material (SCM) to replace Portland cement, because the yearly production of fine glass dust is not in the same order as the yearly consumption of Portland cement, as described in Section 1.2.

Because the fine glass dust consists of small glassy particles (with high amounts of silica) the goal of this was to find a utilization for this powder as a Portland cement replacement for 3D printed concrete. For cast in-situ concrete there are strict regulations that have to be met for SCM's and this would be difficult to achieve with the fluctuating properties of the recycled fine glass dust. However for 3DCP there are fewer regulations and recycled fine glass dust could potentially be used as a cement replacement in 3DCP mixtures.

The clinkering phase of cement production causes large amounts of greenhouse gas emissions, which have a severe impact on the environment in the case of global warming. This use of recycled fine glass dust as cement replacement in 3DCP mixtures reduces the consumption of Portland cement, which reduces the CO₂ emission by cement production, prevents the depletion of natural resources and is a practical utilization of the recycled fine glass dust for the glass recycling industry that would otherwise be incinerated or disposed in landfills.

2.2. Use of glass powder or glass particles in concrete

In section 2.1 it is shown that the recycled fine glass dust has the potential to be used as cement replacement in concrete mixtures and that the performance can be increased by pre-treatment. This

section gives an overview of previous research and experimental investigations on recycled glass particles or glass powder in concrete. Subsection 2.2.1 describes recycled glass cullets that are used as aggregate replacement and subsection 2.2.2 describes waste glass powder that is used as cement replacement in the binder for both conventionally cast concrete and 3D printed concrete. Subsection 2.2.3 describes the potential for dangerous ASR when glass cullets or waste glass powder particles are used in concrete mixtures.

2.2.1. Recycled glass cullets as aggregate replacement

Ting et al. [117] studied the effect of recycled glass cullets as fine aggregates for 3D printing concrete mixture. The reference mixture used natural river sand as fine particles and recycled glass cullets were used to replace 25, 50, 75 and 100% by mass.

The results of this investigation showed that a higher glass content for the aggregates resulted in a slight decrease in static yield stress. Static yield stress is often related to the buildability of the printed material and the ability to withstand the weight of subsequent layers.

An increase in recycled glass cullets content increased the dynamic yield stress and viscosity. This was because of the angular shape and the sharp edges of the glass particles. The increased dynamic yield stress led to a lower material pumpability, because more effort was required to pump the material through the delivery system for 3DCP [117][119]. The printed concrete specimens had lower compressive strength for higher recycled glass content, as illustrated in Figure 2.6.

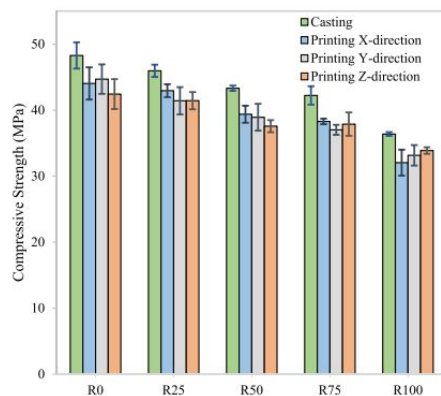


Figure 2.6: Compressive strength for different amounts of recycled glass cullets [117]

This was caused by the weaker adhesion of the glass particles to the cement matrix during hydration. The hydrophobic nature of the glass particles caused more free water in the binder matrix, which resulted in segregation of the glass particles. Not only the compressive strength, but also the interlayer bond strength was found to be lower for higher recycled glass content. This can also be explained by the decrease in adhesion between the printed filaments and the hydrophobic behavior of the glass cullets.

Khan et al. [60] found that crushed glass particles could be used as fine aggregate replacement up to 50% as long as the particle size of the crushed glass was lower than 1 mm. This fine aggregate replacement gave comparable results in terms of compressive and flexural strength as compared to standard reference mortar.

2.2.2. Waste glass powder as cement replacement

As described in chapter 1 and section 2.1, the use of glass powder in concrete as a cement replacement can result in important energy, environmental, cost and performance benefits [82].

When glass powder was used in the binder of cementitious material as cement replacement, the consistency of the fresh state of the mixture was improved [15]. In the hardened state the use of glass powder in the binder increased the porosity and led to a decrease in compressive strength. It was found by Boukhelf et al. that by 30% glass powder cement substitution, the compressive strength at 28 days was 36–41 MPa and at 91 days was 40–45 MPa (see Figure 2.7). This was a reduction in comparison with the reference mixture, but satisfactory performance for structural application.

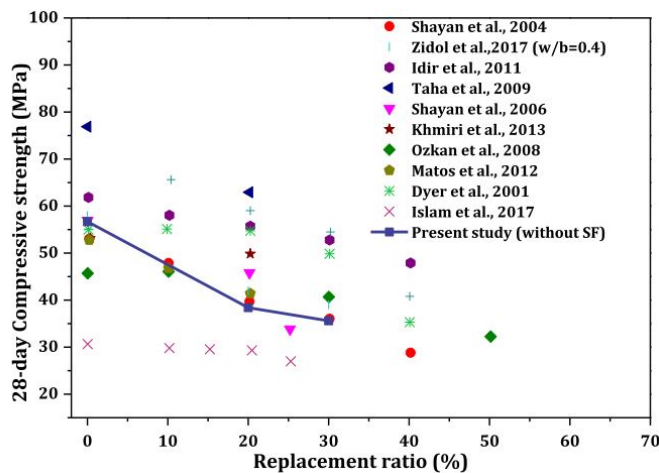


Figure 2.7: Glass powder in concrete binder [15]

If glass powder was used in a sustainable concrete that was produced from a quaternary blend of Portland cement, glass powder, metakaolin and silica fume (volume ratio was 60:20:05:15), the compressive strength of the hybrid concrete was 13,42% higher compared to the control mix after 28 days [21].

Kamali et al. [53] found that glass powders showed to enhance the hydration of cement based on chemical shrinkage measurements. Glass powders in concrete were also found to possess pozzolanic behavior and to improve the cement paste hydration at higher ages. The pozzolanic behavior of glass powder in the cement paste improved the microstructure of the concrete, which enhanced the concrete performance [53].

During the pozzolanic reaction the amorphous silica is detached from the glass powder by the hydroxyl ions in the pore solution during hydration and combines with calcium hydroxide (C-H) from the cement to form calcium silicate hydrate (C-S-H gel) [112]. The additional C-S-H gel that is formed by the pozzolanic reaction can improve the microstructure and mechanical properties of the concrete in the long term [77].

According to Tamanna et al. [113] a pozzolanic material needs three important material characteristics: A large surface area, a high amount of silica and the material should be amorphous. Glass contains sufficient silica and is also amorphous in nature. The surface area of the glass can be increased by grinding the material to a fine glass powder, which activates the pozzolanic behaviour.

The mechanical properties of concrete containing glass powder were strongly influenced by the curing duration, size of the glass powder particles and the content of glass powder [60][30]. Concrete with glass powder had relatively lower strength during the early age, but higher strength in later age compared to standard reference mixture. The slow pozzolanic reaction could enhance the mechanical properties of glass powder concrete in the long term [73][30]. The slump value and workability of glass powder concrete directly after mixing were found to be increased according to Rahman et al. [93] and Vasudevan et al. [121]. This increase in workability for glass powder concrete could be attributed to low water absorption of glass powder and smoother surfaces, which increased the fluidity of the mixtures [46]. On the other hand, research by Nyantakyi et al. [86] showed decreasing slump values with increasing portions of glass powder.

On a durability aspect, it was also shown that when glass powder was incorporated into the binder there was an increase in resistance to moisture absorption [82], acid attack, sulphate attack and chloride penetration [8][73][30]. The pozzolanic potential of glass powder was an advantage to limit concrete degradation and improve durability in the long term, according to Belebchouche et al. [8].

Ahmadah et al. [4] and Kamali et al. [53] showed that improved properties of the concrete occurred when glass powders with extremely fine particle sizes were used. Very fine glass powders were found to possess higher pozzolanic behavior and to improve the hydration of cement paste at early and

later curing ages. Microstructure evaluation indicated pore refinement in the microstructure of cement pastes modified with fine glass powders [52]. The finer the glass powder, the earlier pozzolanic reactions will be activated which resulted in more pozzolanic reactivity [45]. The activation of the pozzolanic reactivity could also be accelerated by increasing the curing temperature [103].

When ground waste glass was blended with Portland cement and lime, an increase in the strength of mortar, more resistance to chloride penetration and higher resistance to sulfate attack could be found in comparison to natural pozzolana and fly ash [112][20]. Due to the high pozzolanic properties, the ground glass could contribute to the hydration of the cement paste and could affect the refinement of the pore structure. When blended cement with glass powder was used, the glass chemical composition played an important role in developing pozzolanic activity [10].

Mirzahosseini et al. [76] studied the reaction kinetics of finely crushed glass powder at different temperatures. Mortar compressive strength and water absorption of the samples at different temperatures and ages were used to give a relation between reaction degree and performance. It was shown that glass behaved pozzolanically if it was fine enough, with a surface area that was larger than $300 \text{ m}^2/\text{kg}$. The pozzolanic reaction occurred between the amorphous silica in the glass powder, calcium hydroxide (C-H) from the cement reaction and water to form additional calcium silicate hydrate (C-S-H) in the cement paste. It was found that finely ground glass powder ($< 25 \text{ }\mu\text{m}$) showed significant pozzolanic behavior at temperatures of 50°C . This was evidenced by a reduction in C-H content in the samples and an increase in the heat of hydration of the samples with temperatures of 50°C [76].

Decreasing the glass powder size from $100 \text{ }\mu\text{m}$ to approximately $10 \text{ }\mu\text{m}$ led to an increase in pozzolanic activity by 49% [43] [2]. It was found that the size of the glass powder played an important role in the pozzolanic behavior of this material. If the glass powder particles are finer, more pozzolanic reactivity and better properties of concrete can be achieved [2] [58].

At a high cement replacement level of 30% with glass powder Carsana et al. [20] showed that the long-term pozzolanic activity of the blended mortar was superior to natural pozzolans and comparable with fly ash. Du et al. [33][32] found that concrete with 30% glass powder as SCM showed lower compressive strength before 28 days, but increased strength at 90 days due to the pozzolanic activity of the glass powder [73]. Glass powders with decreasing particles size and higher curing temperature exhibited more pozzolanic activity. Concrete with cement replacement of 15 and 30% fine glass powder formed compact and homogeneous microstructures, but beyond a replacement level of 30%, the available calcium hydroxide (C-H) became insufficient for the pozzolanic reaction of the glass powder and a reduction in material properties can be observed [32][86]. These observations were also backed by Khan et al. [57] who found that the optimal replacement ratio for cement replacement with fine glass powder was 25%. At higher replacement percentages a reduction in strength and workability was observed [57]. Khan et al. [60] found significant improvement in mechanical properties compared to control samples for up to 25% of cement replacement after 90 days when the average particle sizes of the glass powder were less than $45 \text{ }\mu\text{m}$.

Mejdi et al [75] and Islam et al. [49] found that mortars with glass powder up to 20% replacement showed comparable compressive strength results as standard mortar mixture, after 90 days. Refinement of the microstructure due to the pozzolanic activity of the fine glass powder resulted in the formation of secondary C-S-H gel and improved mechanical properties for the concrete mortar [26].

Aliabado et al. [5] stated that the use of glass powder as cement replacement up to 15% enhanced the properties of the concrete with blended cement after 28 days. A higher replacement percentage led to a decrease in compressive strength compared to the reference mixture. Belebchouche et al. [8] considered 15% replacement of cement by glass powder as the optimal dosage when the compressive strength at 7 and 28 days was taken into account.

According to Gupta et al. [41], the use of glass powder as cement replacement up to 30% enhanced the compressive strength after 90 days, compared to the control mix. It was also found that water absorption and permeability for glass powder concrete were lower than the control mixture [46]. This could be attributed to the filler effect of the fine glass powder and the formation of a more dense microstructure with reduced porosity, caused by the pozzolanic reaction [8] [41].

Khmiri et al. [61] investigated the compressive strength of mortars with waste glass powder as cement replacement in the size ranges 100–80 μm ; 80–40 μm ; <40 μm and < 20 μm fineness. The results showed that pozzolanic activity was low for coarse particle sizes [3] and that the most finely grounded waste glass powder (< 20 μm) showed optimal compressive strength properties and could reach 82%, 95% and 102% of standard mortar strength at 7, 28 and 90 days respectively.

Li et al. [68] showed that 20% waste glass powder with particle sizes 20–44 μm exhibited high fluidity, good cohesion and water retention performance. It was found that the compressive strength was lower than the reference mixture at 7 days, but it was 3.5% and 9.6% higher at 28 and 90 days respectively. These results were backed by TGA-DSC results, which showed that the increase in calcium silicate hydrate gel (C-S-H gel) content increased the most in the period between 28 and 90 days. This indicated high pozzolanic activity and strength gain at later ages [82]. It was also found that a further increase in fineness of the waste glass powder to 15–20 μm did not lead to better results [68].

Lu et al. [69] investigated the fresh properties of cement pastes and mortars with incorporated glass powder. The use of glass powder as cement replacement resulted in a reduction of the heat of hydration at the early stage and an extension of the setting time. This could be attributed to the low reactivity of the glass powder at early ages [69]. These less reactive fine glass particles prevented the contact between unhydrated cement particles and water during the early hydration and therefore reduced the hydration speed. It was also found that the flowability of the glass powder cement mixture could be reduced by increasing the fineness of the glass powder [69].

Ting et al. [119] investigated the rheological and mechanical properties of 3D printed concrete with recycled glass in the binder. It was found that the concrete mixture with recycled glass aggregates demonstrated better flow properties compared to the reference mixture with fine river sand as aggregates. However the buildability and the mechanical performance were lower for the recycled glass particles compared to the reference material. If recycled glass was used in the binder for 3DCP the flow properties were better, because of the lower early hydration reaction rate and thus a slower stiffness development. For 3DCP this can be beneficial, because better flow properties lead to a longer open time, better pumpability and better extrudability of the mixture (see Section 2.3).

In summary, using a specific range of waste glass powder particle size and glass powder content to replace cement in the binder can lead to improvements in the mechanical properties of conventional cast concrete. Owing to the diversification of the different waste glass powder particle sizes, sources and different production lines, the results that were found by previous investigations were diverse and it is difficult to give clear conclusions on the optimal cement replacement percentage. The main findings for glass powder incorporation for conventional cast concrete by different researchers were:

- Decrease of compressive strength at early curing ages
- Increase of compressive strength at long-term curing ages
- Increased pozzolanic activity for fine particle sizes
- Reduction of porosity and water absorption
- Increase of microstructural packing due to C-S-H gel formed by pozzolanic reaction
- Increased durability and resistance against chloride penetration, sulphate attack and acid attack.
- For 3DCP the higher flowability of glass powder concrete can lead to beneficial results for the printing process.

2.2.3. Potential for dangerous ASR when using glass particles in concrete mixtures

Glass powder or glass particles that were used in the concrete mixture contained high amounts of amorphous silica [111]. This increased the risk of Alkali-silica reaction (ASR). ASR is a chemical reaction that occurs between alkalis in cement and reactive amorphous silica in the presence of moisture [36]. This reaction caused unwanted expansion which could lead to cracks and deterioration in hardened concrete over time [36].

The high amount of amorphous silica in glass powder is dissolved under alkali attack and ASR gel is formed [31]. This ASR gel can take up water and therefore expand, which leads to tensile stresses. If these tensile stresses exceed the tensile strength of the concrete, then cracks will occur [36]. These initial cracks will allow opening of the internal structure, accelerating ASR and further widening the cracks. With this mechanism ASR can degrade the concrete quality [31].

If glass powder or glass particles are used in concrete as cement replacement or fine aggregates

then it is important to mitigate the ASR expansion. A possible solution for the glass products is to perform a pre-treatment with a mixture of $\text{Ca}(\text{OH})_2$ and NaOH at $80\text{ }^\circ\text{C}$ for 7 days [110]. This can reduce the ASR expansion by approximately 50% in comparison with untreated glass particles or glass powder. According to Sun et al. [110], glass aggregates were pre-treated with three different solutions: $\text{Ca}(\text{OH})_2$, NaOH and a mixture of $\text{Ca}(\text{OH})_2$ and NaOH . The time-dependent effect was investigated by treatment times of 1, 3 and 7 days. The results showed that ASR was mitigated in all pre-treatments but the best results were shown with a mixture of $\text{Ca}(\text{OH})_2$ and NaOH for 7 days.

It was also found that the size of the fine glass particles has an influence on mitigating ASR. Glass powder with finer particles had an increased ability to mitigate ASR when the glass powder or glass cullets were used as a Portland cement replacement or as an aggregate replacement material [112][2][65].

The fine glass powder particles act as sacrificial particles that react with the alkaline pore solution in the matrix and consume the available alkalis during the pozzolanic reaction [3]. The pozzolanic reaction causes the amorphous silica in the glass powder to react with C-H in the binder to form additional C-S-H gel [73]. This reaction occurs earlier than ASR and will reduce the available alkalis for the aggregates to react with, therefore reducing the ASR potential in the mixture [49][111]. Glass powder also controls ASR by increasing aluminium concentration in the pore solution and therefore reduce the dissolution of amorphous silica from glass particles or reactive aggregates [132]. This was found to be the foremost mechanism of the fine glass powders to mitigate ASR with aggregate particles stated by Matos et al. [73] and Afshinnia et al. [2].

Du et al. [32] found that fine glass powder could be used for suppressing ASR in concrete with glass cullets as aggregates. The mitigation of ASR occurs by reducing the alkalinity in the pore solution and decreasing the permeability and porosity of the cement paste [19][30].

It was found that no deleterious ASR would occur once the glass particles are sufficiently fine (below $75\text{ }\mu\text{m}$) [33][32]. Replacement of Portland cement with finely ground glass powder reduces the expansion due to ASR in the concrete mixture because of enhanced pozzolanic activity, densified microstructure and reduced porosity [30][103]. A higher fineness of glass powder particles in concrete or mortar leads to lower potential ASR activity [30][36].

2.3. 3D Concrete Printing

In this section the 3D concrete printing (3DCP) process is introduced and described. The differences between 3DCP and conventionally cast concrete are reviewed and the different possible printing techniques for 3DCP are reviewed in section 2.3.1. Set-on-demand concrete printing is a recently developed technique that will be elaborated in section 2.3.2. For set-on-demand printing the role of accelerating mixtures is of high importance and the possibilities for accelerators in set-on-demand printing are given in section 2.3.3.

2.3.1. Differences of 3DCP with conventionally cast concrete

3DCP can be considered as a sustainable replacement of conventionally cast concrete in which layers of cementitious material are printed on top of each other from the printing nozzle. The use of 3DCP has many benefits with the main goal to reduce concrete construction, economical and environmental impact. Elimination of formwork in 3DCP compared with conventionally cast concrete reduces waste generation, costs, material use, labor, construction time and provides new architectural possibilities. This leads to environmental and financial benefits for this new manufacturing technique for concrete. 3DCP also allows for optimization in the design methods for structures, so that 3DCP can become a more sustainable and practical fabrication method for concrete structures. [23]

Construction process differences

The design and building process of 3DCP structures has many differences in comparison with conventionally cast concrete. First of all the formwork, which is almost always used for the construction of traditionally cast concrete, can be removed from the construction process for 3DCP structures [89][7]. Normally formwork is created from timber, steel or other materials and is used to withstand the weight of the cast concrete until the concrete has developed enough load-carrying capacity for its own weight. Then the formwork can be removed. If the used formwork is suitable for recycling or reusing depends

on the form of the cast concrete element and the repetition factor of the cast element in a construction. If the formwork is very specific or customized, the chance is very small that the formwork can be reused for other construction activities. For 3DCP no formwork is required, because layers of high stiffness cementitious material are played on top of each other (see Figure 2.8).



Figure 2.8: 3D printed concrete layers [126]

The absence of formwork for 3DCP contributes to the financial and environmental difference between 3DCP and cast concrete and leads to an increase in efficiency and safety for construction workers [128][7].

Next to this comes the fact that freedom in shape allows for more possibilities and complex forms when using 3D printed concrete [64]. An important disadvantage of 3D printed concrete in the construction process is regarding the stacking of the printed layers, also called filaments. These filaments are printed on top of each other and have limited shape stability during the printing process. If a filament is printed it should already have enough early-age strength to be able to withstand the weight of the filaments that are placed on top. To reach this high early-age strength directly after depositing the filaments, changes can be made in the mix design which leads to faster stiffness and strength development of the filaments after printing. Even though these changes in the mix design can cause an improvement in early-age strength, there will be a limit to the stacking ability of the filaments [64].

The implementation of 3D concrete printing in the construction industry is dependent on the accuracy of the printing jobs, the costs of the printing process, the printing time and the availability of the printing materials [127]. Because not many large-scale tests are performed and no design standards are present for 3DCP it is difficult to already use large-scale implementation in constructions. Prior to acceptance of 3D printing for large-scale construction, standards for material and construction process are required [89][59].

For large-scale production of construction elements with 3DCP in the industry, there are two main types of processes that can be used: 3D printing prefab elements and assembly on-site or monolithic 3DCP on-site [128] (see Figure 2.9).

The printability and open time for large-scale on-site 3DCP processes have higher requirements than 3D printed concrete that is produced in a lab for testing only. This is mainly because of the large pumping distance, size of the printing elements and the amount of printed concrete. It is important that the mix design or printing method allows for high printability for as long as possible for large-scale 3DCP in the construction industry [128].

Environmental differences

3D concrete printing is a sustainable construction method with a lower environmental impact in comparison with traditionally cast concrete. For 3DCP the optimized material consumption and the controlled manufacturing process reduce the construction waste and minimize material use [101] [9] [88].

3DCP creates almost zero waste, because efficient material printing requires less transportation during the construction process and this results in a lower carbon footprint for 3D printed concrete

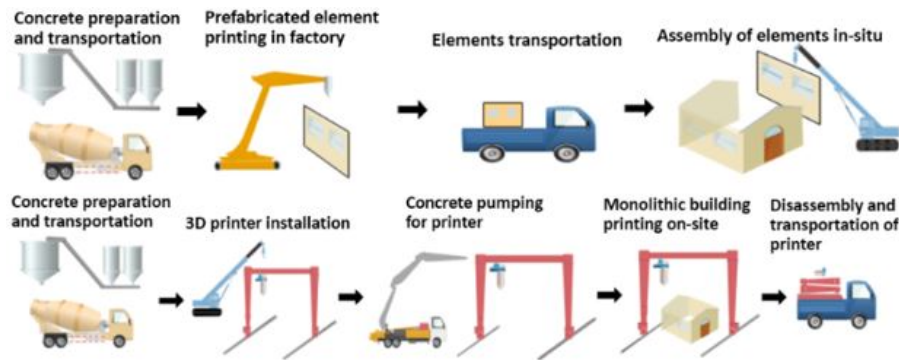


Figure 2.9: 3D printed concrete in practice

in comparison with traditionally cast concrete. Also the absence of formwork for 3DCP reduces the number of trees that have to be cut for timber formwork and reduces the post-construction waste. A cast-in-situ concrete building produces 25% more CO₂ emissions than the same building that is constructed with 3DCP, according to Batikha et al. [7].

In order to increase the sustainability of 3DCP and contribute to the circular economy, it is important that there is a shift toward the use of SCMs, geopolymers, recycled aggregates or waste materials in the concrete mixtures for 3D printed concrete [99].

Economical differences

As described in the previous paragraph for 3DCP there is no formwork required. This is a major difference compared to traditionally cast concrete, where for every concrete element that is created formwork is needed. The costs of this formwork can be up to 35-50% of the total construction costs and the preparation and removal activities regarding formwork can take up to 50-70% of the total construction time [7][80]. The construction time can be reduced by up to 95% compared to the cast-in-situ concrete construction method [7]. It can be stated that the material for the formwork itself is a large financial expense, but also the labor costs for all activities regarding formwork are significant. The total project costs can be decreased if the use of formwork is not needed, as is the case for 3DCP [59][99]. Furthermore with 3D concrete printing there is more freedom in the placement of the deposited filaments and thus ultimately in the products that can be realized [59]. Because of the precise placement of the filaments, optimization of structural elements is possible which reduces material waste and over-dimensioning [29].

On the other hand, the use of 3D printed concrete does not only lead to cost reductions. The initial and operating costs of a good 3D concrete printer and printable mix design cannot be neglected [7] [85]. The printing equipment consists of expensive components and the mix design for 3DCP will be more expensive, because of the use of admixtures to make the mix design suitable for 3D printing [7].

Mix design differences

Traditionally cast concrete mix designs consist of water, cement and aggregates. Normal strength concrete can be obtained by mixing these materials in the right proportions and with the right compaction. For 3DCP the material for the concrete mix consists of high cement content mortar, with a maximum aggregate particle size of approximately 2mm [16]. The use of fine aggregates in the mix for 3DCP is preferred so that no damage is caused to the printing nozzle [99].

The difference for a 3D printed concrete is that the mixture has to be pumpable and buildable [118]. This means that in the pumping phase the concrete mixture has high flowability and low yield stress, to ensure continuous extrusion from the concrete printer without defects on the surface of the filament [118]. Yield stress can be described as the stress at which the material starts flowing. As soon as the filaments are deposited from the printing nozzle the concrete mixture needs to have high yield stress and stiffness to prevent too much deformation and to support the weight of the upper layers without failure [101][99]. These are two contradicting rheological requirements that are difficult to obtain with a regular concrete mixture. In order to fulfill these contradicting rheological properties, only fine aggregate

gates are used and admixtures are added to the mixture for 3DCP.

Superplasticizer is a chemical admixture that increases the flowability of the concrete mixture, which results in a lower water-cement ratio and thus a higher strength concrete [99]. The mechanism of the superplasticizer is the dispersion of cement particles in the mixture, which improves the flow characteristics of the mixture. These good flow characteristics are needed for 3DCP to create a pumpable and extrudable mix design. On the other hand shape stability is essential once the filaments are deposited from the printer. Viscosity Modifying Admixture (VMA) can be used in 3DCP mixtures to increase the shape stability after extrusion. VMA changes the plastic viscosity of the mixture by binding water molecules from polymer chains [99], which can lead to an increase in yield stress and plastic viscosity. The chains of VMA form an intertwined particle structure which gives high shape stability. VMA can positively influence the buildability of a printable mix design. High viscosity of the 3DCP mixture is also needed during the pumping phase to prevent segregation to occur [7].

For 3DCP the rheological behavior of the fresh mix will have a significant influence on the ability of the pumpability and extrudability of the mixture before printing, while the mechanical response of the fresh concrete will influence the buildability of the stacked filaments with bonded interfaces after printing [59][99]. Material selection for the mix design is an important parameter to provide the desired properties of the concrete mixture before and after extrusion. The type of material and dosage that is used for 3DCP, has a large effect on the performance of the mixtures[99].

Mechanical properties differences

Concrete elements that are created by 3DCP have anisotropic properties. This means that the properties of the printed material are not equal in all directions [59]. This is caused by the fact that 3D printed elements are built layer by layer which means that there is an interface between two adjacent layers. This interface between filaments causes deviating element properties in different directions, because the bond strength between these two filaments will be the critical parameter for the mechanical properties of the printed material [125]. These different mechanical properties occur in three different directions: Perpendicular, lateral and longitudinal to the printing direction (see Figure 2.10).

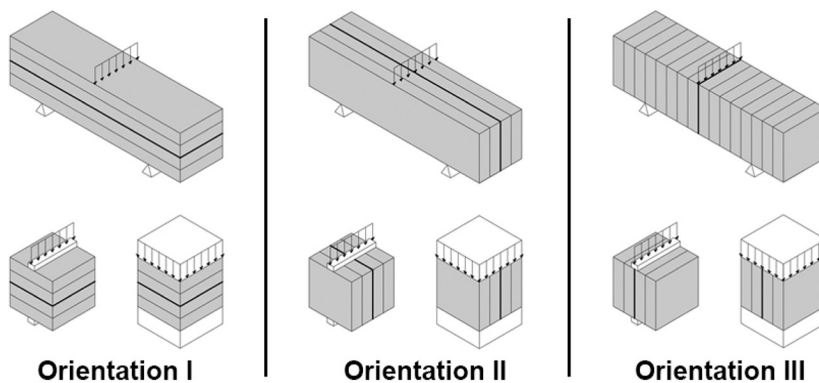


Figure 2.10: Perpendicular (I), lateral (II) and longitudinal (III) directions [125]

Often the interface properties (the bond strength between two filaments) causes the directional dependence of material properties and a reduction of strength can be found [89]. The interaction and bonding between two filaments are mainly dependent on the state of hydration and the time interval between printing the filaments [126]. C-S-H formation due to ongoing hydration on the printed layers results in a higher stiffness over time. Because there is a time interval between two subsequent printed filaments there is a difference in stiffness and this reduces the interlayer bonding. Also at the interface air voids might be present which also weakens the interlayer bonding, which can be seen in Figure 2.11. Because of the time interval between two subsequent printed filaments, air can be entrapped between the two layers. a longer time interval between printing two subsequent layers increases the air void content at the interface zone and this reduces the interlayer bonding. A reduction in interlayer bonding means that the strength of the printed material will be decreased.

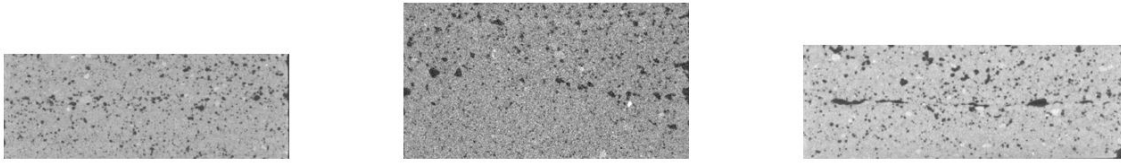


Figure 2.11: Interlayer air voids at 10 sec, 1 min and 10 min intervals [50]

The mechanical properties of 3D printed concrete specimens are also controlled by different parameters than the interlayer interval time. Printing parameters like the shape of the nozzle, complexity of the printed objects, nozzle standoff distance and curing regime of the printed layers can influence the quality of the printed product and therefore determine the mechanical properties of the printed concrete [89][126].

2.3.2. 3D concrete printing techniques

In this subsection the different printing techniques for 3DCP will be reviewed. Extrusion-based concrete printing will be explained in more detail, as this is the most used printing technique nowadays. Secondly set-on-demand concrete printing is described, because this is a promising new development in the concrete printing industry and has some properties that could be beneficial for the 3D concrete printing process for large-scale implementation in the construction industry.

Powder-bed concrete manufacturing

Powder-bed concrete printing works with the principle of depositing a layer of powder in the required geometry and subsequently applying a binder jet on the same deposition path. Afterwards a subsequent layer of the powder is applied on the top by lowering the built structure and the binder jet is applied on top of the powder [59]. This process is repeated for multiple steps until the required geometry is reached.

Powder-bed concrete manufacturing is suitable for relatively small objects and the main advantage of this production method is the freedom to print complicated geometries or sharp corners, which are difficult to realize smoothly with extrusion-based concrete printing [59][99]. Because powder-bed concrete manufacturing is not suitable for producing large construction elements on site, the focus of this thesis will be on extrusion-based concrete printing.

Extrusion-based concrete printing

Most 3DCP systems use an extrusion-based concrete printing strategy. This means that filaments of concrete are placed on top of each other from the concrete printer extruded through a nozzle, which is shown in Figure 2.12 [79][80]. The goal is to form elements by stacking the filaments in the required form and to the required height [115]. The printed filaments must bond together to form different layers as 3D components are built from stacking consecutive filaments. The printed material must have sufficient structural build-up and buildability to remain in position after extrusion and to support the weight of the further layers without collapsing. It is critical for the performance of the printed product that there is a good interface bond between the filaments [64].

The printing systems for 3DCP consist of three main elements: A deposition setup, a control unit and a material conveying system. For the design process in 3DCP the concrete elements are designed as volumetric objects by 3D modeling software. In the next step they are sliced into a series of two-dimensional layers. From this data of two-dimensional layers the G-code is generated. The G-code is exported to the printing machine control unit in order to print the concrete elements by controlled extrusion of the material [64][99].

It is possible to deposit the material with a gantry-based setup (3- or 4-axis) or a robotic arm setup (6-axis), according to Chen et al. [24]. The deposition setup is controlled by the programmed control unit. The goal is to perform a predefined printing path that is made by the user. Gantry-based setups have the possibility for at least 3 translational degrees of freedom and the fourth degree of freedom can provide a rotation. Robotic arm setups can be used to print more complex geometries, because 6

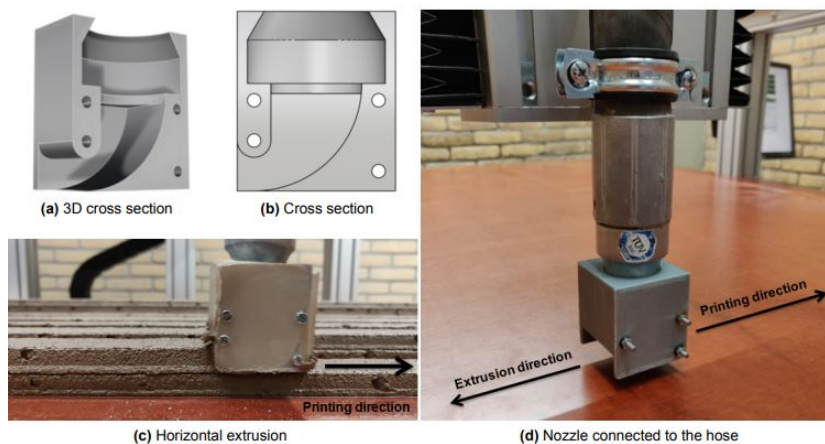


Figure 2.12: Possible printing nozzle for 3DCP [50]

rotational degrees of freedom are allowed with this deposition setup. An advantage of a gantry-based deposition setup is that the height can be easily adjusted and both small and large elements can be printed [24]. An advantage of the robotic arm setup is that there is full freedom in motion and that difficult geometries can be printed with more ease, but often objects with limited scale can be printed.

The material conveying system consists of different components that are working together. These components are a mixing machine, CNC (computer numerical control) system, pump, material hose and printing head with nozzle. Some examples of possible experimental 3D printing setups are shown in Figures 2.13 & 2.14.

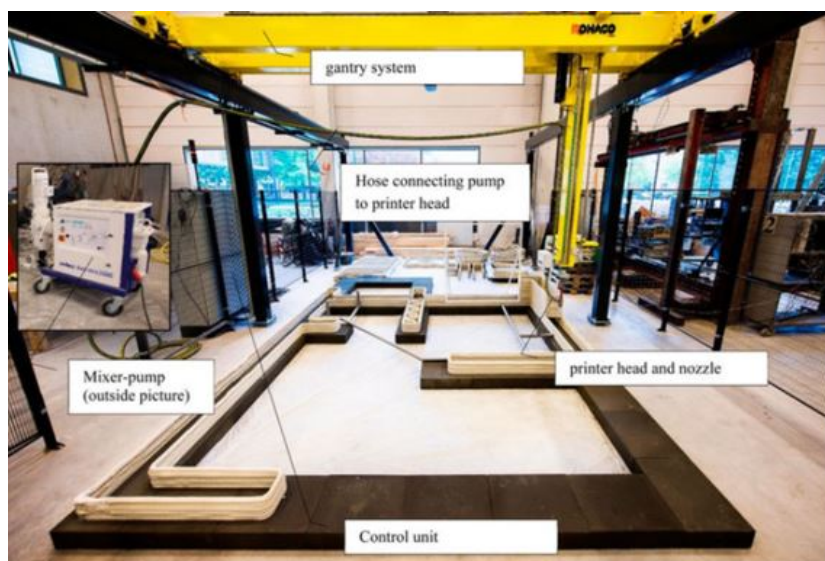


Figure 2.13: 3D printing set-up [23]

The goal of extrusion-based concrete printing is to prepare fresh mixtures and to pump and extrude these mixtures to build concrete elements by stacking printed filaments. In the first stage after mixing, the material needs high flowability, in order to be easily pumped to the print head without too much printing pressure. This means that the mixture has high flowability and low yield stress. It is important that the fresh concrete is conveyed effectively through the pumping system without blocking [64]. As soon as the filaments are extruded from the print head and the print head is no longer supporting the material, the extruded material should be stiff enough to print multiple filaments on top of each other without collapsing. This means that directly after extrusion significant yield stress is needed in combination with adequate thixotropic behavior. The sudden transition from a flowable to a buildable

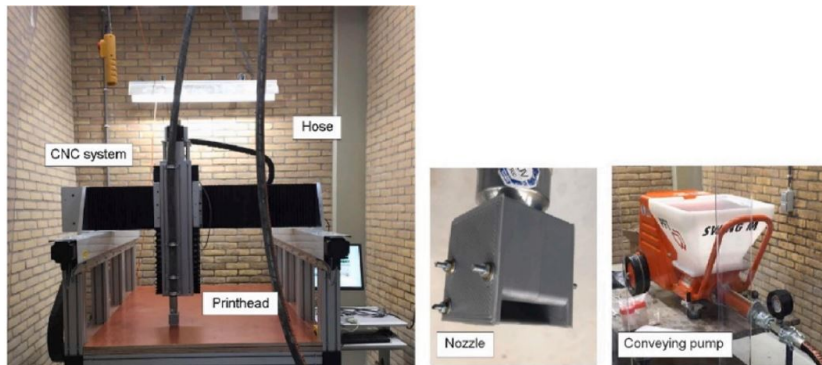


Figure 2.14: 3D printing set-up TU Delft [23]

material calls for contradicting rheological properties [101][59].

Well-chosen additions and admixtures can help to achieve these contradicting rheological properties for the concrete mixture before and after extrusion from the printing nozzle. The hydration reaction should be sufficiently fast to provide a load-bearing internal skeleton of hydration products, which provides strength for the printed concrete filaments. This is the requirement to build layers without significant deformation due to self-weight before setting [64][59].

Set-on-demand concrete printing

The most common printing strategy that is used for 3DCP is the extrusion of high stiffness material from the printing head. The concrete mixture needs to have high stiffness and yield stress in order to have sufficient buildability to stack subsequent filaments of the printed element without collapsing. But this high stiffness concrete mixture has a very limited pumping distance, because there is a very high pumping pressure needed to pump a high stiffness concrete mixture through a hose.

Ideally for 3DCP, the concrete mixture should have a rapid transformation in rheological properties to allow for pumpability and extrudability before depositing filaments (achieved by low yield strength and viscosity). After depositing filaments the mixture should have high buildability and rapid strength build-up (achieved by high yield strength and viscosity) [115][96]. It is shown that these contradictory properties are best achieved with interventions at the print head [24][79][78]. The method that makes use of this mechanism is called set-on-demand concrete printing. With set-on-demand printing accelerating admixtures are added to the concrete mixtures at the printing head just before depositing the filaments (see Figure 2.15) [14].

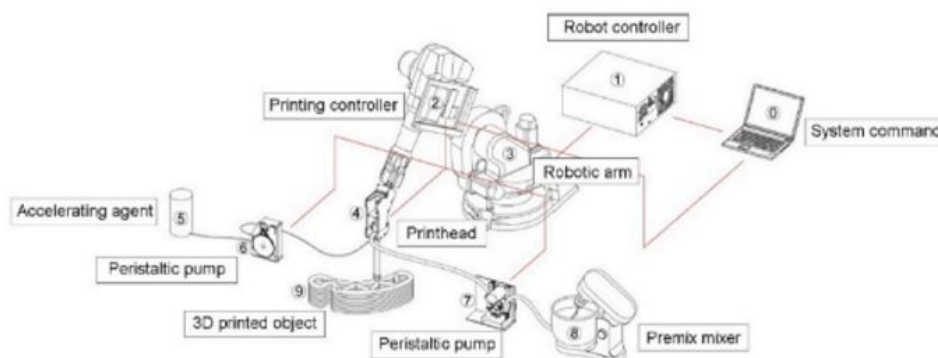


Figure 2.15: Set-up for set-on-demand concrete printing [24]

This method makes use of controlled activation of hydration reaction by accelerators shortly before material placing to ensure structural stability during construction [78]. With this set-on-demand approach the productivity of the 3D printing process can be enhanced without affecting the fresh concrete

pumpability [80][24]. Dispersion of the accelerator to the concrete mixture within the short time inside the printing head is essential to obtain the required buildability after printing [79][115]. This can be achieved by using static or dynamic mixers.

For set-on-demand concrete printing the main idea is to activate the concrete just before extrusion of the filaments. A twin-pipe pumping system (TPP) with a helical static mixer can be used. In this TPP system a pumpable cement-based mixture with high pumpability (cementitious materials, fine aggregates and water without accelerator) and an accelerator slurry (limestone powder based mixture with a high dosage of accelerator) are prepared separately and are transported by two different pumps and material hoses [115]. Then both mixtures are mixed within a helical static mixer just before extrusion from the print-head nozzle (see Figure 2.16). The helical static mixer and the print-head are connected to the CNC system and deposition setup of the 3D printer. The mixing in the helical static mixer allows for a fast increase in the hydration reaction of the pumpable concrete mixture and results in high stiffness deposited filaments. Because the accelerator is added to the fresh cementitious material during the pumping process, the TPP system can also be called an inline mixing system or print head mixing system [78].

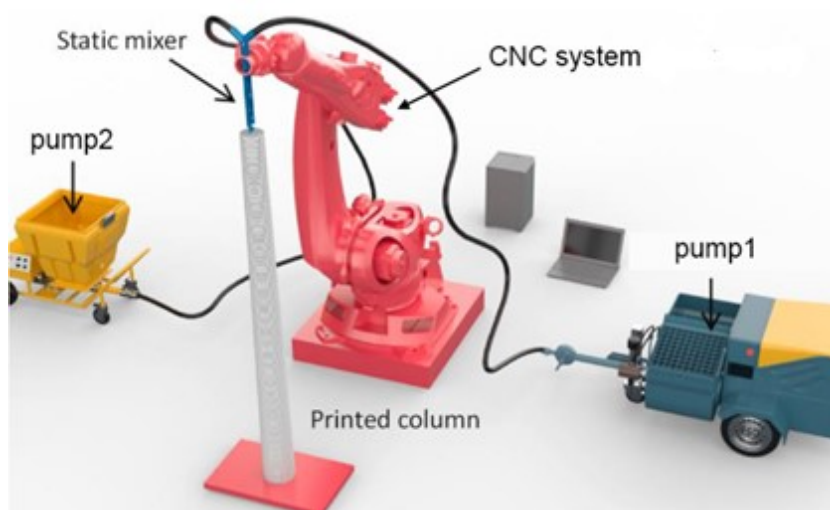


Figure 2.16: Twin-pipe pumping system for 3DCP

Since there is no addition of accelerator during the initial preparation of the pumpable concrete mixture, this has a high pumpability and a long open time [114]. Also the accelerator slurry in the second mixture has no ongoing hydration reactions, which leads to a long open time for the accelerator slurry as well. As the two mixtures pass through the helical static mixer, the mixing elements inside the helical static mixture continuously blend the pumpable concrete mixture with the accelerator slurry (see Figure 2.17a).

During the inline mixing process, which is shown in Figure 2.17b, the accelerator interacts with the cement particles in the pumpable cementitious mixture. This causes a drastic increase in the hydration rate and structural build-up of the cement and results in a fast transition from a flowable mixture to a buildable mixture after the combination of pumpable concrete mix and accelerator slurry leaves the helical static mixer [114]. In this way the contradicting rheological properties that are needed for 3DCP as discussed in section 2.3 can be achieved by set-on-demand concrete printing.

This new set-on-demand concrete printing strategy using a TPP system has the advantage that more flowable mixtures can be used, which drastically extends the open time and thus the possibility to pump the mixture over a longer distance and print more material with the same batch of mixed material before it becomes unusable due to high stiffness development [114][115]. If 3DCP would be used on a large scale for the construction of large structures, it is important that the mixtures have a long open time and are easily pumpable over longer distances. Set-on-demand printing would be a good solution to



(a) Helical static mixer



(b) Twin pump inline mixing

Figure 2.17: Twin pump inline mixing with static mixer [114]

enhance the productivity without affecting the pumpability of the fresh concrete.

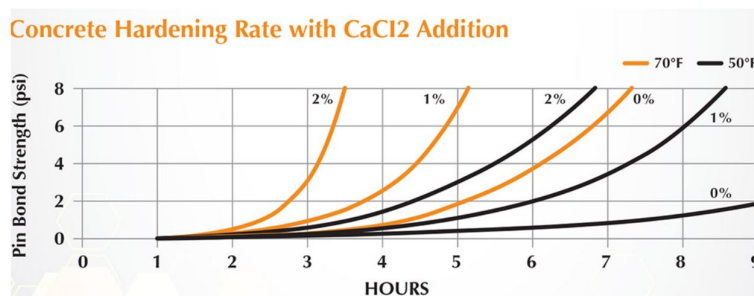
Set-on-demand printing does not only have advantages. A risk of this new TPP system with helical static mixer is that striation patterns are created in the 3D printed concrete. These striations are caused by flow division and insufficient dispersion during mixing of the cementitious mixture and accelerator slurry and can possibly lead to heterogeneous material properties and weak interface zones [114]. The effect of this phenomenon on the material properties has not been studied in detail yet. Also the volume of macropores is found to be higher in the 3D printed specimens with striations, which results in the compressive strength decrease of the printed concrete. If set-on-demand printing strategy is applied, the dispersion of the mixtures during static mixing has to be optimized [115][14].

2.3.3. Accelerator for set-on-demand 3D concrete printing

As described in section 2.3.2 for set-on-demand concrete printing two different mixtures are used: a pumpable cementitious mixture and accelerator slurry. The accelerator slurry is a suspension of limestone powder and accelerator. The accelerator shortens the transition time from plastic to rigid state and increases the early-age strength development when mixed with the cementitious mixture. The accelerator that will be used in the accelerator slurry for this research is CaCl_2 . CaCl_2 is known as the most common accelerator for concrete [109]. In this section the impact of this accelerator on cement hydration is described.

CaCl_2 is an effective accelerator for both setting and hardening of concrete mixtures (see Figure 2.18). This means that not only the stiffness development over time is influenced, but also the early-age strength development is accelerated [72].

The presence of CaCl_2 promotes the supersaturation of C-S-H in the solution, which activates locations

Figure 2.18: Effect of CaCl_2 [72]

in the cementitious solution that would otherwise have been unable to have nucleation. This lowers the free energy barriers to precipitation of hydration products in the solution. The increased rate of precipitation influences the hydration reaction in both nucleation and growth of the hydration products [72].

It is found that CaCl_2 is an effective set and hardening accelerator at 1-4% addition to the concrete mixture and resulted in higher 1-day strength of the mortar than the control mixture. This is caused by the increase in nucleation and growth of the hydration products of the cement. [72]

Research performed on Portland Pozzolan cement showed that adding 1,5% CaCl_2 accelerates the compressive strength development. The increase in compressive strength was 36-48% at 1 day and 29-33% at 3 days. Also in the long term (90 days) an increase in the compressive strength was found [100].

For 3DCP it is possible that multiple different chemical admixtures are added to either the pumpable concrete mixture or the accelerator slurry. For 3D printed concrete the accelerators have shown to rapidly increase the structural build-up rate of the printed mortar. But significantly higher contents are needed if accelerator is used together with superplasticizer to compensate for the repulsive effect [105]. For set-on-demand concrete printing it is possible that superplasticizer admixtures are added to the pumpable concrete mixture to create higher flowability, so the accelerator slurry needs a significant percentage of accelerator to achieve an accelerating effect on the hydration of the printed concrete filaments after mixing in the helical static mixer.

2.4. Fresh-state properties and 3DCP terminology

To characterize the fresh-state properties of the concrete mixtures for 3DCP, different terminology is used in this thesis to describe the behavior of the concrete mixtures before printing and just after printing. In this section an overview of some important terminology regarding 3D concrete printing is given.

Flowability

Flowability is the property of the fresh mixture that indicates the ease of flowing without mechanical effort. It is the ability of the mixture to withhold its shape if no force is applied [64].

Initial setting time

Initial setting time of concrete is the time when the cement paste starts hardening and the stiffness development starts. It is defined as the time between the moment water is added to the cement and the time when the cement paste starts losing plasticity. The final setting time is the time when the cement paste completely loses its plasticity. The initial and final setting times are an indication of the hydration reaction rate in the cement [27].

Pumpability

The pumpability of a mixture is the capacity of a mixture to be transferred through a pipe or a hose. The pumpability is mainly dependent on the flowability of the mixture and is thus determined by the mix design and the use of possible admixtures [64][59].

Extrudability

Extrudability of a concrete mixture can be described as the ability of the mixture to be squeezed out of the printing nozzle as a smooth and continuous filament without defects and discontinuities [118]. If the extrudability is low or the yield stress of the concrete is too high, a high pumping pressure is needed to print the material from the nozzle [64]. If the printing pressure gets too high, damage to the printing equipment is possible and the printed filament displays a lot of defects and discontinuities. For 3DCP it is important that the mixtures have a high extrudability, so that the pressure at the printing nozzle is not too high and that a smooth and continuous filament can be printed [118].

Open time

The open time of a concrete mixture for 3DCP can be described as the available time for printing material with good quality after water is added to the mixture [96][59]. After the open time has passed, the quality of the printed material decreases and is not sufficient anymore. This is caused by the fact that hydration reactions increase the stiffness of the mixture and this has a negative influence on the printability of the material. A longer open time of the mixture means that with the same batch, material can be printed for a longer time without significant loss of quality [64].

Rheology

Rheology is the science of flow and deformation of materials under loads [98]. The rheological principles include the behavior of freshly mixed concrete and the deformation of hardened concrete. For the rheology of the fresh concrete, parameters like stability, compactability and workability have to be taken into account. 3DCP requires contradicting rheological requirements. In the pumping phase before extrusion, the printed material needs high workability and flowability. After extrusion the material needs low workability, high thixotropy and high buildability.

Thixotropy

Thixotropy of concrete can be described as the increase in viscosity and yield stress over time [98][59]. This means that a concrete mixture that has rested a lot after mixing requires more stress to start material flowing than freshly prepared concrete, because of thixotropy effects.

Viscosity

Viscosity can be described as the opposition to flow [98]. This is the resistance of a fluid to change in shape. For freshly mixed concrete the viscosity is low. Over time the viscosity develops and results in high viscosity for hardened concrete. For 3D printable mixtures a higher viscosity is important to prevent segregation of material during the pumping process.

Structural build-up

Structural build-up describes the mechanism that the strength of freshly mixed concrete or paste increases over time, because of hydration reactions of the cement particles with water in the mixture [130][59]. During construction with 3D printed concrete it is important that the structural build-up is high enough to guarantee structural stability. Structural build-up of the material is thus important for the buildability of the printed filaments.

Buildability

For 3DCP the buildability is often described as the shape stability of the material. It is the resistance of the printed material to withstand loads by the layers that are placed on top [130][56]. Material with high shape stability has a low deformation of layers under loads. Buildability is a critical parameter for 3D concrete printing and can be quantified as the maximum number of printed filaments that can be stacked, without failure or significant deformation in the lower filaments [64].

3

Raw material characterization and optimal pre-treatment for the fine glass dust

This chapter aims to determine the raw material characterization of the fine glass dust and to investigate the most effective pre-treatment methods in order to reach comparable fresh-state and hardened properties to standard mortar, when the fine glass dust is used as a cement replacement in concrete binder. Experimental research requires a detailed plan to obtain the desired results. In Section 3.1 the research plan is presented, which is based on the information that is found in the literature study. Section 3.2 describes the materials and the research methodology of the different tests that are performed. In sections 3.3 and 3.4 the results and discussions of the experimental investigation are given.

3.1. Research plan

In order to perform the experimental research for the raw material characterization and investigation on the optimal pre-treatment methods, a research plan was developed. In this research plan it was described which tests were going to be performed to characterize the recycled fine glass dust, a byproduct of the glass-recycling industry. For this fine glass dust the goal of the experimental research in this chapter was to find the optimal pre-treatment method, so that it can be implemented as a Portland cement replacement in concrete mortar with results that approach the fresh-state and hardened properties of standard mortar mixture without fine glass dust. In the research plan it was important to determine which different pre-treatment methods were considered for the fine glass dust in order to reach comparable properties to the reference mixture when it was used in mortar as a cement replacement.

3.1.1. Raw material characterization tests

The recycled fine glass dust is a by-product of the glass recycling industry, but has relatively unknown properties. Because it is a glassy by-product with small particle sizes and high amounts of silica, there is potential for pozzolanic reactivity in concrete and can be used as Portland cement replacement in the binder of mortar mixtures. On this fine glass dust there is performed some research in the past, which is described in section 2.1. The results from these tests had to be validated by own research in this master thesis in order to check the results that were found in the past. There is a possibility that there is a difference between batches of collected material or that the mineral composition of the fine glass dust has changed over time, which means that the results from the previous research [48] can possibly be not accurate anymore. This is the reason that raw material characterization tests were performed. These tests can also be used to compare the fine glass dust before and after pre-treatment in order to check if any major differences in material composition occurred due to different pre-treatments. In the remainder of this subsection the different raw material characterization tests in this research plan are mentioned and the reason why they were performed for this experimental research is given. Section 3.2 describes the performed tests in more detail.

Particle size distribution

Particle size distribution analysis of the fine glass dust was performed, because it has to be checked if it is suitable to use the fine glass dust as a replacement for Ordinary Portland Cement (OPC) in the binder. In order to be applicable for OPC replacement the particle size distribution of the fine glass dust should be comparable with OPC, because bigger particles would decrease the structural packing of the binder and therefore be not beneficial for the strength of the concrete in the long term. A higher porosity of the binder means lower strength and less resistance against deterioration [87].

Thermogravimetric analysis

Thermogravimetric analysis (TGA) was performed in order to determine the behavior of the fine glass dust under elevated temperatures. With the TGA the mass loss can be plotted against the temperature. In this way it could be investigated at which temperatures the organic compounds are removed from the fine glass dust. In section 2.1 it is reported that these organic compounds delay the hydration reaction of the cement in the binder. TGA was performed under Oxygen circumstances, to investigate the temperatures at which the organic compounds are removed from the fine glass dust. The results of the TGA can then be helpful for the determination of possible heat-treatment temperatures for the fine glass dust.

BET-specific surface area analysis

The BET specific surface area (SSA) was determined in order to find the amount of water that will be attracted to the particles of the fine glass dust. A higher specific surface area means that more water can be attracted to the surface of the particles and this means that more water is needed in the mixture to get the same workability. The influence of the pre-treatment on the SSA of the fine glass dust was also investigated, because this could give a possible explanation for the change in behavior of the pre-treated fine glass dust after removal of the organic compounds.

XRD analysis

Research was performed on the recycled fine glass dust by SGS INTRON and the chemical composition was found [48]. For the fine glass dust for this research a new XRD analysis was performed, because it is possible that a different batch of fine glass dust has a slightly different mineral composition. With XRD analysis it was possible to determine the amount of amorphous silica and crystalline compounds in the fine glass dust. The influence of the pre-treatment on the XRD of the fine glass dust was also investigated, because this could give a possible explanation for changing behavior of the fine glass dust after pre-treatment and determine if there was a formation of new crystalline compounds in the fine glass dust after pre-treatment.

3.1.2. Pre-treatment methods for the fine glass dust

As mentioned earlier in the introduction of section 3.1, the main objective of this investigation was to find a pre-treatment for the fine glass dust that gave comparable results to reference concrete mixtures with as little as pre-treatment possible.

Previous research by SGS INTRON [48] has presented that untreated fine glass dust does not have sufficient reactivity to be used as a Portland cement replacement. Organic compounds in the fine glass dust are responsible for the retarding effect if it is used as a cement replacement. Soluble phosphates and sugars have shown to be strong retarders for the hydration reaction of the binder. Other components that have a retarding effect on the hydration reaction of the glass powder are alginic acids, fatty acids and mineral oils [66].

Pre-treatment or material processing of the fine glass dust was needed to increase the reactivity and shorten the initial setting time of the mixtures. The main goal of this pre-treatment was to remove the organic compounds and to increase the pozzolanic reactivity, which could lead to faster strength development and higher values of compressive strength at different curing ages.

The pre-treatment that was used to remove the organic compounds from the fine glass dust in this thesis was a heat-treatment. If the fine glass dust was exposed to elevated temperatures for a certain amount of time, this could remove the organic compounds from the material. The TGA under oxygen

could help to provide information about at which temperatures significant mass loss is experienced. Based on the TGA a temperature for the heat-treatment was chosen and this was used to heat a batch of fine glass dust in an oven at a specific temperature. Before and after heat-treatment the weight was measured and the mass loss could be determined. The removal of organic compounds resulted in less retarding compounds, which could increase the reactivity of the fine glass dust and decrease the initial setting time of the mixtures.

The pre-treatment that was used to increase the initial reactivity and the pozzolanic activity of the fine glass dust was a grinding treatment. In section 2.2.2 it is mentioned that finer particle sizes for glass powder lead to more reactivity, a higher development of compressive strength at early curing ages, but also an increase in the pozzolanic reactivity of the fine glass dust which can potentially cause later age strength development.

3.1.3. Tests after pre-treatment of fine glass dust

In order to determine the optimal pre-treatment for the fine glass dust, tests were performed to compare the fresh-state and hardened behavior of mortar mixtures with untreated glass dust and pre-treated glass dust. In this section it is reported why the different tests were performed to compare the untreated glass dust with the pre-treated glass dust.

Slump and slump flow

For the different mixtures it was important to perform the slump and slump flow test to determine if the mix design was correct and if the mixtures could be used for conventional cast mortar. The flowability after mixing could not be too high, because then the structural build-up will be not sufficient for demoulding the mixture at early curing ages. On the other hand the flowability could not be too low, because this would mean that the mixture is not workable enough to place and compact the mixture in the mould. The slump and slump flow tests were good indicators to investigate the influence of fine glass dust with different pre-treatments on the flowability and workability of the mixtures.

Initial setting time

Initial setting time of the mixture was investigated, because it shows the stiffening of the mortar after adding water to the cementitious materials. If the hydration reaction in the mortar is too slow and the stiffening of the mortar does not occur, then the mixture will not be usable. It was important to check what was the initial setting time of the different mixtures, because this describes the influence of pre-treated fine glass dust on the early-age reactivity of the mortar mixtures with fine glass dust.

Compressive strength

Compressive strength tests were performed in order to investigate the influence of different pre-treatments of fine glass dust on the compressive strength development. Compressive strength is a very important property of concrete. For the development of strength over time it was important that the compressive strength was measured at different times after casting. After 3 days it could tell something about the early age strength development and after 7, 28 and 90 days the longer term strength development could be assessed.

3.2. Materials and Methods

In this section the materials and the different test methods will be explained in more detail. For each of the performed tests the background, test set-up, sample preparation and test procedure are presented. This is based on standards like Eurocode, NEN and ASTM, combined with the information from the literature study in chapter 2.

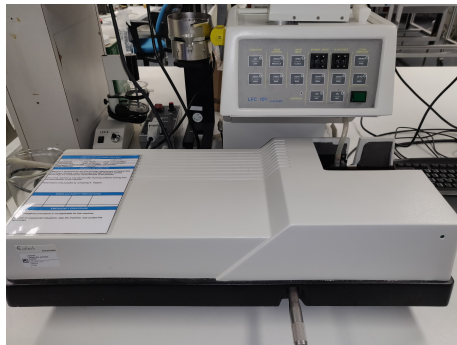
3.2.1. Particle size distribution

The particle size distribution of the fine glass dust was determined, because it had to be checked if the particle size was suitable to use the fine glass dust as a replacement for OPC in the binder.

Test set-up

The particle size distribution was determined with a particle size analyzer. For this thesis The Eyetechn

Ankersmid LFC101 Particle size and shape analyzer was used. The test set-up of this particle size analyzer can be seen in Figure 3.1a.



(a) Eyetech Ankersmid LFC101 for PSD



(b) Lens and laser for PSD

Figure 3.1: Test set-up for Particle size distribution

The LFC101 machine consists of different compartments. Water was collected in the water basin at the top of the machine. Within this water basin there is a rotary axis with a stirrer, which makes it possible to create a water flow. The water was transported by a pump through a small hose and was circulated to pass by the camera and laser. The camera and laser are located at the bottom of the machine and have to be lined up perfectly (see Figure 3.1b). Here it can be seen that the hose passes the water by the lens and the laser. At the front of the machine there is a control panel, which can regulate the pump and the direction of the water flow. Pumping speed and stirrer speed could be adjusted with this panel.

Samples

To determine the particle size distribution of the fine glass dust a sample was prepared. In order to prevent agglomeration of fine glass dust particles in the water, the material was pre-treated in an ultrasonic water bath. For this research the VWR Ultrasonic cleaner was used, which can be seen in Figure 3.2. After ultrasonic pre-treatment a small batch of the fine glass dust (around 5 grams) was used as a sample to be tested.



Figure 3.2: Ultrasonic cleaner for preparation of PSD samples

Procedure

The determination of the particle size distribution started with filling the water basin with sufficient water. Then the pump and stirrer were turned on at the control panel of the machine. It had to be made sure that the water was flowing circularly through the hose and that there was no water leaking. Afterwards, the sample was added to the water basin and was distributed by the stirrer. The water passed the laser and camera. The laser beam was diffracted by the different particles that pass within the water and the camera registered this [35][11]. For different particle sizes there was a laser beam hindrance which was noted by the camera. The camera determined the particle size of the passing particles and with the

help of the software that was connected to the machine and a histogram of the different particle sizes within the sample was produced. Water was pumped by the laser and camera for 180 seconds before the measurements were stopped. The result was a histogram and cumulative distribution graph of the particle size distribution of the sample. For each sample 3 repetitions were performed. The machine was cleaned by draining the pump and cleaning the hose with clean water 3 times.

3.2.2. Thermogravimetric analysis

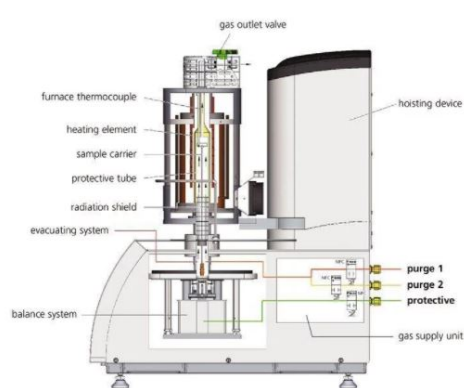
Thermogravimetric analysis (TGA) was performed in order to determine the behavior of the fine glass dust under elevated temperatures. With the TGA the mass loss could be plotted against the temperature.

Test set-up

The thermogravimetric analysis in this thesis was performed with the Netzsch STA 499 F3 Jupiter. The test set-up of this TGA machine can be seen in Figure 3.3a.



(a) Netzsch STA 499 F3 Jupiter at TU Delft



(b) Schematic view of testing apparatus

Figure 3.3: Netzsch STA 499 F3 Jupiter for TGA of the fine glass dust

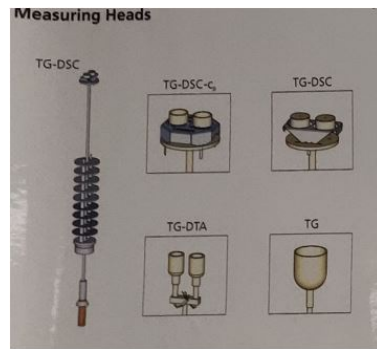
This machine allows for thermal analysis between -150°C and 2000°C . The setup consisted of a balance system, a sample carrier and a heating element with thermocouples. A schematic view of this test set-up is given in Figure 3.3b. With this machine gases were blown by the sample if the hoisting device was brought down and it was possible to perform the TGA under Argon or under Air (oxygen). Under Argon there is an inert atmosphere, which means that there is no chance that the gases will interfere with the thermal treatment of the sample. This means that oxidation of the fine glass powder is prevented. Under Air the gases can react with the fine glass powder and there is a chance for oxidation to occur. The heat-treatment of the fine glass dust in section 3.2.3 will take place in an oven, so the TGA under air provided more valuable results, because in the oven it was also possible that the fine glass dust could react with the oxygen in the air.

There are different possibilities for measuring heads and sample carriers. In this research the TG-DSC set-up was used (see Figure 3.4a). The STA 499 F3 Jupiter runs under Proteus software on Windows. This software allows to plot the temperature against the mass loss of the sample.

Samples

Samples for the TGA were prepared in a small crucible with a cover, which can be seen in Figure 3.4b. First the crucible with cover was weighed. Then the fine glass dust was added to the crucible to fill around half the volume of the crucible. Afterwards, the weight of the crucible and material was measured again. The amount of material that was used for this analysis is around 20-30 mg. If the crucible was filled with material and the cover was placed on top, then the TGA could start.

Procedure



(a) Different possible sample carriers for TGA



(b) TGA sample with cover TU Delft

Figure 3.4: Sample carriers on the TGA apparatus

The procedure of the TGA started with performing a blank test. In this blank test the crucible with cover was placed on the sample carrier in the machine without material and the hoisting device was brought down. Initial gases had to be set until a constant mass was reached and the crucible was heated until the specified temperature. The maximum temperature of heating and also the rate of temperature increase had to be specified. After the maximum temperature was reached, the temperature dropped down to the set-point temperature which was 35°C for this machine. During the analysis, gases were blown by the crucible and the mass loss was measured at the different temperatures. The blank tests were performed in order to correct the TGA of the sample with the weight change in the crucible over the different temperatures.

After the blank test was performed the fine glass dust was added to the crucible and the sample was prepared. The sample was placed on the sample carrier and the TGA was performed under the same circumstances as the blank test. The results for the sample test were corrected with the results of the blank test by the Proteus software. This software plotted a graph of the mass loss of the sample against the temperature.

For this thesis the following TGA was performed for the fine glass dust:

- Under Air: Min. temp = 35°C, Max. temp = 1000°C and temp increase = 10K/min

3.2.3. Heat-treatment of the fine glass dust

The main goal of this investigation was to find a pre-treatment for the fine glass dust that gave comparable results to conventional concrete mixtures as much as possible. The pre-treatment that was used to remove the organic compounds from the fine glass dust in this thesis was a heat-treatment.

Test set-up

The heat-treatment of the fine glass dust was performed with the Carbolite HTF1700 furnace. The test set-up of this oven can be seen in Figure 3.5.

This oven allows materials to be heated up to 1700°C and is connected to a ventilation system which ensures that sufficient oxygen is available in the oven. This oven also allows for heating under different pre-determined time programs. With these temperature-time programs it was possible to ramp up until a certain temperature and stay constant at that temperature for a certain time before continuing with the temperature rise. For higher temperatures this was important to consider, because unexpected reactions could occur if the fine glass dust was heated very quickly.

Samples

Sample preparation for the heat-treatment in the oven consisted of filling a large crucible with a batch of fine glass dust and the mass had to be determined. The largest mass of the fine glass dust that was possible for heating in the oven at TU Delft and with the available crucible was around 500 grams. The crucible had a large surface area and a small depth, which means that there was a large area of fine glass dust at the surface. (see Figure 3.6).



(a) Carbolite HTF1700 furnace



(b) Inside of the Carbolite HTF1700 furnace

Figure 3.5: Carbolite HTF1700 furnace for heat-treatment of fine glass dust



Figure 3.6: Prepared sample for heat-treatment

This large surface area had the advantage that it was easier for the material to be heated uniformly and this could possibly lead to shorter heat-treatment times at a given temperature.

Procedure

Based on the TGA under air circumstances the heat-treatment temperatures could be determined. This was based on the calcination temperature of the fine glass dust. Calcination refers to the removal of volatile substances or impurities in fine glass dust under elevation temperatures [97]. The TGA under air could give an indication of which temperatures caused a large mass loss in the fine glass dust. The goal of testing different heat-treatments was to find the relatively largest mass loss with the lowest possible temperature and time in the oven. The different temperatures that were tested for the heat-treatment were determined based on the results of the thermogravimetric analysis (TGA).

After the sample preparation and mass determination, the sample was placed in the oven. Different temperatures and heat-treatment times were tested. In the first few tests the temperature was gradually increased by hand with 100°C every 30 minutes until the specified heat-treatment temperature. After the heat-treatment time had passed, the oven was cooled down manually. In the next few tests, pre-determined time programs were considered, because this eliminated the need for manual temperature change and the oven cooled down automatically afterwards. For these temperature-time programs the temperature was ramped up by 10°C each minute until a temperature of 450°C was reached. At this

temperature there was a dwell time of 30 minutes before the temperature ramp-up was continued. This dwell time at 450°C was chosen so that there was a chance to reach equilibrium for the fine glass dust after organic compounds were released at lower temperatures. Afterwards, the temperature ramped up at a rate of 10°C per minute until the specified end temperature. The temperature was kept constant for the specified heat-treatment time and afterwards the temperature was cooled down until room temperature.

In the HTF1700 Carbolite oven at the TUDelft it was not allowed to place the fine glass dust directly in an oven of 600°C, because this would cause extreme reaction speeds and smoke development. This caused a risk of explosion and excessive gas development. The temperature-time program was used to gradually heat the material in the oven. The temperature time program that was used for the heat-treatment of 600°C and 1 hour can be described as follows:

- Heating from 0 to 450°C with 10°C per minute
- Dwell time of 30 minutes at 450°C
- Heating from 450 to 600°C with 10°C per minute
- Dwell time of 1 hour at 600°C
- Cooling from 600 to 0°C with 20°C per minute

This process is illustrated in Figure 3.7. The dwell time at 450°C was needed to let the material adjust to the high temperatures before reaching 600°C. This also created time to remove organic compounds from the fine glass dust that were reacting at 450°C and lower. All the heat-treated fine glass dust that was used in the continuation of this thesis was prepared in the way that is presented in Figure 3.7

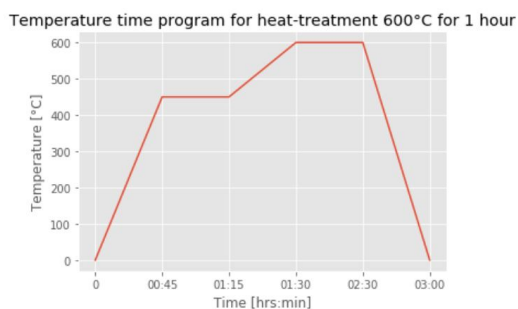


Figure 3.7: Temperature-time program for heat-treatment of 600°C for 1 hour

For this thesis the following heat-treatment temperatures and times were considered:

450°C: 1 hour, 3 hours, 6 hours

600°C: 1 hour, 3 hours, 4 hours, 6 hours, 22 hours

700°C: 3 hours

After each heat-treatment the mass was measured when the sample was cooled down. This was used to determine the mass loss of the sample. For each combination of heat-treatment temperature and time, a minimum of 3 repetitions were performed and the average mass loss was determined.

Determination of organic content

In section 3.1.2 it is declared that the fine glass dust that is delivered from Maltha contains a lot of organic impurities that have a mitigating effect on the hydration reaction in the mortar. The goal of the heat-treatment was to remove these organic compounds from the fine glass dust. To investigate the effectiveness of the heat-treatment the untreated fine glass dust was compared with the heat-treated fine glass dust. Therefore the organic content of both samples was determined. This organic content determination was done according to Makowski et al. [70] and Rodriguez et al. [123].

The powder samples were dried in an oven at 105°C for 24 hours to evaporate all the excess moisture from the samples. Afterwards, the dried samples were weighed and placed in the HTF1700 oven at 600°C for 4 hours. After heating the oven was turned off and the sample was allowed to cool down. After cooling the sample was weighed again and the measured weight loss was recorded as the amount of organic matter present in the original sample. This procedure was performed for both the

untreated fine glass dust and the 600°C heat-treated fine glass dust.

3.2.4. Grinding treatment of the fine glass dust

From section 2.2.2 it can be found in several past experiments that the early age reactivity and pozzolanic activity of the fine glass dust can be increased if the particle size is decreased. In this thesis a grinding treatment was applied to the fine glass dust in order to investigate the effect of different fineness on the mechanical properties of the fine glass dust when it was used in concrete mortar mixtures

Test set-up

The grinding treatment of the fine glass dust was performed with the Eaton QM-30L Ball Mill Machine. The test set-up of this grinding machine can be seen in Figure 3.8.



(a) Outside of the Ball Mill machine



(b) Inside of the Ball Mill machine

Figure 3.8: QM-30L Ball Mill Machine for grinding treatment

This ball milling machine allowed material to be grounded until different particle sizes. The machine operated by rotating around its axis and thereby crushing balls of different sizes into the fine glass dust. Rotation speeds could be manually adjusted, for the grinding of the fine glass dust a rotation speed of 55 rotations per minute was used.

Samples

The heat-treated fine glass dust was collected from the Carbolite HTF1700 furnace as described in section 3.2.3. Afterwards, the powder was directly placed in the milling machine, which was already filled with the milling balls. This can be seen in Figure 3.9.



Figure 3.9: Fine glass dust with milling balls

After the fine glass dust was placed in the machine the top lid was screwed on very tight to ensure that no powder could escape while the grinding machine was rotating.

Procedure

After the top lid was closed, a protective cage had to be placed around the grinding machine. This was done to ensure the safety of other researchers in that area while the machine was grinding the fine glass dust. It was assumed that a longer grinding time would result in a finer particle size of the fine glass dust. In this thesis this assumption was checked by grinding for different time periods and to investigate the corresponding particle size distribution. In this thesis the grinding time intervals that were taken into account: 0 hours, 1 hour, 2 hours, 3 hours, 4 hours, 5 hours and 6 hours.

After each hour of grinding, a small batch of fine glass dust was collected from the grinding machine. This was done by sieving the powder of the milling balls, which is illustrated in Figure 3.10.

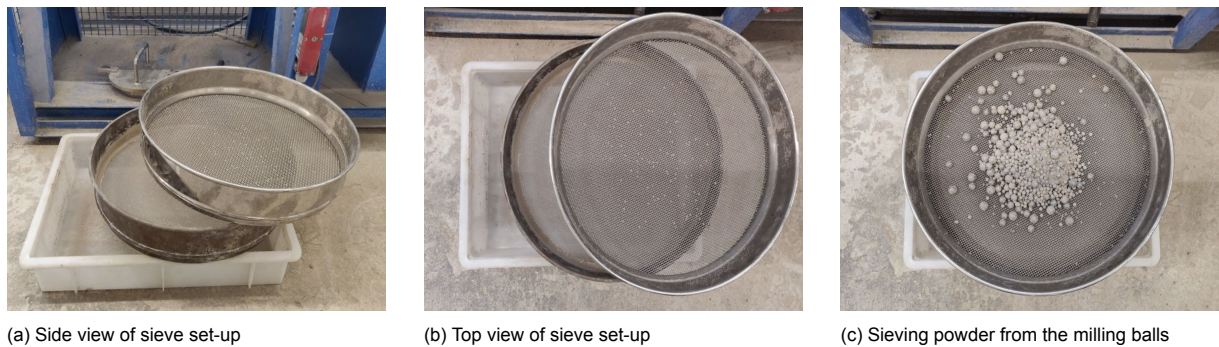


Figure 3.10: Grinding treatment sieve set-up

Two different sieves were used on top of each other to collect the milling balls and to allow the grounded powder to pass through the sieves. The fine glass dust that passed through the sieves was collected underneath and a small batch of material was collected. The collected material of each grinding time interval was used to determine the particle size distribution, as announced in section 3.2.1. In this way the effect of the grinding treatment on the particle size distribution of the fine glass dust was investigated.

Also the company Maltha Glass BV. had performed a grinding treatment on the fine glass dust with their own ball milling machine. The efficiency of the pre-treatment of the fine glass dust increases if it was possible to perform at their own company, so this was the reason that also the Maltha ground material was taken into account in this investigation.

3.2.5. BET specific area analysis

The BET specific surface area (SSA) was determined in order to find the amount of water that would be attracted to the particles of the fine glass dust. A higher BET surface area of the fine glass dust means that the particles have a larger surface area where reactions with water or cement particles can occur [63].

Test set-up

The BET specific surface area analysis in this thesis was performed with the Micromeritics Gemini VII. The test set-up of this machine can be seen in Figure 3.11.

This machine allows for rapid surface area measurements and is also capable of measuring low surface area materials. The Gemini system consists of two reservoirs of equal volume that are connected to an aluminum block for uniformity in temperature. Connected to the reservoirs in the machine are a balance tube and a sample tube. The sample tube was filled with the material that had to be investigated and the balance tube (reference) was filled with glass beads with a volume equal to the material in the sample tube. A liquid coolant dewar was filled with liquid nitrogen and was raised towards the tubes with a small elevator.

Samples

For the sample preparation a heated tube was collected from an oven at around 80°C. This tube was filled with a small amount of fine glass dust (around 3-5 grams). The weight was measured and afterwards the sample tube was connected to the Gemini VII machine. This was done by connecting first



Figure 3.11: Micromeritics Gemini VII for BET analysis

the connector nut, then the ferrule and finally the rubber O-ring (see Figure 3.12).



Figure 3.12: Sample preparation for BET analysis

Then the dewar was filled with liquid nitrogen and was placed in the chamber on the elevator. Two plastic half-lids were placed on both the tubes and the door of the sample compartment was closed.

Procedure

Before the BET analysis could start, the tubes had to be in a vacuum. This was the initializing step of the analysis. If the pressure in the tubes was zero and the vacuum was reached, then the dewar with liquid nitrogen was lifted upwards. This was done so that the balance tube and the sample tube were fully in the dewar. During the BET analysis gases flowed from the reservoirs through the balance tube and the sample tube and the amount of gas absorption in the sample was measured. The rate of gas flow equals the rate of absorption of gas by the sample. An important benefit of this absorptive-rate technique was the increase in analysis speed. At some point, the rate of flow from the sample reservoir (which equals the rate of absorption) falls below a specific level, which signals that equilibrium was reached at the current pressure. Then the sequence started again with an increase in pressure until the highest relative pressure in the pressure table has been reached.

For this thesis a BET analysis was performed for the untreated fine glass dust and for 600°C heat-treated fine glass dust with and without grinding treatment. The goal was to find the influence of heating

and grinding on the specific surface area of the material. Heating removed the organic compounds and impurities from the fine glass dust and grinding lowered the particle sizes of the fine glass dust, so both these pre-treatments were expected to have a positive influence on the BET specific area of the fine glass dust.

3.2.6. XRD analysis

With XRD analysis it was possible to determine the presence of crystalline compounds in the fine glass dust [129]. The influence of the pre-treatment on the crystalline compounds in the XRD results of the fine glass dust was also important to investigate, because this could give a possible explanation for changing behavior of the fine glass dust after heat-treatment.

Test set-up

The XRD analysis in this thesis was performed with the Philips PW 1830 X-ray Diffractometer. The test set-up of this machine can be seen in Figure 3.13.

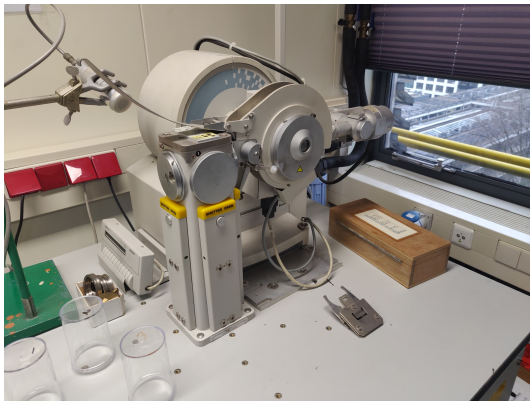


Figure 3.13: Philips PW 1830 X-ray Diffractometer

X-ray diffraction is a non-destructive analytical technique for the identification of various crystalline forms present in the fine glass dust. These crystalline forms are known as phases or compounds. This can be done by comparing the X-ray diffraction pattern from the machine with international databases with known diffraction patterns for all possible crystalline phases. Also the amorphous content of the material can be determined [129][34].

Samples

The sample preparation for the XRD analysis started with placing the thin part of the crucible on a glass plate (see Figure 3.14).



Figure 3.14: Preparation for XRD sample

A small amount of fine glass dust was placed in the circular opening of the crucible. The material was compacted by pressing hard with a steel spatula. Afterwards, the pressed material was broken with a small knife a brought back to the circular opening in the crucible. Now the material was compacted

again by pressing with the spatula. This process was repeated 5 times. Then the excess material was removed from the crucible and the ticker part of the crucible was connected on top. The sample was prepared sufficiently if the crucible could be moved without material dropping out.

Procedure

The XRD analysis started by placing the prepared sample in the machine. During the analysis X-ray beams were sent towards the sample from an X-ray tube. The incoming angle was given by θ . The sample of fine glass dust reflected the incoming X-ray beam and the angle of the reflected outgoing X-ray beam was given by 2θ . Each compound in the sample had its own diffraction angle 2θ . During the analysis the machine detected the diffraction angles and counted the number of hits for each angle. After the analysis the number of hits could be plotted against the diffraction angle 2θ and the result of this XRD measurement is called a diffractogram [34]. The diffractogram showed present phases in the sample material with sharp peaks in intensity. Amorphous compounds were given with a very broad background hump.

Fine glass dust is a by-product of the glass recycling industry. The expectation was to see a large number of amorphous compounds in the material. The high amorphous silica content of the fine glass dust provides interesting pozzolanic properties when it is used as a cement replacement [120]. It was important to check if the heat-treatment of 600°C did not cause a change in the amorphous amount of the fine glass dust and caused a lot of reactive crystalline phases to originate. This could be the case if some compounds in the fine glass dust react with oxygen in the oven at high temperatures. To check the possible change in the amorphous content and crystalline phases of the fine glass dust after heat-treatment, an XRD analysis was performed for the untreated fine glass dust and the 600°C heat-treated fine glass dust and the results were compared.

3.2.7. Mix design

To investigate the influence of the fine glass dust pre-treatments on the properties of concrete mortar different mixtures were developed. To isolate the influence of the pre-treatments without other changing factors in the mixtures, a fixed amount of fine glass dust was used to replace Portland cement. In this part of the thesis a fixed amount of 15% fine glass dust was used. To investigate the effect of the heat-treatment on the fine glass dust, Mix 1 - Mix 3 could be used. To investigate the effect of the grinding treatment, Mix 4 - Mix 6 could be used. The goal of this investigation was to find the most efficient combination of pre-treatments so that the glass dust mortar had similar performance as the reference mix mortar (Mix 1) as much as possible. From Table 3.1 it could be seen that all mixtures used a water/binder ratio of 0.5 and a sand/binder ratio of 3. These values were chosen as constant in order to investigate only the influence of heat-treatment and grinding treatment of the fine glass dust (FGD) when it was used in concrete mortar mixture. CEN standard sand was used, which was based on NEN-EN 196-1 [106]. For the Portland cement (PC) CEM I 42,5N was used. An overview of the different mix designs is given in Table 3.1:

Mix	PC	FGD	Sand	Water	Type of pre-treatment
Mix 1	100	0	300	50	-
Mix 2	85	15	300	50	-
Mix 3	85	15	300	50	600°C heat-treatment
Mix 4	85	15	300	50	600°C heat-treatment and Maltha grinding treatment
Mix 5	85	15	300	50	600°C heat-treatment and 1 hour grinding treatment
Mix 6	85	15	300	50	600°C heat-treatment and 6 hours grinding treatment

Table 3.1: Mix compositions for investigating the effect of pre-treatments (% of binder mass)

The mortar mixtures were prepared with the Hobart N-50 mortar mixer (see Figure 3.15). This mixer has a capacity of 5 liters and is ideally used for the preparation of small to medium quantities of mortar mixture.

The mixtures were prepared by first measuring the required raw materials precisely. Then the dry



Figure 3.15: Hobart N-50 mortar mixer at TUDelft

materials (CEN sand, CEM I 42,5N and fine glass dust) were mixed for one minute at the lowest speed (speed 1). It had to be checked manually if all the materials were mixed properly. Secondly the water could be slowly added while mixing on speed 1. When the water was added, the start of mixing time was determined and there had to be mixed for 1 minute. Afterwards, the material had to be scraped off from the sides of the bowl manually and finally there was mixed once again for 1 minute at speed 2 to ensure proper mixing of all the materials and to complete the preparation of the mortar mixtures.

3.2.8. Slump and Slump flow test

The slump and slump flow tests were good indicators to check the workability and flowability of the designed mixtures. For the different mixtures in section 3.2.7 it was investigated what was the influence of the pre-treatment of the fine glass dust on the slump and slump flow values.

Test set-up

The slump and slump flow tests in this thesis were performed with the Intertest Benelux Compaction table for mini slump test. The test set-up can be seen in Figure 3.16.



Figure 3.16: Set-up on compaction table for mini slump test

This test set-up consists of a compaction table and a mini Hägermann cone. The compaction table has a diameter of 30 cm and the Hägermann cone has a height of 6 cm. At the top the cone has a diameter of 7 cm and at the bottom the diameter is 10 cm. The Hägermann cone has to be oiled before use to minimize friction between the mortar mixture and the surface of the cone.

Samples

The samples for the slump and slump flow test were prepared by filling the Hägermann cone with the concrete mixture. The mortar mixture for the samples was prepared conform NEN-EN 196-3 par. 5.2.1 [107]. After the mixture was prepared, the mortar was transferred immediately to the mould. Any voids were removed from the mortar by compacting the material with a compacting stick 20 times. Excess material was removed from the top of the mould with a sawing motion, which resulted in a smooth upper surface of the prepared sample in the completely filled Hägermann cone (see Figure 3.17a).



(a) Filled mould for the slump test



(b) Slump test after removing the mould

Figure 3.17: Slump test for mortar mixtures

Procedure

After the samples were prepared the slump test was performed by removing the Hägermann mould from the compaction table. This can be seen in Figure 3.17b. The mortar mixture slumps and the height of the mortar after removing the mould was measured from the compaction table to the top of the mortar. The average measured height of the cone after removing the mould is called the slump value of the mixture.

After the slump value was measured, the slump flow test could be performed on the same sample. This was done by turning the compaction table on and dropping the compaction table 25 times. After 25 drops the compaction table was turned off and the flow diameter of the sample was measured. Measurements were taken in different directions and the average value was calculated. The result of a slump flow test can be seen in Figure 3.18.



Figure 3.18: Slump flow test after 25 drops of the compaction table

The different mixtures were described in section 3.2.7. For each mixture 3 repetitions were performed

so that the mean could be calculated. Comparing the results of the different mixtures could describe the influence of heat-treatment and grinding treatment of the fine glass dust on the workability and flowability of the mortar mixtures.

3.2.9. Initial setting time test

Initial setting time of the mixture was important to investigate, because it described the stiffening of the mortar after adding water to the cementitious materials. This could indicate the influence of pre-treatment on the early-age reactivity of the fine glass dust in concrete mortar.

Test set-up

The initial setting time tests in this thesis were performed with the Controls Vicamatic 2 machine. The test set-up can be seen in Figure 3.19.

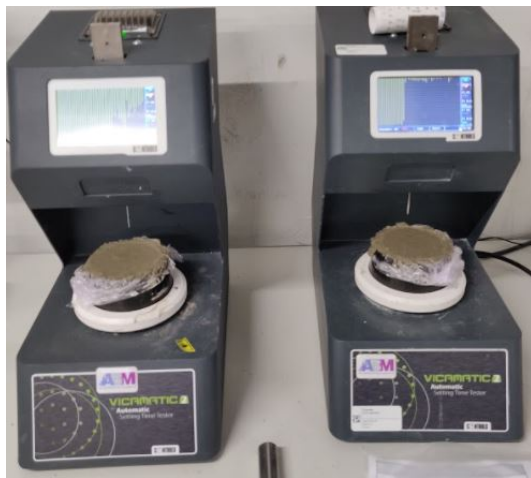


Figure 3.19: Controls Vicamatic 2 machine at TUDelft

The Vicamatic 2 is an Automatic Vicat Apparatus where the material is placed in a mould and a plunger with needle drops into the mortar mixture at regular intervals and in fixed positions. According to NEN-EN 196-3 [107] the plunger has to have a total mass of 300 g and the movement should be truly vertical without significant friction. The Vicat mould to contain the material during the test is made of hard rubber in a truncated conical form of 40,0 mm deep. Under the Vicat mould a rigid glass base plate of 2,5 mm thick is placed to contain the material during the test.

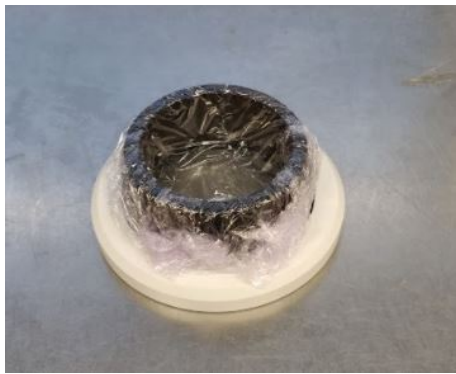
Samples

Before mixing the raw materials, the mould had to be prepared. This was done by placing the Vicat mould on the glass base plate and placing the white ring around the base plate. A thin layer of protective film was placed on the Vicat mould, to prevent stiffened material from sticking to the Vicat mould. Because of this film the Vicat mould could be easily cleaned afterwards. The result can be seen in Figure 3.20a.

The mortar mixture for the samples was prepared conform NEN-EN 196-3 par. 5.2.1 [107]. It was important that the starting time of mixing is noted. After the mixture was prepared, the mortar was transferred immediately to the mould. Any voids were removed from the paste by compacting the material by hand. Excess material was removed from the mould with a sawing motion, which resulted in a smooth upper surface of the prepared sample (see Figure 3.20b).

Procedure

The prepared sample was placed in the Vicat Apparatus. This was done by connecting the white ring to the base plate of the testing machine (see Figure 3.19). On the interface display of the testing machine an automatic testing program was chosen. This program determines at which time interval from



(a) Vicat mould empty



(b) Vicat mould full

Figure 3.20: Preparation of samples for the Vicat test

the start of mixing time and at which locations the needle dropped into the mortar mixture. Before starting the measurements the needle needed to be oiled up, to prevent the material from sticking and hardening at the needle. This could affect future tests with the same machine. Penetration depth of the needle was measured by a sensor with a resolution of 0,1 mm at each drop of the needle. Due to the stiffening process in the mortar mixture over time, the penetration depth decreased and the results were recorded. The initial setting time can be determined as the time when the penetration depth is lower than 36,5 mm [27]. It had to be taken into account that there was a margin of error in the testing machine, because it was possible that penetration of the needle was hindered due to for example large particles. This would result in a low penetration depth, while the material was not hardened enough. This was taken into account with the processing of the results. At the end of the test the pattern of needle drops could be clearly seen in the mortar sample in Figure 3.21.



Figure 3.21: Finished Vicat test

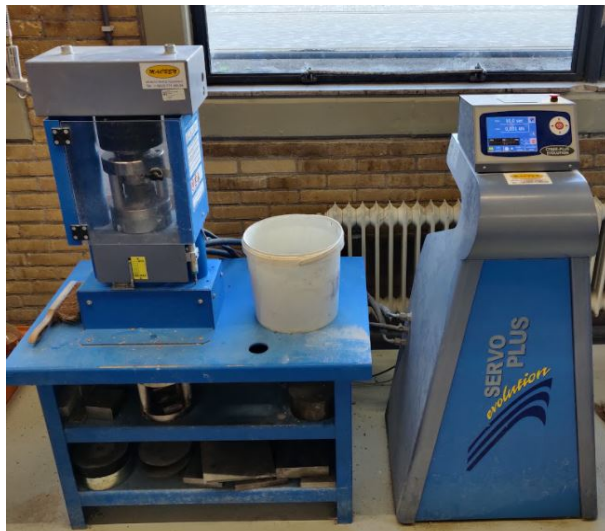
The different mixtures were presented in section 3.2.7. For each mixture 3 repetitions were performed so that the mean could be calculated. Comparing the results of the different mixtures could describe the influence of pre-treatment of the fine glass dust on the early-age hydration reaction in concrete mortar mixtures.

3.2.10. Compressive strength test

Compressive strength tests were performed in order to investigate the influence of heat-treatment and different grinding treatments of fine glass dust on the compressive strength of cast mortar. Compressive strength is a very important hardened property of mortar mixtures. For the development of strength over time it is important that the compressive strength is measured at different curing times after casting.

Test set-up

The compressive strength tests in this thesis were performed with the Macben Servo Plus Evolution machine. The test set-up can be seen in Figure 3.22a.



(a) Overview of the test set-up



(b) Loading jig for compressive strength test

Figure 3.22: Macben Servo Plus Evolution at TUDelft for compressive strength test

With the control panel of this machine the type of test can be selected and also the loading rate can be chosen. Material samples are placed in the loading jig at the left in Figure 3.22a. For the compressive strength test of the mortar the loading jig that was used can be seen in Figure 3.22b.

Samples

According to the NEN-EN 196-1 [106] the test specimens had to be 40 mm x 40 mm x 160 mm prisms. After preparation of the mortar, the samples were moulded immediately, directly from the mixing bowl. The mortar was compacted in the mould by the use of a vibration table. A second layer of mortar was added to the mould, ensuring that there was a surplus of mortar. After compacting, the excess mortar was removed with a metal straightedge in a transverse sawing motion. A plastic film was placed over the top of the moulds for curing in order to prevent too much air and moisture from escaping the mortar during early hydration reaction (see Figure 3.23a). The samples were demoulded 24 hours after casting. After demoulding the samples were stored in a wet room ($20,0 \pm 1,0$ °C and 95% RH) until compressive strength tests had to be performed (see Figure 3.23b).

Procedure



(a) Plastic film for curing of the mortar



(b) Storage of samples in the wet room

Figure 3.23: Curing procedure for mortar prisms

The mixtures and samples were prepared according to NEN-EN 196-1 [106]. Compressive strength tests were performed for each of the six mixtures that are declared in section 3.2.7. For each mixture the compressive strength was determined after 3, 7, 28 and 90 days of curing in the wet room. There

was chosen to test at these curing times because after 1 day not all the mixtures did develop sufficient strength to be tested and also for the possible pozzolanic reaction of the fine glass dust it was important to look at the long-term strength behavior. This was mainly because the pozzolanic reaction is a slow process and will contribute to the later strength development. For each curing age 3 repetitions were made for each mixture.

NEN-EN 196-1 [106] prescribes that the samples first have to be tested on flexural strength with a three-point loading method. For the flexural strength test another loading jig (three-point bending jig) was used in the Macben machine. NEN-EN 196-1 [106] prescribes that the compressive strength test is carried out on the broken halves from the flexural test. Each prism half is loaded on its side face in the loading jig for compressive strength. This can be seen in Figure 3.24.



Figure 3.24: Loading jig with sample for compression test

The load was increased smoothly on the sample by a loading rate of 2400 N/s until fracture of the sample occurred. The compression strength was calculated based on the ultimate load on the sample at fracture. The result of each individual prism half was recorded and the calculated mean was reported [47].

Influence of heat-treatment temperature on the compressive strength development

For the compressive strength investigation of the different types of pre-treatments for the fine glass dust (mix 1 - mix 6) only a heat-treatment of 600°C was taken into account. 600°C was found to be the maximum temperature at which the fine glass dust can be pre-treated and used as a powder afterwards. In section 3.2.3 it could be seen that a lot of different heat-treatment temperatures were investigated in terms of mass loss after heating. It could also be valuable information to look at how these different heat-treatment temperatures influenced the development of compressive strength of the mortar. A lower heat-treatment temperature gave a lower mass loss, which showed that a larger amount of organic compounds was still present in the fine glass dust which could slow down the hydration reaction. By performing compressive strength tests on mortar mixtures with different fine glass dust treatment temperatures, the most optimal heat-treatment could be found in terms of treatment temperature compared to the resulting strength development of the mortar.

The different mixtures that were used for the investigation of the heat-treatment temperature influence on the compressive strength development are given in Table 3.2. It can be seen from this table that a constant amount of 15% FGD was used to replace Portland cement and that only heat-treatment was performed on the fine glass dust. This was done to only investigate the influence of heat-treatment temperatures on the compressive strength development of the mortar. All the mixtures were tested at

3, 7 and 28 days of curing and 3 repetitions for each mixture were performed.

Mix	PC	FGD	Sand	Water	Type of pre-treatment
Mix 0°C	85	15	300	50	0°C heat-treatment
Mix 150°C	85	15	300	50	150°C heat-treatment
Mix 300°C	85	15	300	50	300°C heat-treatment
Mix 450°C	85	15	300	50	450°C heat-treatment
Mix 600°C	85	15	300	50	600°C heat-treatment

Table 3.2: Mix compositions for investigating the effect of heat-treatment temperature (% of binder mass)

3.3. Results

Section 3.2 gave a description of the different material characterization tests, pre-treatment tests and tests that were performed after pre-treatment of the fine glass dust. The goal of these tests was to investigate the influence of fine glass dust and different pre-treatments when it is used as a cement replacement in mortar mixtures. The goal was to find a pre-treatment method for the fine glass dust that approaches the result of a standard reference mortar mixture with as high efficiency as possible. In this section the results of the performed tests are presented in a clear and comprehensible way.

Because of the large number of references to different mix numbers in this section, an overview of the different mix compositions and pre-treatments that were used in this part of the thesis are given in Table 3.3. For more detailed information on the mix designs, section 3.2.7 can be accessed.

Mix	PC	FGD	Sand	Water	Type of pre-treatment
Mix 1	100	0	300	50	-
Mix 2	85	15	300	50	-
Mix 3	85	15	300	50	600°C heat-treatment
Mix 4	85	15	300	50	600°C heat-treatment and Maltha grinding treatment
Mix 5	85	15	300	50	600°C heat-treatment and 1 hour grinding treatment
Mix 6	85	15	300	50	600°C heat-treatment and 6 hours grinding treatment

Table 3.3: Overview of different mix compositions (% of binder mass)

3.3.1. Particle size distribution

Figure 3.25 shows the results of the particle distribution analysis that was announced in section 3.2.1. The particle size distribution analysis was performed for the Portland cement type CEM I 42,5N (PC), the fine glass dust (FGD) and the standard CEN sand. These three components were all the dry materials that were used in the mix design, as described in section 3.2.7. Portland cement consisted of the smallest particle sizes, with particles ranging between 1 and 40 μm . The untreated fine glass dust had larger particle sizes and the distribution of these particles was between 3 and 200 μm . The CEN sand, which was used as the fine aggregates for the concrete mortar had the largest particle sizes, ranging between 100 and 2000 μm .

The cumulative particle size distribution of the fine glass dust showed a small number of particles with sizes <30 μm and the majority of particles ranging between 30 and 200 μm . The D10, D50 and D90 values of the dry materials are presented in table 3.4. The D10 value of Portland cement (PC) means that only 10 % of the particles in the sample was smaller than the specified value. The D50 and D90 values correspond to 50 % and 90 % respectively.

3.3.2. Thermogravimetric analysis

As reported in section 3.2.2 the TGA for the fine glass dust in this thesis was performed under air, because with the heat-treatment of the fine glass dust it was also heated under oxygen circumstances.

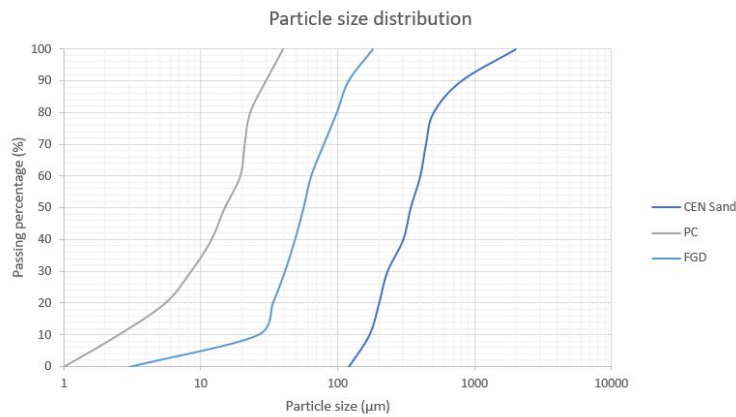


Figure 3.25: Particle size distribution of cement, fine glass dust and CEN sand

	PC	FGD	CEN sand
D10	2.48	25.98	168.83
D50	14.94	56.29	339.62
D90	29.92	120.15	801.33

Table 3.4: D10, D50 and D90 values of dry components (units are μm)

The main goal of the TGA was to find out at which temperatures there was a significant reduction of the fine glass dust mass. These were the temperatures at which part of the organic impurities were removed from the fine glass dust. These impurities had to be removed as much as possible in order to increase the reactivity of the fine glass dust when it was used as a cement replacement material in mortar mixtures. The results of the performed TGA under air are presented in Figure 3.26.

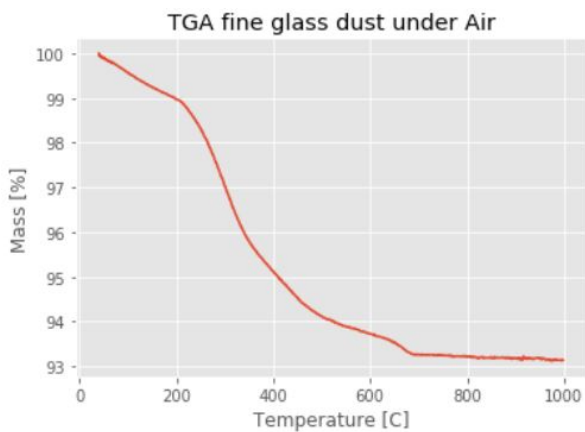


Figure 3.26: TGA results under air

The sample with fine glass dust was heated from 30°C until 1000°C during this TGA. It could be observed that the mass loss of the fine glass dust was minimal at temperatures between 30 and 200°C. The total mass loss over this segment was around 1%. A larger drop in the mass could be noticed at higher temperatures. Between 200 and 450°C the mass loss was around 4.5%, which indicated that a significant amount of organic compounds are removed from the fine glass dust at these temperature ranges. Between 450 and 650°C an additional mass loss of 1% could be found from the results. After 650°C the mass loss was very minimal (<0.5%) until the end point of the thermogravimetric analysis at 1000°C. The total mass loss of the fine glass dust over the full temperature interval was 6.8% (see Figure 3.26).

3.3.3. Heat-treatment of the fine glass dust

Based on the results that were shown in section 3.3.2, the different heat-treatment temperatures and heat-treatment times were chosen and this was reported in section 3.2.3. The heat-treatment temperatures were chosen based on large mass losses of the fine glass dust during the thermogravimetric analysis. It is apparent in figure 3.26 that at 450°C there was a large loss of mass of the fine glass dust and that after 700°C almost no mass loss occurred.

The results of the investigation of different heat-treatment temperatures and times are given in figure 3.27. The goal of this investigation was to find a specific heat-treatment that removed the largest amount of organic compounds as efficiently as possible. This means that for the analysis of the results the total mass loss of the sample had to be taken into account as well as the temperature and heating time, because a higher temperature and longer heat-treatment time, means more energy was consumed during the heat-treatment of the fine glass dust. It was also important to check that the fine glass dust did not melt during the heat-treatment, because then it would be very difficult to use it in a mortar mixture without excessive grinding.

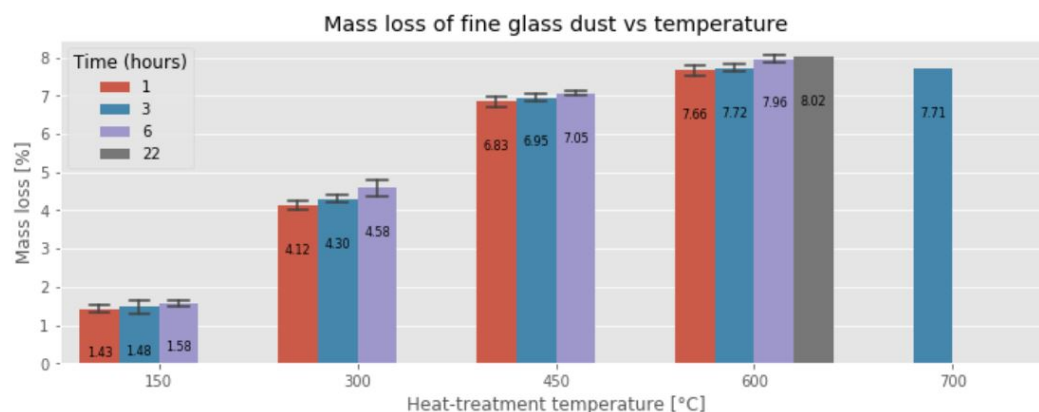


Figure 3.27: Comparison of mass loss at different heat-treatment temperatures and times

From Figure 3.27 it is apparent that for a heat-treatment of 700°C for 1 hour the total mass loss of the sample was 7.71%. The material that came out of the oven was one solid mass and the material was kind of melted. It could also be noticed that the material had a slight change of color. The entire sample that was extracted from the oven had lighter color, which could indicate that some darker organic compounds were removed from the fine glass dust.

For the next iteration the heat-treatment temperature was declined. Based on the results of section 3.3.2 600°C was chosen, because still a significant mass loss was observed for this temperature. For the heat-treatment temperature of 600°C different heat-treatment times were investigated. For all heat-treatments a minimum of 3 repetitions were performed and the mean value is reported in Figure 3.27. It is noticeable that for different treatment times at 600°C the mass loss was between 7.48% and 8.02%. Just as for 700°C, the entire sample that was extracted from the oven had undergone a slight color change and was a little bit lighter. The difference between 700°C and 600°C was that at 600°C the material that was collected from the oven was still in powdered form and could be easily used in a concrete mortar mixture without excessive grinding. For the treatment time of 22 hours it means that the oven has to be burning all night at high temperatures and the extra mass loss of the fine glass dust was relatively small compared to a treatment time of 6 hours (7.96% vs 8.02% respectively).

Because 600°C is still a very high temperature there was also investigated what happened when the temperature was decreased. A decrease in heat-treatment temperature meant that a lot of energy could be saved and the efficiency of the treatment could be improved if the same mass loss could be achieved. Based on Figure 3.26 a lower temperature at which still a significant amount of mass loss occurred was 450°C. Therefore 450°C was taken into account in this investigation for the most optimal and efficient heat-treatment. Three different heat-treatment times at 450°C were taken into account and the results in Figure 3.27 show a mass loss of the fine glass dust between 6.83% and 7.05% for treatment times between 1 and 6 hours. However the extracted samples from the oven at 450°C showed only a slight color change in the top layer of the sample, the bottom layer was completely un-

changed. It was discovered that there was a part of the material in which the organic impurities were not yet removed. This was the case for treatment times of 1, 3 and 6 hours.

Heat-treatment temperatures of 150°C and 300°C were also investigated to check the influence of low temperature heat-treatment on the fine glass dust. Heat-treatment at 150°C resulted in a mass loss of the fine glass dust between 1.43% and 1.58% between 1 and 6 hours of treatment time. At 150°C the temperature was too low to remove a significant part of the organic compounds from the fine glass dust and the mass loss was mainly caused by evaporation of water from the sample. The low mass loss at 150°C heat-treatment was also in agreement with Figure 3.26, in which the results of the TGA showed a mass loss of around 1% for 150°C.

Heat-treatment at 300°C resulted in a mass loss of the fine glass dust between 4.12% and 4.58% between 1 and 6 hours of treatment time. At 300°C the heat-treatment was successful in the removal of part of the organic compounds, but the mass loss was still 46% lower than heat-treatment at 600°C.

Based on the presented results in Figure 3.27 and the observations that were made on mass loss of the extracted samples from the oven during this investigation, the most efficient heat-treatment based on mass loss of the fine glass dust was 600°C for 1 hour. With this heat-treatment all the material undergoes a slight color change and the material from the oven was still in powdered form. The results of this investigation presented that at 600°C, 1 hour was the most efficient heat-treatment time compared to the other investigated treatment times of 3, 6 and 22 hours. The increase in mass loss for longer treatment times was smaller than 0.5%. For the continuation of this thesis there was continued to work with the most optimal and efficient heat-treatment in terms of maximal mass loss of the fine glass dust: 600°C and 1 hour.

Determination of organic content

In section 3.2.3 it was announced that in order to investigate the effectiveness of the heat-treatment, the untreated fine glass dust had to be compared with the heat-treated fine glass dust. Therefore the organic content of both samples had to be determined. The results of the organic content determination are given in Table 3.5

	Temperature (°C)	Mass loss (%)
Untreated FGD	105	1,22
Untreated FGD	600	6,76
600°C heat-treated FGD	105	0,14
600°C heat-treated FGD	600	0,16

Table 3.5: Organic content determination of fine glass dust

The organic content was determined based on the method that is given in section 3.2.3 and this resulted in mass loss of 1.22% for the untreated fine glass dust after 24 hours of drying at 105°C. The organic content of the untreated fine glass dust was found to be 6.76% after heating for 4 hours at 600°C.

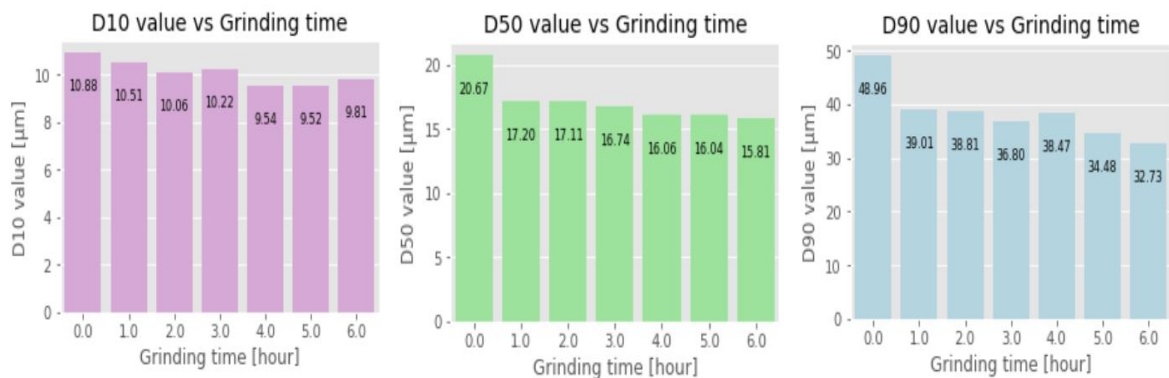
The efficiency of the heat-treatment to remove the organic impurities from the fine glass dust is also shown in Table 3.5. The mass loss after drying at 105°C was 0.14% for the heat-treated fine glass dust and the organic content was determined at 0.16% after heating at 600°C for 4 hours. The results showed that after the heat-treatment of 600°C the fine glass dust still contained a very small amount of organic impurities, but the largest part was effectively removed by the heat treatment. Because of the heat-treatment at 600°C the organic content of the fine glass dust was decreased from 6.76% to 0.16%.

3.3.4. Grinding treatment of the fine glass dust

As reported in section 3.2.4 the main goal of the grinding treatment was to increase the fineness of the fine glass dust particles, because finer glass powder has shown to possess more initial reactivity, pozzolanic activity and better mitigation against ASR [2][132]. Increased pozzolanic reactivity can benefit the early age strength development of the glass dust concrete and can also contribute to later age strength development, because secondary C-S-H products are formed by the pozzolanic reaction of

the fine glass dust [113].

The grinding treatment in the Ball Mill machine was performed for different grinding times. For each of these grinding times a small batch of material was collected and the particle size distribution was determined and also the D10, D50 and D90 values were determined. In section 3.3.1 it was explained what D10, D50 and D90 values mean. The results of the particle size distribution analysis after different grinding times are presented in Figure 3.28a-3.28c. From these results it is apparent that there was a significant reduction in particle sizes after grinding the fine glass dust. It could be observed that the unground fine glass dust had the largest values for D10, D50 and D90 and that these values decreased after grinding. It could also be noticed that a longer grinding time means that the D10, D50 and D90 values decreased. This trend can be seen in Figure 3.28, but the differences in particle sizes between 1 hour grinding and 6 hour grinding were only larger than 15% for the large particles in the D90 values (6.7% for D10, 8.1% for D50 and 16.1% for D90).



(a) D10 particle size

(b) D50 particle size

(c) D90 particle size

Figure 3.28: D10, D50 and D90 particle sizes of fine glass dust after different grinding treatments

The D10 values in Figure 3.28a decreased from 10.88 μm for 0 hours to 10.51 μm for 1 hour to 9.81 μm for 6 hours grinding treatment. The D50 values in Figure 3.28b decreased from 20.67 μm for 0 hours to 17.20 μm for 1 hour to 15.81 μm for 6 hours of grinding treatment. The D90 values in Figure 3.28c decreased from 48.96 μm for 0 hours to 39.01 μm for 1 hour to 32.72 μm for 6 hours of grinding treatment. Observation could be made that the grinding treatment did not very efficiently decrease the smaller particles of the fine glass dust (only 3.4% decrease in particle size for D10 after 1 hour of grinding), but was much more effective in decreasing the large particles of the fine glass dust, which resulted in a larger reduction of D50 and D90 values (16.8% and 20.3% decrease in particle size respectively after 1 hour of grinding).

As declared in section 3.2.4 also Maltha BV had the possibility to perform a grinding treatment at their own factory. The Maltha ground fine glass dust was also taken into account in the mix design in section 3.2.7 and in the tests on compressive strength, initial setting time and slump/slump flow.

For the different grinding times that were investigated in this section only 1 hour grind and 6 hours grind were taken into account for the rest of this research to investigate what is the consequence on the properties of the mortar mixtures was, when ground fine glass dust was used as a cement replacement in the binder.

3.3.5. BET specific surface area

As reported in section 3.2.5 the main goal of the BET specific surface analysis was to investigate the effect of the different pre-treatment methods on the BET specific area of the fine glass dust. A large specific area means that the particles of the fine glass dust have a larger available surface area which can react during the hydration reaction and pozzolanic reaction in the mortar mixture.

The results of the BET specific surface area analysis are presented in Table 3.6. The untreated fine glass dust had a BET surface area of 0.8256 cm^2/g . After the heat treatment at 600°C (section 3.2.3) the surface area of the fine glass dust was increased to 0.9347 cm^2/g . The removal of organic compounds by the thermal treatment had a positive impact on the surface area of the fine glass dust.

If these organic compounds were removed, the surface area of the fine glass dust increased by 13.2% due to the heat-treatment.

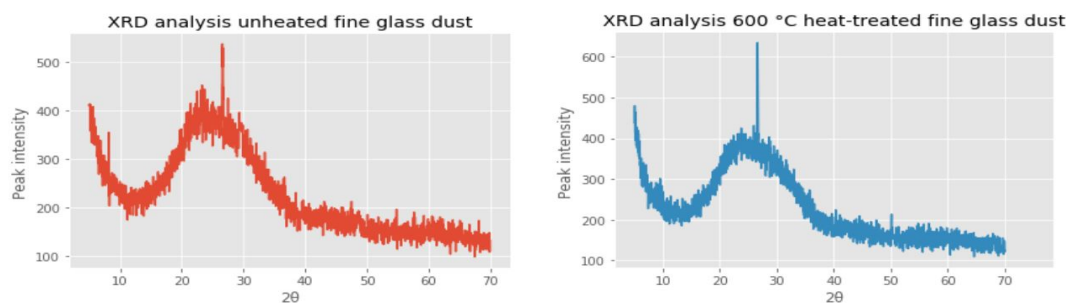
Material	BET specific area (cm ² /g)
Untreated FGD	0.8256
600°C heat-treated FGD	0.9347
600°C heat-treated FGD + 1 hr grinding	2.2232
600°C heat-treated FGD + 6 hr grinding	2.4931

Table 3.6: Results BET analysis for fine glass dust

After a combination of heat-treatment at 600°C and a grinding treatment of 1 hour and 6 hours (section 3.2.4) the surface area increased to 2.2232 and 2.4941 cm²/g respectively. This means that the grinding treatment in the ball mill machine had a large impact on the BET surface area of the fine glass dust, which increased by 137.9% and 166.7% after the grinding treatment of 1 and 6 hours respectively. These findings were also in accordance with the findings in section 3.3.4. The grinding treatment removed the large particles and led to finer particle size for the fine glass dust. An increased fineness of the particles means that there were more small particles, which led to a larger available surface for each gram of material. Based on the results it could be reported that both the heat-treatment as well as the grinding treatment were positively influencing the BET specific surface area of the fine glass dust.

3.3.6. X-Ray Diffraction

The results of the XRD analysis that was described in section 3.2.6 are given in Figure 3.29. The goal of the XRD analysis was to determine if the fine glass dust consisted of amorphous silica and also to check whether the heat-treatment of 600°C did lead to an increase in the number of crystalline phases present. These crystalline phases could have a negative effect on the reactivity of the fine glass dust and therefore on the strength development when the fine glass dust was used in mortar mixtures as Portland cement replacement.



(a) XRD analysis of unheated fine glass dust

(b) XRD analysis of 600°C heat-treated fine glass dust

Figure 3.29: Results XRD analysis of fine glass dust

In Figure 3.29a the diffraction angle 2θ is plotted against the peak intensity for the unheated glass powder. As expected and described in section 2.1 the unheated fine glass dust contained large amounts of amorphous silica. The results showed a broad, amorphous "mountain" between 2θ values of 5 and 70, instead of a graph with sharp peaks. Sharp peaks in intensities would indicate the presence of specific crystalline compounds in the fine glass dust, but the majority of the peak intensities were in the same order and there were almost no specific 2θ values at which a sharp peak could be observed. From Figure 3.29a only a small peak could be noticed around the 2θ value of 26.616. Solving Bragg's Law for the interplanar d-spacing from the 2θ value, led to the crystalline phase of SiO₂ that was present in very small amounts [97]. The major part consisted of amorphous silica and this was also in accordance with the findings of SGS Intron [48] in Figure 2.2.

In Figure 3.29b the XRD analysis results of the 600°C heat-treated fine glass dust are displayed. In this graph also 2θ was plotted against the peak intensity. For the heat-treated fine glass dust it could

also be seen that the major part consisted of amorphous silica and that almost no sharp peak intensities could be observed. Also in this case a small peak at a 2θ value of 26.616 could be noticed, which showed a small amount of SiO_2 that was present in crystalline form [97].

In Figure 3.30 the results of the XRD analysis of the unheated and heat-treated fine glass dust are plotted together in one figure. In this comparison it can be clearly seen that the heat-treatment of the fine glass dust at 600°C did not influence the amorphous silica content and did also not lead to the formation of new crystalline phases under the high temperatures in the oven. The small peak for the crystalline phases of SiO_2 occurred at exactly the same position and was in the same order of peak intensity.

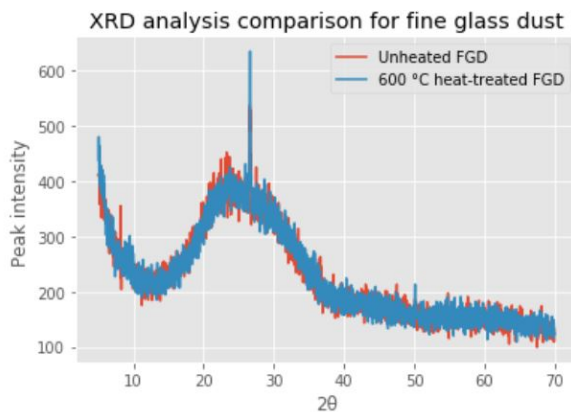


Figure 3.30: XRD analysis comparison of unheated and heat-treated fine glass dust

3.3.7. Slump and Slump flow

Slump and slump flow tests were performed for mix 1 - mix 6. The test procedure was explained in section 3.2.8 and the goal of the slump and slump flow tests was to investigate how the fresh-state properties of the mortar mixtures changed when fine glass dust was added to the mixture. Also the influence of the different pre-treatments of the fine glass dust on the fresh-state behaviour could be investigated.

The results of the slump test are presented in Figure 3.31. For each mixture 3 repetitions were performed and the slump value for each mixture was measured directly after mixing. The slump value was defined as the height after removing the Hägermann cone from the mixture, so a lower slump value meant a larger decrease in height after removing the cone.

The average slump value for the reference mixture (mix 1) was 5.57 cm. If untreated fine glass dust was implemented in the mixture (mix 2) the slump value decreased to 5.37 cm. All the mixtures with heat-treated and/or ground fine glass dust had a slump value in a similar range. The mean slump value for all the mixtures was between 5.67 and 5.27 cm. Between mix 3, mix 5 and mix 6 a small decreasing trend could be discovered. This showed that a grinding treatment for a longer time resulted in a lower slump value. However the differences in this noticed trend were not larger than 7%.

The results of the slump flow tests are presented in Figure 3.32. Also for the slump flow tests for each mixture 3 repetitions were performed directly after performing the slump tests. The slump flow diameter was measured in 4 different directions after 25 drops of the compaction table and the average value was taken. The measured slump flow diameter was an indication of the flowability of the mixtures.

The average slump flow diameter for the reference mixture (mix 1) was 22.17 cm. If untreated fine glass dust was implemented in the mixture (mix 2) the slump flow diameter decreased to 20.17 cm. This meant that the flowability of the mortar mixture slightly decreased by 9.0% if untreated fine glass dust was used as cement replacement in the mixture. For the different pre-treatments (mix 3 - mix 6) the slump flow diameter increased from the untreated fine glass dust mixture, but this difference was a maximum of 2.9%; an increase from 20.17 cm to 20.75 cm for 600°C heat-treatment and 6 hours grinding treatment.

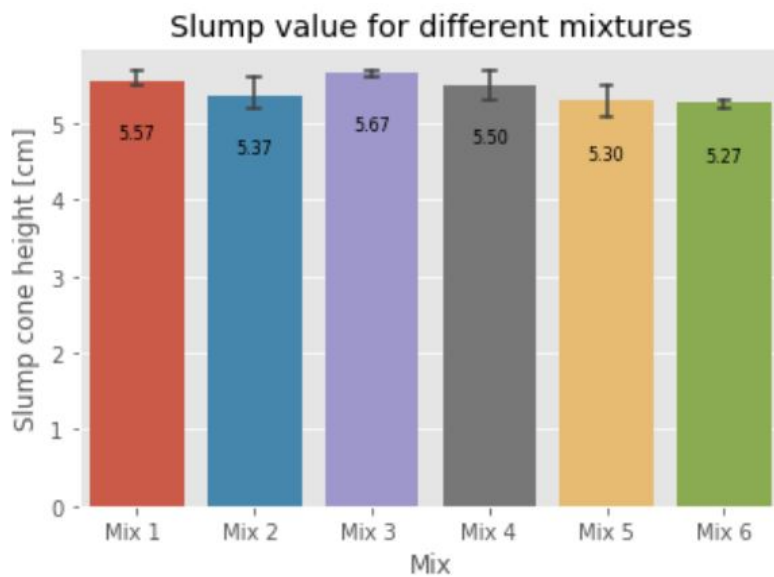


Figure 3.31: Slump results for mix 1-6

Based on the results of the slump and slump flow tests it could be declared that the different pre-treatments and replacement of Portland cement with fine glass dust at 15% had little influence on the investigated fresh-state properties of the mortar mixtures. Similar slump values were found for all different mixtures (maximum 7% difference) and for the slump flow diameter a decrease could be observed if fine glass dust was implemented in the mixtures compared to the reference mixture, but this difference was not very significant, only a reduction of maximum 9%. Between the different pre-treatment methods (Mix 2-Mix 6) the differences in slump flow values were even smaller than 3%.

3.3.8. Initial setting time

Initial setting time tests as described in section 3.2.9 were performed for mix 1 till mix 6. The goal of the initial setting time tests was to investigate the early stage reactivity of the mortar mixtures where fine glass dust with different pre-treatments was implemented in the binder. A comparison of the initial setting times of the different mixtures could say something about the early stiffness development after mixing. For each mixture 3 repetitions were performed and the results of the Vicat tests are presented in Figure 3.33.

The reference mixture without fine glass dust (mix 1) had a mean initial setting time of 219.67 minutes. If fine glass dust was added to the mixture without pre-treatment (mix 2), then the initial setting time increased to an average value of 303 minutes. This increase in initial setting time of 37.9% meant that the stiffness development was slower than for the reference mixture. In section 3.3.3 it was shown that the heat-treatment of 600°C could effectively reduce the number of organic compounds. This was in agreement with the findings in Figure 3.33, where mix 3 had a mean initial setting time of 208 minutes, which was a reduction of initial setting time of 31.3% compared to the untreated fine glass dust. The initial setting time of mix 3 was in the same order as the initial setting time of the reference mix.

The results of mix 4 - mix 6 showed that a heating + grinding treatment led to a slight decrease in the setting time. Additional grinding treatment after heating caused the initial setting time to reduce to 179 and 166 minutes, which was a decrease of 13.9%-20.2% from mix 3 with only heat-treatment. This meant that the increased fineness of the particle sizes could lead to increased reactivity of the fine glass dust and therefore a faster stiffness development. After heating and grinding treatments in all mixtures (mix 4 - mix 6) the initial setting time was lower than for the reference mixture. The results from Figure 3.33 showed that both heat-treatment and grinding treatment led to a higher reactivity and a faster stiffness development for the mortar mixtures when fine glass dust was implemented. This was also in accordance with the findings in sections 3.3.5 and 3.3.9.

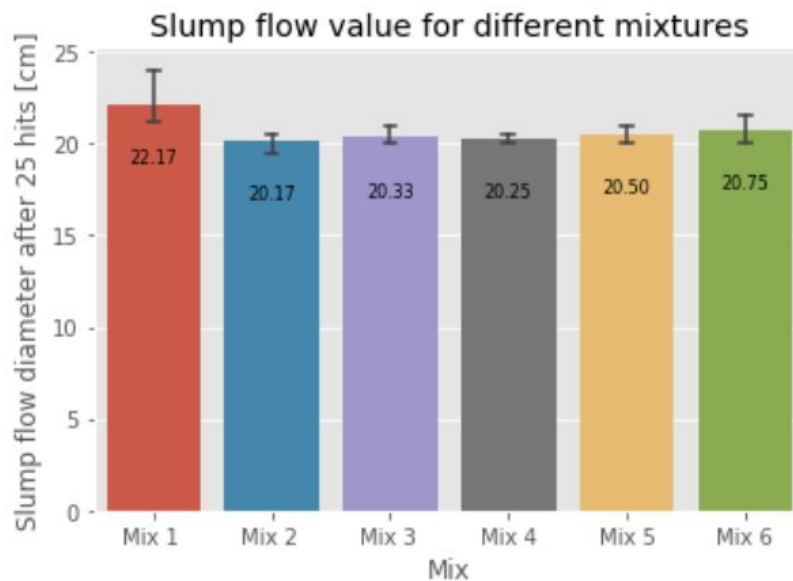


Figure 3.32: Slump flow results for mix 1-6

3.3.9. Compressive strength

As reported in section 3.2.10 compressive strength tests had to be performed in order to investigate the influence of heat-treatment and different grinding treatments of fine glass dust on the compressive strength of mortar mixtures. In this phase of the thesis the goal was to find the optimal pre-treatment for the fine glass dust with as little time and energy consumption as possible. In order to find the most efficient combination of heat-treatment and grinding treatment, different mix designs were developed. The mix designs that were investigated in this part of the thesis were described in section 3.2.7 and given in Table 3.7. Here the percentage replacement of Portland cement (PC) with fine glass dust (FGD) and all other material ratios were constant in order to only investigate the influence of pre-treatment of the fine glass dust.

Mix	PC	FGD	Sand	Water	Type of pre-treatment
Mix 1	100	0	300	50	-
Mix 2	85	15	300	50	-
Mix 3	85	15	300	50	600°C heat-treatment
Mix 4	85	15	300	50	600°C heat-treatment and Maltha grinding treatment
Mix 5	85	15	300	50	600°C heat-treatment and 1 hour grinding treatment
Mix 6	85	15	300	50	600°C heat-treatment and 6 hours grinding treatment

Table 3.7: Overview of different mix compositions (% of binder mass)

Casting session I

The results of the compressive strength tests on mold-cast mortar for the different mix designs are displayed in Figure 3.34. Compressive strength tests were performed at 3, 7, 28 and 90 days. 90 days compressive strength was taken into account because the possible pozzolanic reaction of the fine glass dust is a slow reaction that could contribute to the secondary formation of C-S-H and therefore later stage strength development of the mortar. If the fine glass dust performed pozzolanic activity, then this could be assessed after 90 days of curing. This was discussed in more detail in sections 2.2.2 and 3.2.10.

For all curing ages 6 repetitions were performed for each mixture. The mean value of these results is presented in Figure 3.34 as well as the variation around the mean value. The reference mix without fine glass dust (Mix 1) had a mean compressive strength of 16.15 Mpa after 3 days, which increased to

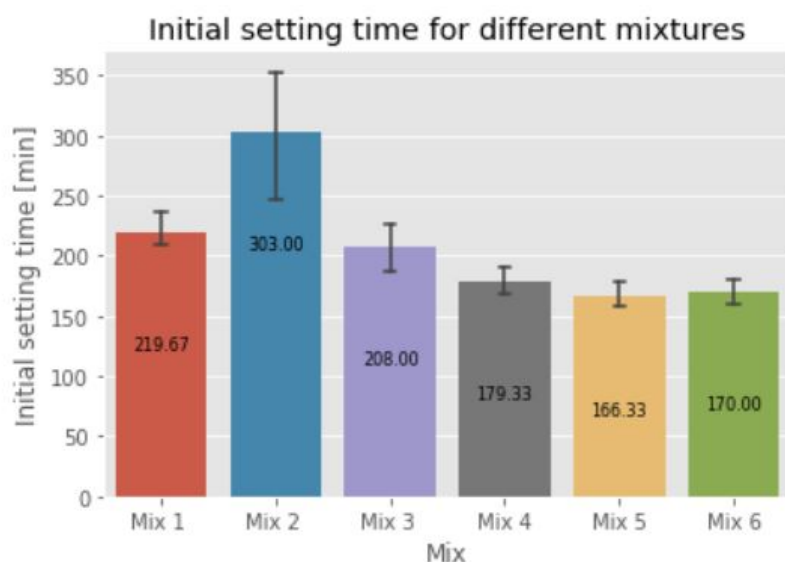


Figure 3.33: Initial setting time results for mix 1-6

24.73 MPa after 7 days, 37.86 MPa at 28 days and 41.98 MPa at 90 days. It was noticeable that early age strength development was fast for the reference mixture compared to the other mixtures, where fine glass dust was used to partially replace Portland cement.

From Figure 3.34 it can be seen that both mix 2 and mix 4 resulted in low strength development. For mix 2 this was expected, because this mix had untreated FGD. Mix 4 had FGD that was heat-treated and ground by Maltha, but provided very low strength development. Mix 3, mix 5 and mix 6 resulted in higher strength development. The additional grinding treatment for mix 5 and 6 caused a fast strength development after 3 days of curing, compared to mix 3. At longer curing ages the differences were small and mix 3, mix 5 and mix 6 reached compressive strength values of 28-31 MPa after 28 days of curing and 36-39 MPa after 90 days of curing.

Compared to the reference mix it can be seen in Figure 3.34 that the mixtures with FGD as cement replacement had lower strength development than the reference mix for all curing ages. Mix 3, mix 5 and mix 6 provided the best results in terms of strength development relative to the reference mix (see Table 3.8). For all investigated curing ages mix 3 with heat-treated FGD reached a relative compressive strength of 73-92% compared to the reference mix. Mix 5 and 6 with heat-treated and ground FGD reached a relative compressive strength of 92-95% after 3 days of curing, but for longer curing ages between 7 and 90 days this percentage dropped to 76-90% compared to the reference mix.

As discussed in section 3.2.10 the fine glass dust could possibly possess any pozzolanic behaviour. Pozzolanic activity of the FGD would mean that there was a slow reaction of secondary C-S-H formation, which caused long-term strength development. When the relative compressive strength percentages in Table 3.8 are reviewed it can be stated that there was higher strength development at curing ages of 90 days for the mixtures with FGD. For mix 3 with the heat-treated FGD an increase in relative strength could be observed and also the mixtures 5 and 6 with heat-treated and ground FGD showed an observable increase after 90 days of curing. The goal of the compressive strength test was to inves-

Curing age	Mix 2	Mix 3	Mix 4	Mix 5	Mix 6
3 days	62	73	70	92	95
7 days	65	78	69	84	88
28 days	61	84	66	79	76
90 days	68	92	65	86	90

Table 3.8: Compressive strength relative to reference mix (%)

investigate what was the influence of different fine glass dust pre-treatments on the compressive strength development of mortar where Portland cement was replaced with FGD. The results showed that untreated FGD (mix 2) provided the worst results, followed by the grinding treatment by Maltha (mix 4). Heat-treatment of the FGD (mix 3) provided a significant increase in strength development compared to the untreated FGD. Grinding of the FGD in addition to the heat-treatment (mix 5 and 6) provided an increase in compressive strength development at an early curing age. The difference between 1 hour and 6 hours of grinding was negligible. Therefore the most promising mixtures to further investigate based on the compressive strength results were mix 3 and mix 5.

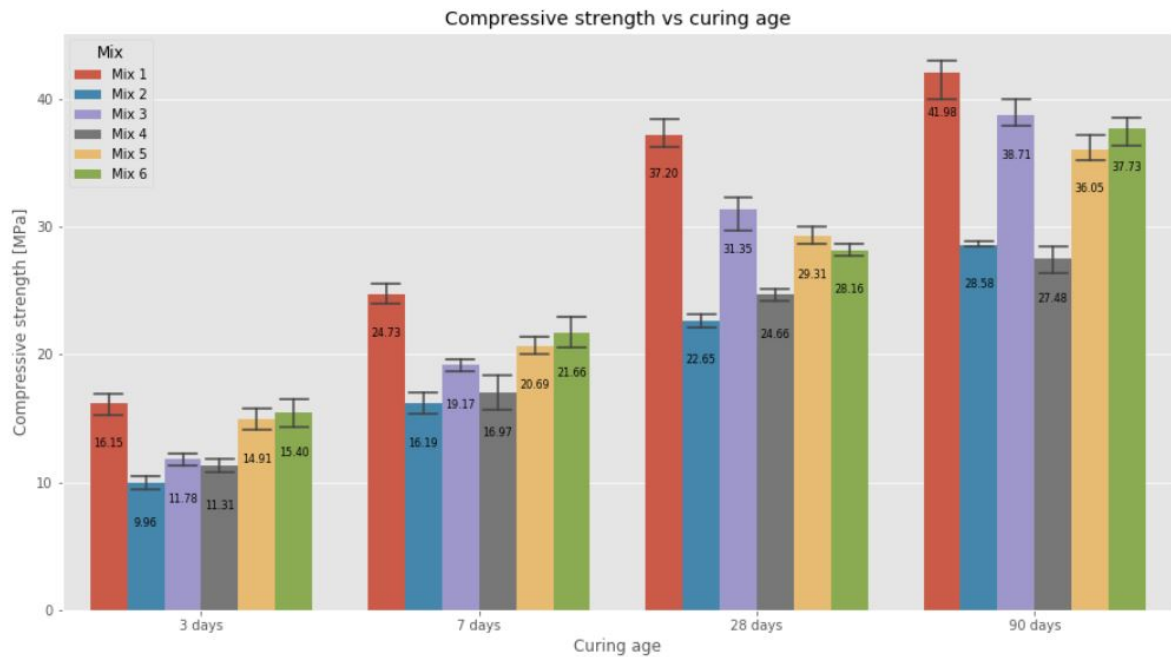


Figure 3.34: Compressive strength results for mix 1-6 at different curing ages

Casting session II

The casting process of mix 1-3 and mix 4-6 was two weeks apart, therefore different casting circumstances or differences in casting quality could be a possible influence on the results of casting session I. To increase the validity of the results and to eliminate the possibility of differences in casting circumstances mix 1, mix 3 and mix 5 were cast again, but all on the same day to ensure equal casting quality. The mixtures were cast with cement type CEM I 52.5R, because in Chapter 5 the focus of the research will be on 3D Concrete printing and CEM I 52.5R is generally used for this. The mix design for the validating casting session II is given in Table 3.9. The replacement percentage of FGD in the binder was kept constant at 15%, just as for the first casting session. Also sand/binder ratio was kept at 3, water/binder ratio was kept at 0.5 and standard CEN Sand was used as fine aggregates.

Mix	PC	FGD	CEN Sand	Water	Type of pre-treatment
Mix 1-2	100	0	300	50	-
Mix 3-2	85	15	300	50	600°C heat-treatment
Mix 5-2	85	15	300	50	600°C heat-treatment and 1 hr grinding treatment

Table 3.9: Mix compositions for validation casting session II (% of binder mass)

After casting the mortar prisms, compressive strength test was performed again for 3 days, 7 days, 28 days and 56 days of curing. For each mixture 6 repetitions were performed for all the curing ages and the mean value was reported. The goal of these renewed tests was to validate the results that are shown in Figure 3.34 and to eliminate casting differences as much as possible. The results of the compressive strength test for casting session II are presented in Figure 3.35.

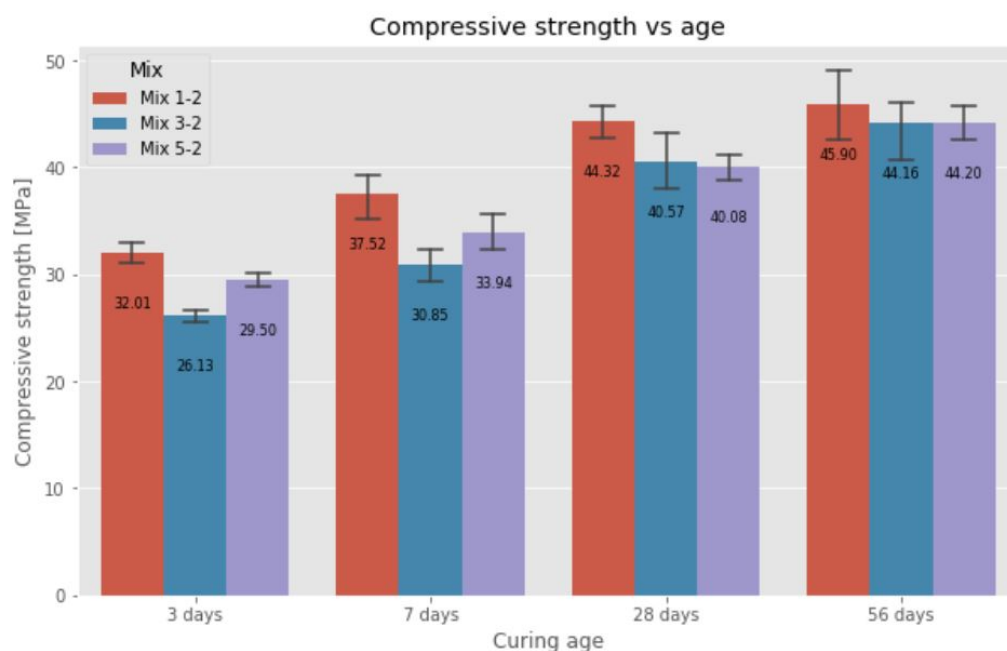


Figure 3.35: Compressive strength development for Mix 1, Mix 3 and Mix 5 in casting session II

After 3 days of curing the reference Mix 1-2 had developed a strength of 32.01 MPa. The rapid strength gain at early age was caused by the cement type CEM I 52.5R that was used. This cement type has a higher cement strength class than CEM I 42.5N and also has high early strength gain, compared to the normal early strength gain for CEM I 42.5N (Rapid vs Normal). From Figure 3.35 it can be seen that at early stages the heating + grinding treatment of the fine glass dust in Mix 5-2 caused more strength gain than only heat-treatment in Mix 3-2. After 3 days Mix 3-2 and Mix 5-2 had a strength of 26.13 and 29.50 MPa respectively. The additional grinding of the fine glass dust caused an increase in the compressive strength of 12.8% after 3 days.

After 7 days of curing the reference Mix 1-2 had developed a strength of 37.52 MPa. The additional grinding treatment of the fine glass dust in Mix 5-2 still caused more strength development after 7 days of curing compared to only heat-treatment in Mix 3-2. After 7 days Mix 3-2 and Mix 5-2 had a strength of 30.85 and 33.94 respectively, so the additional grinding of the fine glass dust caused an increase in the compressive strength of 10% after 7 days.

After 28 days of curing the reference Mix 1-2 had developed a strength of 44.32 MPa. From Figure 3.35 it can be seen that Mix 3-2 and Mix 5-2 showed comparable compressive strength results after 28 days of curing and had compressive strength values of 40.57 and 40.08 MPa respectively. After 28 days the additional grinding in Mix 5-2 did not lead to an increase in compressive strength and gave similar results as Mix 3-2 with only heat-treatment.

After 56 days of curing the reference Mix 1-2 had developed a strength of 45.90 MPa. Mix 3-2 and Mix 5-2 showed comparable compressive strength results after 28 days of curing and had compressive strength values of 44.16 and 44.20 MPa respectively. From Figure 3.35 it can be seen that between 28 and 56 days the increase in strength was larger for the mixtures with FGD than the reference mix and that 96% of reference strength could be reached by both mix 3-2 and mix 5-2.

In Table 3.10 the relative strength indexes compared to the reference mix 1-2 are presented for Mix 3-2 and Mix 5-2. It can be seen that at curing ages 3 and 7 days the mixture with only heat-treatment could reach 82% of the reference mix strength, while the mixture with heat-treatment + grinding could reach a relative strength index of 90-92%. At longer curing ages both Mix 3-2 and Mix 5-2 provided

similar relative strength indexes and between 90-96% of the reference mix strength could be obtained when 15% fine glass dust was used to replace CEM I 52.5R in the binder.

Curing age	Mix 3-2	Mix 5-2
3 days	82	92
7 days	82	90
28 days	92	90
56 days	96	96

Table 3.10: Compressive strength index relative to reference mix for casting session II (%)

When Figures 3.34 and 3.35 are compared it can be seen that a similar trend could be observed between Mix 1, Mix 3 and Mix 5 for both casting sessions. For curing ages 3 and 7 days the additional grinding treatment in Mix 5 could cause an increase in strength development of 10-12%. For curing ages of 28 days and longer the additional grinding treatment did not lead to higher strength development and Mix 3 and Mix 5 provided comparable results. The results of Figure 3.34 were validated by the results that are shown in Figure 3.35 and potential casting differences that could influence the results were eliminated as far as possible. For casting session II the mixtures with fine glass dust could reach up to 90-96% of reference mixture strength.

Influence of heat-treatment temperature on the compressive strength development

In section 3.2.10 it was described that mixtures with different heat-treatment temperatures were tested on compressive strength. This was done to investigate the influence of heat-treatment temperature on the compressive strength development of the mortar. 600°C was found to be the maximum temperature at which the fine glass dust could be pre-treated and used as a powder afterwards. For higher temperatures the materials melted and was not sufficiently treatable anymore. Lower treatment temperatures could provide energy and cost savings if this provided promising results. The results from the heat-treatment temperature investigation are shown in Figure 3.36.

The relation between heat-treatment temperature and compressive strength could be clearly seen for

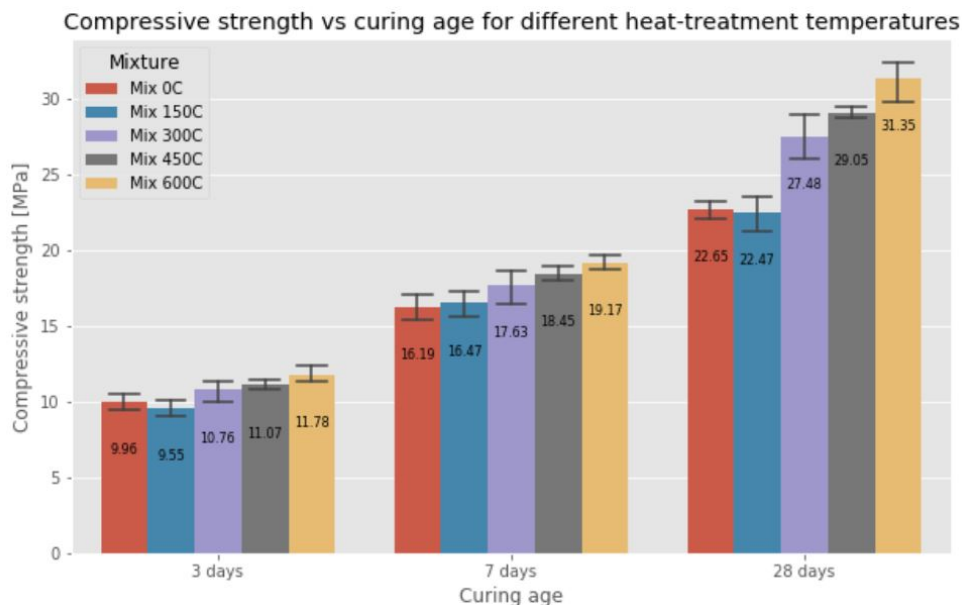


Figure 3.36: Compressive strength development for different heat-treatment temperatures

all curing ages. A higher heat-treatment temperature means that it was more effective for removing organic compounds, which had a delaying effect on the hydration reaction in the mortar. This had a positive influence on the compressive strength development. Fine glass dust without heat-treatment

and fine glass dust with a heat-treatment of 600°C were already investigated in Figure 3.34 in which these represented Mix 2 and Mix 3. Figure 3.36 shows that heat-treatment temperatures of 150, 300 and 450°C provided results that are almost linear between 0 and 600°C. The mixture with 150°C heat-treated fine glass dust provided similar results to the mixture with the untreated fine glass dust for all curing ages. It could be stated that a heat-treatment temperature of 150°C was too low to effectively remove organic compounds from the fine glass dust. Heat-treatment temperatures of 300 and 450°C showed a significant increase in compressive strength development and could reach 27.48 and 29.05 MPa after 28 days of curing, which represented an increase of 21.3% and 28.3% respectively compared to the untreated fine glass dust. The mixture with 600°C heat-treated fine glass dust presented the highest compressive strength development and could reach 31.35 MPa after 28 days of curing. This represented an increase of 7.9% compared to the mixture with 450°C heat-treated fine glass dust.

Based on the provided results from the heat-treatment temperature investigation it could be stated that a higher treatment temperature provides higher strength development. This could be attributed to the fact that at higher temperatures more organic compounds were removed from the fine glass dust, which meant that fewer of these delaying compounds were left to have a slowing effect on the hydration. Heat-treatment of 600°C provided the maximum results for the compressive strength while ensuring that the fine glass dust was sufficiently treatable in powdered form after heating. Lower heat-treatment temperatures could save energy and therefore costs, but this was matched by a loss of compressive strength of around 8% between 450 and 600°C. This was the reason that the 600°C heat-treatment was used for all the fine glass dust that was used in the remainder of this thesis.

3.4. Discussions

3.4.1. The effect of different pre-treatment methods for the fine glass dust on fresh properties

Flowability

The objective of the slump flow test in section 3.3.7 was to find the influence of fine glass dust and different pre-treatments of this fine glass dust on the flowability of mortar mixtures where 15% of Portland cement was replaced by fine glass dust. The results suggest that the slump flow diameter after 25 drops decreased compared to the reference mixture when untreated fine glass dust was used to replace Portland cement in the binder. This means that adding untreated fine glass dust to the mixture would enhance shape retention behaviour, but reduces the flowability of the mixture. Pre-treatment of the fine glass dust in the form of heat-treatment and grinding treatment have shown to increase the slump flow diameters by very small amounts (see Figure 3.32). This means that the heat-treatment and a combination of heat-treatment + grinding reduced the shape retention behaviour a little bit, but a small increase in the flowability of the mixture could be observed. Possible reasons for the changes in flowability by adding untreated or pre-treated fine glass dust to the mixtures are analyzed in this section.

One possible explanation for the reduced flowability when fine glass dust is used in the mixture is due to the large number of organic compounds that are present in the untreated fine glass dust. These organic compounds originate from the production method of fine glass dust and play an important role for the properties of fine glass dust mortar mixtures. Because of the high amount of organic compounds, the fine glass dust consists of a lot of irregularities. This high degree of irregularities in the particles of the fine glass dust decreased the particle packing and caused a lower flowability compared to the reference mixture where only Portland cement was used in the binder [42]. Due to the heat-treatment of the fine glass dust part of the organic compounds can be effectively removed. This means that the flowability of the mixture can be improved by a small amount, but also for the pre-treated fine glass dust mixtures the flowability is lower than the reference mixture. Once again this can be attributed to the higher degree of irregularities when fine glass dust is combined with Portland cement in the binder.

The second possible interpretation for the reduced flowability when fine glass dust is used in the mixture is due to the particle size of the fine glass dust. The untreated fine glass dust has larger particle sizes than the Portland cement, which was shown in Figure 3.25. This difference in particle sizes leads to a sub-optimal particle packing, which causes a decrease in the flowability and workability of the mortar mixtures when untreated fine glass dust is used. Due to the grinding treatment of the fine glass dust

the particle sizes can be decreased, which leads to an increase in particle packing when fine glass dust is combined with Portland cement in the binder. A longer grinding time has shown to reduce the particle sizes and this is also in line with the results of Figure 3.32, where mixtures with longer grinding times presented higher flowability values. The finer fine glass dust might have contributed to improving the flowability, which can be explained by the optimization of particle packing in the mixture but also by the filler effect of the fine particles. This filler effect made the finer particles easier to replace the water which was enclosed in the voids of the structures in the mortar. The released water is then available to reduce the friction between the particles and therefore increase the flowability [18]. Even after 6 hours of grinding there are still differences in particle sizes between the Portland cement and fine glass dust, which means that the flowability is still lower than the reference mixture.

The findings on the effect of fine glass dust and different pre-treatment methods on the flowability of the mortar are in agreement with the findings of Lu et al. [69]. In this research waste glass powders (WGP) with different grinding times were used to replace Portland cement in the binder. It was found that the WGP with the shortest grinding time had the lowest flowability and the WGP with the longest grinding time had the highest flowability. So this research also found that the use of fine glass powder reduced the flowability, but this can be improved by grinding the material until finer particle sizes. However the findings of Lu et al. showed that the flowability of 4 hour ground WGP was similar to the reference mixture, while in this research 6 hours grinding of the fine glass dust was not enough to reach comparable values to the reference mixture. This difference can be explained by the fact that the WGP and the fine glass dust have different particle sizes and irregularities, which both influence the flowability. Also a different percentage of glass powder was used to replace Portland cement in both studies.

So based on the provided results and discussion about the flowability of fine glass dust mortar mixtures it can be indicated that the untreated fine glass dust leads to a reduction of flowability compared to the reference mixture. Both heat-treatment and grinding treatment lead to small improvements in flowability, but still lower than the reference mixture in which no fine glass dust is used.

Initial setting time

The objective of the initial setting time test in section 3.3.8 was to find the influence of fine glass dust and different pre-treatments of this fine glass dust on the initial setting time of mortar mixture where 15% of Portland cement was replaced by fine glass dust. The results indicated that the initial setting time increased compared to the reference mixture when untreated fine glass dust was used to replace Portland cement in the binder. This means that the addition of untreated fine glass dust to the mixture had a negative effect on stiffness development directly after mixing. Pre-treatment of the fine glass dust in the form of heat-treatment at 600°C has shown to decrease the initial setting time to comparable levels as the reference mixture. Additional grinding on top of the heat-treatment could reduce the initial setting time even further, so that the initial setting time of the fine glass dust mixtures was lower and the stiffness development was faster than the reference mixture. This indicated that the pre-treatment in the form of heat-treatment and grinding both had a positive influence on the reduction of the initial setting time. Possible reasons for the changes in initial setting time by adding untreated or pre-treated fine glass dust to the mixture are analyzed in this section.

One possible interpretation for the increase in initial setting time when untreated fine glass dust was used to replace Portland cement in the binder is due to the high amount of organic compounds in the fine glass dust. The main source of stiffness development for the mortar mixtures is the hydration reaction of the cement. With the hydration reaction the unhydrated cement particles were changed into hydration reaction products, which formed a crystallized structure called C-S-H gel. The development of C-S-H gel was the main cause of stiffness development and thus an influence on the initial setting time. When fine glass dust was used to replace Portland cement this meant that fewer cement particles were available for hydration, which caused a slower development of C-S-H gel formation [67]. On top of this came the fact that the fine glass dust consisted of a high amount of organic compounds. These organic compounds are known to have a delaying effect on the hydration of the cement particles in the binder. Organic compounds in the fine glass dust can increase the end time of cement hydration induction and delay the occurrence of a secondary exothermic peak in hydration. This indicated that the organic compounds mainly had a delaying effect on the early stage hydration reaction rate (hydration

induction and acceleration). This prevented the fast formation of hydration reaction products directly after mixing and therefore led to a slower stiffness development and a larger initial setting time.

Heat-treatment of the fine glass dust has shown to be efficient in removing the organic compounds from the fine glass dust in section 3.3.3. After heat-treatment the fine glass dust contains a lower amount of organic compounds, which means that there is less delay in the hydration reaction, there is a faster initial formation of C-S-H gel and thus a reduction in the initial setting time.

A second possible explanation for the increase in initial setting time when fine glass dust was used to replace Portland cement in the binder, is regarding the larger particle size and the smooth surface of the glass particles in the fine glass dust. The larger difference in particle sizes between the fine glass dust and the Portland cement and the smooth surface rendered more water available for initial hydrolysis and this caused an increase in effective water/cement ratio. Cement mortar mixtures with a higher effective water/cement ratio, take a longer time to form a rigid structure of the cement hydration products [17]. This resulted in a slower formation of C-S-H gel, a slower stiffness development and therefore an increase in the initial setting time when fine glass dust is used in the mortar mixture.

Grinding treatment of the fine glass dust has proven to be effective in the reduction of the particle size in section 3.3.4. The reduced particle size of the fine glass dust after grinding led to a smaller difference in particle sizes between the Portland cement and the fine glass dust. Therefore the effective water/cement ratio was decreased and the packing density was increased, which meant that there was a faster formation of a rigid structure of C-S-H gel. The faster initial hydration reaction caused a decrease in the initial setting time for mixtures with ground fine glass dust.

The results provided in Figure 3.33 showed that mixtures with heat-treated fine glass dust reached comparable values to the reference mix, but the mixture with heat-treated + ground fine glass dust showed initial setting time values that were even lower than the reference mixture with only Portland cement. This can possibly be justified by the irregular shape of the fine glass dust particles. These larger irregular particle shapes provided interlocking between the fine glass dust particles to increase the resistance to penetration during the initial setting time test. Increased resistance to penetration could result in lower values for the initial setting time for the mixtures with interlocked fine glass dust particles after the delaying compounds were removed by the heat-treatment.

The findings on the effect of fine glass dust and different pre-treatment methods on the initial setting time of the mortar are in agreement with the findings of Lu et al. [69], in which waste glass powders (WGP) with different grinding times were used to replace Portland cement in the binder. It was found that the longest initial setting time was apparent for the mixture with the shortest grinding time (0.5 hours) and the increase in grinding time had a positive influence on the reduction of the initial setting time of the mortars. However the findings of Lu et al. [69] showed that all the mortar mixtures with WGP had a higher initial setting time than the reference mixture with only Portland cement, while in this study the initial setting time after pre-treatments of the fine glass dust could result in lower initial setting times than the reference mixture. This can be clarified by the fact that in this research not only grinding treatment but also an additional heat-treatment was performed on the fine glass dust. As discussed in this section the heat-treatment was important for removing the delaying organic compounds, which had a significant impact on the initial hydration reaction rate and therefore the initial setting time.

The study of Matos et al. [73] showed that paste mixtures with 10% and 20% Portland cement replacement by glass powder (GP) had a slightly shorter initial setting time than the reference mixture. The initial setting time was reduced by 10 and 15 minutes for the mixtures with 10% and 20% GP respectively. These different results compared to this current research are justified by the fact that the GP that was used in the study of Matos et al. was finely ground in a milling machine for 48 hours. This is a lot longer than the maximum grinding time of 6 hours that was investigated in this study. The grinding treatment of 48 hours resulted in glass powder that had similar particle sizes as the Portland cement and because of the fine particle sizes a small reduction in the initial setting time could be observed.

So based on the provided results and discussion about the initial setting time of fine glass dust mortar mixtures it can be indicated that the untreated fine glass dust leads to an increase in initial setting time compared to the reference mixture. Both heat-treatment and grinding treatment of the fine glass dust lead to faster initial hydration reaction and therefore a reduction of the initial setting time, so that

comparable or even lower values can be reached for the initial setting time compared to the reference mixture.

3.4.2. The effect of different pre-treatment methods for the fine glass dust on the compressive strength development

The objective of the compressive strength test in section 3.3.9 was to find the influence of fine glass dust and different pre-treatments of this fine glass dust on the compressive strength development of mortar mixtures where 15% of Portland cement was replaced by fine glass dust. The results of casting session I suggest that for all curing ages the replacement of 15% Portland cement with untreated fine glass dust led to a decrease in compressive strength compared to the reference mixture. By performing a heat-treatment of 600°C on the fine glass dust the compressive strength development can be significantly increased for all curing ages. Additional grinding on top of the heat-treatment resulted in an increase in compressive strength for early curing ages of 3 and 7 days, but showed comparable results to only heat-treatment for longer curing ages of 28 and 90 days. These results were in agreement with the compressive strength results of casting session II, in which all promising mixtures were cast on the same day to eliminate casting or curing differences. Possible reasons for the changes in compressive strength development by adding untreated or pre-treated fine glass dust to the mixture are analyzed in this section.

One potential reason for the decrease in compressive strength development at all investigated curing ages for the untreated fine glass dust was due to the high amount of organic compounds in the fine glass dust. As mentioned in section 3.4.1 the organic compounds in the untreated fine glass dust delayed the induction phase and acceleration phase of the hydration reaction of the cement and therefore had a negative influence on the initial reactivity of the mortar and this resulted in a slower initial strength development. This is in agreement with the findings in section 3.3.8 on the initial setting time of the mortars. Next to this comes the fact that the fine glass dust replaces part of the Portland cement in the binder, which means that less Portland cement was available for hydration reaction. This is called the dilution effect of the fine glass dust. Because of the dilution effect fewer hydration reaction products could be formed, so this could cause the formation of less dense C-S-H gel structures. This possibly caused the strength to decrease for the untreated fine glass dust mortars, compared to the reference mixture.

As described in section 3.4.1 the heat-treatment of the fine glass dust effectively removed part of the organic compounds and therefore led to a decrease in the delayed effect on hydration for the fine glass dust. This meant that in the mixtures with heat-treated fine glass dust more reaction products could be formed at an early stage, because the initial hydration reaction rate was higher. The increased amount of hydration reaction products formed a dense structure of C-S-H gel, which resulted in a higher compressive strength development of the mixture with heat-treated fine glass dust, compared to the untreated fine glass dust. The strength development was still lower than the reference mixture for all curing ages, because of the dilution effect and thus a lower amount of Portland cement was available for the formation of hydration products.

Another potential reason for the decrease in compressive strength development at all investigated curing ages for the untreated fine glass dust was due to the large particle sizes and smoothness of the glassy particles of the fine glass dust. The large differences in particle sizes caused a sub-optimal particle packing for the binder, which meant that less dense hydration reaction products could be formed and therefore a reduction in the compressive strength development could be observed. The smooth interface of the glass particles in the fine glass dust caused a weak bonding between the glass particles and the fine aggregates in the mortar. This high smoothness could also have led to microcracks in the hydrated C-S-H gel that drives to inadequate adhesion among the fine glass dust and cement interface. This weak bonding between the smooth glass particles, hydration products and the fine aggregates caused the hydrated cement matrix to have less strength and thus a reduction in the compressive strength could be observed for the untreated fine glass dust mixture compared to the reference mixture.

As described in section 3.4.1 grinding treatment of the fine glass dust was efficient in reducing the particle sizes of the fine glass dust, so that the difference in particle sizes between the Portland cement and the grinded fine glass dust was smaller. This could lead to a more optimal particle packing in the

binder. This filler effect of the fine particles of the fine glass dust caused the fine particles to replace water which was enclosed in the voids of the cement matrix in the mortar. This released water could then be available for the hydration reaction of unhydrated cement particles and therefore accelerate the compressive stress development at the early stages. This phenomenon could also explain why the additional grinding treatment of the fine glass dust led to increased compressive stress development at curing ages of 3 and 7 days, but for longer curing ages the effect of the additional grinding treatment becomes negligible.

The large differences in compressive strength results for the investigated mixtures might be influenced by several different factors or errors that were made during the investigation:

- Analytical errors
- Mixing errors
 - Wrong material amounts measured
 - Improper mixing (agglomeration of particles)
 - Different mixing circumstances (temperature differences between days)
- Casting errors
 - Improper vibrating or compaction (causing differences in porosity)
 - Improper scraping off the excess material from the top of the mould
- Curing errors
 - Improper placement of the plastic film during curing in the mould
 - Problems in the wet room during curing
- Testing errors
 - Different loading rates
 - Dry vs wet testing
 - Surface impurities causing stress concentrations

During casting session I some of these errors were made and the mixtures were all prepared during different days. To eliminate most of these errors casting session II was performed, where all the important mixtures were cast again on the same day and under the same conditions (the only difference was that CEM I 52.5R was used instead of CEM I 42.5N). Based on the comparison of the results from casting sessions I and II it can be seen that the trends within the results are largely the same. This can possibly be clarified by the large number of repetitions that were performed for the compressive strength test of each sample (minimum of 6 repetitions), which levels out the made errors and the mean value presents valuable information. The only difference between casting sessions I and II was that higher relative strength values compared to the reference mix were obtained for casting session II. This can be attributed to the increased skill in performing the casting procedure after many repetitions, so for casting session II equal casting procedures were used for all three mixtures.

The reference mixture with Portland cement almost reached its maximum strength after 28 days of curing, which meant that a significant part of the total hydration is done in the short term until 28 days. The mixtures with fine glass dust had a slow initial strength development, but at longer curing ages of 56 and 90 days an increase in strength development rate could be observed. For both casting sessions I and II long-term curing ages caused a small increase in compressive strength development rate compared to the reference mixture. This can be possibly attributed to the slow pozzolanic reaction between the reactive amorphous silica phases in the fine glass dust and calcium hydroxide (C-H) in the cement matrix into the secondary formation of calcium silicate hydrate (C-S-H), which slightly enhanced later age strength development between 28 and 90 days for the mixtures with fine glass dust.

The findings on the effect of fine glass dust and different pre-treatment methods on the compressive

strength development of the mortar are in agreement with the findings of Boukhelf et al. [15], in which waste glass powders (WGP) were used to replace Portland cement in the binder. Boukhelf also found that the replacement of Portland cement with WGP led to a decrease in compressive strength compared to the reference mixture. Slow early age strength development was observed in the WGP mixtures, but an increase in later age strength development could be attributed to the pozzolanic reaction of the WGP. This is also in agreement with the findings of Nassar et al. [82], Nyantaki et al. [86] and Ibrahim et al. [46], in which low initial reactivity was observed for mixtures with waste glass powder resulting in lower strength values than the reference mixture, but a small increase in compressive strength development rate due to pozzolanic activity of the WGP.

On the other hand research by Omer et al. [87], Kamali et al. [53] and Du et al. [33] showed that the replacement of Portland cement with glass powders could enhance the compressive strength development compared to the reference mixture, mostly for longer curing ages. This can be attributed to the high pozzolanic activity of the glass powders that were used for these researches. The glass powders were made from crushing and milling glass bottles until very fine particle sizes, while in this research the particle sizes after grinding were still larger than the Portland cement particles. Also the fine glass dust had a high amount of impurities and did not 100% consist of glass particles. This could be a possible explanation for the lower amount of compressive strength development for the fine glass dust mixtures in this current research.

So based on the provided results and discussion about the compressive strength development of fine glass dust mortar mixtures it can be indicated that the untreated fine glass dust leads to a decrease in compressive strength compared to the reference mixture. Both heat-treatment and grinding treatment of the fine glass dust lead to improvements in compressive strength, but due to the dilution effect of the fine glass dust no investigated mixture could reach comparable strength values as the reference mixture. For casting session II relative compressive strength values between 90-96% could be obtained for the mixture with heat-treated + ground fine glass dust.

3.4.3. Limitations

This section describes the limitations of the study on raw material characterization and optimal pre-treatment method for fine glass dust. For different aspects of the study the limitations are discussed and proposals are made in which the study could be improved based on the limitations.

For the heat-treatment of the fine glass dust no treatment times shorter than 1 hour were investigated. It can be beneficial to investigate shorter heat-treatment times for the fine glass dust to find the minimal treatment time for which a part of the organic compounds is removed from the sample.

The same volume of fine glass dust and oven was used for the heat-treatment during this entire study. The fine glass dust was placed in a crucible where around 500 grams could fit in. This was the largest available crucible at the TU Delft that could fit in the Carbolite HTF1700 furnace. A different volume of fine glass dust that was heated could lead to other results in terms of mass loss. For a large volume of fine glass dust it may be more difficult to heat the entire sample, which could lead to longer heat-treatment times before the organic compounds are successfully removed from the sample.

During this study the heat-treatment temperature of 700°C was disregarded as a possibility for heat-treatment of the fine glass dust, because the material melted and was collected from the oven as one solid mass. Due to insufficient grinding or crushing equipment at the TU Delft this temperature was too high to ensure the usability of the fine glass dust in mortar mixtures. However the study could be improved by investigating treatment temperatures above the melting point in combination with excessive grinding periods afterwards. In this way it can be investigated if higher temperatures may be more effective in removing organic compounds and activating the pozzolanic activity of the fine glass dust.

During this study the only method of removing the organic compounds from the fine glass dust was by heat-treatment temperatures. Other methods like critical CO₂ extraction can also be used for the removal of organic compounds from powdered samples [66]. A combination of heat-treatment and critical CO₂ extraction may provide better results in terms of organic content removal and therefore activating the fine glass dust in mortar mixtures.

For both the heat-treatment and grinding treatment of the fine glass dust there was a material capacity limitation during the study. In the HTF1700 furnace it was possible to only heat around 500 grams of fine glass dust per day. The oven also had to be shared with other researchers, which reduced the capacity even more. In the ball milling machine it was possible to grind around 2.5 kg of fine glass dust per day.

After grinding in the ball mill machine the fine glass dust had to be collected. This was done in this study by sieving the ground material from the milling balls by hand. Sieves of 1 mm and 0.5 mm were placed on top of each other and the fine glass dust was sieved from the milling balls. The large sieve sizes were chosen, because for smaller sieve sizes only small diameter sieves were available which led to fast clogging of the small sieves, when a lot of material had to be sieved. The consequence of using the larger sieve sizes, was that after grinding almost all particles smaller than 0.5 mm were collected. Even though this limitation the grinding treatment showed to be efficient in reducing the particle size of the fine glass dust. The accuracy of the grinding process could be improved by using smaller sieving sizes, but this would be at the expense of a large increase in the sieving time.

The particle size distribution analyzer that was used to determine the efficiency of the grinding treatment was not very accurate for small fractions (between 1 and $10\mu\text{m}$ (the smallest detected value was $10\mu\text{m}$). This caused the fact that the effect of grinding on the finest fractions of the fine glass dust was difficult to observe. This can be improved by using a particle size distribution analyzer which can detect very fine particle sizes.

For the compressive strength test only mortar prisms are tested on a compression surface of 40x40 mm. This standard testing size was good for the comparison of the different pre-treatments. More valuable information could be achieved when different scales of compressive strength tests are included. Larger scale test specimens may lead to other failure mechanisms that could provide valuable information on the hardened properties and the behaviour of fine glass dust in the mortar.

4

Cement replacement percentage investigation for fine glass dust

In Chapter 3 the raw material was characterized and the optimal pre-treatment for the recycled fine glass dust was investigated when fine glass dust is used as a Portland cement replacement in mortar mixtures. In order to only investigate the influence of the different pre-treatments on the behaviour of the fine glass dust a constant replacement percentage of 15% was considered for all mixtures that were investigated in Chapter 3. The most optimal pre-treatment for the fine glass dust was found in terms of time and energy efficiency and the influence on the fresh and hardened properties of the mortar. In this chapter this optimal pre-treatment of the fine glass dust was used and it was investigated what is the influence of different cement replacement percentages for fine glass dust when it is used in mortar mixtures.

Section 4.1 describes the objective and research plan for the cement replacement percentage investigation. In section 4.2 the materials and methods for the cement replacement percentage investigation for the fine glass dust are explained in more detail. Section 4.3 and 4.4 presents the results and discussions about the cement replacement percentage investigation for the fine glass dust.

4.1. Research plan

This section describes the research plan for the cement replacement percentage investigation for fine glass dust. The goal of this research was to investigate the effect on fresh-state and hardened mortar properties when different cement replacement percentages by fine glass dust in the binder of mortar mixtures were used.

From an environmental and financial viewpoint of the glass recycling industry it is preferable to replace the largest amount of Portland cement with fine glass dust, while still meeting sufficient strength requirements. Therefore in this chapter mixtures with different replacement percentages of Portland cement with fine glass dust were investigated. The goal of this investigation was to find the relation between different cement replacement percentages and mortar properties when fine glass dust was used in mortar mixtures. All the fine glass dust that was used for this replacement percentage investigation had received the most efficient pre-treatment from Chapter 3. This means that all the fine glass dust had a heat-treatment of 600°C for 1 hour and a grinding treatment of 1 hour.

To assess the hardened properties of the mixtures with different replacement percentages, compressive strength tests were performed at curing ages of 3 days, 7 days, 28 days and 90 days. The reason for these curing ages was that the early age strength development was important to take into account, but because of the possible pozzolanic activity of the fine glass dust in the mortar mixture it was also important to look at the long-term strength development (90 days). In this way it could be investigated if the fine glass dust caused secondary strength development due to pozzolanic reactivity and how this changed the strength development for different replacement percentages.

Next to the compressive strength tests to look at the hardened properties of the mortar mixtures

also slump and slump flow tests were performed to look at the fresh-state properties of the mixtures directly after mixing. These tests were performed to investigate the influence of different fine glass dust replacement percentages on important fresh-state behaviour like workability and flowability of the mortar mixtures.

Pozzolanic activity test was performed to investigate the potential pozzolanic reaction in the mortar mixtures when pre-treated fine glass dust was used to replace Portland cement in the binder. Secondary formations test was performed to investigate the influence of fine glass dust percentage on the volume stability and the formation of secondary products in the mixtures after casting.

4.2. Material and Methods

This section describes the materials and test methods that were needed for the research plan that is described in section 4.1. The mix designs that were used for the replacement percentage investigation are described and for each of the performed tests the background, test set-up, sample preparation and test procedure are presented. These are based on standards like Eurocode, NEN and ASTM, combined with the information from the literature study in chapter 2.

4.2.1. Mix design for replacement percentage optimization

In the mix designs that were used in section 3.2.7 for the determination of the optimal pre-treatment for the fine glass dust a constant replacement percentage of 15% was used for all the mixtures. In this chapter different replacement percentages were investigated, to find the influence of variable amounts of fine glass dust in the mortar mixtures on hardened and fresh-state properties. The mix designs that were used for the replacement percentage optimization are presented in Table 4.1.

Mix	PC	FGD	Sand	Water	Type of pre-treatment
Mix FGD-0	100	0	300	50	-
Mix FGD-10	90	10	300	50	600°C heat-treatment and 1 hr grinding treatment
Mix FGD-15	85	15	300	50	600°C heat-treatment and 1 hr grinding treatment
Mix FGD-20	80	20	300	50	600°C heat-treatment and 1 hr grinding treatment
Mix FGD-30	70	30	300	50	600°C heat-treatment and 1 hr grinding treatment
Mix FGD-45	55	45	300	50	600°C heat-treatment and 1 hr grinding treatment

Table 4.1: Mix compositions for replacement percentage optimization (% of binder mass)

In Table 4.1 it can be seen that 6 different mixtures were investigated for the replacement percentage optimization. For each mixture the mix compositions were given as a % of the total binder mass. Mix FGD-0 was the reference mixture with 0% fine glass dust and the other mixtures that were investigated contained respectively 10%, 15%, 20%, 30% and 45% Portland cement replacement by fine glass dust (Mix FGD-10 / Mix FGD-45). The different replacement percentages were chosen to investigate the influence of low-level replacement percentages (10% and 15%), but also to investigate the influence of high-level replacement percentages (30% and 45%). As described in section 4.1 The goal of this investigation was to find the relation between different replacement percentages and mortar properties and therefore also high replacement percentages were included in this investigation.

For all the mixtures the water/binder ratio was kept constant at 0.5 and the sand/binder ratio was kept constant at 3. This was done to only investigate the effect of changing the replacement percentage of fine glass dust. If multiple parameters were changing in the mix designs then it was more difficult to determine what was the influence of the changing replacement percentage. For the Portland cement (PC) CEM I 42,5N was used and CEN standard sand was used, which is based on NEN-EN 196-1 [106]. It can also be seen from Table 4.1 that all the fine glass dust had a pre-treatment of 600°C heat-treatment and 1 hour grinding treatment. This was the most efficient pre-treatment that was concluded in Chapter 3.

4.2.2. Slump and slump flow test

Slump and slump flow tests for the replacement percentage investigation were performed with the same test set-up, samples and procedure as described in section 3.2.8. A small Hägermann cone of 6 cm was used for the slump tests and a small compaction table with 25 drops was used for the slump flow tests. For each mixture a minimum of 3 repetitions were performed and the mean value was reported. The goal of these tests was to find the influence of variable amounts of fine glass dust on the workability and flowability of the fresh mixtures.

4.2.3. Compressive strength test

Compressive strength tests were performed to investigate the influence of different replacement percentages of Portland cement by fine glass dust in cast mortar on the compressive strength. Compressive strength is a very important hardened property for concrete and for the replacement percentage investigation it was important to determine the relation between replacement percentage and compressive strength. For the development of strength over time it was important that the compressive strength was measured at different curing times after casting. Compressive strength tests for the replacement percentage investigation were performed with the same test set-up, samples and procedure as described in section 3.2.10.

4.2.4. Pozzolanic activity test

The results that were provided in section 4.3.2 showed a little increase of compressive strength at later curing ages for all different replacement percentages compared to the reference mixture. In section 2.2 and section 4.1 it was described that a higher strength development at later curing ages of 28 and 90 days could be possibly attributed to the pozzolanic activity of the fine glass dust. The high amount of amorphous silica that is present in the fine glass dust could provide a pozzolanic reaction in which the amorphous silica reacts with C-H (Calcium Hydroxide) in the binder matrix to form secondary C-S-H structures (Calcium Silicate Hydrate). These C-S-H structures that are formed by the slow pozzolanic reaction can then contribute to later age strength development of the mortar [53] [103] [61]. However the provided compressive strength results showed a little increase in later age strength development for high FGD mixtures compared to the reference mixture. This raised the question if the fine glass dust possesses pozzolanic activity when it was used as a cement replacement in the binder (Type II addition) or if it only acts as an inert filler material which improved the particle packing, but had no extra strength contribution (Type I addition) [65].

To determine if the fine glass dust had pozzolanic reactivity when it was used as a cement replacement in the binder, a pozzolanic activity test was performed. This pozzolanic activity test was based on research that was performed by Li et al. and Chen et al. [68][25]. With this test TGA was performed on paste samples from different mixtures and the results from the TGA were used to determine if there was any pozzolanic activity of the fine glass dust by comparing the amount of C-H (calcium hydroxide) and the amount of H (chemically bound water) after different curing ages. To perform TGA, the paste samples had to be powdered and hydration had to be stopped after a specific curing age.

Test set-up / Sample preparation

The test set-up for the Thermogravimetric analysis was described in section 3.2.2. The cementitious paste was made with a small mixing machine, it was stored in small cups and left for curing until the specified curing age. Then hydration had to be stopped to ensure that hydration did not continue during the time between powder preparation and TGA testing. The paste sample was then broken into smaller pieces with the help of a hammer and the smaller pieces were collected. Then the material needed to be further ground until it was a powder with very fine particle sizes. This was done in a special grinding bowl, which is shown in Figure 4.1.

The grinding bowl was filled with isopropanol. Isopropanol was used to stop hydration in the paste sample. The isopropanol enters the pores of the paste sample and pushes all the water out of the sample and fills the pores with isopropanol. After removal of the excess isopropanol and water that is pushed out of the sample, the isopropanol evaporates from the pores in the paste and in this way all the water was removed from the paste and the hydration reaction was unable to continue. The small pieces of the paste sample were ground in a solution of isopropanol. This process had to be done for



Figure 4.1: Grinding the paste to a powder in isopropanol

at least 30 minutes to ensure that all the water could be successfully extracted from the sample and also that there is enough time for grinding so that the particle sizes were fine enough for using the TGA. After 30 minutes of grinding in isopropanol the excess isopropanol and water were collected in an Erlenmeyer and removed and the ground paste was filtered out with the use of filter paper.

When all the excess liquid was removed and the ground material was collected in the filter paper, the filter paper was placed in a small basket in an oven at 40°C for at least 2 hours to make sure that all the liquid was removed from the powdered sample and that the isopropanol could successfully evaporate from the pores. After drying the powder could be collected in a plastic zip-lock bag.

For the thermogravimetric analysis the small crucible was filled with around 35 mg of powder and was placed on the sample carrier (see section 3.2.2). The TGA was performed under Argon conditions with temperatures from 40 to 900°C with an increase of 10°C per minute. A gas environment of 30 ml/min argon flow was used. TGA was performed for powdered paste samples of Mixture FGD-0, which was the reference mix and mixture FGD-15, which had a fine glass dust percentage of 15%. For both mixtures hydration was stopped after 7, 28 and 56 days of curing, the paste samples were ground to a powder and thermogravimetric analysis was performed.

Procedure

The results of the thermogravimetric analysis were processed by plotting the mass loss of the samples against the heating temperature. The DTG curve could be obtained by taking the first derivative of the TGA curve. The DTG curve represented the relation between the weight loss rate (%/min) and the temperature. Based on the results of the TGA curve and the DTG curve the pozzolanic activity of the fine glass dust in the paste could be assessed by comparing the results of the reference mix FGD-0 and mix FGD-15 [68]. If the fine glass dust had any pozzolanic activity then the amount of Calcium hydroxide (C-H) would decrease over time and the amount of chemically bound water (H) would increase over time. Chemically bound water is the water that is chemically bound into reaction products of the hydration reaction or pozzolanic reaction. An increase in the chemically bound water amount at later curing ages could indicate secondary C-S-H formation in the paste. By comparing the results of the two separate mixtures at different curing ages, judgement could be made about whether the fine glass dust had any pozzolanic activity or not when it was used as a cement replacement in the binder.

4.2.5. Secondary formations test for mixtures with different FGD percentages

The casting sessions from the cementitious mixtures in section 4.3.2 showed that a high amount of secondary formation occurred in the mixtures where a high replacement percentage of FGD was used to replace the Portland cement in the binder. During the casting process of mixtures with high FGD percentage, expansion and volume instability of the mortar was observed. This could be seen as an

upwards curved top surface of the cast mortar prisms after curing with a plastic film for one day. For some casting sessions even cracking occurred at the top layer, due to high expansion in this area. To find the influence of the replacement percentage of FGD on the expansion and volume instability of the mixtures, secondary formations test was performed. The main purpose of this test was to determine at which FGD percentages the mixtures showed secondary formations in the mixture and also to determine what is the maximum percentage of FGD that can be used in the mixture without significant formation of secondary products. Table 4.2 presents the mixtures that were investigated for the expansion and volume instability test. The investigated mixtures were made in the form of paste, so only binder and water were included and the fine aggregate portion was excluded.

Cementitious mix	CEM I 52.5R	FGD	Water
FGD-25	750	250	300
FGD-10	900	100	300
FGD-7.5	925	75	300
FGD-0	1000	0	300

Table 4.2: Mix compositions for secondary formations test of cementitious mixture (units are grams for 1 liter of mixture)

From Table 4.2 it can be seen that the following replacement percentages of fine glass dust were used for the cementitious mixtures: 25, 10, 7.5 and 0%. A water/binder ratio of 0.3 was used for the mixtures of the secondary formations test, because this would be better in line with the mix designs for 3D Concrete Printing in chapter 5. The goal of the secondary formations test was to find the replacement percentage for which there was no excessive expansion and visible upwards curvature in the top layer of the paste and no cracking occurred during curing.

Test set-up / Samples

The mixtures that are presented in Table 4.2 were prepared by the small Ultra-Turrax T50 mixer. This mixer allows for the mixing of very small amounts of materials and is therefore suitable for the production of paste mixtures. Materials were weighed for 0.2L of paste mixture for each replacement percentage of fine glass dust. First the dry materials were mixed on low speed for 1 minute and then the water was slowly added while mixing. After all the water was added mixing continued for 2 minutes on low speed and 1 minute on high speed. After mixing the paste was added into a large closable cup.

Procedure

After the paste mixtures were added to the closable cups the height of the mixture was measured. After each consecutive day the surface of the paste was observed closely. Measurement photos were taken from the side and the top of the samples to determine the development of secondary products and cracks in the paste. Notes were taken at which curing ages the first expansion products and cracks could be observed for the different paste mixtures.

4.3. Results

4.3.1. Slump and slump flow

The results of the slump test on the mixtures with different replacement percentages are presented in Figure 4.2. From these results it can be seen that the replacement of Portland cement with fine glass dust in the binder reduced the slump cone height after removal of the Hägermann cone. A decreasing trend could be observed for which higher replacement percentages of fine glass dust led to lower values for the slump cone height. The reference mixture Mix FGD-0 had a mean slump value of 5.57 cm. For FGD replacement percentages of 10-20% the slump cone height decreased to 5.30-5.43 cm, which represented a reduction of around 4% compared to the reference mixture. For higher FGD replacement percentages of 30 and 45% the slump cone height decreased to 5.23 and 4.70 cm, which represented a reduction of 6 and 16% respectively.

The results of the slump flow test on the mixtures with different replacement percentages are presented in Figure 4.3. Also for the slump flow test results, the replacement of Portland cement with fine glass

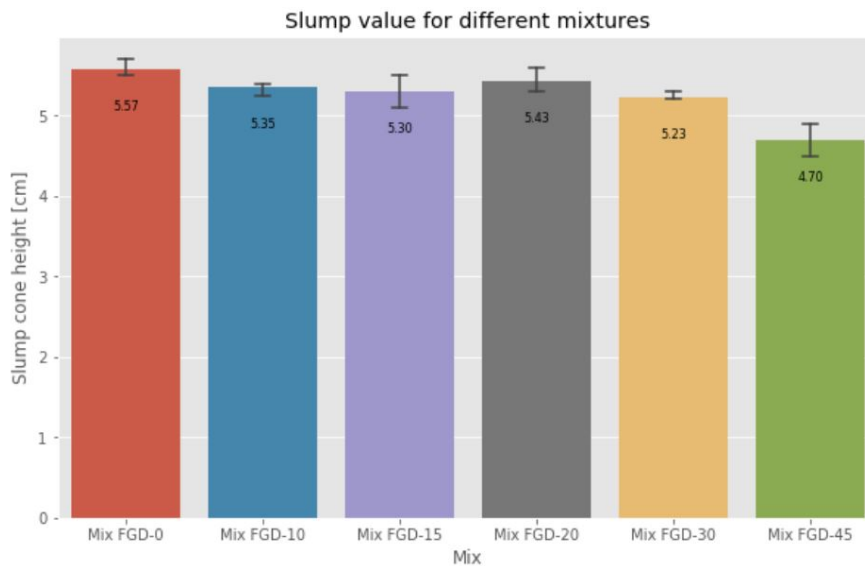


Figure 4.2: Slump results for different replacement percentages of FGD

dust in the binder reduced the slump flow diameter after 25 drops of the compaction table for all different replacement percentages. The reference mixture Mix FGD-0 had a mean slump flow diameter of 22.17 cm. For the different replacement percentages of fine glass dust, no clear trend could be observed. The reduction of slump flow diameter was the largest for Mix FGD-30 and the smallest for Mix FGD-45, which resulted in slump flow diameters between 20.0 and 21.5 cm. This represented a reduction of 3-10% compared to the reference mixture.

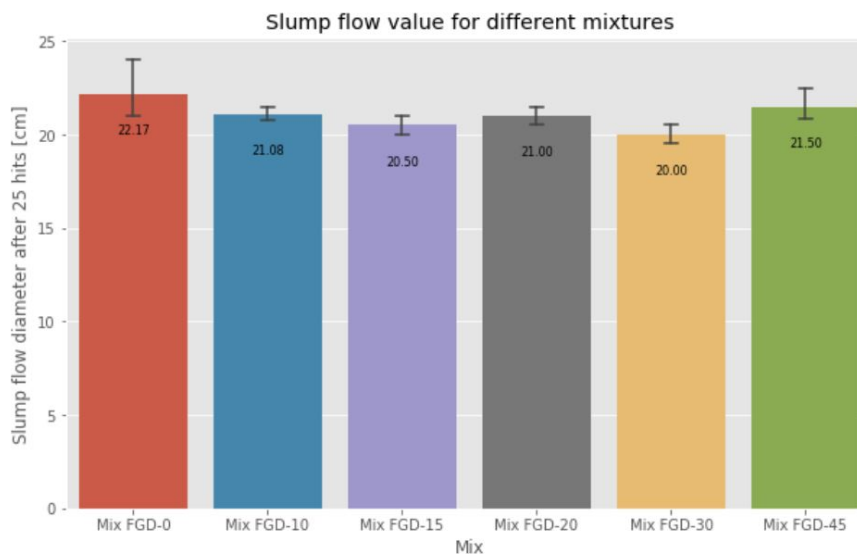


Figure 4.3: Slump flow results for different replacement percentages of FGD

4.3.2. Compressive strength

As reported in section 4.2.3 compressive strength tests had to be performed to investigate the influence of different replacement percentages of fine glass dust on the compressive strength development of mortar mixtures. The different mix designs that were taken into account for this replacement percentage investigation were presented in section 4.2.1. The results of the compressive strength test that is described in section 4.2.3 are presented in Figure 4.4.

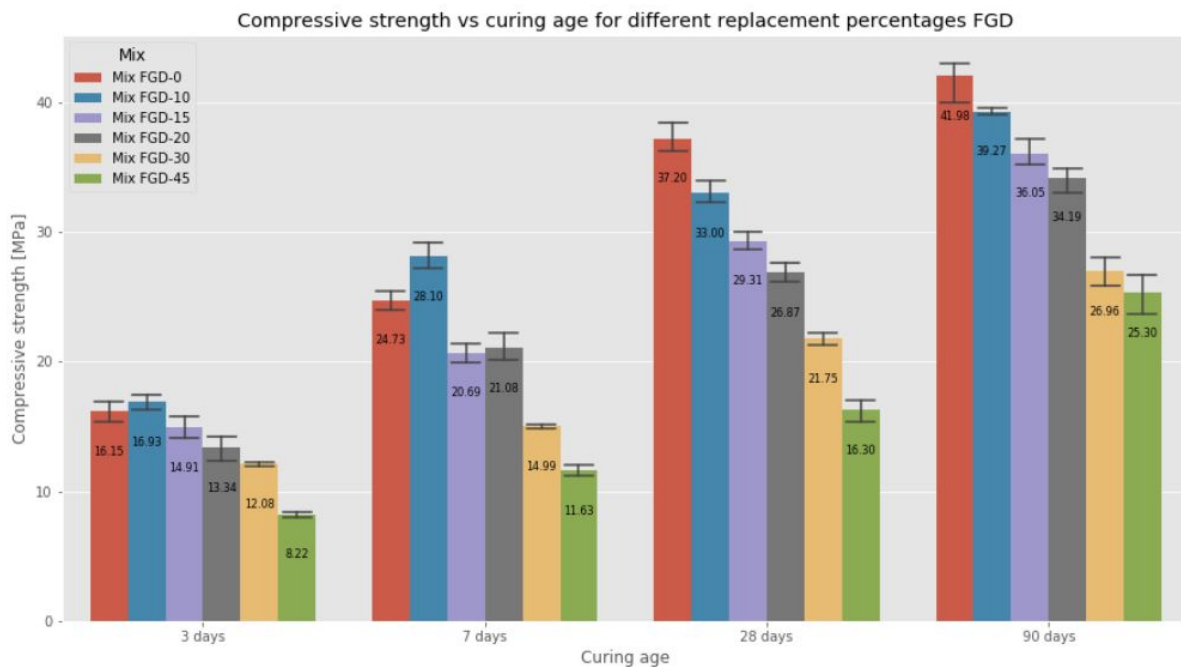


Figure 4.4: Compressive strength development for different replacement percentages of FGD

According to the test results that are shown in Figure 4.4, compressive strength decreased for higher replacement percentages of FGD for all curing ages. Almost all replacement percentages exhibited lower compressive strength than the reference mixture with 0% FGD in the mixture. Mix FGD-10 was the only mix that could exceed the strength development of the reference mixture at early curing ages. Mix FGD-10 reached a mean compressive strength of 16.93 and 28.10 MPa after respectively 3 and 7 days of curing, which was equivalent to 105 and 114% relative to the reference mixture FGD-0. The relative strength index can be defined as the ratio of compressive strength of mortar compared to the control mixture (FGD-0). Table 4.3 presents the relative strength indexes for the investigated mixtures. For longer curing times at 28 and 90 days the relative strength index for Mix FGD-10 decreased to 89 and 94% respectively and after 90 days a strength of 41.27 MPa could be reached for Mix FGD-10.

From Figure 4.4 and Table 4.3 it can be seen that after 3 days of curing Mix FGD-30 and FGD-45 had slow strength development and could only reach 12.08 and 8.22 MPa respectively, which was equivalent to 75 and 51% relative to the reference mixture. Also for longer curing ages (7, 28 and 90 days) it could be seen that the mixtures FGD-30 and FGD-45 had very low strength development compared to the reference mixture. The relative strength index for these mixtures is between 44 and 64% for longer curing ages and after 90 days a strength of 26.96 MPa was reached for Mix FGD-30.

Mix FGD-15 and FGD-20 provided similar results in terms of compressive strength development. After 3 days of curing the strength was 14.91 and 13.34 MPa respectively, which meant a relative strength index of 92 and 83%. After 7 days of curing both Mix FGD-15 and FGD-20 reached a relative strength index of 85%. For longer curing ages at 28 and 90 days both mixtures provided relative strength indexes in the range of 72-86% and after 90 days a strength of 36.05 MPa could be reached for Mix FGD-15.

When the results of Figure 4.4 and Table 4.3 are reviewed a small strength increase compared to the reference mixture was observed for the FGD mixtures at curing ages of 90 days. This showed that the pozzolanic activity of the FGD, which can cause secondary strength development, was potentially present. For the mixtures with high FGD percentages a significant increase in relative strength percentages could be observed between 28 and 90 days of curing. In section 4.2.4 pozzolanic activity test was performed to validate the results from this section and to determine whether the FGD possesses a small amount of pozzolanic activity or not.

The goal of the replacement percentage investigation was to research what was the influence of

Curing age	Mix FGD-10	Mix FGD-15	Mix FGD-20	Mix FGD-30	Mix FGD-45
3 days	105	92	83	75	51
7 days	114	84	85	61	47
28 days	89	79	72	58	44
90 days	94	86	81	64	60

Table 4.3: Compressive strength relative to reference mix for different replacement percentages (%)

different FGD replacement percentages on the compressive strength development of the mortar. The results showed that a higher FGD percentage led to lower compressive strength development for all investigated curing ages between 3 and 90 days. Only 10% FGD showed higher compressive strength than the reference mix at early curing ages, but reached around 90% of strength after 28 and 90 days. A replacement percentage of 20% resulted in 70-85% compressive strength compared to the reference mix. Higher replacement percentages (30 and 45%) experienced even larger strength reductions with the investigated mix designs in this chapter.

4.3.3. Pozzolanic activity of the fine glass dust

In this section the TG and DTG results were used to compare the TGA results for the different mixtures and the boundaries of phases at different curing ages. As described in section 4.2.4 the goal of the TGA was to quantify the amount of C-H (calcium hydroxide) and H (chemically bound water) in the paste samples. According to Chen et al. [25], the amount of H in the paste sample could be quantified by the mass loss between temperatures of 40°C and 600°C. The amount of C-H content in the mixture could be determined by the mass loss between 420°C and 500°C, which is the temperature range at which C-H phases break down. The amount of H and C-H in the paste could be expressed as a percentage of the dry sample weight at 600°C. The following equations were used to calculate the amount of H and C-H based on the TGA results.

H content in the sample (mass percentage):

$$W_{H_2O} = \frac{M_{40^\circ C} - M_{600^\circ C}}{M_{600^\circ C}} \cdot 100\%$$

C-H content in the sample (mass percentage):

$$W_{Ca(OH)_2} = \frac{M_{420^\circ C} - M_{500^\circ C}}{M_{600^\circ C}} \cdot \frac{m_{Ca(OH)_2}}{m_{H_2O}} \cdot 100\%$$

Where:

$M_{x^\circ C}$ = Mass after heating at $x^\circ C$

m_{H_2O} = Molar mass of Chemically bound water (H) = 18g/mol

$m_{Ca(OH)_2}$ = Molar mass of Calcium hydroxide (C-H) = 74g/mol

In Figure 4.5 the results of the TGA of mix FGD-0 (reference mix without FGD) and mix FGD-15 are presented after curing ages of 7 days, 28 days and 56 days. From Figures 4.5a and 4.5c it can be seen that large peaks in mass loss occurred between 100 and 200°C, between 420 and 500°C and a small peak of mass loss occurred around 700°C. For mix FGD-0 the mass loss was larger at longer curing ages. The total mass loss for mix FGD-0 after heating until 900°C was 17.93% after 7 days, 21.99% after 28 days and 22.22% after 56 days.

For mix FGD-15 large peaks of mass loss occurred in the same temperature ranges as for mix FGD-0 (see Figures 4.5b and 4.5d). For mix FGD-15 higher curing ages also led to higher mass loss in the sample, but the difference between curing ages of 28 days and 56 days was slightly larger than for mix FGD-0. For mix FGD-15 a larger reduction in mass could be observed for higher curing ages. The total mass loss for mix FGD-15 after heating until 900°C was 18.48% after 7 days, 20.46% after 28 days and 21.35% after 56 days.

Based on the provided TGA and DTG results in Figure 4.5 the amount of Chemically bound water (H) and Calcium hydroxide (C-H) was quantified with the help of the formulas mentioned earlier in this

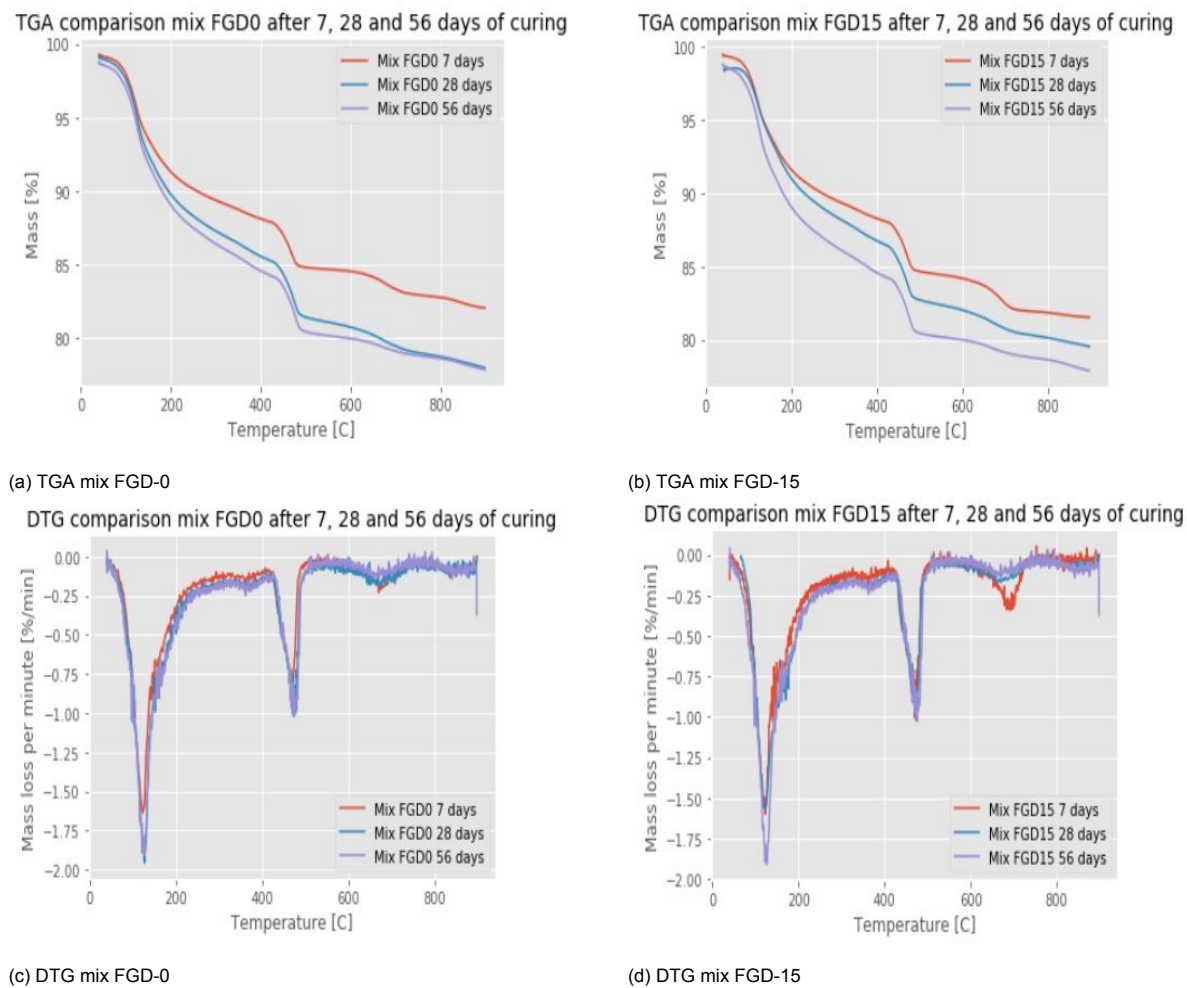


Figure 4.5: TGA results for mix FGD-0 and mix FGD-15 after 7, 28 and 56 days of curing

section. The results of these calculations are presented in Table 4.4. It can be seen that the amount of chemically bound water increased with curing age for both mixtures. For mix FGD-0 the H content increased from 17.41 to 22.78 to 23.26% for curing ages of 7, 28 and 56 days. For mix FGD-15 the H content increased from 18.11 to 20.01 to 20.69% for curing ages of 7, 28 and 56 days. After 7 days the mixture with 15% FGD had a higher chemically bound water content than the reference mixture, but at the curing age of 28 days the H amount was higher in the reference mix. It was also observed that the increase in H between 28 and 56 days was higher for the fine glass dust mixture FGD-15. Between these curing ages the mixture with FGD developed more chemically bound water. This result is in agreement with Figure 4.5 which shows a larger increase in mass loss for the FGD-15 mixture compared to the FGD-0 mixture between 28 and 56 days of curing.

The amount of calcium hydroxide in the paste samples also increased with longer curing ages for both mixtures. For mix FGD-0 the C-H content increased from 15.08 to 19.61 to 19.70 % for curing ages of 7, 28 and 56 days. For mix FGD-15 the C-H content increased from 16.67 to 18.83% for curing ages of 7 and 28 days, but decreased to 18.29% after 56 days of curing. After 7 days the mixture with FGD had a higher calcium hydroxide content than the reference mixture, but at curing age of 28 days the C-H amount was higher in the reference mix. It was also observed that between 28 and 56 days there was an increase in C-H content for mix FGD-0, but a decrease for mix FGD-15. This showed that calcium hydroxide was consumed at curing ages between 28 and 56 days for the mixture with fine glass dust.

Mix	Curing age	W_{H_2O} (% wt.)	$W_{Ca(OH)_2}$ (% wt.)
Mix FGD-0	7 days	17.41	15.08
Mix FGD-0	28 days	22.78	19.61
Mix FGD-0	56 days	23.26	19.70
Mix FGD-15	7 days	18.11	16.67
Mix FGD-15	28 days	20.01	18.83
Mix FGD-15	56 days	20.69	18.29

Table 4.4: Chemically bound water and calcium hydroxide content at different curing ages for mix FGD-0 and FGD-15

4.3.4. Secondary formations of cementitious mixtures

In section 4.2.5 it was described how the small amounts of different paste mixtures were prepared for the secondary formations test and the mix designs can be found in Table 4.2. Directly after mixing the paste mixtures were poured into a closable cup. Figure 4.6 shows the paste mixtures with different fine glass dust percentages from front view and top view. This was determined as the start of the secondary formations test at 0 days after mixing. From Figure 4.6 it can be observed that the top surface of the poured paste samples was not entirely flat for all mixtures and that also some paste material got stuck on the wall of the cup. This could be mainly attributed to improper pouring of the paste into the cups. Mix FGD10 did not have a perfectly flat top surface and for mix FGD0 and FGD7.5 a small amount of material was stuck on the wall of the cups. For the assessment at later curing ages these imperfections had to be taken into account.

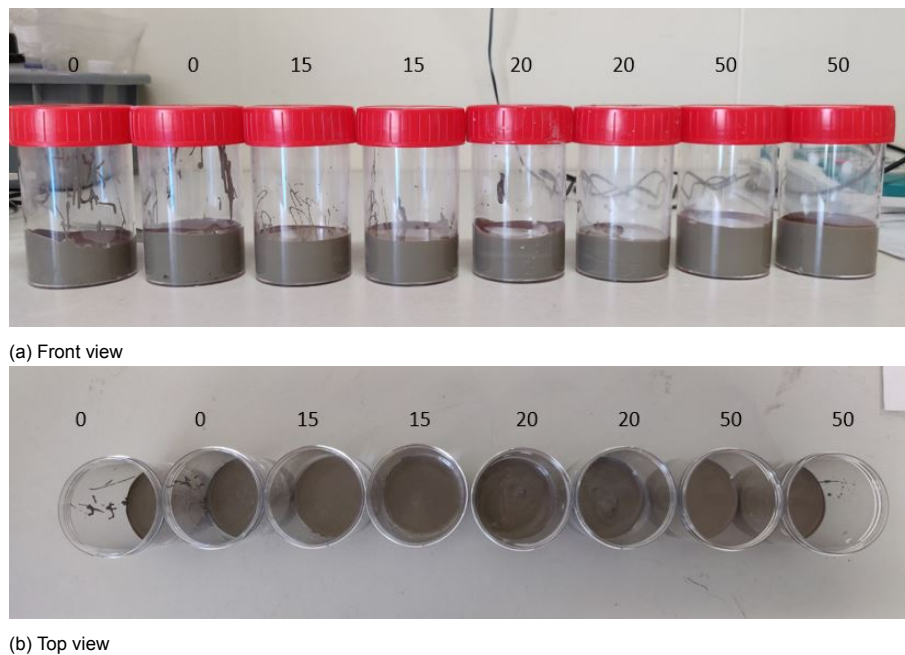


Figure 4.6: Secondary formations test 0 days for different FGD percentages

The results of the secondary formations test after 1 day are presented in Figure 4.7. For all different FGD percentages a close-up picture was taken from front and top view to closely assess the secondary formations (expansion products) in the paste. Figures 4.7a and 4.7b show that after 1 day of curing Mix FGD0 had no visible expansion products formed. Figures 4.7c and 4.7d show that after 1 day of curing Mix FGD7.5 had no visible expansion products formed. Figures 4.7e and 4.7f show that after 1 day of curing Mix FGD10 formed some vague white stripes that could be observed from the front view. This could be explained by the improper pouring at day 0 or the formation of some secondary formations. Figures 4.7g and 4.7h show that after 1 day of curing Mix FGD25 had clear expansion product formation in the upper layer which was visible in the front view and also in the top view. There

was also one very small crack observable from the front view and the top surface curved upwards.

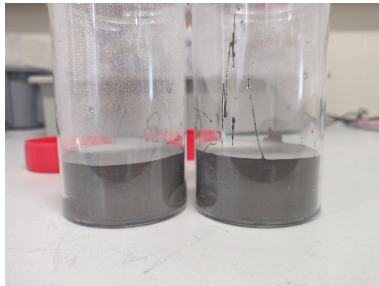
The results of the secondary formations test after 7 days are presented in Figure 4.8. Figures 4.8a and 4.8b show that after 7 days of curing Mix FGD0 had still no visible expansion products formed. Figures 4.8c and 4.8d show that after 7 days of curing Mix FGD7.5 had a small amount of expansion products visible in the top layer, but this was difficult to observe. Figures 4.8e and 4.8f show that after 7 days of curing Mix FGD10 was still in the same condition as after 1 day, in which some white stripes could be observed, but no clear expansion product formation was visible. Figures 4.8g and 4.8h show that after 7 days of curing Mix FGD25 had more clear and larger expansion products formation in terms of thin white lines on top of each other. Small cracks in the upward curved top surface were visible and more cracks could be observed from the front view. After 28 days the results had not much changed



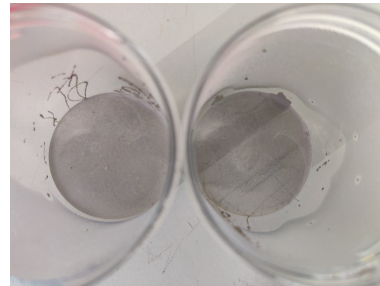
(a) 0% FGD front view 1 day



(b) 0% FGD top view 1 day



(c) 7.5% FGD front view 1 day



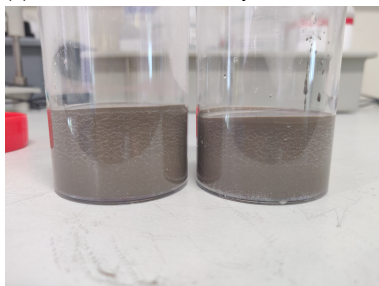
(d) 7.5% FGD top view 1 day



(e) 10% FGD front view 1 day



(f) 10% FGD top view 1 day



(g) 25% FGD front view 1 day



(h) 25% FGD top view 1 day

Figure 4.7: Secondary formations results after 1 day for different FGD percentages

in comparison with the results after 7 days. Still no clear secondary formations could be observed in



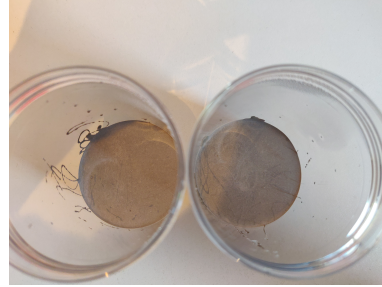
(a) 0% FGD front view 7 days



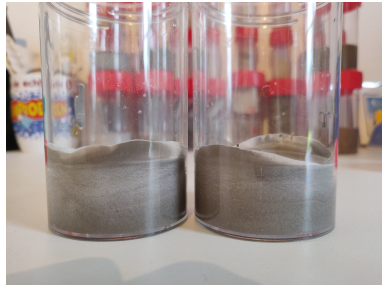
(b) 0% FGD top view 7 days



(c) 7.5% FGD front view 7 days



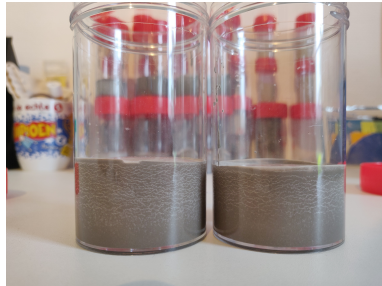
(d) 7.5% FGD top view 7 days



(e) 10% FGD front view 7 days



(f) 10% FGD top view 7 days



(g) 25% FGD front view 7 days



(h) 25% FGD top view 7 days

Figure 4.8: Secondary formation results after 7 days for different FGD percentages

the mixtures with 0%, 7.5% and 10% FGD and very large amounts of secondary formation products could be observed in the mixture with 25% FGD. Mix FGD10 and mix FGD25 were compared under the SEM (scanning electron microscope) after 28 days of curing to visualise the secondary products that were formed. SEM images from both mix FGD25 and FGD10 can be found in Appendix A.

4.4. Discussions

4.4.1. Effect of different fine glass dust replacement percentages on the compressive strength development

The objective of the compressive strength tests as described in section 4.3.2 was to investigate the influence of different replacement percentages of pre-treated fine glass dust on the compressive strength development of mortar mixtures. The data suggests that for all curing ages a higher percentage of FGD led to a lower compressive strength. This indicated that the FGD percentage had a negative impact on the strength development of the mortar. For longer curing times at 90 days a slight improvement in compressive strength was observed, which could indicate secondary strength development due to pozzolanic activity. Possible explanations for the influence of FGD percentage on compressive strength development are analyzed in this section.

A potential interpretation for the decrease in compressive strength with higher fine glass dust percentage is due to the dilution effect of the fine glass dust. Because the fine glass dust has no or very little contribution to the hydration reaction and the strength development at an early age, the compressive strength at short curing ages will be reduced compared to the reference mixture. This is mainly because less Portland cement particles were available for hydration reaction and the fine glass dust mainly had a filler effect at an early age. This could also explain why a larger replacement percentage of fine glass dust led to lower compressive strength values. More fine glass dust in the mixture meant that less Portland cement was available for hydration. This interpretation is in agreement with the findings in section 3.4.2 where all the mixtures with fine glass dust could not exceed the strength of the reference mixture. The high compressive strength values for the FGD-10 mixture at early curing ages could be attributed to optimal particle packing at that specific replacement percentage, which caused the strength of the early age to increase based on the mechanism that is described in section 3.4.2 and can even exceed the compressive strength of the reference mixture at 3 and 7 days. This effect of the optimized particle packing is negligible at later curing ages, when the strength values were in line with the other mixtures with fine glass dust.

For all mixtures with pre-treated fine glass dust as a replacement for Portland cement in the binder a small increase in the compressive strength development rate could be suggested. For all investigated mixtures the relative strength compared to the reference mixture increased between 28 and 90 days. This effect was the smallest for the mixture with the lowest percentage of fine glass dust and the largest for the mixture with the highest percentage of fine glass dust. This data suggests that there could be an indication of pozzolanic activity of the fine glass dust at later curing ages, which caused secondary strength development. This is in agreement with the findings in section 3.4.2 in which the mechanism for the potential pozzolanic reaction is explained in more detail. For high replacement percentages of 30–45% this pozzolanic effect caused a significant increase in strength at later stages, but this was not enough to compensate for the dilution effect of the fine glass dust, so still lower strength values were obtained for the mixtures with these replacement percentages.

The findings on the effect of fine glass dust replacement percentages on the compressive strength development of the mortar are in agreement with the findings of Boukhelf et al. [15], in which waste glass powders (WGP) were used to replace Portland cement in the binder. The results of this research showed a decreasing trend between the compressive strength and the WGP percentage, explained by the dilution effect which is the immediate consequence of replacing a more reactive powder (cement) with a less reactive powder (WGP). These results are also in conformity with the findings of Harrison et al. [43], where it was found that high replacement percentages of Portland cement with glass powder caused detrimental effects on the compressive strength development, because insufficient amounts of CaCO_3 remain to react with the amorphous silica from the glass powder. These results are in line with the findings of Du et al. [33], Khan et al. [57] and Gupta et al. [41], which all showed a decrease in compressive strength development when a higher percentage of glass powder was used for early curing ages. For longer curing ages of around 91 days the pozzolanic reaction of the silica in the glass powder caused an increase in strength development rate. But due to the dilution effect at higher replacement percentages, no higher strength compared to the reference mixture could be obtained.

So based on the provided results and discussion about the compressive strength development of fine glass dust mortar mixtures with different replacement percentages it can be indicated that a higher replacement percentage of pre-treated fine glass dust leads to a decrease in compressive strength compared to the reference mixture. The dilution effect plays possibly an important role in the lower strength development for FGD mixtures. At longer curing ages there could be an indication of pozzolanic activity of the FGD, when an increase in strength development rate could be observed. However this pozzolanic activity was not high enough to cover the strength loss by the dilution effect.

4.4.2. Pozzolanic activity of the pre-treated fine glass dust

The objective of the pozzolanic activity test as described in section 4.3.3 was to determine whether the pre-treated fine glass dust possessed pozzolanic activity when it was used as a Portland cement replacement. The data indicates that the mixture with 15% FGD had a higher initial chemically bound water (H) and calcium hydroxide (C-H) content compared to the reference mixture after 7 days of curing. After 28 days of curing the H and C-H content of the reference mixture were both higher than for the FGD mixture. After 56 days of curing the increase in H accelerated for the 15% FGD mixture compared to the reference mix and a small decrease in C-H content was observed. This indicated that the rate of development of H and C-H is lower for the mixture with pre-treated fine glass dust compared to the reference mixture between 7 and 28 days. For longer curing ages between 28 and 56 days the H development is faster for the FGD mix. In this section it is analyzed what this means for the possibility of pozzolanic activity of the pre-treated fine glass dust in cementitious mixtures.

One possible interpretation of the pozzolanic activity test results is based on the chemically bound water (H) content of the mixtures. H content is a measure of how much water is chemically bound in reaction products of the cement matrix and is therefore a measure of the number of reaction products that are formed. A larger H content suggests that there are more reaction products formed in the hardened mixture either by hydration or by pozzolanic activity. An increase in hydration reaction products causes an increase in strength development for the hardened mixture. Between curing ages of 7 and 28 days the reference mix had a higher rate of H development, which indicated that the formation of hydration reaction products was faster compared to the mixture with pre-treated fine glass dust. This is in agreement with findings in section 4.4.1 where the reference mix had a faster compressive strength development rate than the FGD mixtures between 7 and 28 days of curing. Pozzolanic reaction is a slow reaction that leads to the formation of reaction products at a later stage of curing. For the indication of pozzolanic reactivity an increase in H development rate has to be observed at later curing ages. The test results show a faster increase in H content for the FGD-15 mixture compared to the reference mixture, which indicates a small amount of pozzolanic activity for the pre-treated fine glass dust that caused secondary H development. This is in agreement with findings in sections 3.4.2 and 4.4.1 which showed a small increase in compressive strength development rate at later curing ages for the mixtures with pre-treated fine glass dust compared to the reference mixtures.

A second possible interpretation of the pozzolanic activity test results is based on the calcium hydroxide (C-H) content of the mixtures. Calcium hydroxide is formed by the hydration reaction of Portland cement clinker in the binder, but is also used for the pozzolanic reaction to form secondary calcium-silicate-hydrates (C-S-H) from C-H and silica. A larger C-H content indicates that more cement clinker is hydrated to form calcium hydroxide. The reference mix had a higher rate of C-H development between 7 and 28 days compared to the FGD mixture, which suggests faster hydration of Portland cement clinker at these curing ages. This can be explained by the dilution effect of the fine glass dust. The FGD mixture had a lower amount of Portland cement clinker available for hydration, which reduced the hydration rate and thus the C-H formation at these curing ages. This is in agreement with findings in section 4.4.1 where the reference mix had a faster compressive strength development rate than the FGD mixtures between 7 and 28 days of curing. Between 28 and 56 days of curing the C-H content increased a small amount for the reference mix, which indicated the formation of calcium hydroxide at a lower rate. On the other hand, the decreased C-H content between 28 and 56 days of curing for the fine glass dust mixture suggests small amounts of pozzolanic activity. The calcium hydroxide from the cement matrix might be consumed together with silica from the FGD for the slow pozzolanic reaction to form secondary C-S-H. This consumption of C-H for the pozzolanic reactivity could be a possible

interpretation for the reduction in C-H content at higher curing ages. The secondary formation of C-S-H due to the pozzolanic reaction causes densification of the hydrated cement matrix, which leads to small increases in the compressive strength development rate for the FGD mixtures at later curing ages. This is in accordance with findings and discussion in sections 3.4.2 and 4.4.1

The findings on the pozzolanic activity of the pre-treated fine glass dust are in agreement with the findings of Shi et al. [103], Fanijo et al. [36] and Tamanna et al. [113], which all showed pozzolanic activity for finely ground waste glass powder when it was used as a replacement for Portland cement. The pozzolanic activity was indicated by increases in relative strength indexes at higher curing ages compared to the reference mixture, or a decrease in the C-H content at later curing ages for mixtures with finely ground glass powder. The decrease of C-H indicated calcium hydroxide consumption for the secondary formation of C-S-H due to pozzolanic reaction. However research by Afshinnia et al. [3] showed no pozzolanic reactivity for glass powder from crushed glass particles, because no significant reduction in calcium hydroxide content was observed for the glass powder mixtures at longer curing ages. It was suggested that this might be caused by the large average grain size of the glass powder employed in this research (mean particle size was 70 μm). This average particle size is larger than the ground fine glass dust that is used in this study, where the D50 value was 17.20 μm after 1 hour of grinding. The comparison of pozzolanic activity results with other studies indicates that the pozzolanic activity might be enhanced by the increased fineness of the glass powder particles.

So based on the provided results and discussion about the pozzolanic activity test of fine glass dust it can be indicated that the pre-treated fine glass dust possesses a small amount of pozzolanic activity at longer curing ages. This was indicated by the reduction of C-H content between curing ages of 28 and 56 days for the fine glass dust mixture, which might be caused by the consumption of calcium hydroxide for the secondary formation of C-S-H by pozzolanic reaction. Comparison with other studies suggests that pozzolanic activity for glass powders could be enhanced by longer grinding times to reach a smaller average particle size. Due to the grinding treatment of only 1 hour in this study the pozzolanic activity of the fine glass dust is low, but observable.

4.4.3. Effect of different fine glass dust replacement percentages on the secondary formations in the mixture

The objective of the secondary formations test of section 4.3.4 was to find the influence of fine glass dust percentage in the mixture on the formation of secondary products or expansion products after mixing. The goal was to find a replacement percentage of FGD for which there was volume stability and no significant secondary products would form. The data suggests that the mixture with 25% fine glass dust had a large formation of secondary products and cracks when paste mixture was poured into a small cup after 1 day of curing. After 7 and 28 days of curing the cracks propagated and more cracks could be observed, while the secondary formations were still clearly visible. For a replacement percentage lower than 10% there was no significant formation of secondary products visible in the mixture after 1, 7 and 28 days of curing. This section analyzes the potential explanations for the secondary formations in the mixture with high replacement percentage of FGD.

One potential interpretation for the excessive formation of secondary products of the mortar with high FGD replacement percentages could be attributed to the high amount of calcium oxide (CaO) that was present in the fine glass dust. Free lime is Calcium oxide that has not reacted or is not bound to any other compound in a material. Figure 2.1 shows that XRF analysis on the fine glass dust specimen showed a CaO content of 10.3%. This CaO could be present as free lime in the fine glass dust and could potentially cause unwanted expansion and volume instability in the mortar mixtures. It is possible that all the CaO in the fine glass dust is free lime, however for glass powder the presence of large amounts of free lime is questionable. In this study it was not investigated what part of the CaO was present as free lime in the fine glass dust.

When the fine glass dust with a possibility of free lime (CaO) was used in a mortar mixture, the free lime reacted with water to form Calcium Hydroxide (C-H). For normal mortar the water reacted with calcium and silica to form Calcium Silicate Hydrates (C-S-H). The C-S-H gel formed a network that caused strength development in the mortar, then the C-H took up the available space to make sure that the

mortar is compact and therefore could reach high strength values. With the presence of free lime the water reacted with the free lime from the fine glass dust to form C-H. The hydration of free lime was accompanied by a change in the crystallization system and by a significant increase in the apparent volume of free lime. This led to the development of large pressures within the cement matrix, which caused the increase in expansion [28] [116]. High concentrations of free lime could also probably cause the production of small ettringite crystals, which could be contributing to the expansion of the mixture with high fine glass dust percentage. High expansion could cause volume instability and cracks in the mortar which could be detrimental to the strength and durability of the mortar after hydration.

The proposed solution for the unwanted expansion and volume instability of the mortar in this thesis was to decrease the fine glass dust replacement percentage to find a suitable replacement percentage for which significant expansion did not occur. Lower replacement percentage of fine glass dust in the cementitious mixture, meant less free lime in the binder and therefore less unwanted expansion and volume instability. With the cement replacement percentage of 10% the free lime content was lowered, which resulted in no significant expansion due to hydration of free lime in the mixture.

The findings on the secondary formations of mixtures with pre-treated fine glass dust are in agreement with the findings of Courard et al. [28], Nawaz et al. [84] and Kaewmanee et al. [51], which all showed significant expansion in mixtures with high dosages of free lime. High volume expansion of the hydrated free lime was found to be the main driver of high stresses in the cement matrix that could cause expansion and cracks in the developed mixtures. Deterioration of the mortar could be prevented by lowering the free lime content in the mixtures.

So based on the provided results and discussion about the secondary formations test of fine glass dust it can be indicated that the pre-treated fine glass dust caused a significant amount of expansion products when 25% was used in the binder, potentially due to high free lime content. By lowering the fine glass dust percentage to 10%, the free lime content decreased and no significant expansion could be observed.

4.4.4. Limitations

This section describes the limitations of the study on the cement replacement percentage investigation for fine glass dust. For different aspects of the study the limitations are discussed and proposals are made in which the study could be improved based on the limitations.

For the pozzolanic activity test only mix FGD-0 and mix FGD-15 are investigated to compare the formation of C-H and H at different curing ages. Mixtures with a larger replacement percentage of Portland cement by fine glass dust can be added to the pozzolanic activity test. Mixtures with a higher FGD percentage could show more clearly if there is pozzolanic activity, because the difference with the reference mix is larger.

For the secondary formations test visual observation was used to determine the formation of cracks and expansion products. The credibility of these test results could be improved by using a more accurate method of determining the formation of cracks and expansion products in the mixtures. SEM analysis could be performed at different time intervals after curing to monitor the formation of microcracks and expansion products in the paste mixture, which are not visible to the naked eye. In this way a more credible assessment of the mixtures with different FGD percentages can be made. The SEM analysis results in Appendix A were only performed at one curing age and could therefore not be used to monitor the formation of expansion products over time.

The paste samples for the secondary formations test were poured into a cup after mixing. This meant that the mixtures were not free to expand in all directions, because the cup formed a boundary for expansion. A better research profile would be if the paste samples have freedom for expansion. Then it would be possible to quantify the expansion by measuring the dimensions of the sample at specific time intervals after curing, instead of the visual qualitative assessment of the formation of cracks and secondary formations.

The test profile of the secondary formations test investigated mixtures with 0%, 7.5%, 10% and 25% FGD. The results showed that all mixtures up until 10% showed no significant formation of expansion

products, but the mixture with 25% had significant formation of cracks and expansion products. However with this test profile it is not known what is the percentage at which the expansion products start to form. It should be somewhere between 10 and 25% but the exact percentage remains unknown. This study can be improved by increasing the number of investigated mixtures to check at which percentage the expansion products start to form. In this way it can also be investigated whether this is a gradual transition or a sudden change from no to a significant amount of secondary formations. With this knowledge the maximum fine glass dust percentage without expansion could be optimized.

5

Suitability of fine glass dust for 3D Concrete Printing

In Chapters 3 and 4 fine glass dust was used to replace Portland cement in traditionally mold-cast mortar mixtures. Investigations were performed on the most optimal pre-treatment of the fine glass dust and also the optimal replacement percentage in terms of compressive strength development. In Chapter 2 it was mentioned in section 2.3 that 3D Concrete Printing (3DCP) is a recently developed technique of additive manufacturing of concrete. 3DCP has several advantages over conventionally cast concrete from an environmental, economical and construction process viewpoint (see section 2.3.1). Currently a lot of research is done on 3DCP and in the future this may become the main way of producing concrete structures and buildings. Based on these mentioned reasons, this chapter focuses on the suitability of using fine glass dust as a cement replacement for 3D Concrete Printing.

In section 5.1 the objective and research plan are presented to determine the suitability of fine glass dust for 3DCP. Section 5.2 describes the materials that are used for 3DCP mixtures and explains the performed tests in more detail. Section 5.3 and 5.4 presents the results and discussions on the performed tests about the suitability of fine glass dust as a Portland cement replacement for 3DCP.

5.1. Research plan

The goal of this chapter was to investigate the suitability of Portland cement replacement by fine glass dust for 3D Printed Concrete. In section 2.3.2 different 3D Printing Concrete techniques were described. For this thesis the recently developed set-on-demand concrete printing technique was used. This means that a pumpable cementitious mixture and an accelerator slurry were prepared separately and were mixed at the printing head just before printing. The accelerator slurry causes a fast activation of the hydration reaction in the cementitious mixture and after mixing at the printing head and a fast strength development occurs. For more information on set-on-demand printing, section 2.3.2 can be consulted.

5.1.1. Pumpable cementitious mixtures

For this thesis, in the pumpable cementitious mixture part of the Portland cement was replaced by the fine glass dust, which had the most optimal pre-treatment as described in Chapter 3. The mix design for 3DCP mixtures had a lower water/binder ratio and also a lower sand/binder ratio was used. This means that in comparison with conventionally cast concrete, 3DCP mixtures contain relatively more Portland cement. High amount of Portland cement in 3DCP mixtures means that there will be high strength development. Because of this high strength development, it was possible to replace a larger percentage of Portland cement with fine glass dust while still reaching acceptable strength levels. For 3DCP the mixtures need to have sufficient flowability and high viscosity. High flowability is needed to make sure that the mixture is pumpable and easily flowable. High viscosity for 3DCP mixtures is needed to prevent segregation during the pumping process. To reach flowable mix designs, Superplasticizer (SP) was added to the mixtures and the goal was to find the optimal SP dosage for the chosen mix design. The different mixtures that were investigated are described in section 5.2.1.

The prepared pumpable cementitious mixtures were tested on flowability (slump flow test) at different time intervals after mixing. This was done to determine how the flowability and consistency of the mixtures change over time. The flowability could not be too high, because then the structural build-up would be insufficient. On the other hand, the flowability could not be too low, because this means that the mixture would not be workable enough. The slump flow tests were good indicators to see if the designed mixture could be used for 3DCP. Compressive strength tests were performed for each of the pumpable cementitious mixtures after 7 days of curing. This was done to compare the strength development of the mixtures with different SP dosages. Longer curing days are not taken into account, because long-term strength values provide only valuable information for the cementitious mixture + accelerator slurry.

Based on the flowability and compressive strength test the mixture with the most promising result was selected to continue to work with. With this mixture a pumpability test was performed to check the pumpability of the designed cementitious mixture. For a mixture to be pumpable it is important that the mixture stays consistent under pressure in the pumping hose and that no segregation occurs. During the pumpability test also the material flow rate was measured to determine the optimal pumping speeds for each mixture. Based on the pumpability test one single optimal pumpable cementitious mixture was selected.

5.1.2. Pumpable cementitious mixtures + accelerator slurry

In the next stage of the 3DCP research the behaviour of the optimal cementitious mixture when it was mixed with the accelerator slurry was investigated. This was important, because during set-on-demand printing the cementitious mixture and accelerator slurry were mixed at the printing head. The printed filaments from the printer are a combination of both mixtures.

For the accelerator slurry a limestone powder based mix design was used in this thesis. The amount of accelerator dosage in the accelerator slurry was changed to check the influence of different accelerator dosage on the behaviour of the material. For the combination of pumpable cementitious mixture and accelerator slurry flowability and compressive strength tests were performed, for the same reasons that were mentioned in section 5.1.1. For the combination of cementitious mixture and accelerator slurry also the initial setting time test was performed. This was done to check the influence of changing accelerator dosages in the accelerator slurry on the setting time of the combined mixture. The working mechanism of the accelerator is correct if a larger accelerator dosage leads to a lower initial setting time.

Based on the flowability test, compressive strength test and the initial setting time test, 1 combined mixture (pumpable cementitious mixture + accelerator slurry) was selected to continue to work with. With this mixture a buildability test was performed, which meant that layers of printed material were placed on top of each other. Because of the very labor-intensive work of handling a 3D printer only 1 mixture of the original design could really be printed. Buildability test was performed to investigate the structural build-up of the printed filaments. A faster strength development means a higher structural build-up and this means that more layers can be printed on top of each other without failure.

After the buildability test small samples were sawed out of the printed material. These sawed-out samples were used for compressive strength testing of the 3D printed material. This was done to investigate the strength development of the stacked filaments after printing. Because 3DCP prints layers on top of each other an interface between the layers is formed. This interface between filaments causes deviating element properties in different directions and this means that compressive strength test on the printed sample had to be performed in three directions: Longitudinal, lateral and perpendicular to the printing direction (see Figure 2.10). The strength of the printed sample could then also be compared to the strength of the cast-mortar sample of the same combined mixture.

5.2. Materials and Methods

5.2.1. Mix design for pumpable cementitious mixtures

The mix designs that were used in this thesis for the pumpable cementitious mixtures are given in Table 5.1. The reference mix design had a specific gradation of sand that had proven to be successful for 3DCP in the past. Based on this reference mixture the mix designs for the replacement of PC by FGD in this thesis were made. The type of Portland cement (PC) that was used for 3D concrete printing was CEM I 52.5R. All the fine glass dust that was used had the same pre-treatment: 600°C heat-treatment and 1 hour grinding treatment. The water/binder ratio that was used is 0.3 and the sand/binder ratio that was used in the reference mixture for 3D concrete printing was 1.0 in all mixtures. For the superplasticizer MasterGlenium 51 con.35% NL was used.

In this thesis two different cement replacement percentages were investigated. For mix FGD20 20% of

Mix	PC	FGD	SP	Water	Sand (0.125-0.25 mm)	Sand (0.25-0.5)	Sand (0.5-1)	Sand (1-2)
Reference	1000	0	0	300	280	520	180	20
FGD50-SP0.25	500	500	2.5	300	280	520	180	20
FGD50-SP0.4	500	500	4	300	280	520	180	20
FGD50-SP0.45	500	500	4.5	300	280	520	180	20
FGD50-SP0.5	500	500	5	300	280	520	180	20
FGD20-SP0.25	800	200	2.5	300	280	520	180	20
FGD20-SP0.35	800	200	3.5	300	280	520	180	20
FGD20-SP0.4	800	200	4	300	280	520	180	20
FGD20-SP0.5	800	200	5	300	280	520	180	20

Table 5.1: Mix compositions for pumpable cementitious mixtures (units are grams for 1 liter of mixture)

the Portland cement in the binder of the cementitious mixture was replaced with pre-treated fine glass dust and for mix FGD50 50% of the Portland cement was replaced with fine glass dust. This can be seen in Table 5.1. It has to be taken into account that set-on-demand concrete printing was used. This means that the pumpable cementitious mixture was mixed with the accelerator slurry in a ratio of 1:1. This means that for the 3D printed concrete (the combined mixtures) the amount of PC per liter mixture was halved and only 250 grams of PC was available per liter for the 50% FGD cementitious mixture.

The reason for the replacement percentage of 20% in the cementitious mixture was mainly chosen because of the secondary formations test in section 4.3.4. These results showed that a total mixture with 10% FGD was the largest percentage that had volume stability and did not lead to significant formation of expansion products. When the cementitious mixture with 20% FGD is combined with accelerator slurry in a ratio of 1:1, this would not lead to any volume instability based on the test results of section 4.3.4.

The cementitious mixture with 50% cement replacement by FGD would lead to a total mixture with 25% FGD after combination with the accelerator slurry during printing. Based on the results in section 4.3.4 it was known that this mixture would lead to volume instability and significant formation of expansion products. However for 3DCP mix designs a high amount of PC was used. In the reference mixture 1000 grams of PC was used for 1 liter of mixture. A high PC amount in a mixture means high strength development after printing. When 50% of the Portland cement amount was replaced with pre-treated fine glass dust, then still 500 grams of PC was used for 1 liter of the pumpable cementitious material. Despite the high expansion of the mixture it was interesting to look at the fresh-state properties when 50% of FGD was used to replace cement for the pumpable cementitious mixture for 3DCP. With the investigation of two different fine glass dust percentage mixtures it was also possible to study the influence of changing FGD percentage on the properties of the fresh 3DCP mixtures when 50% FGD and 20% FGD could be compared with each other.

It can be seen from Table 5.1 that for the cementitious mixtures different Superplasticizer (SP) amounts were used. The goal of the SP addition in the mixture was to investigate the effect on the flowability of the mixtures in section 5.2.2. For a mixture to be pumpable the flowability could not be too high, but also not too low. Different SP amounts were used to investigate what was the SP amount that could be

used the best for the pumpable cementitious mixture with 20% and 50% Portland cement replacement by fine glass dust.

The mixtures were prepared by first measuring the required raw materials precisely. Then the dry materials (Sand, CEM I 52.5R and fine glass dust) were mixed for one minute at the lowest speed (speed 1). It had to be checked manually if all the materials were mixed properly. Secondly the water + SP could be slowly added while mixing on speed 1. It had to be made sure that that the water was added in small increments and that after each increment all the water was properly mixed before adding the next increment. This was done to prevent agglomeration of material in the mixture and to the side of the mixing bowl. When all the water was added, the start of mixing time was determined and there had to be mixed at slow speed for 4 minutes. Afterwards the material was scraped off from the sides of the bowl manually to make sure all the material could properly mix and there was mixed once again for 1 minute on speed 1. Afterwards the speed was increased to speed 2 for 2 minutes to ensure proper mixing of all the materials at high speed and to complete the preparation of the mortar mixtures.

5.2.2. Flowability test for cementitious mixtures

Flowability is an important property for a pumpable mixture for 3D concrete printing. If the flowability is too low, then the material is difficult to pump through the pumping hose which can cause high pumping pressures and possible damage to the printing equipment. If the flowability is too high then the material can't be pumped correctly, because there is a high risk of segregation of the material during the pumping process. If segregation occurs during pumping this means that the mixture loses its consistency and the material that is pumped through the hose is not mixed properly anymore. The goal of the flowability test was to find the mix design with the optimal SP dosage for the pumpable cementitious mixture. The mixtures with different SP dosages that were used for the flowability test are presented in Table 5.1. To determine the flowability of the mixtures, slump flow tests were performed. For 3D concrete printing it was not only sufficient to look at the flowability directly after mixing, but it was more valuable to investigate the change in flowability at different time periods after mixing. This was done, because with 3D concrete printing the material was not printed directly after mixing but it needed to be printable for a longer period of time. With this flowability test it was investigated how the flowability changed over time for the mixtures with different superplasticizer dosages.

Test set-up

Test set-up for the flowability test (slump flow test) was described in section 3.2.8.

Samples

Sample preparation for the flowability test was described in section 3.2.8.

Procedure

The goal of the flowability test was to investigate the change of the flowability of the mixtures with different SP dosages over time. As described in the introduction of this subsection the flowability of the mixtures was tested by performing slump flow tests at different time periods after mixing. The flowability of the pumpable cementitious mixtures was tested at 15, 30, 45 and 60 minutes after mixing and the time of mixing was determined as the moment when all the water and SP were added. When the materials were mixed properly and the sample for the slump flow test was prepared, the first slump flow test could be performed exactly 15 minutes after mixing. The Hägermann cone was removed and the compaction table was dropped 25 times. After 25 drops the diameter of the spread mortar was measured in 4 directions and the mean value was determined. Then the mortar was collected and placed in a zip-locked plastic bag. This was done to prevent excessive water loss by evaporation from the material during the time between two consecutive slump flow tests. The Hägermann cone and the compaction table were cleaned properly to prepare for the next slump flow test. For each mixture the slump flow test was performed at 4 different time periods after mixing and the mean flow diameter was measured. The result gave 4 data points for each mixture in which the flowability change over time could be determined. For each of the mixtures with different SP dosages (see section 5.2.1) 3 repetitions were performed to increase the validity and accuracy of the results.

5.2.3. Compressive strength test for cementitious mixtures

The mix designs that were used for the investigation of pumpable cementitious mixtures had a Portland cement replacement percentage of 20% and 50% by pre-treated fine glass dust (see section 5.2.1). In section 4.3.2 it could be seen in Figure 4.4 that high replacement percentages of FGD led to a significant reduction of compressive strength for conventional cast mortar. For a replacement percentage of 45% FGD, the strength reduction compared to the reference mixture was 50%, 53% and 56% for curing ages of 3 days, 7 days and 28 days respectively.

For 3D concrete printing mix designs with lower water/binder ratio and lower sand/binder ratio were used. This means that relatively more cement was used in these mixtures which caused a higher rate of strength development. Also the cement type CEM I 52.5R was used, which provided rapid strength gain at early curing ages. Compressive strength tests were performed on the pumpable cementitious mixtures to investigate the influence of changing FGD amount on the compressive strength development. Also it was important to investigate how the different superplasticizer dosages in the mixtures influenced the compressive strength development.

Test set-up / Samples / Procedure

The test set-up, sample preparation and procedure for the compressive strength test were described in section 3.2.10. For the comparison of the pumpable cementitious mixtures, 2 L of mixture was prepared and compressive tests were only performed after 7 days of curing to find the influence of different SP dosages. For each mixture 6 repetitions were performed.

5.2.4. Pumpability test for cementitious mixtures

The results of the slump flow test that was described in section 5.2.2 showed the change of flowability of the different mixtures over time. For 3D concrete printing the flowability had to be in a specified range of spread diameter during the printing process. Based on the results of the flowability test for the cementitious mixtures given in section 5.3.1, the mixture with the optimal dosage of superplasticizer was chosen to continue for the pumpability test for the cementitious mixtures. The pumpability test required a lot of material preparation and was labor-intensive work, so this was the reason that the pumpability test was only investigated for one mixture.

The pumpability test was performed to investigate the ability of the cementitious mixture to be pumped through a pumping hose. It was important to investigate if the material properties changed during the pumping process and if the mixture could contain its consistency during printing. High viscosity of a 3D printed mixture was needed, because otherwise there was a risk of segregation of materials in the mixture during the printing process. Pumpability test was also performed to monitor the pressure during the pumping of cementitious material. The mixture needed to possess enough flowability to be easily pumped through the pumping hose without high pressures to occur. High pumping pressures could lead to possible damage to the printing nozzle, once the mixture was used for a real 3D printed test.

The objective of the pumpability test was to find the material flow rate of the cementitious mixture for different pumping speeds. The material flow rate at a specific pumping speed was the determining factor for the linear moving speed of the printing nozzle during the 3D printing process. The material flow rate determined how much material was pumped through the hose each second and if the cross-section of the printing nozzle is known, the linear moving speed of the printing nozzle for 3D printing could be determined to print filaments without discontinuities (if the nozzle moves too fast) or material accumulation (if the nozzle moves too slow).

Test set-up

The pumpability test for the cementitious mixture in this thesis was performed with the PFT Swing-M type material conveying pump. The test set-up can be seen in Figure 5.1. The test set-up consisted of a material conveying pump connected to a pumping hose. The material conveying pump provided the primary forces for pumping the cementitious mixture and was based on a rotor and stator configuration. The rotor was connected to the pump and consisted of a steel spiral component that was screwed into the stator, which was a rubber cover around the rotor (see Figure 5.2a). Friction-induced heating could occur if the material passes the stator-rotor system. In the hopper of the pump up to 38 L of fresh cementitious mixture could be placed. Driven by the motor and the rotor-stator system, the mixture

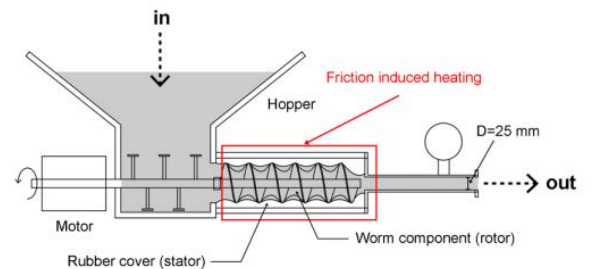


Figure 5.1: Test set-up of the material conveying pump

was pumped through the pumping hose at a specific material flow rate, depending on the different motor speeds and rheology of the cementitious mixture. A pressure gauge was placed directly after the rotor-stator system to prevent high pumping pressures in the pumping hose. A schematic view of the material conveying pump is given in Figure 5.2b.



(a) Rotor-stator system



(b) Schematic view of the material conveying system [22]

Figure 5.2: Material conveying system

A material pumping hose with an inner diameter of 25 mm and a length of 3 m was connected to the pump. Based on the forces provided by the material conveying pump, the material was passed through the pumping hose and was extruded at the end of the hose.

Samples

For the pumpability test a minimum of 7 L of fresh cementitious mixture was needed. This was to ensure that there was sufficient material to be pumped through the hose and that the hopper of the material conveying pump was sufficiently filled. The mixture that was used for the pumpability test was mix FGD50-SP0.40. The mix design for 1 L of mixture can be seen in Table 5.1. The results from section 5.3.1 showed similar flow behaviour for mixtures FGD50-SP0.40 and FGD20-SP0.35 in terms of spread diameter over time. Because of low availability of pre-treated fine glass dust during this thesis, only mix FGD50-SP0.40 was investigated for the pumpability test and it was assumed that mix FGD20-SP0.35 would possess similar flow behaviour during the pumping process.

Procedure

If the test set-up was prepared and all the components were connected and cleaned, the sample of fresh cementitious mixture could be placed in the hopper. The objective was to find the material flow rates for the cementitious mixture at different motor speeds from the material conveying pump. After placement of the material the motor was turned on at speed 2, the lowest speed that was investigated. First the excess water was removed from the pumping hose and it was checked if the cementitious mixture was pumped through the hose. During the pumping process the pressure gauge had to be monitored to avoid high pumping pressures. If the first cementitious material was fully pumped through the hose, the motor was turned off and the conveying end of the pumping hose was placed above the hopper. This was done to reuse the cementitious material after it had passed through the hose and to collect the material for the pumpability test (see Figure 5.3).



Figure 5.3: Pumpability test material pumping

For the start of the pumpability test, the motor was turned on at speed 2 and it had to be made sure that the mixture was properly pumped through the hose. Then for a time interval of 10 seconds the pumped material from the hose was collected in a zip-lock plastic bag. At motor speed 2 there were 2 repetitions performed. Afterwards the motor speed was increased to speed 3. After increasing the motor speed the material was pumped through the hose at a higher pace, so for a short period of time the pumping process had to adjust to the higher pumping speed. Then for a time interval of 10 seconds the pumped material was collected in a zip-lock plastic bag and also for speed 3 there were 2 repetitions performed. Afterwards the speed of the motor was increased to speed 4 and speed 5 and for both these speeds also 2 repetitions were performed and the pumped material from the hose was collected.

Afterwards the pumping hose and the hopper were cleaned, the rotor-stator system was disassembled and all the other connecting components of the material conveying pump were cleaned and dried. The mass of pumped cementitious material that was collected at different pumping speeds was measured. With the unit weight of the cementitious material the collected mass after 10 seconds of pumping was then converted to the material flow rate at different pumping speeds.

5.2.5. Mix design for cementitious mixtures + accelerator slurry

As described in section 5.1.2 after the formulation of the mix design for the pumpable cementitious mixture, the next step in the process was to investigate the behaviour and properties of the combination of cementitious mixture and accelerator slurry. This was investigated because for set-on-demand concrete printing the pumpable cementitious mixture and the accelerator slurry were mixed at the printing head with a helical static mixer (see section 2.3.2). The interaction between the cementitious mixture

and the accelerator slurry had to stimulate rapid strength gain and stiffness development after extrusion from the printing nozzle, because the printed filaments needed to have sufficient strength to withstand the load from the subsequent layers that were placed on top during the printing process.

From sections 5.3.1 and 5.3.3 it could be seen that the pumpable cementitious mixture FGD50-SP0.4 provided the best results for the flowability change over time and also provided good results during the pumpability test. In this mixture 50% of the CEM I 52.5R was replaced with pre-treated fine glass dust. All the fine glass dust that was used had the same pre-treatment: 600°C heat-treatment and 1 hour grinding treatment. For the mixtures with 20% replacement by fine glass dust mix FGD20-SP0.35 provided the most optimal results in terms of flowability change over time (see section 5.3.1). The accelerator that was used in the accelerator slurry was CaCl_2 . The amount of accelerator dosage in the accelerator slurry was varying during this investigation to research what was the influence of different accelerator dosages on the fresh-state behaviour and hardened properties of the combination of cementitious mixture + accelerator slurry. The different mix designs that were investigated are presented in Table 5.2.

In Table 5.2 it is shown which different accelerator dosages were investigated for the accelerator slurry

Mix	PC	FGD	SP	Water	Sand (0.125-0.25 mm)	Sand (0.25-0.5)	Sand (0.5-1)	Sand (1-2)
FGD50-SP0.4	500	500	4	300	280	520	180	20
FGD20-SP0.35	800	200	3.5	300	280	520	180	20
Mix	LP	FGD	CaCl_2 (33%)	Water	Sand (0.125-0.25 mm)	Sand (0.25-0.5)	Sand (0.5-1)	Sand (1-2)
Acc0%	1000	-	0	300	280	520	180	20
Acc2%	1000	-	10	293.3	280	520	180	20
Acc5%	1000	-	25	283.25	280	520	180	20
Acc8%	1000	-	40	273.20	280	520	180	20
Acc10%	1000	-	50	266.50	280	520	180	20

Table 5.2: Mix compositions for cementitious mixture and accelerator slurry (units are grams for 1 liter of mixture)

mix design. The accelerator dosage was calculated as a percentage of the Portland cement that was used in the cementitious mixture FGD50. For 1 liter of cementitious mixture, the amount of Portland cement that was used in mix FGD50 was 500 grams, so the mixture Acc2% consisted of 10 grams of CaCl_2 solution. The CaCl_2 solution that was used consisted of 33% CaCl_2 and 67% water. The amount of water that was used in the mix design for the total accelerator slurry had to be adjusted for the amount of water that was present in the CaCl_2 solution. For the mixture Acc2% this meant that $0.67 \cdot 10 = 6.7$ grams of water was present in the CaCl_2 solution and the remaining part of the water that needed to be added to the mixture is $300 - 6.7 = 293.3$ grams. If this adjustment for the amount of water in the CaCl_2 solution was not made this meant that for higher accelerator dosages there was a larger amount of water in the mixture, which meant that the flowability of the accelerator slurry increased. In order to solely investigate the influence of variable accelerator dosage in the mixtures, the total amount of water in the mixture needed to be constant. Both pumpable cementitious mix FGD50-SP0.40 and mix FGD20-SP0.35 were combined with accelerator slurry to also investigate the effect of different FGD percentages on the fresh properties of the combined mixture (cementitious mix + accelerator slurry)

The combination of accelerator slurry and cementitious mixture was prepared by first measuring the raw materials of both mixtures separately. Then the dry materials of the accelerator slurry were mixed in the small Hobart mixing machine. After 1 minute of mixing the water and the CaCl_2 solution were slowly added to the mixture. When all the water was added there was mixed for 2 minutes at slow speed. Then the material was scraped off the sides and bottom of the mixing bowl and mixing was continued for another minute at slow speed. Afterwards the speed of the mixer was increased to speed 2 and there was mixed for another 2 minutes. Then a plastic cover was placed on top of the mixing bowl of the accelerator slurry to prevent excessive water loss during the time period when the cementitious mixture was prepared. Preparation of the cementitious mixture was exactly the same as for the

accelerator slurry. First the dry materials were mixed and then the water and superplasticizer were added. The mixing times were also kept constant. After both the accelerator slurry and the cementitious mixture were prepared separately, the mixtures were combined in the mixing bowl of the large Hobart mixing machine. The combined mixture was mixed for another 1 minute at low speed. This was done to simulate the mixing process in the helical static mixer for set-on-demand concrete printing in which the cementitious mixture and accelerator slurry are combined just before extrusion from the printing head. As presented in Table 5.2 the preferred pumpable cementitious mixtures for FGD50 and for FGD20 from section 5.2.1 were combined with 5 different accelerator slurry mixtures to investigate the influence of accelerator dosage on the fresh-state and hardened properties of the combined mixtures.

5.2.6. Flowability test for cementitious mixtures + accelerator slurry

For the combined mixture of cementitious mixture + accelerator slurry it was important to determine the influence of varying accelerator dosage on the flowability directly after mixing. During the concrete printing process with the set-on-demand method, the combined mixture was extruded from the printing head shortly after mixing the two separate mixtures together. Therefore the flowability of the combined mixtures with different accelerator dosages that were presented in section 5.2.5 was investigated by performing slump flow tests directly after mixing.

Test set-up / Samples / Procedure

The test set-up, sample preparation and procedure for the slump flow test for flowability of the combined mixtures were described in section 3.2.8. For each combination of cementitious mixture + accelerator slurry 3 repetitions were performed and the mean value of the slump flow diameter after 25 drops of the compaction table was calculated.

5.2.7. Initial setting time test for cementitious mixtures + accelerator slurry

For set-on-demand concrete printing the extruded mixture from the printing head was a combination of the pumpable cementitious mixture and accelerator slurry. This combined mixture needed to possess high stiffness and sufficient structural build-up, so that the printed filaments could withstand the loads from the subsequent layers that were printed on top during the printing process. For the combined mixtures it was essential to investigate the influence of the different accelerator dosages on the initial setting time. For high early age stiffness development in a mixture, a short initial setting time was needed. If the accelerator works properly, then a larger accelerator dosage leads to a shorter initial setting time. For set-on-demand concrete printing the combined mixture of cementitious mixture + accelerator slurry needed to have an initial setting time of around 90 minutes. If the initial setting time was too low, this meant that the stiffness development was too fast and that the mixtures could not be properly extruded from the printing nozzle. If the printed material has a high stiffness this can lead to high pressures at the printing nozzle and a large number of surface deflections in the printed filaments. On the other hand, if the initial setting time was larger than 90 minutes, this meant that the stiffness development of the combined mixture was slow, which results in the extrusion of highly flowable material from the printing nozzle. If the printed filaments have high flowability and low stiffness this leads to low structural build-up of the mixture and low buildability if multiple layers are printed on top of each other.

Test set-up / Samples / Procedure

The test set-up, sample preparation and procedure for the initial setting time test for the combined mixtures were described in section 3.2.8. For each combination of cementitious mixture + accelerator slurry 3 repetitions were performed and the mean value of the initial setting time was calculated.

5.2.8. Isothermal calorimetry test for cementitious mixtures + accelerator slurry

Isothermal calorimetry test was performed to study the heat flow and heat evolution of the combined mixture of cementitious mix + accelerator slurry during the first seven days of hydration. The goal was to find the influence of variable fine glass dust amount on the heat evolution of the hydration reaction, but also to investigate the influence of different CaCl_2 dosages in the accelerator slurry on the heat evolution.

Test set-up

The isothermal calorimetry test in this thesis was performed by an eight-channel TAM Air calorimeter. This machine was used to investigate the heat evolution of paste samples and can be seen in Figure 5.4.



Figure 5.4: TAM Air calorimeter with eight channels

This TAM Air machine consists of eight different channels which work independently and a channel consist of two separate glass vessels. One vessel was used for the reference and the other vessel was used for the sample. Because paste samples had to be placed in the vessels, the sand fractions were left out of the mixture.

Samples

Before the test could start, the reference vessels were filled with a fine sand fraction (0.125 - 0.25 mm). The weight of this reference sand was calculated to have the same specific heat capacity as the sample that was tested. Before mixing the samples a baseline was recorded for about 30 minutes in which the test conditions could be calibrated. After the baseline was initiated the fresh mixtures were prepared by first mixing the dry materials together and afterwards the water, superplasticizer and accelerator were added to the mixture. The fresh paste was mixed for about 2-3 minutes. Then 6 grams of freshly prepared paste was collected in a sample vessel of 20 mL. When the sample vessel and reference vessel were both prepared, they were simultaneously placed into the channel.

Procedure

During the isothermal calorimetry test the temperature inside the calorimeter was kept constant at 20°C during the entire test. The heat flow values of each sample were recorded every 20 seconds to determine the heat evolution of the different mixtures. This was continued for 168 hours, which is equal to 7 days. The mixtures that were investigated in the calorimeter were (see Table 5.2):

- Cementitious Mix FGD20-SP0.35 + Acc Slurry with 0% CaCl_2
- Cementitious Mix FGD20-SP0.35 + Acc Slurry with 5% CaCl_2
- Cementitious Mix FGD20-SP0.35 + Acc Slurry with 8% CaCl_2
- Cementitious Mix FGD50-SP0.4 + Acc Slurry with 0% CaCl_2

The goal was to find the influence of FGD amount and CaCl_2 dosage in the Acc slurry on the heat evolution of the combined mixture of cementitious mixture + accelerator slurry.

5.2.9. Compressive strength test for cementitious mixtures + accelerator slurry

Compressive strength tests were performed for the combination of cementitious mixture and accelerator slurry based on two reasons. Firstly to determine the influence of combination of cementitious mixture and accelerator slurry on the compressive strength development compared to only cementitious mixture (which was investigated in sections 5.2.3 and 5.3.2). Accelerator slurry only had limestone powder and no extra Portland cement (PC) in the mix design, so this meant that when the mixtures were combined in a ratio of 1:1 the total amount of Portland cement (which caused the main strength development) decreased per volume of the combined mixture. This meant that a liter of material only had 250 grams of PC instead of 500 grams of PC for mixture FGD50. Compressive strength tests were performed to investigate the changes of the combined mixture on compressive strength development.

Secondly compressive strength tests were performed to determine the influence of different accelerator dosages in the accelerator slurry on strength development of the combined mortar. The mixtures with different CaCl_2 dosages were tested on the compressive strength development with the goal to investigate the influence of CaCl_2 on the strength development of the combined mixtures. Together with the results of the initial setting time test of section 5.2.7 it could be determined if the accelerator has a positive effect on the setting and/or hardening development of the combined mixtures of cementitious mixture + accelerator slurry.

Test set-up / Samples / Procedure

The test set-up, sample preparation and procedure for the compressive strength test for the combined mixtures were described in section 3.2.10. For each combination of cementitious mixture + accelerator slurry 3 repetitions were performed and the mean value of the compressive strength was calculated. Compressive strength tests were performed at curing ages of 7 days and 28 days for each combination of cementitious mixture and accelerator slurry. This was done to determine the influence of varying accelerator dosage on strength development at shorter and longer curing ages.

5.2.10. Buildability test for 3D Printed Concrete

The main advantage of set-on-demand 3D concrete printing compared to regular concrete printing is the ability to make two separate mix designs for the pumpable cementitious mixture and the pumpable accelerator slurry. These mixtures can both have high flowability and low yield stress, which causes lower pumping pressures and a longer open time during the printing process. A longer open time means that more material can be printed with the same batch of material before the stiffness development is too high to print extra filaments without significant surface defects. However after both mixtures are combined in the helical static mixer just before extrusion, the material needs to have sufficient yield strength and structural build-up if the filaments are extruded from the printing nozzle. High structural build-up of the printed layers is needed to withstand the load of the subsequent layers that are printed on top during the printing process and to ensure the stability of the printed sample. During the inline mixing process the accelerator comes into contact with the cement particles in the pumpable cementitious mixture. This causes a drastic increase in the hydration rate and structural build-up of the mixture and results in a fast transition from a flowable mixture to a buildable mixture after the combination of pumpable cementitious mixture and accelerator slurry leaves the helical static mixer. In this way the contradicting rheological properties that are needed for 3DCP can be achieved by set-on-demand concrete printing.

Buildability test in this thesis was performed on the printed filaments to investigate the structural build-up of the combination of cementitious mixture and accelerator slurry. A faster strength development means a higher structural build-up and this means that more layers can be printed on top of each other without failure. The goal of the buildability test was to find the maximum number of layers that could be printed on top of each other before failure occurred. In section 4.2.5 it was described that the cementitious mixture with 50% replacement of PC by fine glass dust had volume instability and led to the formation of expansion products during curing. Due to volume instability and material shortage this mixture was not included in the buildability test. The pumpable cementitious mixture with 20% fine glass dust was included for the buildability test, because this was the maximum replacement percentage that did not lead to the formation of excessive amounts of expansion products in section 4.2.5 and was therefore a safer mix design to be used in practice.

Test set-up / Samples

The test set-up for the buildability test is shown in Figure 5.5. This test set-up consisted of two separate material conveying pumps and two pumping hoses that were connected to the helical static mixer.



Figure 5.5: Two material conveying pumps with separate pumping hoses

The helical static mixer was connected to the 3D concrete printer as shown in Figure 5.6. The material conveying pumps were connected in the same way as for the pumpability test that was described in section 5.2.4 with a rotor-stator system and a pressure gauge. Both material pumping hoses had an inner diameter of 25 mm. The helical static mixer also had a diameter of 25 mm and was connected to a circular printing nozzle. The 3D concrete printer at TU Delft is based on a 3-axis gantry system, which means that the printing nozzle can move in longitudinal, lateral and vertical direction. The concrete printer was connected to a computer numerical control (CNC) system, which determined the printing path of the extruded filaments.

For the design process in 3DCP the concrete elements were designed as volumetric objects by 3D modelling software. In the next step they were sliced into a series of two-dimensional layers. From this data of two-dimensional layers the G-code was generated. The G-code was exported to the CNC system to print the concrete elements by controlled extrusion of the material.

In order to make sure that the quality of the extruded material was sufficient it was important that the linear moving speed of the printing nozzle was determined based on the material flow rate of the mixtures in the material conveying system. As mentioned in section 5.2.4 this could significantly influence the quality of the printed filaments. In this study a nozzle moving speed of 3600 mm/min was used for printing the buildability test.

For the buildability test a minimum of 11 L of both fresh cementitious mixture and accelerator slurry was needed, to ensure that there was sufficient material for printing and that the hopper of the material conveying system was sufficiently filled. The cementitious mixture that was used for the buildability test was FGD20-SP0.35. The accelerator slurry mixture that was used for the buildability test was Acc8%. The mix designs for 1 L of these mixtures can be seen in Table 5.2. During the printing process the mixtures were added together in the ratio of 1:1. This meant that the motor speed and the material flow rate of both mixtures had to be similar to ensure that equal amounts of material were mixed in the helical static mixer. The mixtures were divided into two batches of 7 L, because this would otherwise exceed the capacity of the Hobart N-50 mixer. The mixing procedure for the cementitious mixture and the accelerator slurry was the same as described in section 5.2.4. First the accelerator slurry was prepared and poured into the hopper of one of the two material conveying pumps. The hopper was then



Figure 5.6: Helical static mixer set-up with printing nozzle (Yu Chen)

covered with a towel to prevent excessive water loss during the time that the cementitious mixture was prepared. Secondly the cementitious mixture was prepared and the fresh mixture was poured into the hopper of the second material conveying pump.

Procedure

When the test set-up was prepared and all the components were connected and cleaned, the fresh mixtures could be placed in the two separate hoppers. The objective of the buildability test was to find the maximum number of layers that can be stacked on top of each other without failure. The number of subsequent stacked layers was a measurement for the structural build-up of the material just after extrusion from the printing nozzle. The buildability test was also performed to investigate the quality of the printed filaments of a mixture with high expansion and volume instability.

For the buildability test a cylindrical column was printed and also a prism was printed for the compression test in section 5.2.11. This was done by preparing the G-code on the CNC system for this cylinder and prism divided into layers. The printed column had a diameter of 180 mm and the prism had a length of 800 mm. A nozzle moving speed of 3600 mm/min was used for the printing session, which means that the time between two subsequent filaments was 9.42 seconds for the cylindrical column and 13.3 seconds for the prisms. For printing vertical objects there are two possibilities to adjust the height: Gradually increasing the height over the printing path or step increasing the height at a specific location. For the cylinder of the buildability test the gradually increasing height was used of 15 mm per layer, which meant that extrusion of printed material was continuous and that no discontinuities occurred at the location where step increase height happened due to accumulation of material.

Before printing a plastic film was applied to protect the printing table. The printing nozzle was moved to the starting position and the printing process was started. Both material conveying pumps were turned on at the same time and with the same motor speed. Printing of the column was continued until failure occurs. The number of printed layers before failure was measured and photos of the printed results were taken. During the printing process different failure modes can occur: Global failure of the printed specimen (plastic collapse down or to the side), local failure of a printed filament (stress concentrations due to printing process) or discontinuities in the printed filaments (high stiffness development causes problems with extruding the material). If one of these three failure mechanisms occurred on the cylinder, then the buildability test was stopped and the maximum number and height of deposited

layers before collapsing were recorded as indicators for the buildability of the printed material.

5.2.11. Compressive strength test on 3D Printed Concrete

The objective of the compressive strength test was to investigate the compressive strength development of the 3D printed samples of mix FGD20-SP0.35-Acc8%. These samples were tested in three different directions, because anisotropic properties of the printed samples were expected. The printed samples were compared with the cast samples of the same mixture to investigate the effect of the printing process on the compressive strength of the mixture.

Test set-up / Samples / Procedure

The test set-up for the compressive test was described in section 3.2.10. The printed prism (length=800mm, width=25mm, height=6 layers) from the printing session was used to prepare the samples for the compressive strength test. The 3D printed prism was used to saw out cube samples of 40 x 40 x 40 mm to fit into the compressive strength testing machine. Due to anisotropic mechanical properties of the printed mortar, the samples from the printed prism were tested in 3 different directions. Compression load was applied in the longitudinal, lateral and perpendicular to the printing direction (see Figure 2.10). For each direction 3 repetitions were performed after 7 days of curing and the average value was calculated. The compression strength values of the 3D printed samples were compared to the cast mortar of mix FGD20-SP0.35-Acc8% to investigate the influence of the printing process on the compressive strength. The testing procedure for the compressive strength test is identical as described in section 3.2.10.

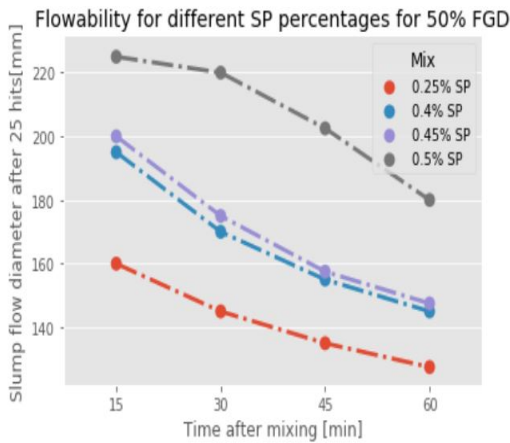
5.3. Results

5.3.1. Flowability for cementitious mixtures

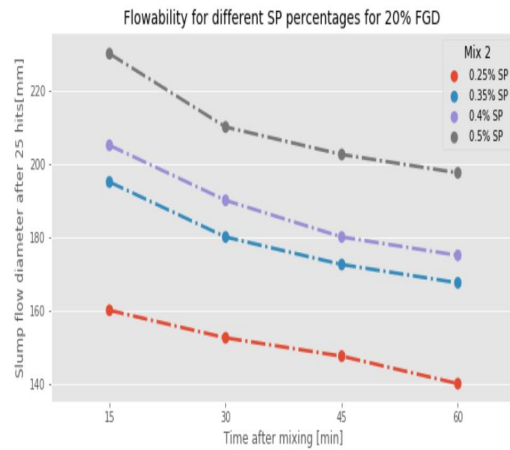
As reported in section 5.2.2 the goal of the flowability test was to find a suitable mix design for a pumpable cementitious mixture. This was done by adding different dosages of superplasticizer (SP) to the mixture in order to influence the flowability of the mixtures. For the 3D printable mix designs 50% and 20% of the Portland cement in the binder was replaced with pre-treated fine glass dust and the different SP dosages that were taken into account for this investigation are given in Table 5.1. For each of these mixtures the flowability change over time was investigated by measuring the slump flow diameter at different time intervals after mixing. The results are presented in Figures 5.7a and 5.7b. For all cementitious mixtures the slump flow diameter was measured at 15, 30, 45 and 60 minutes after mixing. From Figure 5.7a the effect of superplasticizer addition to the mixture on the flowability could be clearly seen. For mix FGD50 15 minutes after mixing the addition of 0.4% SP led to a slump flow diameter increase of 22% compared to the mixture with 0.25% SP. The addition of 0.5% SP to the mixture led to a slump flow diameter increase of 41% compared to the mixture with 0.25% SP. A higher dosage of SP led to a larger slump flow diameter at each time interval between 15 and 60 minutes after mixing for both mix FGD50 as well as mix FGD20. For the mix FGD50-SP0.25 with the least amount of SP (0.25%) the slump flow diameter 15 minutes after mixing was 160mm and decreased to 127.5mm for 60 minutes after mixing. The results for 0.40% SP and 0.45% SP were in a similar range and for all investigated time intervals after mixing and the difference is smaller than 3%. For the mix FGD50-SP0.5 with the largest amount of SP (0.5%) the slump flow diameter 15 minutes after mixing was 225mm and decreased to 180mm for 60 minutes after mixing.

For the 20% fine glass dust replacement the mix FGD20-SP0.25 with the least amount of SP (0.25%) the slump flow diameter 15 minutes after mixing was 160mm and decreased to 140mm for 60 minutes after mixing (see Figure 5.7b). The results for 0.35% SP and 0.40% SP were in a similar range and for all investigated time intervals after mixing and the difference is smaller than 5%. For the mix FGD20-SP0.5 with the largest amount of SP (0.5%) the slump flow diameter 15 minutes after mixing was 230mm and decreased to 197.5mm for 60 minutes after mixing.

For a mixture to be suitable for 3D concrete printing the flowability over time should be within specific boundaries for as long as possible. The flowability had to be ideally between 150 and 200mm for as long as possible after mixing. Based on the presented results in Figure 5.7a it can be seen that both mix FGD50-SP0.4 and FGD50-SP0.45 gave slump flow diameters of 200 and 195mm for 15 minutes after mixing and slump flow diameters of 147.5 and 145mm for 60 minutes after mixing. This meant that both



(a) FGD50



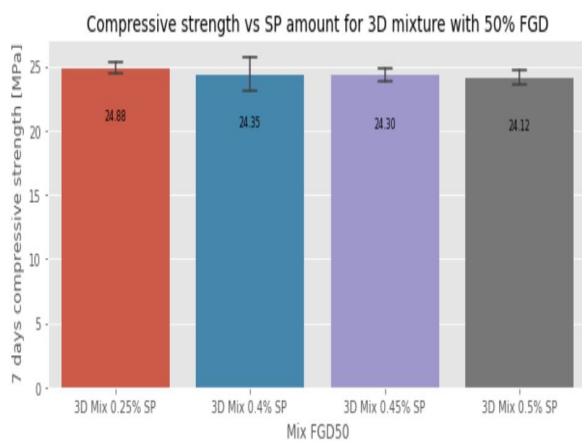
(b) FGD20

Figure 5.7: Flowability graph for pumpable cementitious mixtures

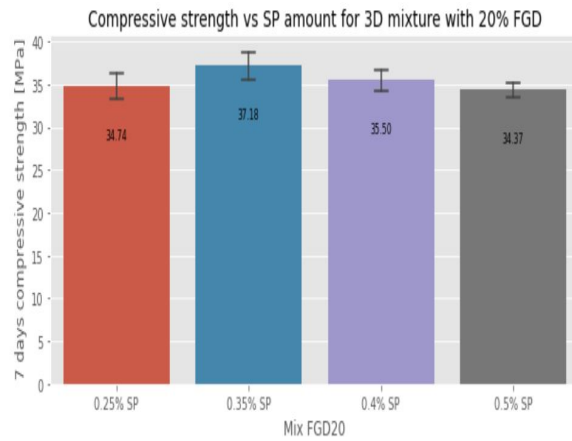
the 0.4% SP and the 0.45% SP mixtures had flowability values within the specified boundaries between 15 and 60 minutes after mixing for FGD50. The mixture with 0.25% SP had too little flowability and provided lower slump flow diameters than 150mm from 30 minutes after mixing. The mixture with 0.5% SP was too flowable and only reached slump flow diameters of 200mm from 45 minutes after mixing. Based on the presented results for the flowability test it was stated that both the mix FGD50-SP0.4 and mix FGD50-SP0.45 could be used as a pumpable cementitious mixture. For the pumpability test in section 5.2.4 only one mixture was chosen for the remainder of this thesis. Based on the lower amount of superplasticizer amount Mix FGD50-SP0.4 was considered for the pumpability test in section 5.2.4. For the investigated mixtures with 20% FGD the mix FGD20-SP0.35 provided the most optimal results in terms of flowability change over time (see Figure 5.7b). The slump flow diameter was between 195 and 167.5 mm for the time interval between 15 and 60 minutes, which represented values within the specified boundaries for 3D Concrete Printing.

5.3.2. Compressive strength for cementitious mixtures

The cementitious mixtures that were described in section 5.2.1 were tested on compressive strength after 7 days of curing to compare the strength development in the mixtures with different superplasticizer dosages. The results of the compressive strength test that was described in section 5.2.3 are presented in Figures 5.8a and 5.8b



(a) Mix FGD50



(b) Mix FGD20

Figure 5.8: 7 days compressive strength for pumpable cementitious mixtures

For 50% FGD the cementitious mixture with the lowest SP dosage had the highest strength development after 7 days and reached a mean compressive strength of 24.88 MPa. The mixture with the highest SP dosage had the lowest strength development after 7 days and reached a mean compressive strength of 24.12 MPa. The difference between the investigated mixtures was smaller than 3% and was therefore not significant. The different SP dosages that were applied in the pumpable cementitious mixtures did not have a significant effect on the compressive strength development of the mixtures with 50% FGD.

For 20% FGD the cementitious mixture FGD20-SP0.35 had the highest strength development after 7 days and reached a mean compressive strength of 37.18 MPa. The mixture with the highest SP dosage (mix FGD20-SP0.5) had the lowest strength development after 7 days and reached a mean compressive strength of 34.37 MPa. The difference between the investigated mixtures was smaller than 7.5% and is more significant than for the FGD50 mixtures, but no clear trend could be observed. The optimal SP dosage for compressive strength development of FGD20 mixtures was the same as for the flowability, namely mix FGD20-SP0.35.

The pumpable cementitious mixtures that were investigated for the 3D printing process had a Portland cement replacement percentage of 50% and 20% of the binder mass by pre-treated fine glass dust. The strength that was reached after 7 days of curing was in the range of 24-25 MPa for FGD50 and in the range of 34-37 MPa for FGD20. This could be attributed to the large amount of cement that was used for 3D concrete printing mixtures and the use of CEM I 52.5R, which caused rapid strength gain at an early age.

5.3.3. Pumpability for cementitious mixtures

The results of the pumpability test for the cementitious mixture FGD50-SP0.4 that was described in section 5.2.4 are presented in Table 5.3. During the pumpability test the pumpable cementitious mixture was passed through the hose at different motor speeds and the material was collected for a time interval of 10 seconds. From table 5.3 it can be seen that a higher motor speed gave a higher collected mass after 10 seconds. The collected mass was converted to mass per second. The unit weight of the pumpable cementitious mixture converted the collected mass per second to the material flow rate through the hose in cm^3/s . The unit weight of the cementitious mixture was determined by determining the mass of a known volume after compaction. The unit weight of the mixture FGD50-SP0.4 was found to be 2172 kg/m^3 and this value was used to calculate the material flow rate at different motor speeds.

The material flow rate of the cementitious mixture at different pumping speeds was an important

Speed	Mass collected (gram)	Mass per second (gram/s)	Material flow rate (cm^3/s)
Speed 2	387.1	38.71	17.82
Speed 2	373.9	37.39	17.21
Speed 3	587.9	58.79	27.06
Speed 3	580.5	58.05	26.73
Speed 4	765.8	76.58	35.25
Speed 4	770.3	77.03	35.47
Speed 5	1039.1	103.91	47.84
Speed 5	944.6	94.46	43.49

Table 5.3: Pumpability test results for pumpable cementitious mixture FGD50-SP0.4

property to investigate, because this determined the linear speed of the 3D concrete printer during the printing process. Figure 5.9 presents the average value of the material flow rate of the pumpable cementitious mixture for each pumping speed. For set-on-demand concrete printing both the material flow rate of the pumpable cementitious mixture as well as the material flow rate of the accelerator slurry had to be taken into account. Both mixtures were pumped through a separate pumping hose, but were combined in the helical static mixer just before extrusion at the printing head. Because the two mixtures had to be combined in a ratio of 1:1, pumping speeds at the two different pumps had to be used so that the material flow rate was similar for both the cementitious mixture and the accelerator slurry.

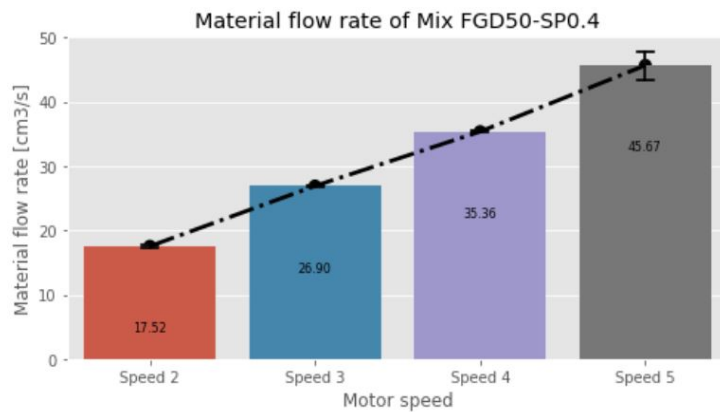


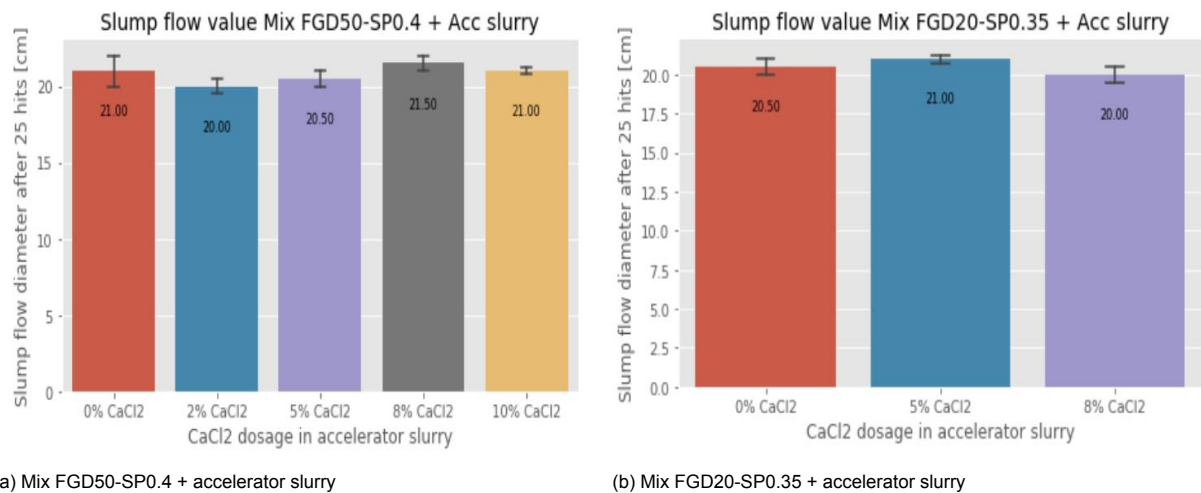
Figure 5.9: Material flow rate at different motor speeds for mix FGD50-SP0.4

The cementitious mixture FGD50-SP0.4 with 50% replacement of PC with FGD in the binder and the addition of 0.4% SP by binder mass had a material flow rate between 17.52 and 45.67 cm³/s for pumping speeds 2-5 (see Table 5.3 and Figure 5.9). For all pumping speeds during the pumpability test the pumping pressure stayed in acceptable ranges, so that no risk of damage to the printing equipment occurred. Also for all pumping speeds the extruded material from the hose was continuous and the material was pumped through the hose properly without congestion or blockages in the pumping hose. Based on the provided test results the mixture FGD50-SP0.4 was a pumpable cementitious mixture and will be used for set-on-demand printing to combine with accelerator slurry. Based on material shortage during the thesis, no pumpability test was performed for the mixture with 20% fine glass dust. Because mix FGD20-SP0.35 provided similar results in terms of flowability change over time, it was assumed that this mixture also possessed good pumpability properties and could be used as a pumpable cementitious mixture. In section 5.2.5 different mix designs for the accelerator slurry were combined with the pumpable cementitious mixtures for both 50% and 20% FGD to find the best combination of cementitious mixture + accelerator slurry in terms of fresh-state and hardened properties.

5.3.4. Flowability for cementitious mixtures + accelerator slurry

In section 5.2.5 it was described that both the cementitious mixture and the accelerator slurry were prepared in a separate small mixing bowl and were shortly combined afterwards. Directly after mixing slump flow test was performed on the combined mixture to determine the flowability of the combined mixture and the influence of the different accelerator dosages on the flowability. The results of the flowability test, that was described in section 5.2.6, are presented in Figures 5.10a and 5.10b. The combination of cementitious mixture FGD50-SP0.4 and accelerator slurry with 0% of CaCl₂ had a mean slump flow diameter of 21.0 cm. After addition of a small amount of 2% CaCl₂ to the accelerator slurry, the slump flow diameter dropped to a mean value of 19.5 cm, which represented a reduction of around 8%. For the addition of 5%, 8% and 10% of CaCl₂ to the accelerator slurry the slump flow diameter of the combined mixture showed comparable values to the accelerator slurry with 0% CaCl₂, namely in the range between 20.5 and 21.5 cm. The combination of cementitious mixture FGD20-SP0.35 and accelerator slurry with 0%, 5% and 8% CaCl₂ all resulted in slump flow diameters between 20.0 and 21.0 cm directly after mixing.

Based on the results that are provided in Figures 5.10a and 5.10b it could be stated that the addition of higher dosages of CaCl₂ to the accelerator slurry had no significant effect on the slump flow diameter of the combined mixtures directly after mixing for both FGD50 and FGD20. The mean value was around 21.0 cm for 4 out of 5 tested mixtures for mix FGD50-SP0.4. The reduction in slump flow diameter for the mixture with 2% accelerator could be caused by different mixing circumstances or a small material measurement error with the dry materials or the water/accelerator amount which could reduce the flowability of the mixture. The mean value for the mixtures with FGD20-SP0.35 was 20.5 cm, which means the largest difference between the results was smaller than 5%.



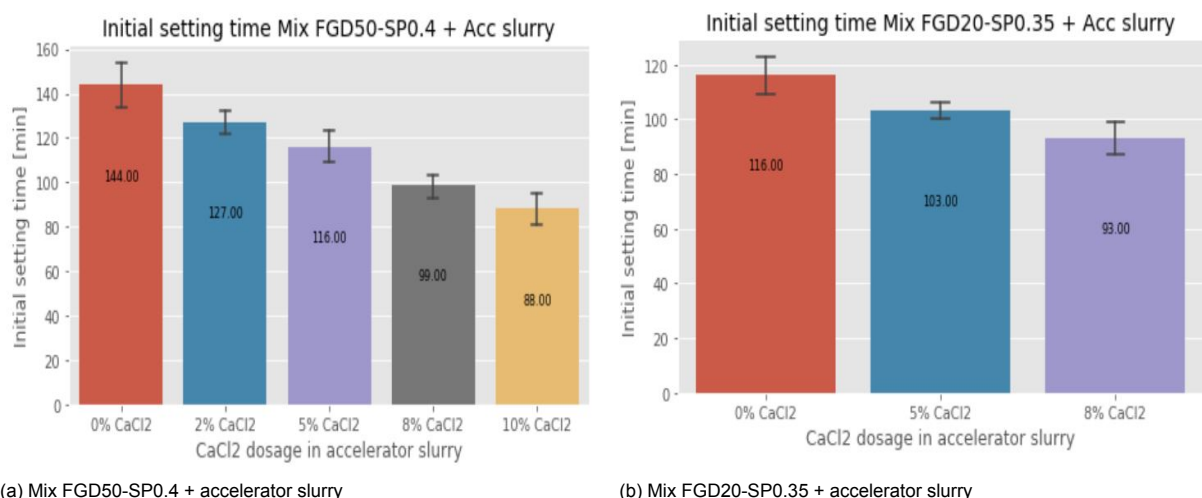
(a) Mix FGD50-SP0.4 + accelerator slurry

(b) Mix FGD20-SP0.35 + accelerator slurry

Figure 5.10: Flowability results for cementitious mixture + accelerator slurry for different CaCl₂ dosages

5.3.5. Initial setting time for cementitious mixtures + accelerator slurry

As described in section 5.2.7 the initial setting time test was performed to investigate the effect of different accelerator dosages and different FGD dosages on the setting time of the combination of cementitious mixture and accelerator slurry. The results of the initial setting time test are shown in Figures 5.11a and 5.11b. The effectiveness of the accelerator could be shown by the test if a higher CaCl₂ percentage led to a decrease in the initial setting time, which indicated faster stiffness development of the combined mixture. The goal of the test was to find an accelerator dosage which caused a fast initial setting time of around 90 minutes, which was suitable for set-on-demand concrete printing.



(a) Mix FGD50-SP0.4 + accelerator slurry

(b) Mix FGD20-SP0.35 + accelerator slurry

Figure 5.11: Initial setting time results for cementitious mixture + accelerator slurry for different CaCl₂ dosages

From Figure 5.11a it can be seen that if 0% CaCl₂ was used in the accelerator slurry that the initial setting time had a mean value of 144 minutes for FGD50. For higher CaCl₂ dosages in the accelerator a decrease in initial setting time could be seen, which showed that the addition of CaCl₂ solution to the accelerator slurry had an accelerating effect on the stiffness development of the combined mixture. For the mixture with 2% CaCl₂ in the accelerator slurry the initial setting time decreased to 127 minutes and for 5% CaCl₂ in the accelerator slurry this further decreased to 116 minutes for FGD50. Even higher additions of accelerator dosage led to shorter initial setting times and at 10% CaCl₂ in the accelerator slurry the mean initial setting time of the combined mixture of cementitious mixture + accelerator slurry was 88 minutes, which was below 90 minutes for the first time. By addition of 10% CaCl₂ to the accelerator slurry the initial setting time could be decreased with by 39% compared to the mixture with 0%

CaCl₂ for FGD50.

From Figure 5.11b it can be seen that if 0% CaCl₂ was used in the accelerator slurry that the initial setting time had a mean value of 116 minutes for FGD20. For the mixture with 5% CaCl₂ in the accelerator slurry the initial setting time decreased to 103 minutes and for 8% CaCl₂ in the accelerator slurry this further decreased to 93 minutes for FGD20. By addition of 8% CaCl₂ to the accelerator slurry the initial setting time could be decreased by 20% compared to the mixture with 0% CaCl₂ for FGD20. So in order to reach an initial setting time of around 90 minutes for FGD50 there was 10% CaCl₂ needed and for FGD20 there was 8% CaCl₂ needed.

The provided results in Figures 5.11a and 5.11b both showed that higher dosages of CaCl₂ solution in the accelerator slurry had a beneficial effect on the stiffness development of the cementitious mixtures + accelerator slurry.

5.3.6. Isothermal calorimetry for cementitious mixtures + accelerator slurry

As described in section 5.2.8 the isothermal calorimetry test was performed to investigate the effect of different accelerator dosages and different FGD dosages on the early stage hydration of the combination of cementitious mixture and accelerator slurry. Faster early age hydration of a mixture would indicate a more rapid hardening and therefore a higher structural build-up. The results of the isothermal calorimetry test are presented in Figure 5.12.

According to the normalized heat flow results in Figures 5.12a and 5.12b, it is shown that incorporating higher dosages of CaCl₂ in the accelerator slurry resulted in a shorter induction period. For the mixtures with 20% FGD it can be seen that mix FGD20-Acc0% has the longest induction period and that mix FGD20-Acc8% has the shortest induction period. The main hydration peak of the mix FGD20-Acc8% was shifted to the left to occur at an earlier stage and also had a higher heat flow intensity. In addition, the effect of fine glass dust percentage on the normalized heat flow of the mixture can also be seen in Figures 5.12a and 5.12b. When the normalized heat flow values of mix FGD20-Acc0% and mix FGD50-Acc0% were compared, it was found that mix FGD20-Acc0% had a shorter induction period, the time to reach the main hydration peak was earlier and the height of the main hydration peak was larger.

If the main hydration peaks of mixtures FGD20-Acc0% / FGD20-Acc8% are compared it can be seen in Figure 5.12b that for higher CaCl₂ dosages the main hydration peak was higher and more narrow. For Mix FGD20-Acc5% and FGD20-Acc0% the main hydration peak was more spread out and even a second shoulder peak after the main hydration peak was observed. In the mixture with 50% FGD this secondary peak was also observed. The second shoulder peak of mixtures with 20% FGD was found to be at a lower intensity than the main hydration peak, but for the mixture with 50% FGD this peak was found to be higher than the main hydration peak.

The results from the normalized cumulative heat in Figure 5.12c were in agreement with the findings of the normalized heat flow. It was found that the mix FGD50-Acc0% released less amount of cumulative heat than all the mixtures with 20% FGD. The reduction of cumulative heat was around 30% after 90 hours. The three mixtures with 20% FGD provided similar cumulative heat results after 90 hours. At early material ages the mix FGD20-Acc8% had a higher increase in cumulative heat compared to mix FGD20-Acc5% and mix FGD20-Acc0%, which was caused by the high hydration peak in the heat flow curve around 5 hours.

Based on the results in Figure 5.12 it was found that a lower amount of FGD caused a shorter induction period and a higher hydration peak, which occurred at an earlier age compared to the mixture with a higher FGD dosage. It was also found that a higher dosage of CaCl₂ in the mixture caused a shorter induction period and a higher hydration peak at an earlier age. Both the FGD dosage and the CaCl₂ dosage had an influence on the hydration reaction and heat flow of the combined mixture of cementitious mixture + accelerator slurry.

5.3.7. Compressive strength for cementitious mixtures + accelerator slurry

As described in section 5.2.9 the compressive strength test was performed to investigate the effect of different accelerator dosages and different FGD dosages on the compressive strength development of the combination of cementitious mixture and accelerator slurry for curing ages of 7 and 28 days. The

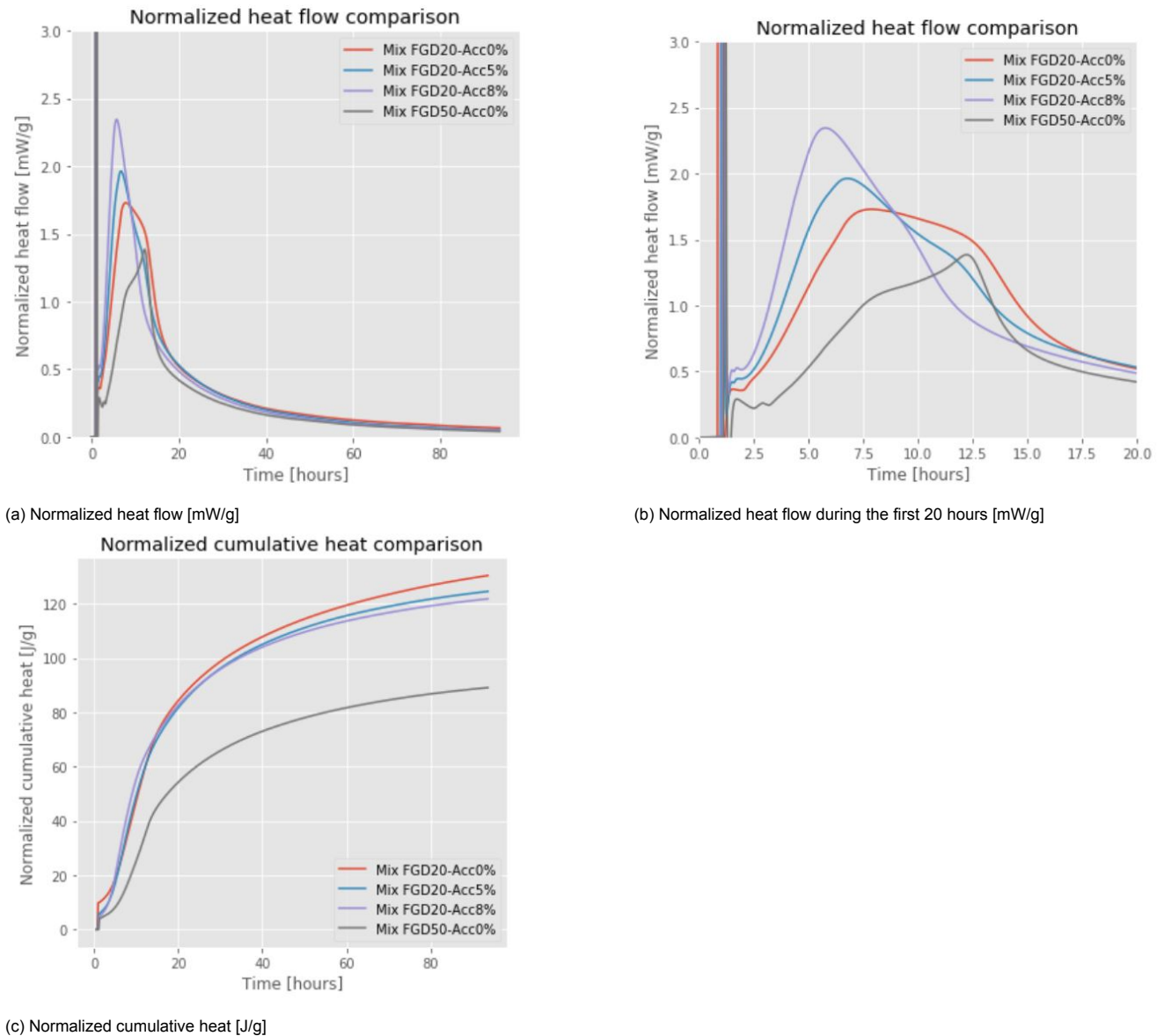
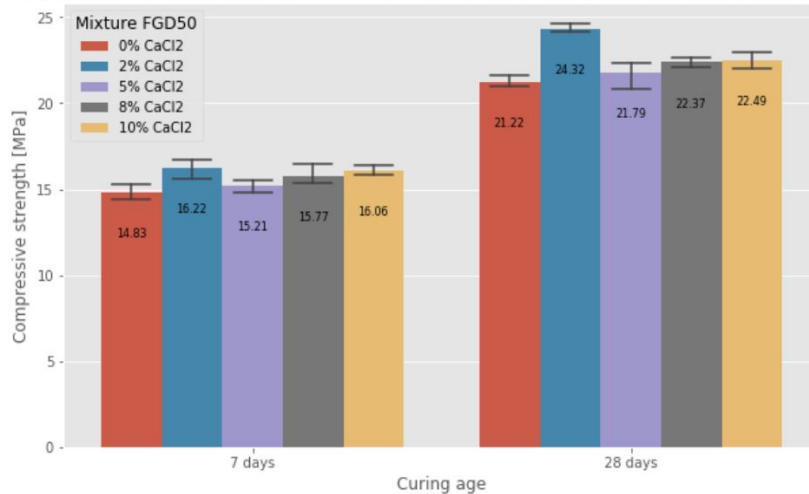


Figure 5.12: Isothermal calorimetry results for mixtures FGD20 and FGD50 with different CaCl_2 dosages in accelerator slurry

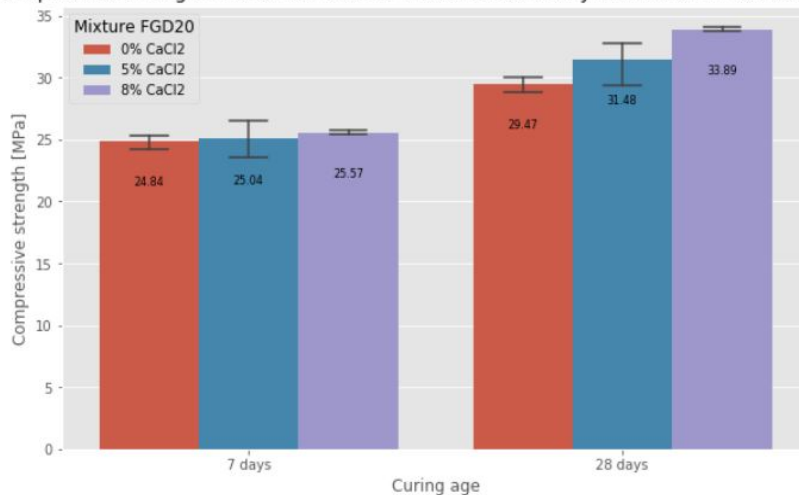
results of the compressive strength test are shown in Figures 5.13a and 5.13b.

For FGD50 the compressive strength for the combined mixture with 0% CaCl_2 was 14.83 MPa after 7 days of curing. When this strength is compared with the result from Figure 5.8a it can be seen that the 7 day strength decreased from 24.35 to 14.83 MPa, because of the addition of accelerator slurry to the cementitious mixture in mass ratio 1:1. This represents a decrease in compressive strength of 39%, which could be attributed to the lower amount of Portland cement per unit of mass as discussed in section 5.2.1. For FGD20 the 7 day compressive strength decreased from 37.18 to 24.84 MPa (compare Figure 5.8a with Figure 5.13b), because of the addition of accelerator slurry to the cementitious mixture in mass ratio 1:1. This represents a decrease in compressive strength of 33%.

For FGD50 the compressive strength of the combined mixtures increased for higher CaCl_2 dosages in the accelerator slurry for both 7 and 28 days of curing. From Figure 5.13a it can be seen that the mixture with 2% CaCl_2 in the accelerator slurry was an outlier, which could be potentially attributed to a small error in material measurement or a change in the casting or curing process. For the rest of the investigated mixtures the compressive strength increased from 14.83 to 16.06 MPa after 7 days of curing for 0% and 10% CaCl_2 respectively. The compressive strength increased from 21.22 to 22.49 MPa after 28 days of curing for 0% and 10% CaCl_2 respectively. For FGD50 the addition of 10% CaCl_2

Compressive strength Mix FGD50-SP0.4 + Accelerator slurry with different CaCl₂ dosages

(a) Mix FGD50-SP0.4 + accelerator slurry

Compressive strength Mix FGD20-SP0.35 + Accelerator slurry with different CaCl₂ dosages

(b) Mix FGD20-SP0.0.35 + accelerator slurry

Figure 5.13: Compressive strength results for cementitious mixture + accelerator slurry for different CaCl₂ dosages

in the accelerator slurry caused an increase in compressive strength of 6-8% for both 7 and 28 days of curing.

For FGD20 the compressive strength of the combined mixtures also increased for higher CaCl₂ dosages in the accelerator slurry for both 7 and 28 days of curing. From Figure 5.13b it can be seen that the compressive strength increased from 24.84 to 25.57 MPa after 7 days of curing for 0% and 8% CaCl₂ respectively. The compressive strength increased from 29.47 to 33.89 MPa after 28 days of curing for 0% and 8% CaCl₂ respectively. For FGD20 the addition of 8% CaCl₂ in the accelerator slurry caused an increase in compressive strength of 3% for 7 days of curing and 15% for 28 days of curing.

Based on the results that are provided in Figures 5.13a and 5.13b it can be stated that the accelerator slurry has a small hardening effect. For both 50% and 20% mixtures the addition of higher CaCl₂ dosages led to an increase in compressive strength after both 7 and 28 days of curing.

5.3.8. Buildability for 3D Printed Concrete

As described in section 5.2.10 the goal of the buildability test was to investigate whether the developed mixture FGD20-SP0.35-Acc8% was printable with set-on-demand printing, where a helical static mixer was used to mix the cementitious mixture and the accelerator slurry just before extrusion from the

printing nozzle. During the printing session a cylinder was printed for the buildability test and a prism was printed for the compression strength test of the 3D printed concrete.

The results of the printing session are shown in Figure 5.14a. During the printing process it was observed that the developed mixture FGD20-SP0.35-Acc8% was printable. Both the cementitious mixture and the accelerator slurry could be pumped through the hose without high pressures and the two separate mixtures were mixed properly in the helical static mixer. The combined mixture that was extruded from the printing nozzle was uniform and no striations could be observed. According to Tao et al. [114], striation patterns in the extruded filaments are an indication of improper mixing of the materials, but for mix FGD20-SP0.35-Acc8% this was not observed.

The prisms were printed with a height of 6 layers with 13.3 seconds time interval between each subsequent layer. During the printing of the prisms no failure occurred in the printed filaments, only small deformations could be observed in the bottom filament.

The buildability test showed that 10 layers of a cylinder with a diameter of 180mm with 9.42 seconds time interval between each subsequent layer could be printed before failure of the cylinder occurred. From Figure 5.14b it can be seen that the bottom filament had large deformation and had insufficient strength to carry the weight of the filaments that were printed on top. Failure of the bottom filament was the governing factor for the buildability test of the developed mixture.



Figure 5.14: Results of printing session for mix FGD20-SP0.35-Acc8%

5.3.9. Compressive strength of 3D Printed Concrete

As described in section 5.2.11 the goal of the compressive strength test was to investigate the compressive strength development of the 3D printed samples of mix FGD20-SP0.35-Acc8%. These samples were tested in three different directions, because anisotropic properties of the printed samples were expected. The printed samples were compared with the cast samples of the same mixture to investigate the effect of the printing process on the compressive strength of the mixture. Figure 5.15 shows the results of the compressive strength test on the printed samples in three different directions: perpendicular, longitudinal and lateral compared to the printing direction (as presented in Figure 2.10).

Figure 5.15 shows that the cast sample reached a mean compressive strength of 25.57 MPa after 7 days of curing. This strength was the same in all directions, as the cast mortar was isotropic under compression loading. Anisotropic properties were observed for the printed samples. When the printed sample was loaded perpendicular to the printing direction, compressive strength of 26.85 MPa was reached after 7 days of curing. This was a 5.0% increase compared to the cast sample of the same mixture. When the printed sample was loaded longitudinally to the printing direction, compressive strength of 25.51 MPa was reached, which represented a 0.2% decrease compared to the cast sample. The compressive strength lateral to the printing direction was 19.56 MPa, which represented a decrease of 23.5% compared to the cast sample.

The results of the compressive strength test on the printed samples showed that the printed mixture

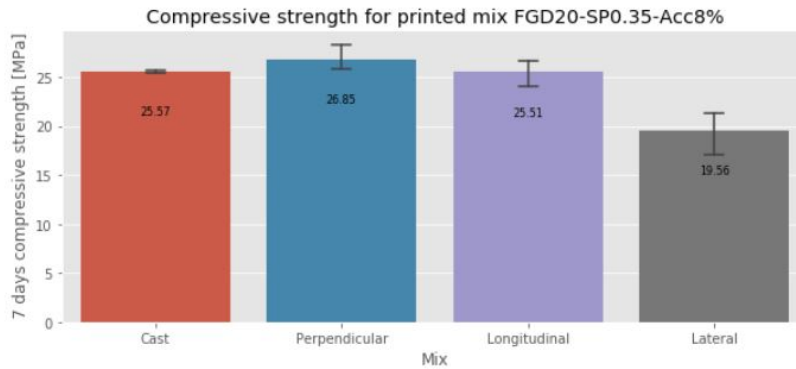


Figure 5.15: Compressive strength results for the printed samples of mix FGD20-SP035-Acc8%

developed similar strength to the cast sample for the perpendicular and longitudinal directions. For the lateral direction a significant reduction was observed compared to the cast sample.

5.4. Discussions

5.4.1. Pumpable cementitious mixtures

Flowability

The objective of the flowability test for cementitious mixtures as described in section 5.3.1 was to find a suitable mix design for a pumpable cementitious mixture and to investigate the influence of Superplasticizer (SP) and fine glass dust (FGD) dosage on the flowability. The results suggest that for both mixture FGD50 and FGD20 an increasing amount of SP resulted in a larger slump flow diameter after 25 drops for all investigated time intervals after mixing. Therefore the SP amount had a positive influence on the flowability of the cementitious mixtures. Figure 5.16 shows the flowability comparison between the collected data on mixtures with 50% FGD and mixtures with 20% FGD for some of the investigated superplasticizer dosages. The possible reasons for the changes in flowability by adding different SP dosages and the effect of FGD percentage on the flowability will be assessed in this section.

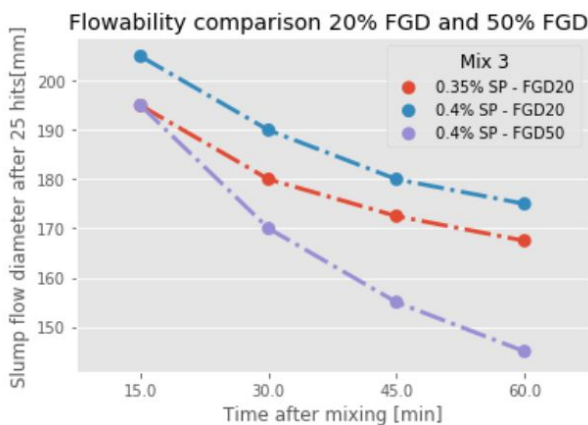


Figure 5.16: Flowability comparison for mix FGD50 and FGD20

One feasible interpretation for the increased flowability for mixtures with a larger dosage of SP is due to the working mechanism of the superplasticizer. The surface of the cement particles in the mortar mixture carries both positive and negative charges. The SP polymers are negatively charged and therefore counterbalance the positive charges on the cement particle surface. This results in making the entire surface of the cement particles appear fully negative. The negatively charged cement particles repel each other, creating a dispersing effect that allows for more water permeation. This higher water permeation in the mixture causes a higher flowability. Another possible working mechanism of SP is steric hindrance, which controls the selectivity in the cementitious mixture and prevents cement particles from

agglomerating. This assures space between particles and within this space the water can move more easily, which results in a higher flowability for the mixture when SP is added. For higher dosages of SP for the cementitious mixture this effect became stronger, which increased flowability. For 3D Concrete Printing it is important that the mixture is not too stiff, because this could cause high pressures during pumping or printing. On the other hand the flowability can also not be too high, because in that case there could be a risk of segregation of the material during the pumping or printing process (as described in sections 5.2.1 and 5.2.2). The boundaries for flowability of the mixtures for 3D Concrete Printing are within 150 and 200mm for the largest possible time interval. Based on those boundaries mix FGD50-SP0.40 and Mix FGD20-SP0.35 were chosen for the cementitious mixture.

The flowability comparison in Figure 5.16 shows that mix FGD20 possessed a higher flowability than mix FGD50 for all investigated time intervals after mixing for the same superplasticizer dosage of 0.4%. This higher flowability for mix FGD20 can potentially be explained by the difference in particle size between the Portland cement and the FGD. As discussed in section 3.4.1 the particles of the FGD are larger and have a smaller specific surface area than the particles of the Portland cement even after grinding treatment of the FGD. This resulted in a sub-optimal filler effect and particle packing of the fine glass dust combined with the Portland cement particles. This indicates that when a higher percentage of FGD was used in the binder that more water is captured in the voids between the particles of different sizes. This enclosed water is not available to reduce the friction between the particles and therefore decreases the flowability. This could clarify why the FGD50 mix had a lower flowability than the FGD20 mix with the same superplasticizer amount.

Another possible explanation is that the working mechanism of the SP mainly affects the cement particles and had less effect on the FGD particles. For a higher replacement percentage mixtures, there were fewer cement particles available which meant that the SP was less effective in increasing the flowability of the mixtures. Therefore a higher dosage of SP was needed for the FGD50 mixture to reach similar flowability to the FGD20 in which more cement particles were available. This meant that to reach similar flowability a lower superplasticizer dosage was sufficient for mix FGD20. For mix FGD20 it was sufficient to add 0.35% superplasticizer to the mixture to reach flowability values within the boundaries of 3D Concrete Printing.

The findings on the effect of fine glass dust and superplasticizer dosage on the flowability of the cementitious mixture are in agreement with the findings of Lu et al. [69] and Rahma et al [92]. These findings also showed a reduction in flowability for mixtures with a larger amount of glass powder as a replacement for Portland cement, interpreted due to the high surface tension of the glass powder. This high surface tension was justified by the large surface area of the glass powder particles. Rahma et al. also showed the flowability enhancing effect when superplasticizer was added to mixtures with glass powder. A larger dosage of SP led to a larger increase in flowability.

On the other hand research by Fanijo et al. [36] showed an increase in flowability when glass powder was used to replace Portland cement in the binder. The difference between this research and the research of Fanijo et al. was the particle size of the glass powder. Fanijo et al. used a mean particle size of 10 μm which was almost twice as fine as the mean particle size of 17.20 μm which was used in this study. The fine particles of the glass powder had an increased filler effect, because of the smaller difference in particle sizes with the Portland cement. The increase in flowability could then be clarified by the poor cohesion and the lower absorption capacity of the smooth glass powder particles.

So based on the provided results and discussion about the influence of superplasticizer and FGD amount on the flowability of cementitious mixtures it can be indicated that a higher amount of pre-treated FGD in a mixture led to a reduction of flowability compared to a lower amount of FGD mixture. The flowability of mixtures with SP could be effectively increased by adding SP to the mixture. The optimal mix designs for the pumpable cementitious mixture for 3D Concrete printing were mix FGD50-SP0.4 and mix FGD20-SP0.35.

Compressive strength

The main intention of the compressive strength tests for the cementitious mixtures in section 5.3.2 was to investigate the influence of superplasticizer (SP) dosage and fine glass dust (FGD) percentage on compressive strength development for pumpable cementitious mixtures for 3D concrete printing. The

results indicate that there was a difference in compressive strength development for the cementitious mixtures with 50% and 20% FGD. For all investigated superplasticizer dosages mix FGD20 had a higher compressive strength development than mix FGD50. The results also suggested that SP dosage did not have a significant influence on the compressive strength development.

One possible explanation for the decrease in compressive strength development for the mixture with higher FGD percentage is due to the dilution effect of the FGD. The replacement of Portland cement by FGD in the binder of the mixtures resulted in a lower amount of cement particles that were available for hydration and thus a lower rate of hydration reaction, which is responsible for the strength development of the mixtures at early curing ages. At a curing age of 7 days the fine glass dust mainly had a filler effect in the binder, which indicated no significant contribution to the strength development of the mixtures in terms of pozzolanic activity. So also for the pumpable cementitious mixture for 3D concrete printing the dilution effect played an important role. Because of the high amount of Portland cement in the standard mix design for the pumpable cementitious mixtures, high compressive strength values in the range of 24-25 MPa were achieved for mix FGD50 and 34-37 MPa for mix FGD20 mixture after 7 days of curing.

The results in section 5.3.2 also suggest that the superplasticizer dosage did not have a significant influence on the compressive strength development of the mixtures. Neither the mixtures with 20% FGD nor the mixtures with 50% FGD experienced significant strength gain or loss by the added superplasticizer in the mixture. This can potentially be clarified by the fact that the superplasticizer working mechanism only influenced the flowability of the mixtures by the repulsion effect or steric hindrance on particles, but had no influence on the hydration reaction and the amount of hydration reactions that are formed. Therefore no significant trend could be observed between SP dosage and compressive strength development. The small changes in compressive strength results for different superplasticizer dosages could be attributed to different casting and compacting conditions due to the flowability changes in the mixtures. The investigated mixtures with low SP dosage possessed low flowability which complicated the vibrating and compacting conditions while filling the mould. The investigated mixtures with high SP dosage possessed high flowability which caused a lot of water loss during vibrating and compacting.

As described in section 3.4.2 the findings on the effect of fine glass dust on the compressive strength development of the cementitious mixtures for 3D concrete printing are in agreement with the findings of Boukhelf et al. [15], Nassar et al. [82], Nyantaki et al. [86] and Ibrahim et al. [46], in which low initial reactivity was observed for mixtures with waste glass powder resulting in lower strength values than the reference mixture. Because the mixtures were only tested at a curing age of 7 days, no influence of pozzolanic activity of the FGD could be indicated and the dilution effect of the FGD caused the lower strength development for mixtures with higher glass powder percentages.

Research by Hassouna et al. [44] showed that superplasticizer dosage can have an effect on the compressive stress development of cementitious mixtures. The results suggested that if a very low dosage of SP was used, but also if a very high dosage of SP was used, the compressive strength would be decreased. In between there was an optimum SP dosage which resulted in the highest strength. The main difference between the research of Hassouna et al. and this research is the mix design that is used as well as the range of SP dosage that was investigated. The research of Hassouna et al. investigated SP dosages ranging from 0-5%, but in this study only ranges of 0.25-0.5% were investigated. The large range of investigated SP dosages gave a more wide spread of results, which could clarify the more obvious trend in results for the research of Hassouna et al.

So based on the provided results and discussion about the compressive strength development of cementitious mixtures with different FGD percentages and SP dosages it can be indicated that a higher FGD percentage led to a decrease of compressive strength, due to the dilution effect of the FGD. The investigated range of SP dosage did not have a significant influence on the compressive strength development of either FGD50 mix or FGD20 mix.

5.4.2. Pumpable cementitious mixture + accelerator slurry

Initial setting time

The main goal of the initial setting time test in section 5.3.5 was to investigate the effect of FGD percentage and CaCl_2 dosage on the initial setting time of the pumpable cementitious mixture + accelerator slurry. The results suggest that the CaCl_2 dosage in the accelerator slurry had a decreasing effect on the initial setting time of the cementitious mixture + accelerator slurry. For all investigated mixtures an increase in the CaCl_2 dosage led to a decrease in the initial setting time. Figure 5.17 shows the initial setting time comparison between the mixtures with 50% FGD and mixtures with 20% FGD for the investigated CaCl_2 dosages. This figure indicates that a higher percentage of FGD led to an increase in initial setting time for the same CaCl_2 dosage. The possible reasons for the changes in initial setting time by adding different CaCl_2 dosages and the effect of FGD percentage on the initial setting time will be assessed in this section.

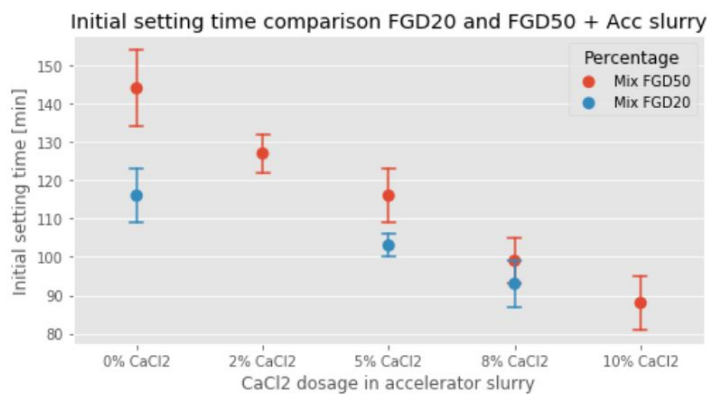


Figure 5.17: Initial setting time comparison for mix FGD50 and FGD20

One potential explanation for the accelerating effect of CaCl_2 dosage on the initial setting time of the cementitious mixture + accelerator slurry is due to the working mechanism of the CaCl_2 . The results indicate that accelerator slurry with a higher dosage of CaCl_2 caused a faster initial setting time for both FGD50 and FGD20 mixtures. Early-age hydration of ordinary Portland cement originates from nucleation and crystal growth of calcium-silicate-hydrates (C-S-H). CaCl_2 is known to have an accelerating effect on Portland cement hydration not only during the acceleration phase of the hydration reaction, but throughout the full early-age hydration (approximately 24 hours). CaCl_2 has an accelerating effect on hydration by providing supersaturation of C-S-H during early age hydration of Portland cement. Supersaturation affects the hydration reaction by surface activation. Nucleation can take place on surfaces depending on the contact angle between the surface and the precipitating phase [104]. Precipitation can occur where C-S-H is supersaturated with respect to the solution. In the presence of CaCl_2 , the degree of C-S-H supersaturation increased. This led to lower free energy barriers to precipitation and this enabled surfaces to act as nucleation sites for C-S-H in presence of CaCl_2 , which were previously inactive. So the presence of CaCl_2 increased the number of surfaces that are active nucleation surfaces for C-S-H during the cement hydration. This meant that because of the presence of CaCl_2 the nucleation and crystal growth of C-S-H nuclei was accelerated, which caused the hydration reaction rate to increase [104]. A faster early-age hydration reaction rate meant faster stiffness development and therefore a decrease in the initial setting time. A higher dosage of CaCl_2 had an enhanced effect on the initial reactivity and this could be a possible interpretation for the lower initial setting time at higher CaCl_2 dosages.

For 3D Concrete Printing it is important to have a fast initial setting time for the combination of cementitious mixture + accelerator slurry, because this ensures sufficient stiffness development of the printed filaments after extrusion from the printing nozzle. This high stiffness development prevents the printed filaments from collapsing under the load of the subsequent filaments that are printed on top during the printing process. On the other hand the initial setting time can not be too fast, because this could cause possible damage to the printing equipment. If the stiffness development of the combined

mixture is too fast, there is a risk of material accumulation and high pressures at the printing nozzle if the material can not be extruded properly. This also imposes the risk of improper quality of the printed filaments when the stiffness development is too high before deposition of the filaments. To ensure proper printing quality during 3D Concrete Printing the initial setting time should be in the range of 90 minutes. Based on the provided results in the initial setting time tests the cementitious mixture + accelerator slurry were formed by mix FGD50-SP0.4-Acc10% (10% CaCl_2) and mix FGD20-SP0.35-Acc8% (8% CaCl_2).

Figure 5.17 shows the comparison of the mixtures with 50% and 20% FGD for different CaCl_2 dosages in the accelerator slurry. The data suggest that the initial setting time for the FGD20 mixture was lower than the FGD50 mixture for the same CaCl_2 dosage. For the FGD20 mixture 8% of CaCl_2 was sufficient to reach an initial setting time of around 90 minutes, while for the FGD50 mixture 10% CaCl_2 was needed. This meant that the FGD amount in the mixture had a delaying influence on the initial setting time.

This can be potentially clarified by the fact that a lower amount of pre-treated FGD in the FGD20 mixture means that there was more Portland cement in the mixture. This higher amount of Portland cement particles increased the C-S-H precipitation on nucleation sites, which was responsible for the faster hydration reaction and faster stiffness development. This is in agreement with section 3.4.1 in which it was discussed that the FGD possesses compounds that had a delaying effect on the hydration reaction and the stiffness development. For the FGD50 mixture, more Portland cement was replaced by FGD, which had a delaying contribution to the nucleation and crystal growth of C-S-H structures. This decreased the initial hydration reactivity and delayed the stiffness development. This led to a higher initial setting time for the FGD50 mixture and thus more CaCl_2 was needed to reach an initial setting time of 90 minutes.

Another possible explanation is that the CaCl_2 worked most effectively on the acceleration of hydration of Portland cement particles. In the FGD20 mixture, more Portland cement particles were present, so the accelerator could maximize its effect on all the cement particles to accelerate the hydration reaction. As discussed earlier, this was potentially done by increasing the C-S-H supersaturation, which meant that more surfaces were available for cement particles to form C-S-H crystals on. In the FGD50 mixture less Portland cement particles were present, so more CaCl_2 was needed to reach the same effect for the acceleration of the early-age hydration reaction.

The findings on the initial setting time of the cementitious mixture + accelerator slurry are in agreement with the findings of Mansell et al. [72], which showed that the presence of CaCl_2 promotes the supersaturation of C-S-H in the solution, which activates locations in the cementitious solution that would otherwise have been unable to have nucleation. The increased rate of precipitation has an influence on the hydration reaction in both nucleation and growth of the hydration products, which results in a faster initial setting time when CaCl_2 was added to the mixture. These results are in conformity with the findings of Steger et al. [109], Salain et al. [100] and Souza et al. [105], which all showed that CaCl_2 could be effectively used to increase the stiffness development and therefore decrease the initial setting time of cementitious mixtures. Souza et al. [105] found that higher contents are needed if accelerator is used together with superplasticizer to compensate for the repulsive effect. This is in line with the findings in this research in which 10% CaCl_2 was needed for the FGD50 mix and 8% CaCl_2 was needed for the FGD20 mix, because superplasticizer was used for the pumpable cementitious mixture.

So based on the provided results and discussion about the initial setting time of the cementitious mixture + accelerator slurry it can be indicated that a higher percentage of pre-treated fine glass dust led to an increase in initial setting time. A higher dosage of CaCl_2 in the accelerator slurry could effectively reduce the initial setting time by accelerating the early-age hydration reaction. To reach an initial setting time of around 90 minutes mix FGD50-SP0.4-Acc10% and mix FGD20-SP0.35-Acc8% were used.

Heat evolution

The main objective of the isothermal calorimetry test in section 5.3.6 was to investigate the effect of CaCl_2 dosages and FGD percentages on the heat evolution during the early-age hydration of the combination of cementitious mixture + accelerator slurry. The results indicate that a lower amount of FGD

in the mixture had a positive influence on the hydration reaction rate. The mixture with 20% FGD had a shorter induction period, a higher heat flow during the main hydration peak and a larger normalized cumulative heat value than the mixture with 50% FGD for the same accelerator dosage. The results also suggest that the CaCl_2 dosage caused a shorter induction period and a higher heat flow during the main hydration peak at an earlier age. This means that the CaCl_2 dosage had a positive influence on the acceleration of the hydration reaction at an early age. It was also found that the accelerator dosage had no significant effect on the total normalized cumulative heat that was developed, but only caused an increase in hydration reaction rate during the main hydration peak. So both the FGD dosage and the CaCl_2 dosage influence the early-age reaction rate and the heat flow of the combined mixture of cementitious mixture + accelerator slurry, which is in accordance with the initial setting time discussion in section 5.4.2.

One potential explanation for the decrease in main hydration peak for the FGD50 mix compared to the FGD20 mix is due to the dilution effect of the FGD. The replacement of Portland cement by FGD in the binder of the mixtures resulted in a lower amount of cement particles that were available for hydration reaction. The particle size of the FGD was also larger than the particle size of the Portland cement. The larger FGD particles with lower surface area provided a reduced number of nucleation sites compared to the Portland cement particles, which resulted in a decline in hydration reaction. The larger fine glass dust particles decreased the precipitation rate of dissolved cement particles and therefore reduced the amount of C-S-H crystals that could originate and grow. The amount of FGD particles had a negative influence on the hydration rate at an early age and this could clarify the lower peak in hydration for the FGD50 mixture compared to the FGD20 mixture. The lower rate of hydration additionally affects the total amount of C-S-H structures that are formed during the hydration and therefore influences the total heat of hydration. This could also explain the lower cumulative heat value for the FGD50 mix compared to the FGD20 mix.

The heat flow results suggest pozzolanic activity for the FGD50 mix as a second hydration peak could be observed which was higher than the initial peak. The initial hydration peak is known for the hydration of C_3S , the main component of cement clinker. For the mixtures with FGD20 this peak was higher than for the FGD50 mix, because more cement particles were available and therefore more hydration of C_3S occurred. The pozzolanic activity of the fine glass dust is slower and generates less heat than the cement, because the reaction is similar to the hydration of C_2S . For the FGD50 mix this secondary hydration peak could be clearly observed, which could indicate pozzolanic activity of the mixture with 50% FGD. This second shoulder peak may also be attributed to the delayed hydration reaction of specific compounds in the cementitious mixture, according to Scrivener et al. [102]. According to Quennoz et al. [91], this peak might be regarded as the secondary formation of ettringite. For the investigated mixtures with 20% FGD this secondary hydration peak could also be observed around the same time, but these were less significant than for the FGD50 mixture. This could be interpreted by the difference in fine glass dust particles available for pozzolanic reaction between the FGD50 and FGD20 mixture.

As described earlier in this section in the discussion on the initial setting time in section 5.4.2 the working mechanism of the CaCl_2 in the accelerator slurry might have an acceleration effect on the hydration reaction by higher nucleation and growth rate of C-S-H nuclei in the presence of CaCl_2 . During the C_3S hydration the Ca^{2+} ion concentration could influence the growth of the C-S-H structures by higher nucleation and growth rate. This indicates a faster formation of hydration reaction products in the presence of higher CaCl_2 dosages. The calcium and chloride ions in the accelerator mainly affect the C_3S hydration and C_3S is the main component of Portland cement clinker, so the working mechanism of the CaCl_2 accelerator is enhanced if more Portland cement is available. For the investigated mixtures with 20% FGD, the addition of higher dosages of CaCl_2 caused a shorter induction period and a sharper and higher peak of hydration. This indicates that the CaCl_2 mainly influenced the induction phase and the acceleration phase of the hydration reaction. As suggested by the cumulative heat results, the CaCl_2 did not influence the total amount of hydration products that are formed, the process was only accelerated during the early age.

The findings on the heat evolution of the pumpable cementitious mixture + accelerator slurry are in agreement with the findings of Boukhelf et al. [15] and Kamali et al. [52], which both showed a de-

crease in main hydration peak height when a larger percentage of glass powder was used to replace Portland cement in the binder. This could be mainly attributed to the dilution effect of the Portland cement as the main hydration peak is caused by the hydration of C_3S . Higher replacement percentages mean that less C_3S particles were available in the binder to produce heat during the main hydration peak. The glass powder is mainly contributing to the heat evolution by pozzolanic activity, which produced less heat than the hydration of C_3S . This could explain the lower amount of cumulative heat for mixtures with more glass powder.

Rapp et al. [94], Yum et al. [131] and Kishar et al. [62] were in accordance with the findings on the acceleration effect of $CaCl_2$ on the early-age heat flow development of cementitious mixtures. The results of these researches showed an increase in initial hydration reactivity which contributed to a shorter induction period and a faster and higher main hydration peak. Yum et al. showed that secondary hydration peaks could be observed when supplementary cementitious materials are used to replace Portland cement. The height of these secondary hydration peaks was lower than the main hydration peak, likely due to the fact that the chemical reactivity of the supplementary cementitious material was lower than that of Portland cement clinker. In this current study the secondary hydration peak was higher than the main hydration peak for the mixture with 50% FGD. The differences between the results of these researches could be interpreted by a large difference in investigated replacement percentages 50% of cement replacement in this research compared to 20% cement replacement in the research of Yum et al [131].

So based on the provided results and discussion about the heat evolution of the cementitious mixture + accelerator slurry it can be indicated that a higher percentage of pre-treated fine glass dust led to a decrease in heat flow evolution during the main hydration peak and a reduction in total amount cumulative heat that was produced. A higher dosage of $CaCl_2$ in the accelerator slurry could effectively reduce the induction period and increase the heat flow during the main hydration peak by accelerating the early-age hydration reaction.

5.4.3. 3D Printed Concrete

Buildability and compressive strength of printed samples

The main objective of the buildability and compressive strength test in sections 5.3.8 and 5.3.9 was to investigate the printability and compressive strength development of the designed mixture FGD20-SP0.35-Acc8%. The buildability test showed that the developed mixture was printable at a printing speed of 3600 mm/min and a time interval of 9.42 seconds between subsequent layers. 10 layers could be printed with the developed mixture before failure of the cylinder. The bottom filaments had large deformation and had insufficient strength to carry the weight of the filaments that were printed on top. The compressive strength test showed anisotropic properties for the printed samples, in which the perpendicular and longitudinal directions provided similar results as the cast sample. However for the lateral direction a significant reduction in compressive strength was observed. Possible reasons for these results are analyzed in this section.

One potential interpretation for the buildability result is that the structural build-up was not strong enough. This means that the bottom layer had not developed sufficient strength and stiffness to withstand the loads of the subsequent filaments that were printed on top. Under this high load the bottom layers had a significant deformation, which eventually could lead to the failure of the printed cylinder after 10 layers. The structural build-up of the printed filaments could potentially be improved by adding a higher dosage of $CaCl_2$ to the accelerator slurry, which could lead to faster stiffness development in the bottom layers after printing. This suggests that more filaments could be stacked upon the bottom filaments before failure occurs.

A second possible influencing factor for the buildability results was the time duration between mixing and printing. During the mixing process of the buildability test there were 2 mixers available, which meant that the mixing procedure could be fast. This led to the fact that the time between mixing and printing was very short and the material had high flowability. At the start of the printing session the printed filaments had a large layer width due to the high flowability of the mixtures. These flowable printed filaments were loaded by the filaments on top, which caused even more deformation and even-

tually led to failure of the printed cylinder. The buildability of the developed mixture could potentially be improved by a small increase in the time between mixing and printing, or a small reduction in the superplasticizer dosage, so that the bottom layers have a little less flowability and more shape retention when printed. The buildability could also potentially be improved by changes in the nozzle moving speed. With a lower nozzle moving speed the time interval between subsequent layers will be longer. This means that the printed filaments will have more time available for strength and stiffness development before the subsequent layers are printed on top. Higher strength and stiffness development in the extruded filaments could cause an increase in structural build-up of the developed mixture.

A potential explanation for the anisotropic compressive strength development of the printed samples might be due to the interface between the printed filaments and the printing quality. The layer-by-layer extrusion process of concrete printing created interfaces between the printed filaments. These interfaces often have lower strength compared to the printed filaments and therefore might be governing the anisotropic properties under different loading directions [126] [89].

The results indicated that the perpendicular and longitudinal loading relative to the printing direction resulted in similar strength values as the cast sample after 7 days of curing. Lateral loading compared to the printing direction resulted in a significant strength reduction. The high strength of the perpendicular direction could possibly be explained by compaction of the printed filaments in the vertical direction during the printing session. The weight of the subsequent layers that are printed on top could cause increased compaction in the bottom layers and this high compaction could be responsible for the high compressive strength of the samples that were loaded perpendicular to the printing direction. The high strength of the longitudinal direction could potentially be explained by the motion pattern of material in the printing process. The longitudinal direction is the same direction as the printing direction. Therefore the particles in the middle of the printed filaments in the longitudinal direction may be better placed and compacted during extrusion from the nozzle. This better placement and compaction leads to a denser structure, which could potentially improve the strength in the longitudinal direction. The reduction in strength for the lateral direction might be explained by the sample geometry after sawing. After sawing the samples to the required size for compressive strength testing, the layered surface from printing was still present on the sides of the sample. During the extrusion process very little compaction of particles occurred, which means that a less strong structure is formed in this direction. Also for testing compressive strength in the lateral direction, this layered surface had to be placed into the loading jig. The applied load on the layered surface might have caused uneven loading on the surface and therefore caused stress concentrations in the sample. These stress concentrations together with low interlayer bonding and low compaction of the particles could potentially be responsible for the lower strength in the lateral direction.

The high strength of extruded material compared to the cast sample might also be justified by the formation of a denser matrix during the printing of the filaments [89]. During the extrusion process of filaments from the nozzle, pressure is applied to the fresh state material, which could potentially help to reduce the voids in the printed filaments. This lower void content could contribute to high strength filaments. However for multiple layers of extruded material this mechanism might not be so dominant, as the interlayer surface between printed filaments significantly influences the material properties.

The findings on the compressive strength development of the printed samples are in agreement with the findings of Wolfs et al. [126] and Bos et al. [13], which both indicated anisotropic properties of printed concrete caused by a weak interlayer surface due to stacking printed filaments on top of each other. For the strength of the printed samples compared to the cast sample of the same mixture there is a lot of variation between different studies [24] [16] [89] [125] [126]. These studies showed variation in the compressive strength of the printed samples, which could be higher or lower compared to the cast mixture. Also the loading direction which resulted in the highest strength showed a lot of differences between the studies. This can potentially be caused by a large variety of concrete printers, printing processes and printing parameters. Printing parameters were variable in each study, like the time interval between printing two subsequent layers, layer thickness of linear nozzle speed of the printer. Because there are no regulations or standards for 3D Concrete Printing yet it is difficult to compare the results of different studies.

So based on the provided results and discussion about the buildability and compressive strength development of the 3D printed concrete it can be indicated that the developed mixture FGD20-SP0.35-Acc8% was printable and that failure of the printed cylinder occurred after printing 10 layers with an interval time of 9.42 seconds between subsequent layers. Failure was potentially caused by insufficient structural build-up of the bottom printed filaments. Compressive strength development of the printed samples was comparable to the cast samples for the perpendicular and longitudinal loading direction. For the lateral loading direction a significant reduction in compressive strength was observed.

5.4.4. Limitations

This section describes the limitations of the study on the suitability of fine glass dust for 3D Concrete Printing. For different aspects of the study the limitations are discussed and proposals are made in which the study could be improved based on the limitations.

The flowability test on the pumpable cementitious mixtures was performed to determine the influence of superplasticizer (SP) dosage on the flowability of the mixture. However the flowability tests were all performed with the same volume of mixtures, as for all tests 1 liter of mixture was prepared. This means that the volume effect of the superplasticizer was not taken into account. When the same dosage of SP is used for a mixture with a larger volume, the increase in flowability will be larger because of the volume effect of the superplasticizer [44]. In this study only small material quantities were used for flowability tests, so this led to unpredictability when large amounts of mixture had to be prepared for the printability test, because it was not known how the flowability would change with large batches of material. This could be improved by investigating the flowability of different volumes of mixture with the same SP dosage.

The same holds for the initial setting time of this study. For the investigation of the accelerating effect of CaCl_2 dosage on the initial setting time of the mixture, similar material volumes were prepared for all investigated mixtures. With this research design it was not possible to determine the effect of CaCl_2 dosage in larger material quantities and how this changed the accelerating mechanism of the CaCl_2 .

Material supply was a significant limitation during the study of the suitability of fine glass dust for 3D Concrete Printing. As described in section 3.4.3 the pre-treatment of the fine glass dust was a slow process, due to oven capacity and availability. Therefore the amount of pre-treated fine glass dust was limited during this part of the research. Pumpability test and buildability test both required large material quantities, which was difficult with the material shortage of pre-treated fine glass dust. Due to the limited supply of material only one pumpability test was performed (for mix FGD50-SP0.4) and only one buildability test was performed (for mix FGD20-SP0.35-Acc8%). This could be improved by a larger oven capacity, which could cause a larger supply of pre-treated fine glass dust during the study.

For the isothermal calorimetry tests no FGD50 mixtures with CaCl_2 were included. Due to this test profile the two things that could be investigated during the isothermal calorimetry test were the effect of FGD percentage and CaCl_2 dosage on the heat evolution of the paste mixtures. However it was not possible to investigate the heat evolution effect of different CaCl_2 dosages on FGD20 mixtures compared to FGD50 mixtures. By implementing mixtures with different CaCl_2 dosages with FGD50 the accelerating effect of calcium chloride on FGD50 compared to FGD20 could be investigated.

6

Applicability of the developed mixture in practice

This research investigated 3D printable mixtures with two different fine glass dust percentages to replace Portland cement in the binder. Set-on-demand printing technique was used, which meant that both a pumpable cementitious mixture and an accelerator slurry had to be defined. For the pumpable cementitious mixture different dosages of superplasticizer were used to find the optimal flowability properties for pumpability. For the accelerator slurry different CaCl_2 dosages were added to find a suitable setting time for 3D concrete printing when the cementitious mixture and accelerator slurry were added together. From the test results in Chapter 5 it was evident that both mix FGD50-SP0.40-Acc10% and mix FGD20-SP0.35-Acc8% provided good results in terms of flowability, pumpability and initial setting time. However mix FGD20-SP0.35-Acc8% showed higher compressive strength development at all curing ages and was therefore chosen in section 5.2.10 to perform the buildability test to check the structural build-up after printing. Next to this comes the fact that mix FGD50-SP0.40-Acc10% showed high expansion and volume instability. It is unknown how the volume instability of this mixture will influence the 3D printability of the mixture and the structural build-up and stability of the printed filaments.

Based on the reasons mentioned above, the mix FGD20-SP0.35-Acc8% might be more suitable for future 3D concrete printing applications. This chapter aimed to provide an outlook for the applicability of mix FGD20-SP0.35-Acc8% for 3DCP in practice for structural applications. The suitability of the developed mixture with fine glass dust in a structural application is discussed based on a case study for a concrete bus shelter in Canberra, Australia. The goal of this chapter was to investigate if it was possible to produce a concrete bus shelter with the developed 3D printable mixture and to determine if this was strong enough to withstand the loads based on a finite element analysis. Also a feasibility analysis for the developed mixture is performed to evaluate the potential of the recycled fine glass utilization in 3DCP mixtures.

6.1. Background information on concrete bus shelter

The concrete bus shelters in Australia's capital city Canberra are considered as an icon in the environment. Cylindrical concrete bus shelters are placed throughout the entire city and remain a landmark value for almost 50 years now (see Figure 6.1). The bus shelters were designed in 1974 by the architect Clem Cummings [38][54]. The design was for a cylindrical bus shelter made from concrete, with window frames on each side and a bench inside, which was made from fiberglass. The orientation of the opening in the cylindrical concrete shelters is that the passengers that are inside can see in the direction of the arriving busses. Construction and installation of the concrete bus shelters started in 1975 and at least 477 bus shelters were produced and placed by the government in the city of Canberra. On February 1977, a new bus transport system was launched in Canberra, the ACT Internal Omnibus Network (ACTION) which made use of transportation along these concrete bus shelters [40][54]. To this date still 455 of these bus shelters remain in use, which means that over a time span of almost 50 years only 22 bus shelters were put out of use because of damage or other means [38]. Between

1980 and 1990 the inside murals of the bus shelters were painted by school children and community groups to discourage vandalism and promote community art [40]. Over the years the concrete shelters have become an admired element of Canberra's urban landscape and the locals often refer to the bus shelters as their "iconic bunkers".



(a) Total view



(b) 3D model

Figure 6.1: Canberra bus shelter made out of concrete

The reason for the concrete bus shelters in Canberra and the main advantages are that they are durable and cheap. The construction cost of a single shelter in 1977 was around 2300 dollars. This provided a durable concrete bus shelter that remains in service for almost 50 years to this date [54]. The concrete bus shelter provides protection against sun, rain and all other types of extreme weather possibilities in Australia and provides a safe waiting area for bus travelers. The bus shelter also has high protection against vandalism, because a concrete shelter is more difficult to damage than glass bus shelters. This decreases the cost and labor hours for repair or renovation works and leads to a long lifespan for the concrete shelters. As described in the previous paragraph the concrete bus shelters in Canberra are seen as an iconic landmark by many people. These are both inhabitants of Canberra as well as visiting tourists from other countries. The cultural value of these concrete bus shelters is further increased by displaying community art and local school children's paintings on the inside concrete walls, as presented in Figure 6.2 [40].



Figure 6.2: Canberra bus shelter with art displayed on the inside

Newcastle artist Trevor Dickinson increased the popularity of the concrete bus stops by making a museum exhibition consisting of a 50-photo-long gallery from different concrete bus shelters all around Canberra [54]. Dickinson called his exhibition: The beautiful bus shelters of Canberra, in which he showed real images and artist impressions of the concrete bus shelters placed in different environments. This gallery raised more awareness and appreciation for the concrete bus shelters in Canberra. Based on the success of the gallery exhibition Dickinson decided to write a book on the beautiful bus

shelters of Canberra with the goal of further putting the concrete shelters back on the map.

6.2. Design of the concrete bus shelter

During construction of the concrete bus shelters in 1975 the walls and roof structure were made out of precast concrete elements. These large concrete elements were produced in a large concrete factory and transported by road to their placement location all around Canberra. Once arrived at the placement location the concrete bus shelter was hoisted from the transportation vehicle and placing it on the ground [38].



Figure 6.3: Transportation of the prefabricated bus shelters [38]

The design that was used for the construction of the concrete bus shelters can be seen in Figure 6.4. All the bus shelters that are placed throughout Canberra have the same design and dimensions. The design is made in a cylindrical form with an opening on one side. This opening is placed to make the bus shelters easily accessible and that the bus travelers can look in the direction of the arriving busses. The height of the cylindrical wall structure is 2100 mm. On top of this cylindrical wall the roof structure is placed with a height of 500 mm and a roof slab thickness of 100 mm. The total height of the bus shelter from the ground to the top is 2600 mm. The roof structure expands over the entire cylindrical area, to protect the bus travelers from rain falling into the bus shelter. The outer diameter of the cylindrical concrete wall is 2740 mm and the walls have a thickness of 75 mm, so this means that the inner diameter is 2590 mm. This is the available area for the bus travelers to wait for their arriving bus. On the inside of the shelter a 75 mm thick concrete slab is placed on the floor. Under the floor a shallow foundation is made from concrete blocks and slabs that are placed in the ground. Fiberglass seats and back plates are placed on galvanized steel brackets to provide a seating area in the back of the concrete bus shelters. The bench inside the shelter provides seating area for a maximum of 3 people at once. On both sides of the bench windows are made in the concrete wall to provide a view for the waiting bus travelers. The windows are made from fiberglass and have a diameter of 600 mm. From the design drawings it can be seen that the opening in the wall structure is 1/3 of the full circle (see bottom middle design drawing in Figure 6.4). This means that the perimeter of the cylindrical wall is $(2/3) \cdot 2 \cdot \pi \cdot 1332.5 = 5581.56mm$.

6.3. Design verification of 3D printable mixture for concrete bus shelter

For the design verification of the wall structure of the concrete bus shelter, the loads on the wall had to be determined. For this case study it was assumed that the loads on the wall consisted of the self-weight from the roof structure and the wall itself and a wind load that was placed on the side of the wall. The self-weight of the concrete structure was placed as a line load on top of the wall and the wind load was placed as an area load on the side of the wall. For the calculations of the loads the dimensions from Figure 6.4 were used.

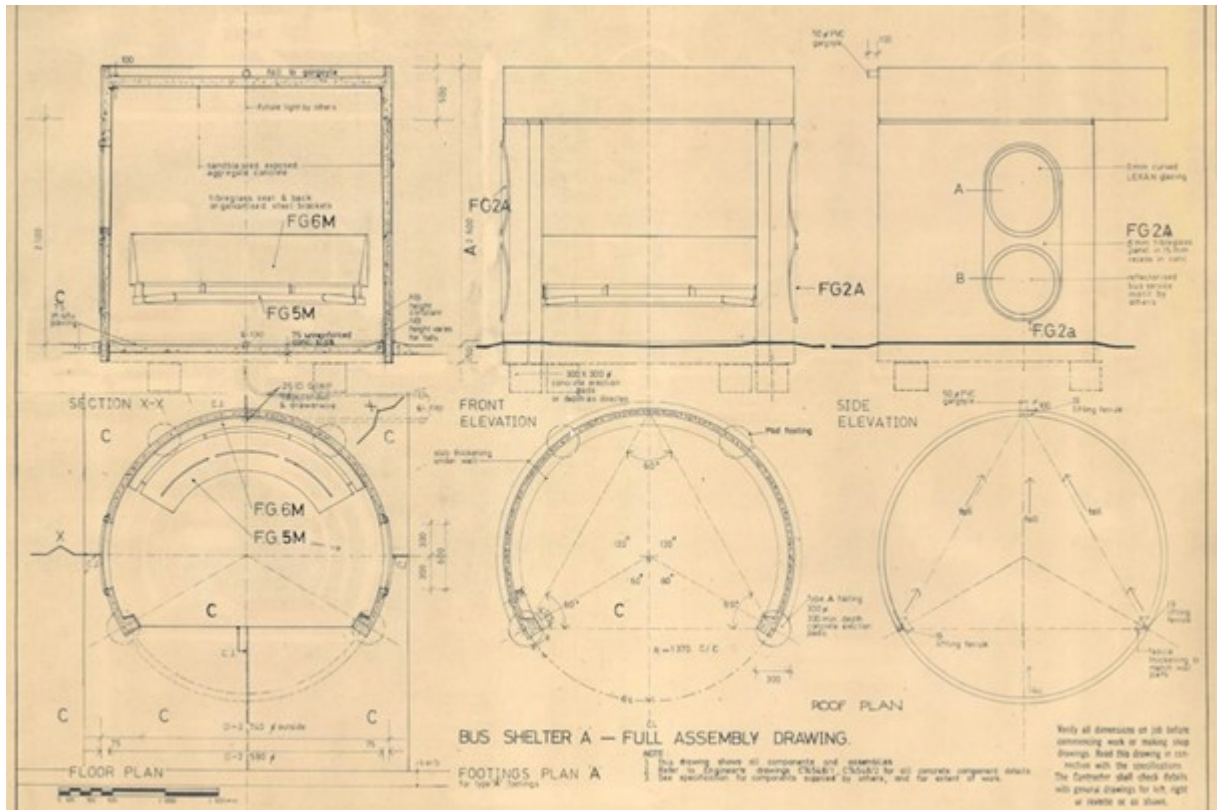


Figure 6.4: Design drawing for the concrete bus shelters [40]

Calculation of the self-weight:

- Volume of the roof slab: $t_{roof} \cdot 0.25 \cdot \pi \cdot d_{roof}^2 = 0.1 \cdot 0.25 \cdot \pi \cdot (2.59^2) = 0.53m^3$
- Volume of the roof wall: $h_{roof} \cdot t_{wall} \cdot 2 \cdot \pi \cdot r_{wall} = 0.5 \cdot 0.075 \cdot 2 \cdot \pi \cdot 1.3325 = 0.31m^3$
- Volume of the wall: $h_{wall} \cdot t_{wall} \cdot \frac{2}{3} \cdot 2 \cdot \pi \cdot r_{wall} = 2.1 \cdot 0.075 \cdot \frac{2}{3} \cdot 2 \cdot \pi \cdot 1.3325 = 0.88m^3$
- Total volume of concrete: $0.53 + 0.31 + 0.88 = 1.72m^3$
- Total mass of concrete: $Volume_{concrete} \cdot \rho_{concrete} = 1.72 \cdot 2400 = 4127.79kg$
- Total weight of concrete: $Mass_{concrete} \cdot 9.81 = 4127.79 \cdot 9.81 = 40493.6N$
- Line load on top of the wall: $Weight_{concrete} / (\frac{2}{3} \cdot 2 \cdot \pi \cdot r_{wall}) = 40493.6 / (\frac{2}{3} \cdot 2 \cdot \pi \cdot 1.3325) = 7254.89N/m$

So the self-weight of the roof structure and the wall were modeled by a line load of 7254.89 N/m on top of the cylindrical wall.

Calculation of the wind load:

The wind calculation was based on the Australian Standard AS/NZS 1170.2 [1].

Design wind speed for the bus shelter: $V_{des} = V_r \cdot M_d \cdot M_{z,cat} \cdot M_s \cdot M_t$

Where:

V_r = Regional zone 3 seconds gust wind speed; Canberra is region A2; $V_r = 46m/s$

M_d = Wind direction multiplier; Assume wind can come from all directions; $M_d = 1.0$

$M_{z,cat}$ = Terrain/height multiplier; Terrain category 2 (relatively open) and height smaller than 3 m;

$M_{z,cat} = 0.91$

M_s = Shielding multiplier; Assuming no very large blocking buildings; $M_s = 1.0$

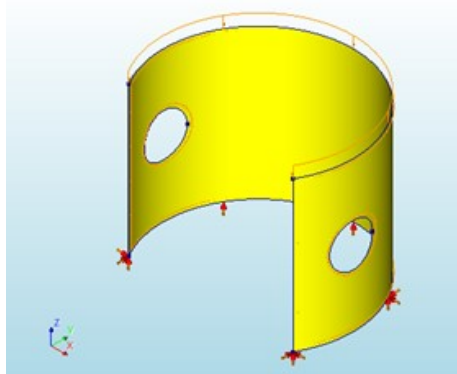
M_t = Topographic multiplier; Assuming no peaks or hills; $M_t = 1.0$

Design wind speed for the bus shelter: $V_{des} = 46 \cdot 1.0 \cdot 0.91 \cdot 1.0 \cdot 1.0 = 41.86m/s$

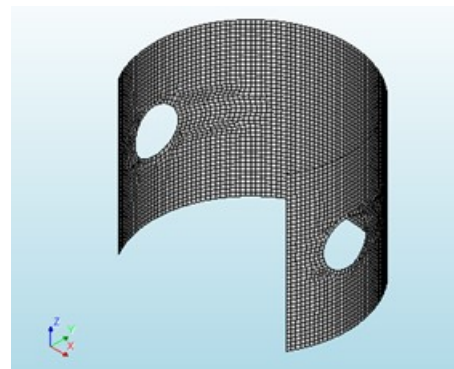
Design wind pressure: $p = 0.5 \cdot \rho_{air} \cdot (V_{des})^2 = 0.5 \cdot 1.2 \cdot (41.86)^2 = 1051.35Pa = 1051.35N/m^2$

So the wind load on the concrete bus shelter was modeled by an area load of 1051.35 N/m^2 on the side face of the cylindrical wall. In order to validate the maximum stresses in the cylindrical wall, the wind had to be placed in the most unfavorable direction. For the design of the bus shelter the most unfavorable direction was if the wind load was placed on the back side of the cylindrical wall (in the opposite direction of the opening in the shelter). More additional information on the full load calculation on the concrete bus shelter can be found in Appendix B.

Once the loads on the cylindrical wall were determined, the cylindrical wall of the bus shelter was modeled to validate the stresses that would occur when the loads were placed on the wall. The model of the cylindrical wall was made with Finite Element Method (FEM) software called DIANA. With the use of the Finite element method the model could be divided into very small elements, for which the stresses could be calculated. The finite element model for the cylindrical wall is shown in Figure 6.5. Based on the dimensions of the design drawings in Figure 6.4, the cylindrical wall is modeled as 2/3 of a full circle with the same dimensions as the original design. In Figure 6.5a it can be seen that available space for the windows was included in the wall by cutting out circular windows with a radius of 300 mm. For this design verification the window openings are not filled within the DIANA model, because the circular openings in the cylindrical wall could cause stress concentrations under the applied load during construction before the windows were placed and this could be governing for the design verification. This problem can be solved by integrating the windows directly in the printing process, however this solution for the printing procedure was beyond the scope of this case study. At the bottom the cylindrical wall had a clamped support, which means that it was not allowed to rotate or move in any direction at the base. The clamped support was used to model the shallow foundation under the bus shelter which prevented the wall from moving and/or rotating. From Figure 6.5a it can also be seen that two different loads were placed on the wall. First a line load of 7254.89 N/m was placed on top of the wall in vertical direction (negative Z-direction). Secondly an area load of 1051.35 N/m^2 was placed on the side of the wall in the most unfavorable direction (negative Y-direction). These two loads represented the self-weight and the wind load on the bus shelter. In Figure 6.5b it can be seen that the model is divided into very small elements. For this 3-dimensional model quadratic quadrilateral finite elements were used and a mesh size of $50 \times 50 \text{ mm}^2$ was applied.



(a) DIANA model



(b) DIANA mesh

Figure 6.5: Diana model for the cylindrical wall of the bus shelter

The finite element model of the cylindrical wall was used to run a linear static analysis, which means that the loads are placed on the wall and the deformations and stresses in each of the elements were calculated. The goal of this analysis was to determine the maximum stresses in the cylindrical wall under the applied loads. The maximum stresses could then be compared with the strength of the developed 3D printable mixture in order to determine if the mixture would be suitable for the construction of this concrete bus shelter. The results of the FEM analysis are presented in Figure 6.6.

From Figure 6.6a it can be seen that the maximum stress in the horizontal X-direction was $7.49 \cdot 10^4 \text{ N/m}^2$ which is equal to 74.9 kPa . The maximum stress in the horizontal x-direction occurred in the top

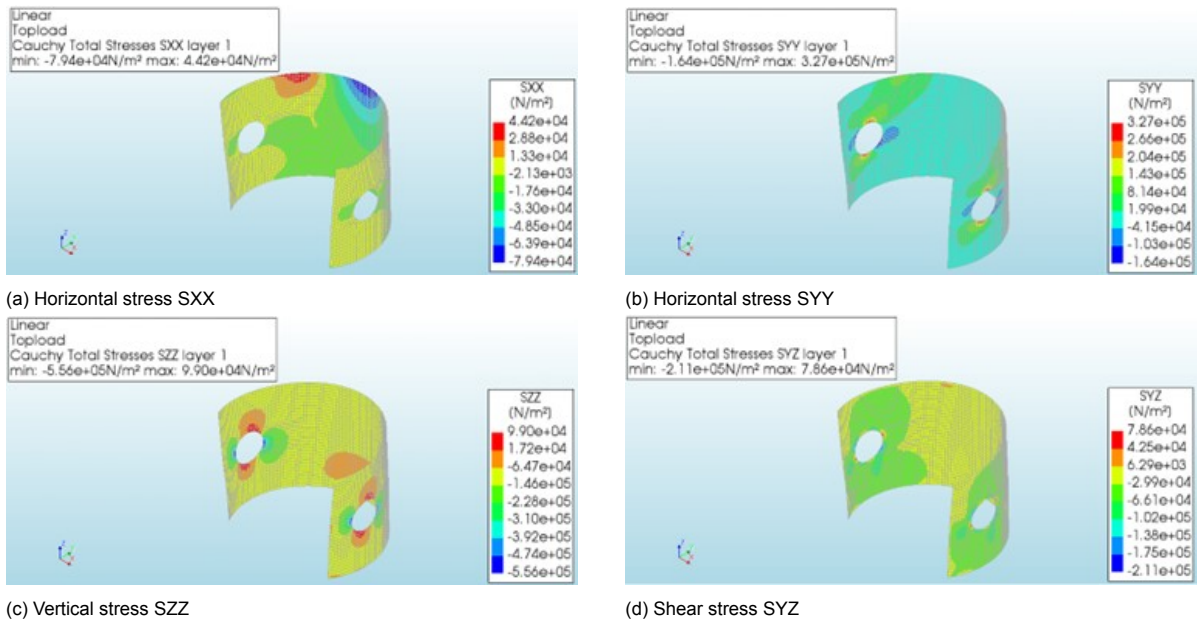


Figure 6.6: DIANA analysis results for cylindrical wall of bus shelter

part of the cylindrical wall at the location opposite to the opening. From Figure 6.6b it can be seen that the maximum stress in the horizontal Y-direction for the cylindrical wall was $3.27 \cdot 10^5 \text{ N/m}^2$ which is equal to 327 kPa. The maximum stress in the horizontal Y-direction occurred at the top and bottom part of the circular window openings in the cylindrical wall. From Figure 6.6c it can be seen that the maximum stress in the vertical Z-direction was $5.56 \cdot 10^5 \text{ N/m}^2$ which is equal to 556 kPa. The maximum stress in the vertical Z-direction occurred at the left and right sides of the circular window openings in the cylindrical wall. From Figure 6.6d it can be seen that the maximum shear stress in the YZ-direction for the cylindrical wall was $2.11 \cdot 10^5 \text{ N/m}^2$ which is equal to 211 kPa. The maximum shear stress in YZ-direction occurred at the diagonals of the circular window openings.

From the FEM results in Figure 6.6 it becomes clear that the circular window openings in the cylindrical wall of the concrete bus shelter were the main location for high stresses during the linear static analysis. The reason for this is that the window openings caused a discontinuity in the cylindrical wall during the construction process which prevented a vertical load transfer from the top of the wall (where the line load is applied) to the bottom of the wall (where the base of the wall is supported). Because of the circular openings the load transfer can not be fully vertical but has to go around the openings, which means that stress concentrations occur at that location. This process of stress concentration is clarified in Figure 6.7.

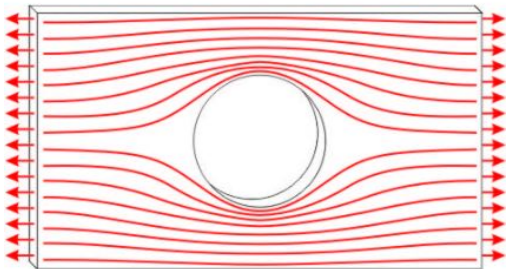


Figure 6.7: Force flow around a circular opening

For the applicability of the developed printable mixture FGD20-SP0.35-Acc8% the maximum stresses in different directions from the FEM analysis in Figure 6.6 are compared with the compressive strength

results of the 3D printed sample of section 5.3.9. In Figure 5.3.9 it is shown that the strength of the printed samples perpendicular to the printing direction was 26.85 MPa after 7 days of curing. The highest compressive stress in the vertical direction (SZZ) was $5.56 \cdot 10^5 \text{ N/m}^2$, which corresponds to 0.56 MPa (Figure 6.6c). The strength of the printed samples longitudinal and lateral compared to the printing direction were 25.51 and 19.56 MPa respectively after 7 days of curing. The highest compressive stresses in both horizontal directions (SXX and SYY) were $7.94 \cdot 10^4 \text{ N/m}^2$ and $1.64 \cdot 10^5 \text{ N/m}^2$, which correspond to 0.08 and 0.16 MPa respectively.

The printed concrete of the designed mixture FGD20-SP0.35-Acc8% developed sufficient compressive strength after 7 days of curing to withstand the designed loads in this case study on compression (self-weight and wind load). The strength of the printed filaments was way higher than the designed stresses during the use phase of the construction in this simplified case study. It would provide valuable information if the strength of the printed filaments was determined at earlier curing ages, for example very shortly after printing. As discussed in section 5.4.3 the buildability of the developed mixture FGD20-SP0.35-Acc8% could be increased by increasing the CaCl_2 dosage in the accelerator slurry. If the bottom filaments are able to withstand the loads of the subsequent filaments and have sufficient structural build-up, the buildability of the printed mixture will be higher and this mixture could potentially be used for the printing of the concrete bus shelter.

6.4. Suitability of developed mixture for 3D printable concrete bus shelter

Section 6.3 showed that the developed mix design FGD20-SP0.35-Acc8% was strong enough for the realisation of the bus shelter. The maximum stresses in this case study in three different directions were lower than the strength of the printed samples of the developed mixture after 7 days of curing. So the developed mixture is strong enough to withstand the loads on the bus shelter. This section analyses two possible methods for the construction of the concrete bus shelter by 3D printing with the developed mixture in this study. This is done to assess the suitability of the developed mixture for 3D printing a concrete bus shelter structure with concrete. For each construction principle the construction procedure is described and advantages and disadvantages are discussed to compare the two possible methods for printing the concrete bus shelter with the developed mixture FGD20-SP0.35-Acc8% from this study.

On-site 3D concrete printing

The first possible principle on how to make the concrete bus shelter printable is based on on-site printing. With on-site printing a 3D concrete printer is used to print the concrete bus shelter on the desired placement location. With on-site printing the concrete bus shelter is printed in one session, which means that the cylindrical wall, the wall of the roof and the roof slab are all printed together in one session. In order to print the difficult geometry of the concrete bus shelter, an inflatable air cushion with specific geometry can be used on the inside of the bus shelter, like the construction of concrete domes [122] [74]. The concrete is printed around the inflated air cushion in the desired geometry of the bus shelter and if the material is hardened enough to support its own weight the air cushion can be deflated. Because the developed mixture contains a high amount of CaCl_2 in the accelerator slurry this stiffening process will be fast and the air cushion does not need to give support for a very long time. The inflatable air cushion is needed, because with concrete printing it is not possible to print the roof slab directly on top of the wall, because there is insufficient support for the printed filaments. With 3D concrete printing it is only possible to directly print filaments on top of each other so that the printed filaments can support and carry the weight of the filaments that are printed on top. The air cushion creates temporary support for the roof wall and roof slab in the early stage, until these can support their own weight.

Because the entire structure is printed in one session the connections between the cylindrical wall, roof wall and roof slab are all monolithic, this means that no additional connection is needed to keep the structure stable. On the other hand monolithic connections have a low tolerance for deformations, which can cause damage to the concrete bus shelter in the case of imposed deformations due to temperature changes. The printing session of the entire structure together has the advantage that the printing speed can be high, which means a low printing time and low labour time for the concrete workers that control the concrete printer.

If the entire structure is printed on site it is possible to realise the printing path of the cylindrical wall in one line. In this way the wall can be realised by printing multiple lines next to each other depending on the width of the printing nozzle and the printed filaments to reach the total wall thickness of 75 mm. The printing path of the wall can then be $2/3$ of a circle for multiple filaments next to each other to form the entire layer of the wall, which is shown in Figure 6.8. This relatively simple printing path has the advantage that it saves printing time, due to the simple geometry. But on the other hand the disadvantage is that the wall will be printed as a massive unit of concrete which leads to the fact that there is no available space to apply reinforcement bars vertically in the structure. This printing path of the wall makes it very difficult to place or integrate any form of reinforcement for the wall during or after the printing process. The absence of reinforcement decreases the durability of the printed bus shelter.

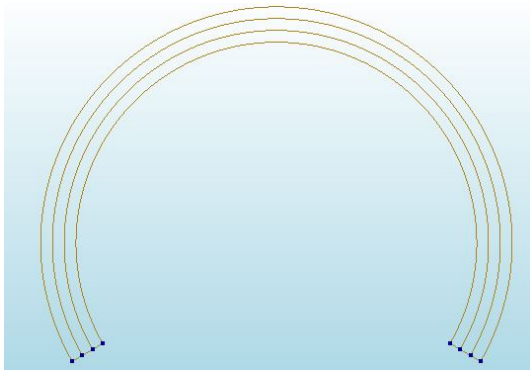


Figure 6.8: Top view of printing path for cylindrical wall for on-site printing

When the concrete bus shelter is printed on-site there is one large 3D concrete printer needed to print all the parts of the entire bus shelter continuously. This has the advantage that there is no need for the transportation of heavy concrete elements from the production factory to the placement location, because the material is directly printed on the placement location. A large printer that can cover the entire bus shelter and sufficient material supply is needed to ensure good printing quality during the printing process. A disadvantage of on-site printing are the unpredictable outside weather circumstances. Changes in temperature, wind and humidity can all influence the concrete properties and therefore influence the printing quality of the concrete bus shelter with the developed mixture.

Prefabricated 3D concrete printing

The second possible principle on how to make the concrete bus shelter printable is based on constructing with prefabricated 3D concrete printed elements. With this construction principle the different elements of the bus shelter are 3D printed separately in the factory and are then transported to the placement location of the concrete bus shelter where they are assembled. This means that the cylindrical wall, the wall of the roof and the roof slab are printed separately and are connected later. This leads to a more easy printing path for the separate elements, which can all be printed from the ground. No special balloon or other form of temporary mould is needed to support the weight of the printed filaments, but all three separate elements can be printed by stacking layers on top of each other. Because the total structure of the concrete bus shelter is divided into separate elements a smaller concrete printer is sufficient for this construction principle. Another advantage of the prefabrication of the 3D printed elements is that in the construction factory the printing circumstances can be kept almost constant, which means that there is no influence of weather changes and standard printing quality can be ensured for all prefabricated elements. However this has the disadvantage that the prefabricated elements have to be transported from the production factory to the placement site, which leads to high transportation and installation costs. At the placement site the separate elements of the bus shelter are connected to ensure structural stability of the structure. These connections can be very costly or difficult to fabricate, which increases the cost of the construction process. On the other hand with the free choice of connections it is possible to design connections in the shelter that allow deformations

until a certain limit. This deformation freedom decreases the stresses by imposed deformations on the structure and therefore increases the durability of the printed bus shelter.

The prefabricated cylindrical wall is printed with a specific printing path. This printing path consists of a geometry in which an inner and outer layer are printed for the wall to reach a total wall thickness of 75 mm with diagonals that are placed in between. A possible printing path for the cylindrical wall of the concrete bus shelter is presented in Figure 6.9.

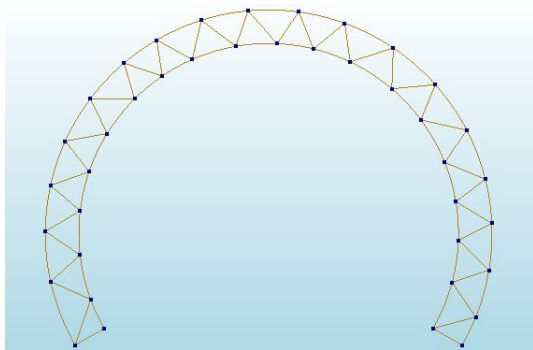


Figure 6.9: Top view of printing path for cylindrical wall for precast printing

The diagonals in the printing path allow for structural stability of the wall during the printing process. After the printing process of the cylindrical wall, the space between the printed filaments provides room for insulation and the placement of reinforcement bars. After the reinforcement bars are placed, the spaces in the wall are filled up with cast concrete so that it results in a massive wall structure. In this way it is possible to add reinforcement to a 3D concrete printing structure. Prefabrication makes this process easier, because elements are printed separately and the connection of the different elements happens at the placement site. The reinforcement bars in the printed cylindrical wall increase the durability of the structure, which means that the lifespan of the concrete bus shelter can be expanded. The developed mixture in this study consists of CaCl_2 as an accelerator that allows for rapid stiffness development of the printed filaments. However it has been shown in previous studies that the interaction between standard steel reinforcement bars and calcium chloride increases the corrosion rate of the reinforcement bars [124] [6]. Corrosion of the reinforcement bars will lead to the deterioration of the reinforcing steel and weakening of the bond between concrete and reinforcement bars, which can ultimately result in spalling and cracks on the concrete surface. Therefore in mixtures with calcium chloride as an accelerator, the use of steel reinforcement bars might not be the best choice.

So in order to apply reinforcement in the concrete, other possibilities for reinforcement of the cylindrical wall have to be explored. One potential solution for the reinforcement in combination with the CaCl_2 in the developed mixture is the use of bamboo reinforcement [71] [12]. Long bamboo sticks are placed vertically in the openings of the printed wall structure to replace the steel reinforcement bars and the remaining space is filled with cast mortar. In this way bamboo can function as reinforcement for the cylindrical wall of the bus shelter. One of the advantages of bamboo is that bamboo is a very strong natural fibre with a tensile strength comparable to steel reinforcement bars. Bamboo is very lightweight compared to steel, which means that bamboo is almost six times stronger than steel by weight [55]. Another important advantage is that bamboo is easily available in nature and has a very fast regrowing capacity. This indicates that the use of bamboo as reinforcement is a cheap and sustainable solution as a replacement for steel reinforcement bars. Also bamboo contains an almost impermeable protection in the outer layer which protects from rotting due to moisture in the cementitious mixtures [55].

However on the other hand bamboo has some important disadvantages for the use as a reinforcement in concrete. The main disadvantage of bamboo as reinforcement is the lower durability compared to steel reinforcement bars. Bamboo is prone to fungus and insect attacks and these are important degradation mechanisms that can deteriorate bamboo over time. Bamboo has also shown to be a brittle material with a low modulus of elasticity and therefore can crack under high deflections. Compared to yielding of the reinforcement steel cracks in the bamboo can possibly lead to failure of the cylindri-

cal wall under high loads [71]. Also for bamboo the adherence to the mortar mix is lower than steel reinforcement, as the steel reinforcement bars have ribs for additional bond capacity and the surface of the bamboo reinforcement is mainly smooth and flat.

Another potential solution for the reinforcement in combination with the CaCl_2 in the developed mixture is the use of fibre reinforced polymers (FRP). Fibre Reinforced Polymer materials are composite materials that typically consist of strong fibres embedded in the cement matrix which can take up the tensile stresses in the concrete [95] [81]. The fibres provide stiffness and strength to the cementitious mixture and generally carry most of the applied loads along the length of the fibres. The fibres are anisotropic, which means the properties vary in different directions. The best mechanical properties are in the direction of fibre placement. The cement matrix acts to bond the fibres, protects the fibres and provides stress transfer from fibre to fibre through shear stresses [95]. Different types of fibres can be used for fibre reinforced polymers. The most common fibres are carbon, glass and synthetic fibres [81]. The fibres are lightweight and have very high strength characteristics, which makes them ideal for reinforcement in the cylindrical wall. In the available space between the printing path of the cylindrical wall a cast in-situ mortar can be placed with a high dosage of fibre reinforced polymers. These fibres can act as a replacement for steel reinforcement bars. The fibre reinforced polymers are non-conductive and non-corrosive, which means that these can be combined with the CaCl_2 in the developed mix design for the concrete bus shelter.

Based on the analyzed construction principles it is suggested that prefabricated 3D concrete printing would be the optimal solution for printing the concrete bus shelter with the developed mixture. The advantages of the prefabricated 3D printing principle outweigh the disadvantages. Separate production of construction elements, constant printing quality due to constant weather conditions and the possibility of integrating FRP reinforcement in the structure to increase the strength and durability of the structure all contribute to the applicability of the developed mixture FGD20-SP0.35-Acc8% in practice.

6.5. Feasibility for the utilization of fine glass dust in 3DCP mixtures

Sections 6.3 and 6.4 showed a potential applicability for the developed fine glass dust 3DCP mixtures and proved that on a technical aspect the cement replacement in 3DCP mixture provided a suitable utilization for recycled fine glass dust. This section presents a discussion on the feasibility of utilizing fine glass dust as cement replacement in 3DCP mixtures. This section presents the value and relevance of the developed mixture in this study and also suggestions are proposed to increase the feasibility of the pre-treated fine glass dust in practice.

The yearly production of recycled fine glass dust by Maltha BV is 5000 tons per year. Based on the capacity of this recycling plant it is estimated that the total yearly production of fine glass dust is 200.000 tons per year for the entire glass recycling industry in Europe (D. Timmers, personal communication, August 31, 2022). With the developed Mix FGD20-SP0.35-Acc8% for 3DCP this means that $1.0 \cdot 10^9$ L which equals 1.0 million cubic meters of 3D printed concrete can be produced in Europe every year with the developed fine glass dust mixture in this thesis. With 1.0 million cubic meters of 3D printed concrete per year the equivalent of 580.000 concrete bus shelters could be printed with the developed mix design. This would result in a decrease of 200.000 tons per year of Portland cement clinker consumption and the utilization of the fine glass dust that would otherwise be incinerated or used as landfill. The CO_2 emissions related to Portland cement clinker are found to be around 830 kg CO_2 /ton according to Prakasan et al. [90]. This means that every year the emission of CO_2 into the atmosphere due to the concrete construction industry in Europe could be reduced by 166 million kg when the developed mixture with fine glass dust is used for 3D concrete printing. This not only has an advantageous contribution to the sustainability of the concrete industry by replacing part of the Portland cement with fine glass dust, but this application is also beneficial for the circularity of the glass recycling industry. This byproduct from the glass recycling industry otherwise was difficult to recycle, had limited applications and would mainly be placed in landfill, however this study presented a new utilization for the fine glass dust as a cement replacement in 3DCP mixtures, which could contribute to closing the loop for glass recycling.

An important topic to address for the feasibility of the fine glass dust as cement replacement for 3DCP mixtures is the large variation in organic content and material composition between different batches of fine glass dust. This is caused by the difference in recycled glass products and the various amount of impurities and food waste on the glass products that are delivered to the glass recycling plant. Because of the small particle sizes of the fine glass dust, these impurities and organic compounds are difficult to remove during the recycling process. The varying organic content and material composition make it difficult to accurately predict the properties when different batches of fine glass dust are used as cement replacement in 3DCP mixtures. Sufficient heat-treatment has shown in this thesis to remove a large part of the organic compounds from the fine glass dust and can ensure a more consistent material composition between different batches of fine glass dust.

A larger material production with a more constant quality could potentially be achieved by using the fine glass fraction. Every recycling plant in Europe has a fine glass fraction after recycling and separation with a particle size between 0-6 mm. This fine glass fraction has a comparable material composition as the fine glass dust, only with a higher silica content (around 75%) and a lower organic content, because food waste and impurities in the glass stream can be removed more efficiently on larger particles. Nowadays this fine fraction is partly used as aggregate replacement in concrete, but mainly used as landfill. With this process a lot of material goes to waste and this does not contribute to the circularity of the glass recycling stream. Based on the promising results of the fine glass dust as cement replacement in this study, there could be a possibility to grind the fine glass fraction until glass powder. For sufficiently long grinding times the particle sizes can be reduced to comparable sizes as the fine glass dust. In this case a ground fine glass powder can be produced with a lower organic content, a higher silica content and similar properties to the fine glass dust in this study. The main advantage is that the production capacity of the ground fine glass powder is a lot higher. From every glass recycling plant in Europe an estimated 10% is fine glass fraction that can potentially be ground to fine glass powder (D. Timmers, personal communication, August 31, 2022). From a total of 13 million tons per year of recycled glass products in Europe [37], an estimated amount of 1.3 million tons of fine glass fraction per year could potentially be produced to ground glass powder. With the developed Mix FGD20-SP0.35-Acc8% for 3DCP this means that $6.5 \cdot 10^9$ L which equals 6.5 million cubic meters of 3D printed concrete can be produced every year with the developed fine glass dust mixture in this thesis. By using the developed printable mixture in this thesis for 3DCP the amount of Portland cement that is used, is lowered by 1.3 million tons per year. This equals a reduction of 1.08 billion kg of CO₂ emission for the concrete industry every year when this ground fine glass powder could be used to replace 20% of Portland cement in 3DCP mixtures [90]. The only disadvantage of this utilization is that it requires an extra step of grinding and sieving for the glass recycling industry. This extra production step requires extra time and money during the recycling process, but if done correctly this could potentially decrease the environmental burden of cement clinker production by replacing part of the Portland cement with this fine glass powder in the mixtures for 3DCP. Also the utilization of this fine glass fraction in cementitious mixtures further contributes to the circularity of the glass recycling industry.

For the fine glass dust to be feasible for the 3D Concrete printing industry the advantages of the cement replacement have to outweigh the disadvantages. This means that the financial burden of an extra production step or an extra pre-treatment step for the fine glass dust and the loss in strength compared to the reference mix have to be covered by the potential advantages analyzed earlier in this section. The advantages of using fine glass dust as a cement replacement for 3DCP could be enhanced by financial support from the government for using a lower carbon footprint cementitious mixture. Another possibility could be the implementation of mandatory regulations in Europe that necessitate the use of recycled material as a cement replacement in the binder of concrete mixtures to reduce the CO₂ emissions from the construction industry. Financial support or regulations regarding the use of recycled material for cementitious mixtures could provide a promising solution, which would increase the feasibility and applicability of the pre-treated fine glass dust in this thesis as cement replacement in 3DCP mixtures. In this way the utilization of fine glass dust as a cement replacement in 3DCP mixtures can contribute to increase the sustainability of the construction industry and the circularity of the glass recycling industry.

Conclusions and recommendations

Based on the provided results and discussions conclusions were formulated in section 7.1 to answer the research questions from section 1.4. Recommendations for further research based on this thesis are formulated and presented in section 7.2.

7.1. Conclusions

Based on the presented results in Chapter 3, the following conclusions could be formulated with regards to the raw material characterization and the optimal pre-treatment methods for fine glass dust.

- The most efficient heat-treatment of the fine glass dust in terms of mass loss could be achieved by placing the fine glass dust in an oven at 600°C for 1 hour. The material that was collected from the oven was still in powdered form and the corresponding mass loss of this heat-treatment was 7.66%. Determination of organic content had shown that at this temperature the organic compounds were effectively removed from the fine glass dust.
- The most efficient grinding treatment for the fine glass dust was achieved by grinding in the ball mill machine for 1 hour. Results had shown that the grinding treatment led to a significant reduction of particle sizes for the fine glass dust and it especially decreased the number of large particles. After 1 hour of grinding the D90 value of the fine glass dust decreased from 48.96 to 34.92 μm .
- BET specific surface area analysis had shown that both the heat-treatment and the grinding treatment had a positive influence on the specific area of the fine glass dust. This could be attributed to the removed organic compounds and the finer particle sizes.
- The heat-treatment at 600°C did not lead to the formation of new crystalline phases in the fine glass dust. The amorphous silica content of the fine glass dust after heat-treatment was not significantly changed as was shown by the results of the XRD analysis.
- Both the heat-treatment and the grinding treatment had a positive influence on the early age compressive strength development of mortar mixtures with 15% cement replacement by fine glass dust. The delaying effect on hydration was reduced by the heat-treatment and reactivity of the fine glass dust was increased by the grinding treatment. This led to an increase in early age strength development.
- Heat-treatment of the fine glass dust had a positive influence on the later age compressive strength development of mortar mixtures with 15% cement replacement by fine glass dust. Additional grinding of the fine glass dust showed comparable results to the mix with only heat-treated fine glass dust and did not lead to further strength increase for the mortar mixtures at longer curing ages.

The mixtures with pre-treated fine glass dust showed slightly higher strength development at later curing ages compared to the reference mixture. Between 28 and 90 days of curing the compressive strength relative to the reference mix was increased and secondary strength development

was observed. This indicated that the possibility for the fine glass dust to possess some pozzolanic activity after pre-treatment when 15% was used to replace Portland cement in the binder was likely.

- Compression strength results showed that the mixture with heat-treated and ground fine glass dust could approach the reference mixture strength up to 90% for curing ages between 3 and 90 days.
- The dilution effect on hydration for the untreated fine glass dust (Mix 2) increased the initial setting time compared to the reference mixture (Mix 1) from 220 minutes to 303 minutes. After only heat-treatment (Mix 3) the initial setting time was reduced to 208 minutes. The heat treatment and grinding treatment combined led to a further reduction of the initial setting time to 166 minutes for Mix 5.
- The heat-treatment and grinding treatment did not cause any major differences for the fresh-state properties of the mortar mixtures. For the slump value and slump flow diameters very small differences were observed for all investigated mixtures.
- Based on the presented results and discussions it was observed that both heat-treatment and grinding treatment were beneficial to the fresh state and hardened properties of mortar mixtures with fine glass dust. However the difference between 1 hour grinding and 6 hours grinding was not very significant in terms of compressive strength development and initial setting time. Therefore this investigation concluded that the most optimal pre-treatment for the fine glass dust was a combination of a heat-treatment at 600°C for 1 hour and a grinding treatment of 1 hour.

Based on the presented results in Chapter 4, the following conclusions were formulated with regards to the cement replacement percentage investigation.

- A higher replacement percentage of fine glass dust resulted in a lower compressive strength development for all investigated curing ages between 3 and 28 days. This showed that the fine glass dust had no significant contribution to the strength development of the mortar and mainly had a filler function at early curing ages.

The mixtures with the investigated cement replacement percentages of fine glass dust showed slightly higher strength development at later curing ages compared to the reference mixture. Between 28 and 90 days of curing the compressive strength relative to the reference mix was increased and secondary strength development was observed. This indicated that the possibility for the fine glass dust to possess pozzolanic activity after pre-treatment was possible not only for 15%, but also for higher replacement percentages.

- Higher fine glass dust replacement percentages had no significant influence on the investigated fresh-state properties of the mortar for replacement percentages between 0 and 30%. For high replacement percentages (45%) a sharp reduction in slump value was observed. No clear trend could be observed for the slump flow values for low to medium replacement percentages. For high replacement percentages (45%) the slump flow value increased, which indicated an increase in flowability for high FGD percentages.
- The pre-treated fine glass dust showed small amounts of pozzolanic activity when it was used to replace 15% Portland cement in the binder of concrete mortar. This was indicated by the reduction of C-H content between curing ages of 28 and 56 days for the fine glass dust mixture, which might be caused by the consumption of calcium hydroxide for the secondary formation of C-S-H by pozzolanic reaction. This was also in agreement with the increase of secondary compressive strength development at higher curing ages compared to reference mixtures.
- The mixture with 25% Portland cement replacement by fine glass dust caused volume instability and significant formations of secondary products. For a cement replacement percentage lower than 10% by fine glass dust, no significant secondary formations could be observed.

Based on the presented results and discussion in Chapter 5, the following conclusions can be given with regards to the suitability of fine glass dust for 3D Concrete Printing.

- Optimal flowability for 3DCP for the cementitious mixture with 50% FGD was achieved by adding 0.4% SP to the mixture. Optimal flowability for the cementitious mixture with 20% FGD was achieved by adding 0.35% SP to the mixture. Both Mix FGD50-SP0.4 and Mix FGD20-SP0.35 proved to be cementitious mixtures with good pumpability and suitable for the pumping process of 3D Concrete Printing with set-on-demand printing technique.
- Superplasticizer dosage had a negligible effect on the 7 day compressive strength development for both mixtures with 50% and 20% FGD. Investigated cementitious mixtures with 20% FGD had higher compressive strength development after 7 days of curing than cementitious mixtures with 50% FGD.
- Variable CaCl_2 dosage in the accelerator slurry had no significant effect on the flowability of the combination of cementitious mixture + accelerator slurry. Both mixtures with 50% and 20% FGD showed comparable slump flow results for all investigated CaCl_2 dosages.
- Initial setting time of the combination of cementitious mixture + accelerator slurry could be significantly shortened by the addition of higher CaCl_2 dosages in the accelerator slurry. For cementitious mixture FGD50-SP0.40 accelerator slurry with 10% CaCl_2 was sufficient to reach an initial setting time of 90 minutes. For cementitious mixture FGD20-SP0.35 accelerator slurry with 8% CaCl_2 was sufficient to reach an initial setting time of 90 minutes.
- A lower amount of FGD caused a shorter induction period for the hydration reaction and a higher hydration peak, which occurred at an earlier age compared to the mixture with a higher FGD dosage. A higher dosage of CaCl_2 in the mixture caused a shorter induction period and a higher hydration peak at an earlier age. Both the FGD dosage and the CaCl_2 dosage influenced the hydration reaction and heat flow of the combined mixture of cementitious mixture + accelerator slurry.
- CaCl_2 dosage in the accelerator slurry had a small hardening effect. For both the mixtures FGD50-SP0.4 and FGD20-SP0.35 the addition of higher CaCl_2 dosages led to a small increase in compressive strength development after 7 and 28 days of curing. Investigated cementitious mixtures + accelerator slurry with 20% FGD had higher compressive strength development after 7 days of curing than cementitious mixtures + accelerator slurry with 50% FGD.
- The developed mixture FGD20-SP0.35-Acc8% proved to be printable with set-on-demand concrete printing. A cylindrical column could be printed up to 10 layers and failure of the printed specimen was potentially caused by insufficient structural build-up of the bottom printed filaments. Compressive strength development of the printed samples was comparable to the cast samples of the same mixture for the perpendicular and longitudinal loading direction. For the lateral loading direction a significant reduction in compressive strength was observed.

Based on the presented results in Chapter 6, the following conclusions were formulated with regards to the applicability and feasibility of the developed mixture for 3DCP in practice.

- The printed specimens of the developed printable mixture FGD20-SP0.35-Acc8% are strong enough to withstand the modeled self-weight and wind loads on the concrete bus shelter. Therefore the developed 3DCP mixture could be applicable for producing the concrete bus shelters in practice.
- The suggested construction principle for the 3D printed concrete bus shelter with the developed mixture is based on prefabricated 3D concrete printing. With this principle separate elements of the structure are produced in a factory and reinforcement can be added to the printed concrete structure by designing a specific printing path for the wall. For the reinforcement Fibre Reinforced Polymer reinforcement is suggested to be compatible with high CaCl_2 dosages in the developed mixture.
- The utilization of fine glass dust in 3DCP mixtures not only has an advantageous contribution to the sustainability of the concrete industry by replacing part of the Portland cement and therefore reducing CO_2 emission significantly, but this application promises also to be beneficial for the circularity of the glass recycling industry by utilizing a byproduct that would otherwise be mainly disposed as landfill.

7.2. Recommendations for further study

The objective of this thesis was to investigate the suitability of fine glass dust for 3D Concrete Printing with set-on-demand printing technique. Based on the presented results, discussions and limitations, recommendations for further study are summarized in this section.

- Investigating the effect of a combination of Portland cement, pre-treated fine glass dust and an other Supplementary Cementitious Material (SCM), like silica fume or fly ash in the binder of the cementitious mixture for 3D printing. By combining three different constituents in the binder a ternary blend can be produced and the positive aspects of all constituents can be combined. Mixtures with fly ash have shown to increase the compressive strength development compared to the reference mixture in a study by Nath et al. [83]. When fly ash is added to the fine glass dust mixture, this could potentially compensate for the decrease in strength for the fine glass dust mixtures. By investigating mixtures with different ternary blends as binder a potentially higher strength than the reference mixture could be obtained, while still having sustainable benefits reducing the Portland cement content in the binder.
- Investigating the effect of large aggregate fraction in the fine glass dust mixtures. In this thesis only mortar mixtures with sand as fine aggregates were used. For 3D Concrete Printing the largest aggregate fraction had to be smaller than 2 mm, because there was a risk of damage to the printing equipment, when larger aggregate particles were used. However for practical applications with cast concrete not only mortar mixtures with small aggregates, but also concrete mixtures with large aggregates are used. Therefore it could be interesting to investigate the interaction between the fine glass dust and the large aggregates in concrete mixtures.
- Investigating the ASR effect on the fine glass dust mixtures. Alkali-Silica reaction is a potential danger for the deterioration of concrete, especially when fine glass dust with a large silica content is used to replace Portland cement in the binder. However on the other hand research by Huang et al. [45], Taha et al. [111] and Du et al. [31] showed that finely ground glass powder may inhibit possible ASR reaction. So investigation of the effect of fine glass dust on the possible acceleration or inhibition of ASR in concrete mixtures would provide valuable insights.
- Investigating longer grinding times or a better sieving procedure after grinding. Due to large batches of material and limited capacity, grinding times not longer than 6 hours were investigated in this thesis. After grinding relatively large sieve sizes were used for sieving the ground material, so larger particles may have passed through the sieve. Also the analyzer for the particle size distribution was not very accurate in analyzing particles smaller than $10\mu\text{m}$. Research by Shi et al. [103] and Du et al. [32] showed that very fine glass powder was achieved by long grinding times, which could significantly improve the pozzolanic activity and compressive strength development of glass powder mortars. Therefore it would be interesting to investigate longer grinding times with a better sieving procedure and PSD analyzer, to reach better properties of the fine glass dust mixtures.
- Investigating the secondary formations in the mixtures with high fine glass dust percentage. In this thesis the unwanted secondary formations, potentially caused by volume expansion of hydrated free lime, were briefly investigated with SEM analysis, but no significant conclusion could be formulated from this. It would be interesting knowledge to study the secondary formations of the mixtures in more detail, by analyzing the type of compounds that form and also how to reduce the formation of these compounds in the mixture. If the secondary formations could be reduced and volume stability of the mixture is achieved, it would potentially be possible to use higher Portland cement replacement percentages in the cementitious mixture for set-on-demand printing.
- Investigating glass powder with higher silica content. As shown in Figure 2.1 the fine glass dust that was used for this study had a silica content of 55.90% and a high organic content. As described in the feasibility study in section 6.5 a possibility would also be to grind the fine glass fraction to a powder, which results in a powder with higher silica content and lower amount of organic compounds. This material composition could potentially lead to an increase in pozzolanic reactivity of the glass powder when it is used as a cement replacement. Another potential application as cement replacement could be the use of borosilicate glass, which is a glass product with a typical composition of 80-81% of SiO_2 [39].

A

SEM images for secondary formations test

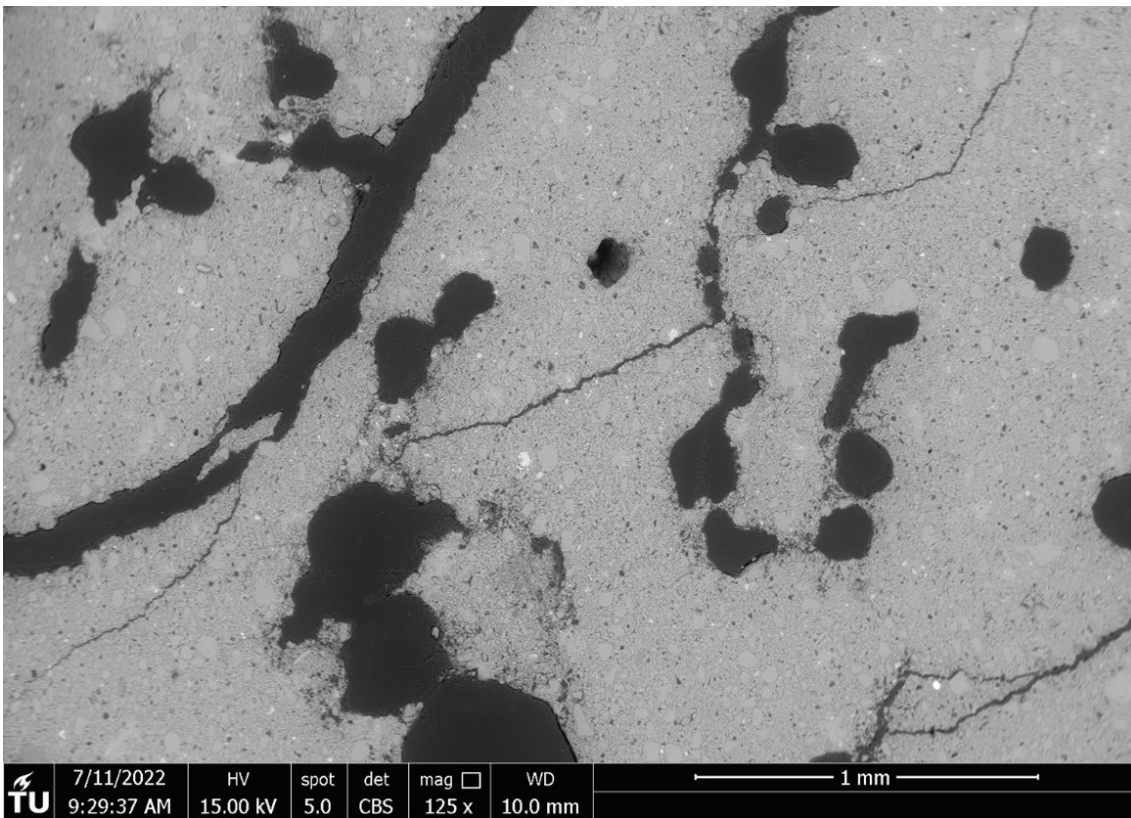


Figure A.1: Overview SEM image mix FGD50 (zoom 125x)

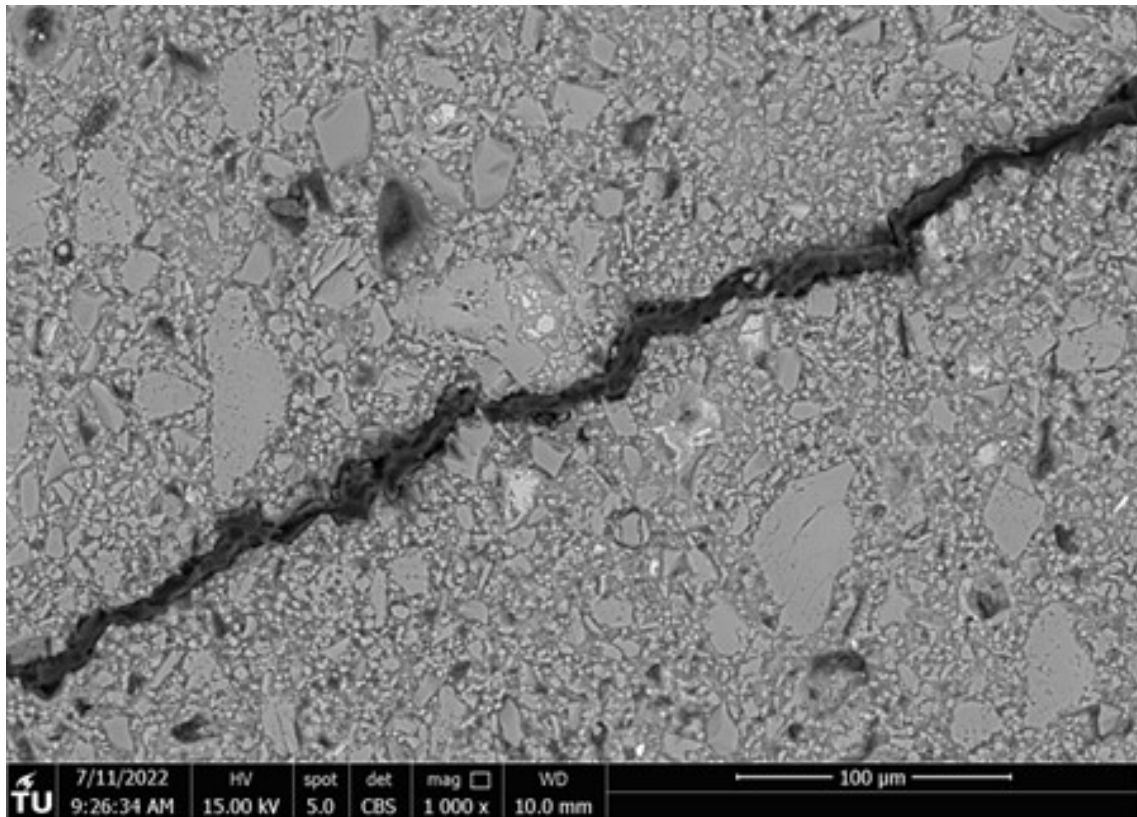


Figure A.2: Close-up SEM image 1 mix FGD50 (zoom 1000x)

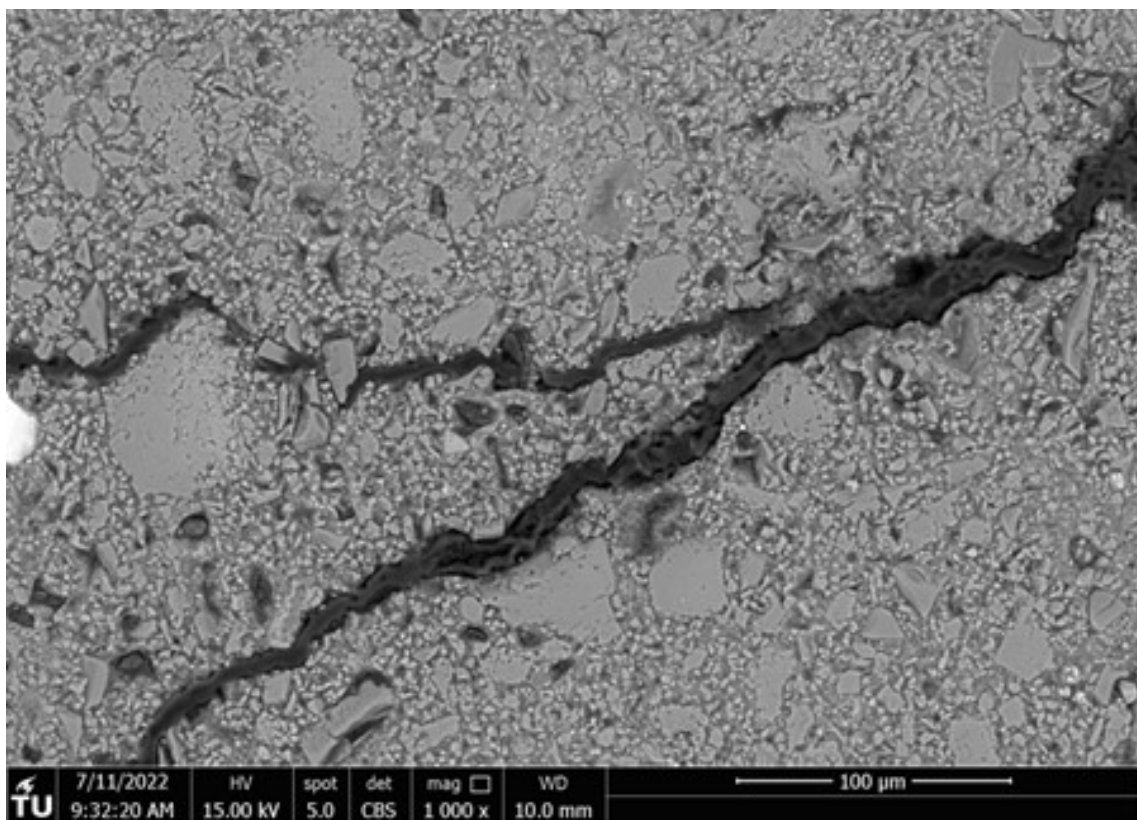


Figure A.3: Close-up SEM image 2 mix FGD50 (zoom 1000x)

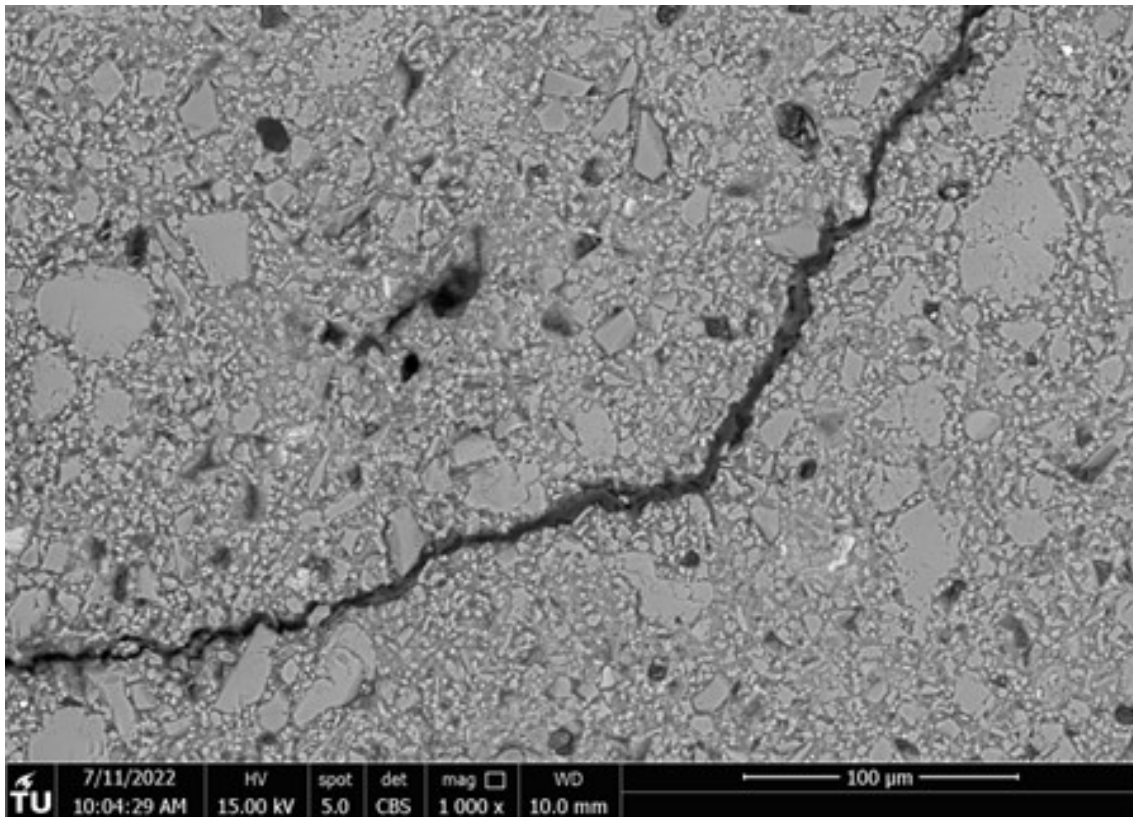


Figure A.4: Close-up SEM image 3 mix FGD50 (zoom 1000x)

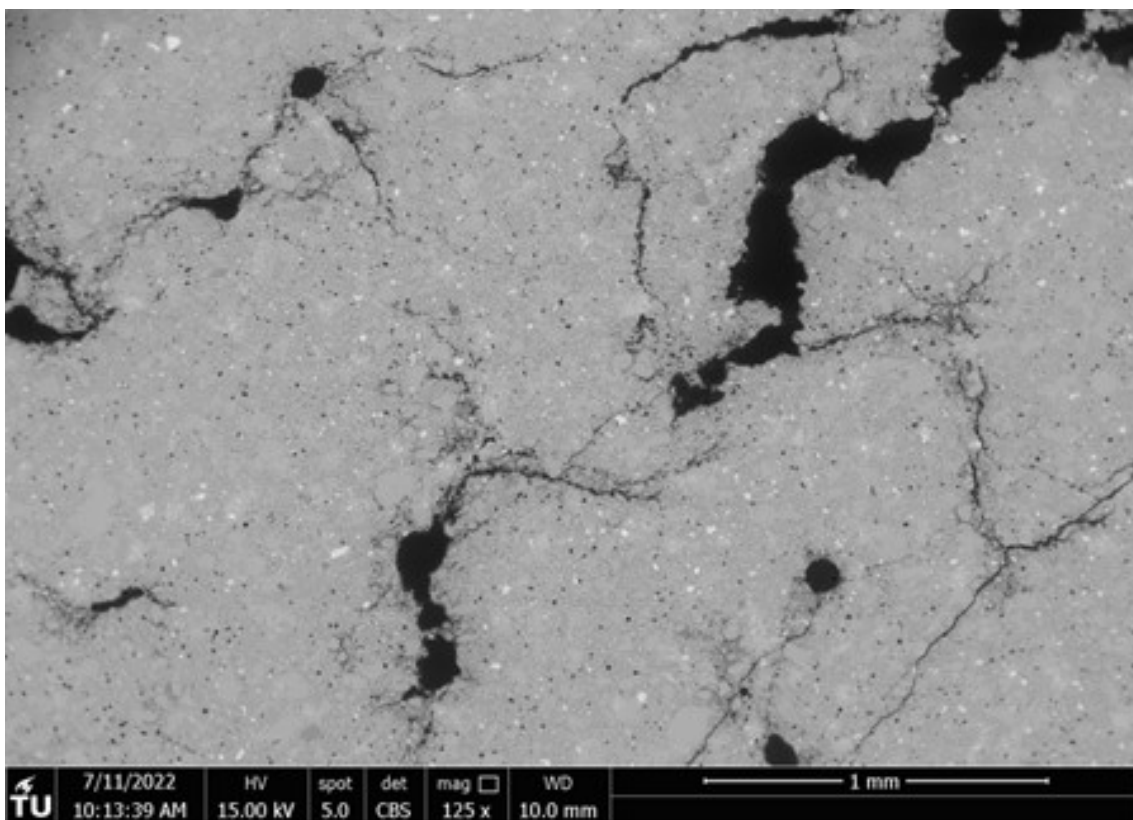


Figure A.5: Overview SEM image mix FGD20 (zoom 125x)

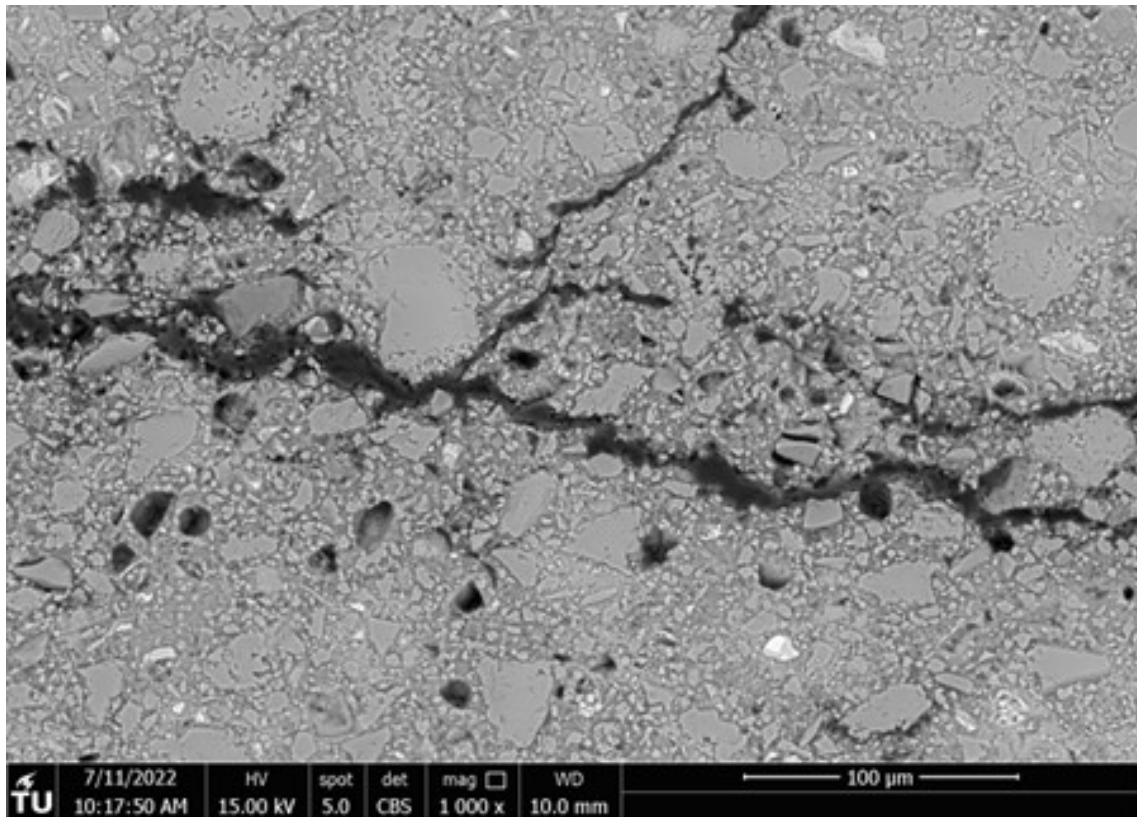


Figure A.6: Close-up SEM image 1 mix FGD20 (zoom 1000x)

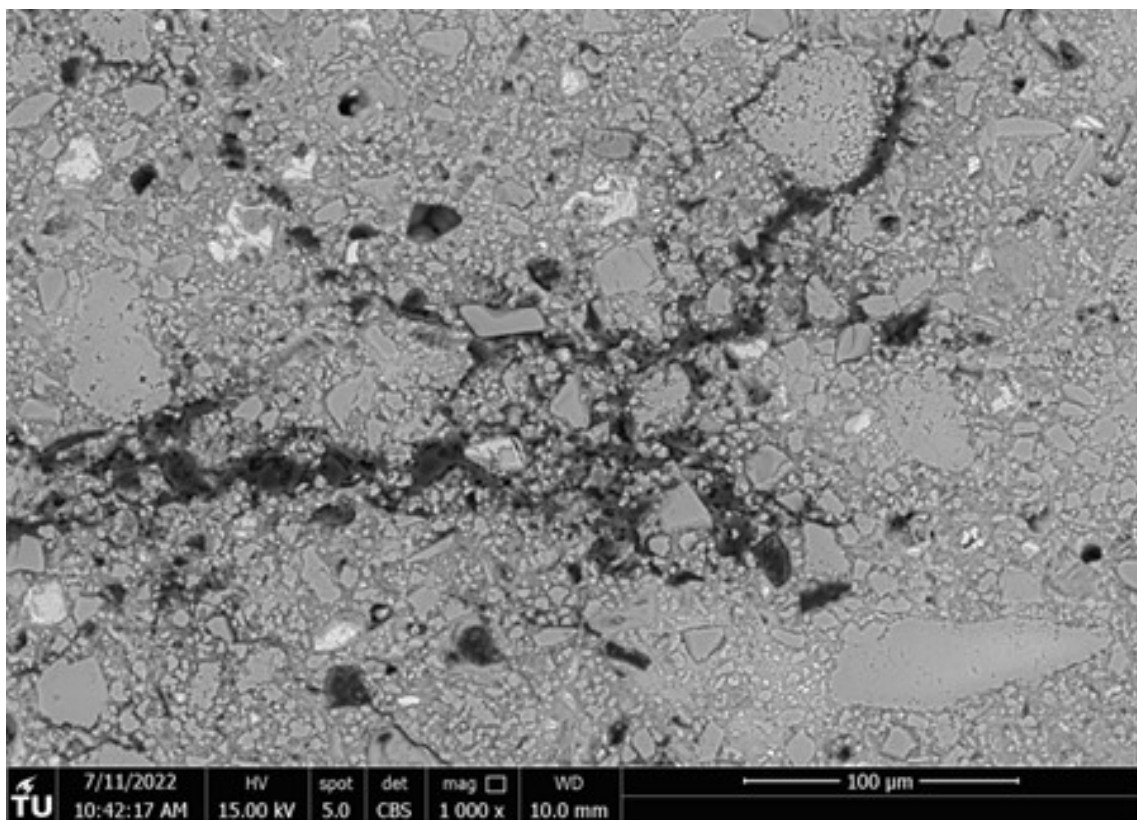


Figure A.7: Close-up SEM image 2 mix FGD20 (zoom 1000x)

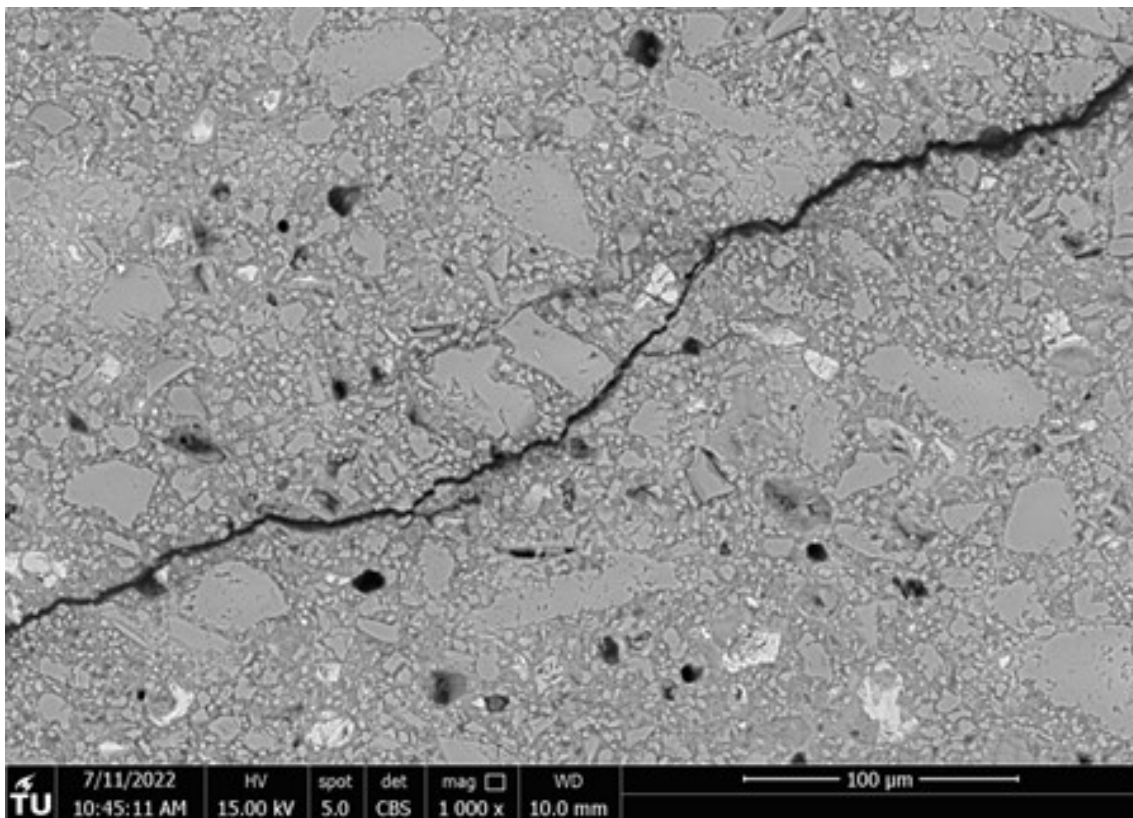


Figure A.8: Close-up SEM image 3 mix FGD20 (zoom 1000x)

B

Load calculation for concrete bus shelter

Concrete bus shelter calculation			The wall of the shelter is 2/3 of a full cylinder	Height wall is 2100 mm
Constant	Value	Unit	The roof of the shelter is a full cylinder	Height roof is 500mm with 100 mm slab
p concrete	2400	kg/m ³		
E concrete	30	Gpa		
v concrete	0.2	-		
h wall	2.1	m	Weight calculation	(The total weight of the structure is placed as a line load on the top of the wall)
t wall	0.075	m		
t roof	0.1	m	Volume roof slab = $0.1 \cdot 0.25 \cdot \pi \cdot (2.590)^2$	0.526853 m ³
h roof	0.5	m	Volume roof wall = $0.5 \cdot 0.075 \cdot 2 \cdot \pi \cdot 1.3325$	0.313963 m ³
d roof	2.59	m	Volume wall = $2.1 \cdot (2/3) \cdot 0.075 \cdot 2 \cdot \pi \cdot 1.3325$	0.879096 m ³
r wall	1.3325	m	Total volume	1.719912 m ³
Vr	46	m/s	Total self-weight = total volume * p concrete	4127.789 kg
Md	1	-	Convert mass to newton = total mass * 9.81	40493.61 N
Mz,cat	0.91	-	Circumference of the wall = $2/3 \cdot 2 \cdot \pi \cdot 1.3325$	5.581563 m
Ms	1	-	Load on top of the wall	7254.887 N/m
Mt	1	-		
p air	1.2	kg/m ³		
Cfig	1	-		
Cdyn	1	-		
Vminimum	30	m/s		

(a) Self-weight calculation for the concrete bus shelter

SOURCE	AS/NZS 1170.2:2021	Structural design acti Part 2: Wind actions
	https://skyciv.com/docs/tech-notes/loading/asnz-1170-2-wind-load-calculation-example/	
Wind calculation	(wind is placed as an area load from the most unfavorable direction)	
	Wind comes from the back of the shelter	
Vdes = Vr * Md * Mz,cat * Ms * Mt		
Vdes = $46 \cdot 1.0 \cdot 0.91 \cdot 1.0 \cdot 1.0$	41.86 m/s	
p = $0.5 \cdot p_{air} \cdot (Vdes^2) \cdot Cfig \cdot Cdyn$		
p = $0.5 \cdot 1.2 \cdot (Vdes^2) \cdot 1.0 \cdot 1.0$	1051.356 Pa = N/m ²	

(b) Wind load calculation for the concrete bus shelter

Figure B.1: load calculation for the concrete bus shelter

Bibliography

- [1] AS/NZS 1170.2:2021. "Structural design actions, Part 2: Wind actions". In: (2021).
- [2] Kaveh Afshinnia and Prasada Rao Rangaraju. "Influence of fineness of ground recycled glass on mitigation of alkali-silica reaction in mortars". In: *Construction and Building Materials* 81 (2015). ISSN: 09500618. DOI: 10.1016/j.conbuildmat.2015.02.041.
- [3] Kaveh Afshinnia and Prasada Rao Rangaraju. "Mitigating alkali-silica reaction in concrete: Effectiveness of ground glass powder from recycled glass". In: *Transportation Research Record* 2508 (2015). ISSN: 03611981. DOI: 10.3141/2508-08.
- [4] Oumayma Ahmadah et al. "A new mix design method for low-environmental-impact blended cementitious materials: Optimization of the physical characteristics of powders for better rheological and mechanical properties". In: *Cement and Concrete Composites* 128 (Apr. 2022), p. 104437. ISSN: 09589465. DOI: 10.1016/j.cemconcomp.2022.104437.
- [5] Ali A. Aliabdo, Abd Elmoaty M. Abd Elmoaty, and Ahmed Y. Aboshama. "Utilization of waste glass powder in the production of cement and concrete". In: *Construction and Building Materials* 124 (Oct. 2016), pp. 866–877. ISSN: 09500618. DOI: 10.1016/j.conbuildmat.2016.08.016.
- [6] M. Babaei and A. Castel. "Chloride-induced corrosion of reinforcement in low-calcium fly ash-based geopolymer concrete". In: *Cement and Concrete Research* 88 (Oct. 2016), pp. 96–107. ISSN: 00088846. DOI: 10.1016/j.cemconres.2016.05.012.
- [7] Mustafa Batikha et al. "3D concrete printing for sustainable and economical construction: A comparative study". In: *Automation in Construction* 134 (Feb. 2022), p. 104087. ISSN: 09265805. DOI: 10.1016/j.autcon.2021.104087. URL: <https://linkinghub.elsevier.com/retrieve/pii/S0926580521005380>.
- [8] Cherif Belebchouche et al. "Mechanical and microstructural properties of ordinary concrete with high additions of crushed glass". In: *Materials* 14 (8 2021). ISSN: 19961944. DOI: 10.3390/ma14081872.
- [9] Joseph J. Biernacki et al. "Cements in the 21st century: Challenges, perspectives, and opportunities". In: *Journal of the American Ceramic Society* 100 (7 2017). ISSN: 15512916. DOI: 10.1111/jace.14948.
- [10] M. C. Bignozzi et al. "Glass waste as supplementary cementing materials: The effects of glass chemical composition". In: *Cement and Concrete Composites* 55 (2015), pp. 45–52. ISSN: 09589465. DOI: 10.1016/j.cemconcomp.2014.07.020.
- [11] Simon Blott and Debra Croft. *Particle size analysis by laser diffraction*. Geological society London, 2004, pp. 63–73. URL: <http://sp.lyellcollection.org/>.
- [12] Bor. "Alternative Reinforcement for Concrete in Corrosive Environments". In: (). URL: <https://www.usbr.gov/research/>.
- [13] Freek Bos et al. "Additive manufacturing of concrete in construction: potentials and challenges of 3D concrete printing". In: *Virtual and Physical Prototyping* 11.3 (July 2016). Publisher: Taylor and Francis Ltd., pp. 209–225. ISSN: 17452767. DOI: 10.1080/17452759.2016.1209867.
- [14] Federica Boscaro et al. "Eco-Friendly, Set-on-Demand Digital Concrete". In: *3D Printing and Additive Manufacturing* (Aug. 2021). Publisher: Mary Ann Liebert Inc. ISSN: 2329-7662. DOI: 10.1089/3dp.2020.0350.
- [15] Fouad Boukhelf et al. "On the hygrothermal behavior of concrete containing glass powder and silica fume". In: *Journal of Cleaner Production* 318 (Oct. 2021). Publisher: Elsevier Ltd. ISSN: 09596526. DOI: 10.1016/j.jclepro.2021.128647.

- [16] R. A. Buswell et al. "3D printing using concrete extrusion: A roadmap for research". In: *Cement and Concrete Research* 112 (Oct. 2018), pp. 37–49. ISSN: 00088846. DOI: 10.1016/j.cemconres.2018.05.006.
- [17] G.C. Bye. "Portland cement". In: (1999).
- [18] Wenjing Cai et al. "Effect of Particle Packing on Flow Property and Strength of Concrete Mortar". In: ().
- [19] Yamei Cai, Dongxing Xuan, and Chi Sun Poon. "Effects of nano-SiO₂ and glass powder on mitigating alkali-silica reaction of cement glass mortars". In: *Construction and Building Materials* 201 (2019). ISSN: 09500618. DOI: 10.1016/j.conbuildmat.2018.12.186.
- [20] Maddalena Carsana, Massimiliano Frassoni, and Luca Bertolini. "Comparison of ground waste glass with other supplementary cementitious materials". In: *Cement and Concrete Composites* 45 (2014). ISSN: 09589465. DOI: 10.1016/j.cemconcomp.2013.09.005.
- [21] Gaurav Chand, Sugandh Kumar Happy, and Shobha Ram. "Assessment of the properties of sustainable concrete produced from quaternary blend of portland cement, glass powder, metakaolin and silica fume". In: *Cleaner Engineering and Technology* 4 (Oct. 2021). Publisher: Elsevier Ltd. ISSN: 26667908. DOI: 10.1016/j.clet.2021.100179.
- [22] Yu Chen. "Investigation of limestone-calcined clay-based cementitious materials for sustainable 3d concrete printing". In: (2021). URL: <https://doi.org/10.4233/uuid:a0d9289b-9f24-4805-86ab-09f12714a946>.
- [23] Yu Chen. *Sustainable Cementitious Material for 3D Concrete Printing View project*. Tech. rep. Jan. 2017. URL: <https://www.researchgate.net/publication/331803002>.
- [24] Yu Chen et al. "A review of printing strategies, sustainable cementitious materials and characterization methods in the context of extrusion-based 3D concrete printing". In: *Journal of Building Engineering* 45 (Jan. 2022). Publisher: Elsevier Ltd. ISSN: 23527102. DOI: 10.1016/j.jobeb.2021.103599.
- [25] Yu Chen et al. "Effect of different grade levels of calcined clays on fresh and hardened properties of ternary-blended cementitious materials for 3D printing". In: *Cement and Concrete Composites* 114 (Nov. 2020). ISSN: 09589465. DOI: 10.1016/j.cemconcomp.2020.103708.
- [26] S. H. Chu et al. "Recycling of waste glass powder as paste replacement in green UHPFRC". In: *Construction and Building Materials* 316 (2022). ISSN: 09500618. DOI: 10.1016/j.conbuildmat.2021.125719.
- [27] Constructor. "Initial Setting Time and Final Setting Time of Concrete - The Constructor". In: (2019). URL: <https://theconstructor.org/concrete/initial-final-setting-time-concrete/25819/>.
- [28] Luc Courard, Hervé Degée, and Anne Darimont. "Effects of the presence of free lime nodules into concrete: Experimentation and modelling". In: *Cement and Concrete Research* 64 (2014), pp. 73–88. ISSN: 00088846. DOI: 10.1016/j.cemconres.2014.06.005.
- [29] Henri Van Damme. "Concrete material science: Past, present, and future innovations". In: *Cement and Concrete Research* 112 (Oct. 2018), pp. 5–24. ISSN: 00088846. DOI: 10.1016/j.cemconres.2018.05.002.
- [30] Wenkui Dong, Wengui Li, and Zhong Tao. "A comprehensive review on performance of cementitious and geopolymeric concretes with recycled waste glass as powder, sand or cullet". In: *Resources, Conservation and Recycling* 172 (2021). ISSN: 18790658. DOI: 10.1016/j.resconrec.2021.105664.
- [31] Hongjian Du and Kiang Hwee Tan. "Effect of particle size on alkali-silica reaction in recycled glass mortars". In: *Construction and Building Materials* 66 (Sept. 2014), pp. 275–285. ISSN: 09500618. DOI: 10.1016/j.conbuildmat.2014.05.092.
- [32] Hongjian Du and Kiang Hwee Tan. "Properties of high volume glass powder concrete". In: *Cement and Concrete Composites* 75 (Jan. 2017), pp. 22–29. ISSN: 0958-9465. DOI: 10.1016/J.CEMCONCOMP.2016.10.010.

- [33] Hongjian Du and Kiang Hwee Tan. "Waste glass powder as cement replacement in concrete". In: *Journal of Advanced Concrete Technology* 12 (11 2014). ISSN: 13468014. DOI: 10.3151/jact.12.468.
- [34] J. Epp. "X-Ray Diffraction (XRD) Techniques for Materials Characterization". In: *Materials Characterization Using Nondestructive Evaluation (NDE) Methods* (Apr. 2016), pp. 81–124. DOI: 10.1016/B978-0-08-100040-3.00004-3.
- [35] G. Eshel et al. "Critical Evaluation of the Use of Laser Diffraction for Particle-Size Distribution Analysis". In: *Soil Science Society of America Journal* 68.3 (May 2004). Publisher: Wiley, pp. 736–743. ISSN: 03615995. DOI: 10.2136/sssaj2004.7360.
- [36] Ebenezer O. Fanijo, Emad Kassem, and Ahmed Ibrahim. "ASR mitigation using binary and ternary blends with waste glass powder". In: *Construction and Building Materials* 280 (2021). ISSN: 09500618. DOI: 10.1016/j.conbuildmat.2021.122425.
- [37] FEVE. "Industry Data - FEVE". In: (). URL: <https://feve.org/glass-industry/data/>.
- [38] Sonya Gee. "Are Canberra's iconic bus shelters found anywhere else in the world?" In: <https://www.abc.net.au/news/canberra/2016-08-08/canberras-iconic-bus-shelters-are-there-others-like-it/7681568> (Aug. 2016).
- [39] Ace Glass. "Raw Borosilicate Glass Data Chart 828 Technical Info Raw Borosilicate Glass Data". In: (2007). URL: <http://www.aceglass.com/rawglass.html>.
- [40] Rohan Goynes. "The Cummings concrete bus shelter, Canberra 100". In: <https://www.capitalhistoryhere.com/home/2010no-2-the-cummings-concrete-bus-shelter> (2021).
- [41] Jagriti Gupta, A.S. Jethoo, and P.V. Ramana. "Evaluating long term properties of concrete using waste beverage glass". In: *Materials Today: Proceedings* (2021). ISSN: 22147853. DOI: 10.1016/j.matpr.2021.09.446.
- [42] M. Harini, G. Shaalini, and G. Dhinakaran. "Effect of size and type of fine aggregates on flowability of mortar". In: *KSCE Journal of Civil Engineering* 16 (1 Jan. 2012), pp. 163–168. ISSN: 12267988. DOI: 10.1007/s12205-012-1283-4.
- [43] Edward Harrison, Aydin Berenjian, and Mostafa Seifan. "Recycling of waste glass as aggregate in cement-based materials". In: *Environmental Science and Ecotechnology* 4 (Oct. 2020), p. 100064. ISSN: 2666-4984. DOI: 10.1016/J.ESE.2020.100064.
- [44] Fady M A Hassouna and Hussein Abu-Zant. "Effects of Superplasticizers on Fresh And Hardened Portland Cement Concrete Characteristics". In: (2016). ISSN: 2277-8691. URL: <https://www.researchgate.net/publication/316157363>.
- [45] Da Huang et al. "Study on the effect and mechanism of alkali-silica reaction expansion in glass concrete". In: *Sustainability (Switzerland)* 13 (19 2021). ISSN: 20711050. DOI: 10.3390/su131910618.
- [46] K. I.M. Ibrahim. "Recycled waste glass powder as a partial replacement of cement in concrete containing silica fume and fly ash". In: *Case Studies in Construction Materials* 15 (2021). ISSN: 22145095. DOI: 10.1016/j.cscm.2021.e00630.
- [47] Instron. "What is Compression Testing? - Instron". In: (2019). URL: <https://www.instron.com/en/our-company/library/test-types/compression-test?region=Global%20Site&lang=en>.
- [48] SGS INTRON. *Analyserapport Residual glass streams*. 2020.
- [49] G. M.Sadiqul Islam, M. H. Rahman, and Nayem Kazi. "Waste glass powder as partial replacement of cement for sustainable concrete practice". In: *International Journal of Sustainable Built Environment* 6 (1 2017). ISSN: 22126104. DOI: 10.1016/j.ijbsbe.2016.10.005.
- [50] K. Jansen. *The influence of printing process parameters on the mechanical properties, numerical modelling, and the exploration of sustainable printable solutions for humanitarian problems*. Tech. rep. URL: [http://repository.tudelft.nl/..](http://repository.tudelft.nl/)
- [51] Krittiya Kaewmanee et al. "Effect of free lime content on properties of cement-fly ash mixtures". In: *Construction and Building Materials* 38 (Jan. 2013), pp. 829–836. ISSN: 09500618. DOI: 10.1016/j.conbuildmat.2012.09.035.

- [52] Mahsa Kamali and Ali Ghahremaninezhad. "An investigation into the hydration and microstructure of cement pastes modified with glass powders". In: *Construction and Building Materials* 112 (June 2016), pp. 915–924. ISSN: 09500618. DOI: 10.1016/j.conbuildmat.2016.02.085.
- [53] Mahsa Kamali and Ali Ghahremaninezhad. "Effect of glass powders on the mechanical and durability properties of cementitious materials". In: *Construction and Building Materials* 98 (2015). ISSN: 09500618. DOI: 10.1016/j.conbuildmat.2015.06.010.
- [54] Julia Kanapathippillai. "Canberra bus shelters move to new locations in the ACT". In: <https://www.canberratime.com.au/news/canberra-bus-shelters-rehomed-across-the-act/> (Jan. 2021).
- [55] N. S. Kathiravan et al. "State of art of review on bamboo reinforced concrete". In: *Materials Today: Proceedings* 45 (2021), pp. 1063–1066. ISSN: 22147853. DOI: 10.1016/j.matpr.2020.03.159.
- [56] Ali Kazemian et al. "Cementitious materials for construction-scale 3D printing: Laboratory testing of fresh printing mixture". In: *Construction and Building Materials* 145 (Aug. 2017). Publisher: Elsevier Ltd, pp. 639–647. ISSN: 09500618. DOI: 10.1016/j.conbuildmat.2017.04.015.
- [57] Fasih Ahmed Khan et al. "Development of environment-friendly concrete through partial addition of waste glass powder (Wgp) as cement replacement". In: *Civil Engineering Journal (Iran)* 6 (12 2020). ISSN: 24763055. DOI: 10.28991/cej-2020-03091620.
- [58] Kaffayatullah Khan et al. "Effect of Fineness and Heat Treatment on the Pozzolanic Activity of Natural Volcanic Ash for Its Utilization as Supplementary Cementitious Materials". In: *Crystals* 12 (2 Feb. 2022), p. 302. ISSN: 20734352. DOI: 10.3390/cryst12020302.
- [59] M. A. Khan. "Mix suitable for concrete 3D printing: A review". In: *Materials Today: Proceedings*. Vol. 32. ISSN: 22147853. Elsevier Ltd, Jan. 2020, pp. 831–837. DOI: 10.1016/j.matpr.2020.03.825.
- [60] Md Nabi Newaz Khan, Ashish Kumer Saha, and Prabir Kumar Sarker. "Reuse of waste glass as a supplementary binder and aggregate for sustainable cement-based construction materials: A review". In: *Journal of Building Engineering* 28 (2020). ISSN: 23527102. DOI: 10.1016/j.jobbe.2019.101052.
- [61] A. Khmiri, M. Chaabouni, and B. Samet. "Chemical behaviour of ground waste glass when used as partial cement replacement in mortars". In: *Construction and Building Materials* 44 (2013), pp. 74–80. ISSN: 09500618. DOI: 10.1016/j.conbuildmat.2013.02.040.
- [62] Essam A. Kishar et al. "Effect of calcium chloride on the hydration characteristics of ground clay bricks cement pastes". In: *Beni-Suef University Journal of Basic and Applied Sciences* 2 (1 Mar. 2013), pp. 20–30. ISSN: 23148535. DOI: 10.1016/j.bjbas.2013.09.003.
- [63] Particle Technology Labs. "BET Specific Surface Area - Particle Technology Labs". In: (2022). URL: <https://www.particletechlabs.com/analytical-testing/gas-adsorption-and-porosimetry/bet-specific-surface-area>.
- [64] T. T. Le et al. "Mix design and fresh properties for high-performance printing concrete". In: *Materials and Structures/Materiaux et Constructions* 45.8 (Aug. 2019), pp. 1221–1232. ISSN: 13595997. DOI: 10.1617/s11527-012-9828-z.
- [65] Gerry Lee et al. "Effects of crushed glass cullet sizes, casting methods and pozzolanic materials on ASR of concrete blocks". In: *Construction and Building Materials* 25 (5 May 2011), pp. 2611–2618. ISSN: 09500618. DOI: 10.1016/j.conbuildmat.2010.12.008.
- [66] University of Leuven. "Rapport Dienstverlening SR_Lim_2021_001". In: ().
- [67] Duan Le Li et al. "Influence of Organic Esters on Portland Cement Hydration and Hardening". In: *Advances in Materials Science and Engineering* 2018 (2018). ISSN: 16878442. DOI: 10.1155/2018/3203952.
- [68] Qiong Li et al. "Performance of waste glass powder as a pozzolanic material in blended cement mortar". In: *Construction and Building Materials* 324 (Mar. 2022). ISSN: 09500618. DOI: 10.1016/j.conbuildmat.2022.126531.

- [69] Jian xin Lu, Zhen hua Duan, and Chi Sun Poon. "Fresh properties of cement pastes or mortars incorporating waste glass powder and cullet". In: *Construction and Building Materials* 131 (Jan. 2017), pp. 793–799. ISSN: 0950-0618. DOI: 10.1016/J.CONBUILDMAT.2016.11.011.
- [70] Christopher Makowski and Kirt Rusenko. "Recycled glass cullet as an alternative beach fill material: Results of biological and chemical analyses". In: *Journal of Coastal Research* 23 (3 May 2007), pp. 545–552. ISSN: 07490208. DOI: 10.2112/06-0715.1.
- [71] Pankaj R. Mali and Debarati Datta. "Experimental evaluation of bamboo reinforced concrete beams". In: *Journal of Building Engineering* 28 (Mar. 2020). ISSN: 23527102. DOI: 10.1016/j.jobbe.2019.101071.
- [72] Brooke Mansell et al. *The impact of accelerating admixtures on blended cement hydration for early age strength enhancement*. Tech. rep. 2021.
- [73] Ana Mafalda Matos and Joana Sousa-Coutinho. "Durability of mortar using waste glass powder as cement replacement". In: *Construction and Building Materials* 36 (2012). ISSN: 09500618. DOI: 10.1016/j.conbuildmat.2012.04.027.
- [74] Will Mclean. "Skill: Inflatable Concrete Domes". In: *The architectural review* (2013). URL: <https://www.architectural-review.com/essays/craft/skill-inflatable-concrete-domes>.
- [75] Mehdi Mejdi et al. "Hydration and microstructure of glass powder cement pastes – A multi-technique investigation". In: *Cement and Concrete Research* 151 (Jan. 2022). ISSN: 00088846. DOI: 10.1016/j.cemconres.2021.106610.
- [76] Mohammadreza Mirzahosseini and Kyle A. Riding. "Effect of curing temperature and glass type on the pozzolanic reactivity of glass powder". In: *Cement and Concrete Research* 58 (2014). ISSN: 00088846. DOI: 10.1016/j.cemconres.2014.01.015.
- [77] Thanaa Khalaf Mohammed and Sheelan Mahmoud Hama. "Mechanical properties, impact resistance and bond strength of green concrete incorporating waste glass powder and waste fine plastic aggregate". In: *Innovative Infrastructure Solutions* 7 (1 2022). ISSN: 23644184. DOI: 10.1007/s41062-021-00652-4.
- [78] Shravan Muthukrishnan, Sayanthan Ramakrishnan, and Jay Sanjayan. "Set on demand geopolymer using print head mixing for 3D concrete printing". In: *Cement and Concrete Composites* 128 (Apr. 2022), p. 104451. ISSN: 09589465. DOI: 10.1016/j.cemconcomp.2022.104451.
- [79] Shravan Muthukrishnan, Sayanthan Ramakrishnan, and Jay Sanjayan. *Set-on-demand approaches for geopolymers in concrete 3D printing*. Tech. rep. 2022.
- [80] Shravan Muthukrishnan, Sayanthan Ramakrishnan, and Jay Sanjayan. "Technologies for improving buildability in 3D concrete printing". In: *Cement and Concrete Composites* 122 (Sept. 2021). ISSN: 09589465. DOI: 10.1016/j.cemconcomp.2021.104144.
- [81] M. Z. Naser, R. A. Hawileh, and J. A. Abdalla. "Fiber-reinforced polymer composites in strengthening reinforced concrete structures: A critical review". In: *Engineering Structures* 198 (Nov. 2019). ISSN: 18737323. DOI: 10.1016/j.engstruct.2019.109542.
- [82] Roz Ud Din Nassar, Parviz Soroushian, and Muhammad Sufyan-Ud-Din. "Long-term field performance of concrete produced with powder waste glass as partial replacement of cement". In: *Case Studies in Construction Materials* 15 (2021). ISSN: 22145095. DOI: 10.1016/j.cscm.2021.e00745.
- [83] P. Nath and P. Sarker. "Effect of fly ash on the durability properties of high strength concrete". In: *Procedia Engineering* 14 (2011), pp. 1149–1156. ISSN: 18777058. DOI: 10.1016/j.proeng.2011.07.144.
- [84] Adnan Nawaz et al. "Effect and limitation of free lime content in cement-fly ash mixtures". In: *Construction and Building Materials* 102 (Jan. 2016), pp. 515–530. ISSN: 09500618. DOI: 10.1016/j.conbuildmat.2015.10.174.
- [85] Venkatesh Naidu Nerella, Martin Krause, and Viktor Mechtcherine. "Direct printing test for buildability of 3D-printable concrete considering economic viability". In: *Automation in Construction* 109 (Jan. 2020). ISSN: 09265805. DOI: 10.1016/j.autcon.2019.102986.

- [86] Emmanuel Kwesi Nyantakyi et al. "Partial Replacement of Cement with Glass Bottle Waste Powder in Concrete for Sustainable Waste Management : A Case Study of Kumasi Metropolitan Assembly , Ashanti Region , Ghana". In: *Journal of Civil Engineering Research* 10 (2 2020).
- [87] Brwa Omer and Jalal Saeed. "Characterizations and modeling the influence of particle size distributions (Psd) of glass powder on the mechanical behavior of normal strength concrete". In: *Civil Engineering and Architecture* 8.5 (Oct. 2020). Publisher: Horizon Research Publishing, pp. 993–1005. ISSN: 23321121. DOI: 10.13189/cea.2020.080526.
- [88] Neri Oxman et al. "Towards robotic swarm printing". In: *Architectural Design* 84 (3 2014). ISSN: 15542769. DOI: 10.1002/ad.1764.
- [89] Suvash Chandra Paul et al. "Fresh and hardened properties of 3D printable cementitious materials for building and construction". In: *Archives of Civil and Mechanical Engineering* 18.1 (Jan. 2018). Publisher: Elsevier B.V., pp. 311–319. ISSN: 16449665. DOI: 10.1016/j.acme.2017.02.008.
- [90] Sanoop Prakasan, Sivakumar Palaniappan, and Ravindra Gettu. "Study of Energy Use and CO2 Emissions in the Manufacturing of Clinker and Cement". In: *Journal of The Institution of Engineers (India): Series A* 101 (1 Mar. 2020), pp. 221–232. ISSN: 22502157. DOI: 10.1007/S40030-019-00409-4.
- [91] Alexandra Quennoz and Karen L. Scrivener. "Interactions between alite and C3A-gypsum hydrations in model cements". In: *Cement and Concrete Research* 44 (Feb. 2013), pp. 46–54. ISSN: 00088846. DOI: 10.1016/j.cemconres.2012.10.018.
- [92] Afif Rahma, Nabil El Naber, and Sherzad Issa Ismail. "Effect of glass powder on the compression strength and the workability of concrete". In: *Cogent Engineering* 4 (1 Jan. 2017). ISSN: 23311916. DOI: 10.1080/23311916.2017.1373415.
- [93] S. Rahman and M. N. Uddin. "Experimental investigation of concrete with glass powder as partial replacement of cement". In: *Civil Engineering and Architecture* 6 (3 2018). ISSN: 23321121. DOI: 10.13189/cea.2018.060304.
- [94] Paul Rapp. "EFFECT OF CALCIUM CHLORIDE ON PORTLAND CEMENTS AND CONCRETES". In: *Part of Journal of Research of the National Bureau of Standards* 14 (1935).
- [95] Sara Reichenbach et al. "A review on embedded fibre-reinforced polymer reinforcement in structural concrete in Europe". In: *Construction and Building Materials* 307 (Nov. 2021). ISSN: 09500618. DOI: 10.1016/j.conbuildmat.2021.124946.
- [96] Lex Reiter et al. "Setting on demand for digital concrete – Principles, measurements, chemistry, validation". In: *Cement and Concrete Research* 132 (June 2020). Publisher: Elsevier Ltd. ISSN: 00088846. DOI: 10.1016/j.cemconres.2020.106047.
- [97] Daniel Véras Ribeiro and Marcio Raymundo Morelli. "Effect of calcination temperature on the pozzolanic activity of Brazilian sugar cane bagasse ash (SCBA)". In: *Materials Research* 17 (4 July 2014), pp. 974–981. ISSN: 19805373. DOI: 10.1590/S1516-14392014005000093.
- [98] Nicolas Roussel. "Rheological requirements for printable concretes". In: *Cement and Concrete Research* 112 (Oct. 2018), pp. 76–85. ISSN: 00088846. DOI: 10.1016/j.cemconres.2018.04.005.
- [99] Hatice Gizem Şahin and Ali Mardani-Aghabaglou. "Assessment of materials, design parameters and some properties of 3D printing concrete mixtures; a state-of-the-art review". In: *Construction and Building Materials* 316 (Jan. 2022). ISSN: 09500618. DOI: 10.1016/j.conbuildmat.2021.125865.
- [100] I. M. A. K. Salain. "Using calcium chloride as an accelerator for Portland pozzolan cement concrete compressive strength development". In: *IOP Conference Series: Materials Science and Engineering*. Vol. 615. ISSN: 1757899X Issue: 1. Institute of Physics Publishing, Oct. 2019. DOI: 10.1088/1757-899X/615/1/012016.
- [101] Geert De Schutter et al. "Vision of 3D printing with concrete — Technical, economic and environmental potentials". In: *Cement and Concrete Research* 112 (Oct. 2018), pp. 25–36. ISSN: 00088846. DOI: 10.1016/j.cemconres.2018.06.001.

- [102] K. L. Scrivener and H. F. W. Taylor. "Delayed ettringite formation: a microstructural and microanalytical study". In: *Advances in Cement Research* 5 (20 Oct. 1993), pp. 139–146. ISSN: 0951-7197. DOI: 10.1680/adcr.1993.5.20.139.
- [103] Caijun Shi et al. "Characteristics and pozzolanic reactivity of glass powders". In: *Cement and Concrete Research* 35 (5 May 2005), pp. 987–993. ISSN: 00088846. DOI: 10.1016/j.cemconres.2004.05.015.
- [104] J Skalny and J N Maycock. "MECHANISMS OF ACCELERATION BY CALCIUM CHLORIDE: A REVIEW". In: *ASTM Journal of Testing and Evaluation* 3 (4 1975).
- [105] Marcelo Tramontin Souza et al. "Role of chemical admixtures on 3D printed Portland cement: Assessing rheology and buildability". In: *Construction and Building Materials* 314 (Jan. 2022). Publisher: Elsevier Ltd. ISSN: 09500618. DOI: 10.1016/j.conbuildmat.2021.125666.
- [106] EUROPEAN STANDARD. "nen-en 196-1 Beproevingmethoden voor cement - Deel 1". In: (2013).
- [107] EUROPEAN STANDARD. "nen-en 196-3 Beproevingmethoden voor cement - Deel 3". In: (2013).
- [108] Statista. "• Europe: cement production by country | Statista". In: (). URL: <https://www.statista.com/statistics/1291068/european-cement-production-volume-by-country/>.
- [109] Laurent Steger et al. "Experimental evidence for the acceleration of slag hydration in blended cements by the addition of CaCl₂". In: *Cement and Concrete Research* 149 (Nov. 2021). Publisher: Elsevier Ltd. ISSN: 00088846. DOI: 10.1016/j.cemconres.2021.106558.
- [110] Lianfang Sun et al. "Alkali-silica reaction and strength of concrete with pretreated glass particles as fine aggregates". In: *Construction and Building Materials* 271 (Feb. 2021). Publisher: Elsevier Ltd. ISSN: 09500618. DOI: 10.1016/j.conbuildmat.2020.121809.
- [111] Bashar Taha and Ghassan Nounu. "Using lithium nitrate and pozzolanic glass powder in concrete as ASR suppressors". In: *Cement and Concrete Composites* 30 (6 2008). ISSN: 09589465. DOI: 10.1016/j.cemconcomp.2007.08.010.
- [112] Nafisa Tamanna and Rabin Tuladhar. "Sustainable Use of Recycled Glass Powder as Cement Replacement in Concrete". In: *The Open Waste Management Journal* 13 (1 Mar. 2020), pp. 1–13. ISSN: 1876-4002. DOI: 10.2174/1874347102013010001.
- [113] Nafisa Tamanna et al. "POZZOLANIC PROPERTIES OF GLASS POWDER IN CEMENT PASTE". In: *Journal of Civil Engineering, Science and Technology* 7 (2 Sept. 2016), pp. 75–81. DOI: 10.33736/jcest.307.2016.
- [114] Yaxin Tao et al. "Mechanical and microstructural properties of 3D printable concrete in the context of the twin-pipe pumping strategy". In: *Cement and Concrete Composites* 125 (Jan. 2022). Publisher: Elsevier Ltd. ISSN: 09589465. DOI: 10.1016/j.cemconcomp.2021.104324.
- [115] Yaxin Tao et al. "Stiffening control of cement-based materials using accelerators in inline mixing processes: Possibilities and challenges". In: *Cement and Concrete Composites* 119 (May 2021). Publisher: Elsevier Ltd. ISSN: 09589465. DOI: 10.1016/j.cemconcomp.2021.103972.
- [116] Thermoscientific. "Free Lime Determination in Clinker ARL 9900 Series with IntelliPower™ Simultaneous-Sequential XRF Spectrometer Key Words • ARL 9900-3600W • Cement • Free lime • Integrated XRF-XRD • X-ray Fluorescence". In: (). URL: www.thermoscientific.com.
- [117] Guan Heng Andrew Ting, Yi Wei Daniel Tay, and Ming Jen Tan. "Experimental measurement on the effects of recycled glass cullets as aggregates for construction 3D printing". In: *Journal of Cleaner Production* 300 (June 2021). Publisher: Elsevier Ltd. ISSN: 09596526. DOI: 10.1016/j.jclepro.2021.126919.
- [118] Guan Heng Andrew Ting et al. "Extrudable region parametrical study of 3D printable concrete using recycled glass concrete". In: *Journal of Building Engineering* 50 (June 2022). ISSN: 23527102. DOI: 10.1016/j.jobeb.2022.104091.

- [119] Guan Heng Andrew Ting et al. "Utilization of recycled glass for 3D concrete printing: rheological and mechanical properties". In: *Journal of Material Cycles and Waste Management* (2019). Publisher: Springer Tokyo. ISSN: 16118227. DOI: 10.1007/s10163-019-00857-x.
- [120] Monique Tohoue Tognonvi et al. "Reactivity of Recycled Glass Powder in a Cementitious Medium". In: *New Journal of Glass and Ceramics* 10 (03 2020). ISSN: 2161-7554. DOI: 10.4236/njgc.2020.103003.
- [121] Gunalaan Vasudevan, Seri Ganis, and Kanapathy Pillay. "Performance of Using Waste Glass Powder In Concrete As Replacement Of Cement". In: *American Journal of Engineering Research* 02 (12 2013).
- [122] Viatechnik. "The Basics of Inflatable Concrete Dome Construction". In: (2019). URL: <https://www.viatechnik.com/the-basics-of-inflatable-concrete-dome-construction/>.
- [123] Elena. Rodriguez Vieitez et al. "End-of-waste criteria for glass cullet : technical proposals." In: (2011).
- [124] Tran Huyen Vu et al. "Chloride induced corrosion of steel reinforcement in alkali activated slag concretes: A critical review". In: *Case Studies in Construction Materials* 16 (June 2022). ISSN: 22145095. DOI: 10.1016/j.cscm.2022.e01112.
- [125] R. J. M. Wolfs, F. P. Bos, and T. A. M. Salet. "Early age mechanical behaviour of 3D printed concrete: Numerical modelling and experimental testing". In: *Cement and Concrete Research* 106 (Apr. 2018). Publisher: Elsevier Ltd, pp. 103–116. ISSN: 00088846. DOI: 10.1016/j.cemconres.2018.02.001.
- [126] R. J. M. Wolfs, F. P. Bos, and T. A. M. Salet. "Hardened properties of 3D printed concrete: The influence of process parameters on interlayer adhesion". In: *Cement and Concrete Research* 119 (May 2019). Publisher: Elsevier Ltd, pp. 132–140. ISSN: 00088846. DOI: 10.1016/j.cemconres.2019.02.017.
- [127] Peng Wu, Jun Wang, and Xiangyu Wang. "A critical review of the use of 3-D printing in the construction industry". In: *Automation in Construction* 68 (Aug. 2016), pp. 21–31. ISSN: 09265805. DOI: 10.1016/j.autcon.2016.04.005.
- [128] Jianzhuang Xiao et al. "Large-scale 3D printing concrete technology: Current status and future opportunities". In: *Cement and Concrete Composites* 122 (Sept. 2021). ISSN: 09589465. DOI: 10.1016/j.cemconcomp.2021.104115.
- [129] XOS. "X-Ray Diffraction (XRD) - XOS". In: (2021). URL: <https://www.xos.com/XRD>.
- [130] Q. Yuan et al. "A feasible method for measuring the buildability of fresh 3D printing mortar". In: *Construction and Building Materials* 227 (Dec. 2019). Publisher: Elsevier Ltd. ISSN: 09500618. DOI: 10.1016/j.conbuildmat.2019.07.326.
- [131] Woo Sung Yum et al. "Effects of CaCl₂ on hydration and properties of lime(CaO)-activated slag/fly ash binder". In: *Cement and Concrete Composites* 84 (Nov. 2017), pp. 111–123. ISSN: 09589465. DOI: 10.1016/j.cemconcomp.2017.09.001.
- [132] Keren Zheng. "Pozzolanic reaction of glass powder and its role in controlling alkali–silica reaction". In: *Cement and Concrete Composites* 67 (Mar. 2016), pp. 30–38. ISSN: 0958-9465. DOI: 10.1016/J.CEMCONCOMP.2015.12.008.